Fabrication of Novel Cytocompatible Membranes for Ocular Application, Concentrating in Particular on Age-Related Macular Degeneration (AMD)

A thesis submitted to the University of Manchester for the degree of Doctor of Philosophy in the Faculty of Engineering and Physical Sciences

2014

Atikah Shahid Haneef

School of Materials

Table of Contents

Final Word Count:

54,516

List of Figures (Thesis)

List of Tables (Thesis)

List of Figures (Publication #1)

(Note: Thesis p. 87, publication pages as follows)

List of Tables (Publication #1)

List of Figures (Publication #2)

(Note: Thesis p. 88, publication pages as follows)

List of Tables (Publication #2)

List of Abbreviations

AMD/ARMD: age-related macular degeneration

PS: polystyrene

PET: poly(ethylene terephthalate)

PU: polyurethane

BM: Bruch's membrane

RPE: retinal pigment epithelial cells

IAESG: International ARM epidemiological study group

AREDS: age-related eye disease study

CNV: choroidal neovascularization

HDL: high density lipoproteins

LDL: low density lipoproteins

FDA: US Food and Drug Administration

VEGF: vascular endothelial growth factor

AMOPS: advanced macular oxidation products

BL: basal lamina

ICL: inner collagenous layer

EL: elastin layer

BCE-ECM: bovine corneal endothelial extra-cellular matrix

ECM: extracellular matrix

PLLA: poly-L-lactic acid

PTFE: polytetrafluoroethylene

NaOH: sodium hydroxide

PLGA: poly-lactic-glycolic-acid

O_2: oxygen

NH_3: ammonia

PLA: polylactic acid

ATP: adenosine triphosphate

PEDF: pigment epithelium derived factor

REL: retinal exclusion limit

VEC: vascular endothelial cells

WBC: white blood cells

PLAGA: poly-lactic acid-glycolic acid

PCL: polycaprolactone

CA: cellulose acetate

PVC: polyvinylcarbazole

PC: polycarbonate

DCM: dichloromethane

PMSQ: polymethylsilsequioxane

MC: methylene chloride

DMF: dimethyl formamide

PMMA: polymethylmethacrylate

PVA: polyvinylalcohol

N6: Nylon 6

PVP: poly(vinylpyrrolidone)

EPN: electrospun polyamide nanofibres

EPP: etch pore polyester

TCP: tissue culture plastic

RGD: Arginine-Glycine-Aspartic Acid tripeptide motif

HF: hexafluoropropylene

NN: N,N-dimethylaminoethyl methacrylate

MA: methacrylate

Mw: molecular weight

THF: tetrahydrofuran

DCM: dichloromethane

v/v: volume/volume

w/v: weight/volume

EtOH: ethanol

HFIP: 1,1,1-3,3,3-hexafluoroisopropanol

TFA: trifluoroacetic acid

NaCl: sodium chloride

SEM: scanning electron microscopy

EHT: electron high tension

WCA: water contact angle

XPS: X-ray photoelectron spectroscopy

DMEM: Dulbecco's modified Eagle's medium

$NaHCO_3$: sodium hydrogen carbonate

FBS: foetal bovine serum

AB: antibiotic/antimycotic mixture

L-gluts: L-glutamine

ARPE-19: spontaneously arising retinal pigment epithelial cells

PBS: Dulbecco's phosphate buffered saline

EDTA: ethylenediaminetetracetic acid

UV: ultraviolet light

HMDS: hexamethyldisilazane

TEER: transepithelial electrical resistance

SD: standard deviation

NIHR: National Institute for Health Research

i4i: Invention for Innovation programme

NHS: National Health Service

HOMO: highest occupied molecular orbital

LUMO: lowest unoccupied molecular orbital

PLCL: poly(L-lactide-co-ε-caprolactone)

Abstract
The University of Manchester

Atikah Shahid Haneef

Doctor of Philosophy (PhD)

Fabrication of Novel Cytocompatible Membranes for Ocular Application, Concentrating in Particular on Age-Related Macular Degeneration (AMD)

April 2014

The aims of this research were to investigate polymer fibre morphology, overall mat morphology, mechanical properties and general handling of the mats, and ideal mat thickness in order to fabricate a suitable substrate for potential use in cell transplantation for application as a permanent substrate for the treatment of dry age-related macular degeneration (AMD). Polystyrene (PS), poly(ethylene terephthalate) (PET) and polyurethane (PU) were electrospun to ascertain the ideal electrospinning parameters to reproducibly obtain fibres to construct a mat as a potential candidate for a replacement Bruch's membrane (BM). After identifying the ideal spinning parameters, mats were fabricated, their fibre morphology, overall mat morphology, and handling during processing were examined. This allowed the shortlisting of PS and PET substrates, which were suitable to be taken forward for further testing and cell culture. PU was found to be unsuitable as it had a tendency to become entwined and stick to itself, which would destroy the gross mat morphology. Therefore PU was excluded from further testing.

Further handling, both quantitative and qualitative, and thickness and porosity were tested for PS and PET mats. Electrospun PET demonstrated greater handling and durability properties compared to PS mats, which were more fragile. PET was able to withstand twisting, folding, and rolling, whereas PS could not undergo twisting and fell apart. PS mats were thicker and more porous compared to PET mats, which was attributed to the widely spaced placement of the larger PS fibres and the fluffy gross morphology of the PS mats, in comparison to the closer fibre placement of the smaller PET mats which had a smooth gross mat morphology. Considering this, PS mats were compressed and thickness and porosity was reduced, while maintaining its fibrous structure. However the compressed PS mats became extremely fragile and could not withstand much handling. Although PET mats were thinner than PS mats, it did not match the native BM thickness and so experiments in varying collection time during electrospinning to match the native BM thickness were undertaken. Tensile tests, thickness and porosity measurements showed that PET tensile properties, thickness, and porosity reduced with reduced collection time.

For the purposes of surface treatment and cell culture, uncompressed mats collected for 60 minutes were used since sufficient PS fibres were able to be collected to form a mat that was able to withstand processing at this collection time. Effect of UV/ozone surface treatment was tested for both PS and PET mats. Treatment of both substrate types affected protein adsorption, with evidence of aminolysis observed on PET substrates. Short-term initial growth and survival of retinal pigment epithelial cells (RPE cells) on electrospun, surface oxidised PS and PET was investigated. Untreated PS did not support cell proliferation and although treated PS did, the resultant RPE cell morphology was undesirable, therefore was not taken forward to long term cell culture. Treated and untreated PET supported cell proliferation, and was taken forward to the long term culture study, where cells exhibited the desired monolayer morphology. In this work it has been demonstrated that electrospun PET may potentially be a suitable candidate as cell carrier substrate for subsequent implantation in application towards AMD treatment.

Declaration

No portion of the work referred to in the thesis has been submitted in support of an application for another degree or qualification of this or any other university or other institute of learning.

Copyright Statement

i. The author of this thesis (including any appendices and/or schedules to this thesis) own certain copyright or related rights in it (the "Copyright") and she has given The University of Manchester certain rights to use such Copyright, including for administrative purposes.

ii. Copies of this thesis, either in full or in extracts and whether in hard or electronic copy, may be **only** in accordance with the Copyright, Designs and Patents Act 1988 (as amended) and regulations issued under it or, where appropriate, in accordance with licensing agreements which the University has from time to time. This page must form part of any such copies made.

iii. The ownership of certain Copyright, patents, designs, trade marks and other intellectual property (the "Intellectual Property") and any reproductions of copyright work in the thesis, for example graphs and tables ("Reproductions"), which may be described in this thesis, may not be owned by the author and may be owned by third parties. Such Intellectual Property and Reproductions cannot and must not be made available for use without the prior written permission of the owner(s) of the relevant Intellectual Property and/or Reproductions.

iv. Further information on the conditions under which disclosure, publication and commercialisation of this thesis, the Copyright and any Intellectual Property and/or Reproductions described in it may take place is available in the University IP Policy (see http://www.campus.manchester.ac.uk/medialibrary/policies/intellectual-property.pdf), in any relevant Thesis restriction declarations deposited in the University library, The University Library's regulations (see http://www.manchester.ac.uk/library/aboutus/regulations) and in The University's policy on presentation of Theses.

Dedications & Acknowledgements

My work is dedicated to my family, without whose continued, and very much needed support this definitely would not have been possible. My Mum who is my go to and my biggest enthusiast, my Dad who keeps me straight and focused when maybe I am being a little silly, my Sister for putting up with my eccentricity (of which there is plenty), and my Brother for being my distraction when I need it most. Alhamdulillah, I've got the best of the lot.

Thanks to everyone at the Biomaterials Department that did their bit.

About the Author

My background is in chemistry. I graduated from the University of Manchester in 2010 with a MChem (with Honours). I have experience in working with air-sensitive and water sensitive materials, and have much experience in working under inert conditions. My experience also includes nuclear magnetic resonance (NMR) spectroscopy and infra-red (IR) spectrometry. My interest in medical related science developed when I was working on synthesising anti-cancer gold complexes as my final year undergraduate project. From then on I wanted to work in applied science. Biomedical materials fit my interests, and have found that because of its diverse interdisciplinary nature, it is constantly moving forward. This project has been interesting and very challenging as the learning curve, coming from a pure science background and changing to an applied science, was a very steep one. But it has also been an enjoyable experience. I am now experienced in cell culture, aseptic technique, and have learned a range of biochemical assay techniques. I have also gained experience in scanning electron microscopy (SEM), fluorescent microscopy and electrospinning.

Chapter 1: Introduction

1.1 The Eye

Loss of vision can severely affect an individual's quality of life. It can range from poor visual acuity, or blurriness, which is the least incapacitating, to partial sight loss, through to complete loss of sight. Blurriness, which can be due to refractive error of the lens, can be easily corrected either via contact lenses or glasses, which may need regular changing if vision continually degrades. Central vision loss can be particularly debilitating, as the object being looked at directly cannot be seen and one must learn to look slightly away from the object in order to use the peripheral vision. Peripheral vision does not have as high a visual acuity as central vision. Therefore, although this is a form of managing loss of central vision, it can become frustrating for the individual hence cannot be labelled as a long term solution.

Upon gross examination of the eye, it is evident that it contains distinct layers that enable us to see.[1] Visual acuity is controlled by; the pupil, which controls the amount of light that enters the eye, a lens that is responsible for 22 % of the refraction of light and the cornea, which works in conjunction with the sclera to give the eye support, strength and shape. Without a functioning retina however, all of the previous structures would be rendered futile.

The retina is the transparent, photographic plate that is made up of photoreceptors responsible for vision. One particular area of the retina that is of interest is the macula, which is situated in the fundus of the eye. The fundus is an area of the retina directly behind the lens and includes structures such as the optic disc: the blind spot where nerves lead to the brain, the macula: a yellow spot which contains the fovea an area responsible for high resolution central vision which is located in the middle of the macula and also the posterior pole: an area of retina between the macula and optic disc (Figure 1).

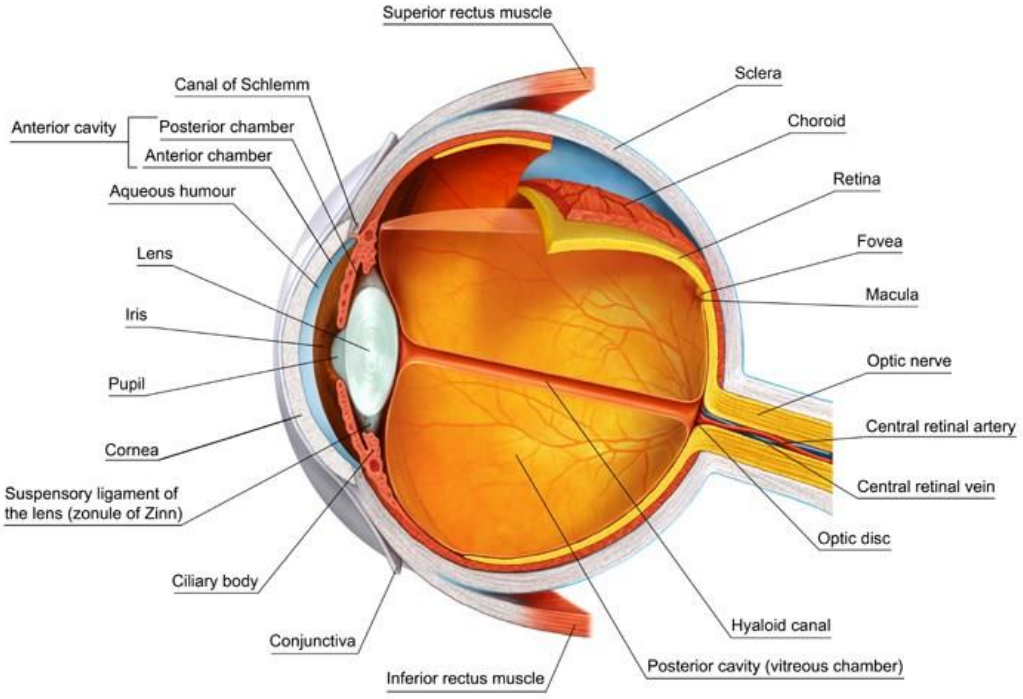

Figure 1: Cross section of a normal human eye, with labels of the gross anatomy. From this it can be seen that the macula is located in the fovea, which is directly behind the lens and is responsible for central vision. Image obtained from http://www.virtualmedicalcentre.com [2]

1.2: The Macula, Bruch's Membrane & Retinal Pigment Epithelium

The macula is the area of the retina containing a concentrated density of rods and cones, the photoreceptors responsible for vision, and is most important for detailed vision.

Meticulous imaging of the eye via electron microscopy illustrated the complex nature of the layers within.[3] Particularly the membrane found between the retina and the choroid called the Bruch's membrane (BM) or the lamina vitrea (Figure 2).

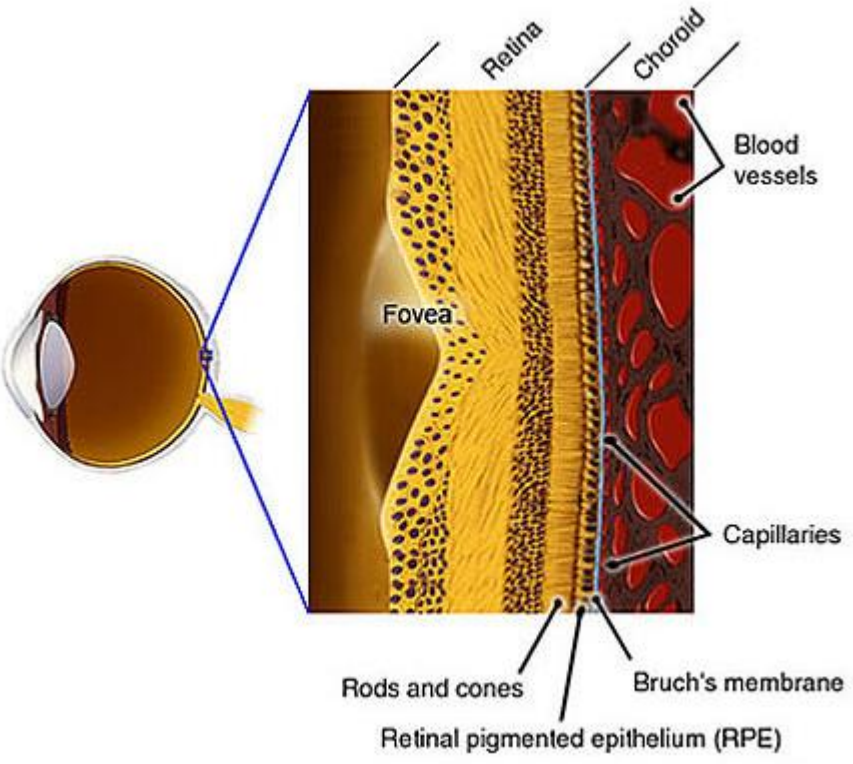

Figure 2: Cross section of a healthy human macula, with the anatomical labels. From this it can be seen that the Bruch's membrane is a very thin layer upon which the retinal pigment epithelial cells are sat. Directly underneath the Bruch's membrane are capillaries which are the blood supply and the means of receiving nutrients and help remove waste products. Image obtained from http://www.brightfocus.org/macular [4]

The choroid is a highly vascular tissue that supplies blood to the retina.[1,3] From microscopic inspection it was realised that the tight junctions between the cells of a retinal

pigment epithelium (RPE) and BM constitutes a blood-retina barrier that prevents penetration of blood vessels through the retina and is a selectively permeable membrane to allow the movement of molecules across it.[3]

The BM is a 2-4.7 μm thick membrane[5,6] which consists of five distinct layers: a basal lamina that RPE cells attach to (RPE-BL) described as a meshwork of fine fibres that contains collagen IV, but fibre measurements have not been reported;[7] an inner collagen fibre membrane (ICL) described as containing 70 nm diameter fibres of collagen I, III, V in a multi-layered criss-cross;[7] an elastin layer (EL) described as being able to confer biomechanical properties, consisting of stacks of elastin fibres that also contain collagen VI, fibronectin and other proteins, criss-crossing to form a sheet, which allows collagen fibres from the ICL and outer collagen layer (OCL) to cross it, with inter-fibre spaces of approximately 1 μm; an OCL that is described as being similar to the ICL, however the OCL has regular extensions toward the choriocapillary lumens called intercapillary pillars,[7] and a choriocapillaris basal lamina (ChC-BL) upon which capillary endothelial cells of the choroid attach to has been described as being important for inhibiting endothelial cell migration into the Bruch's membrane.[3,6-9]

The BM has two functions, it provides support and provides a means for metabolic exchange; allowing nutrients to permeate through to the RPE and metabolic products to be removed via the opposite pathway.[6,7] The RPE is a layer of highly active metabolic cells that continuously deposit metabolic products into the BM. The RPE relies on the permeability of the BM to remove these waste products. The BM also allows a supply of blood via the choroid and oxygen to reach the RPE and it also possesses filtering abilities; thus preventing large proteins from entering the retina or the vitreous body of the eye and stops cell invasion. This filtering ability is explained by the highly fenestrated and folded characteristics of the membrane, which also provides a large surface area to aid ion and material transport.[3] Sumita also found that between the basal layer of the RPE and the

basement layer for the RPE (the top most layer of the BM) was a gap, which occasionally consisted of filamentous connections. This may be the filamentous growths of the RPE cells themselves.[3]

1.3: Age-Related Macular Degeneration

1.3.1 Prevalence

According to the World Health Organisation (WHO), age-related macular degeneration (AMD) is the third largest cause of blindness in the world, causing 8.7 % of cases (Figure 3).[10]

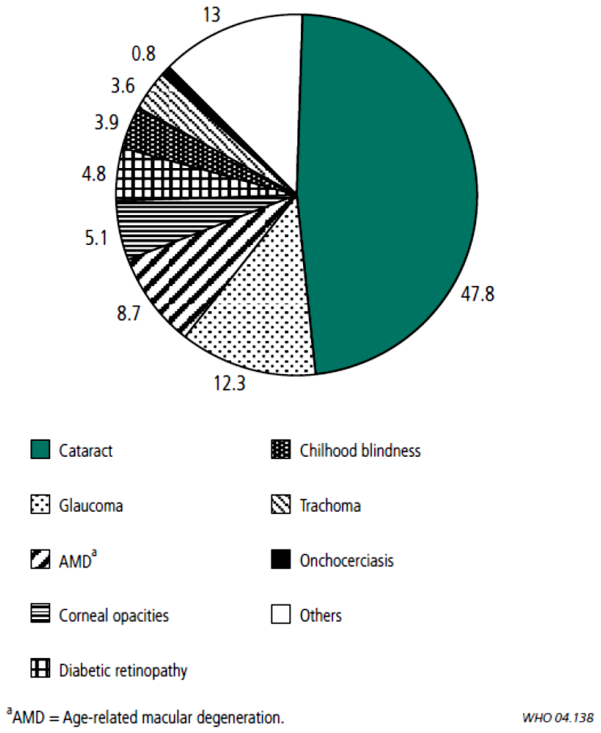

Figure 3: Pie-chart showing the World Health Organisation's statistics on the major causes of blindness worldwide. All values are given in percentages. From this it can be seen that AMD is the third most prevalent cause of blindness worldwide, coming in at 8.7 % of recorded cases. Image obtained from Resnikoff *et al.* 2004.[10]

AMD, also referred to as ARMD, is one of the largest registered causes of blindness in the UK[11] and is the leading cause of severe and irreversible vision loss in the West in people over the age of 50, but is more prominent in people aged 65 and above.[12] It is typically described as a disorder of the retina and has been suggested that it is much more prevalent

in females than males; however this may be due to statistics that women, in general, live longer than men. In addition, most of the reviews are based on hospital records in which women may be over represented.[11] Pooled data from three prominent studies into AMD prevalence; Beaver Dam Eye Study, Blue Mountains Eye Study and Rotterdam Eye Study have revealed that no gender difference is present in the risk of AMD.[11,13,14] There is however a predominance found in Caucasian people, with AMD found to be responsible for more than 8 million blind people worldwide.[14]

Owen *et al.* compiled a statistical analysis to investigate the prevalence of AMD in the UK.[11] Although the study involved the majority of the data coming from the USA, North Europe and Australia, the individuals involved in the study were representative of the majority of the UK population, and so Owen *et al.* were able to generalise findings.[11] However obvious geographical differences and possible effects of diet, sun exposure and environment as extenuating circumstances were also taken into account.[11] This study found that dry AMD was rare in people between 50 and 69 but by age 69 and upwards, prevalence increased with age, eventually peaking at 80-84 years of age.

1.3.2 Classification of AMD

AMD comes under the main umbrella of disorders of the retina and is a disorder of the region of the retina called the macula. It is thought to be caused by a variety of things, some being; ocular trauma, retinal detachment or chorioretinal infective/inflammatory process. The definitive cause of the disease isn't known, only that age is a factor and that debris like material called "drusen" accumulates below the RPE on the BM (Figure 4). It has been suggested that with age the macula undergoes degenerative changes. Not all patients experience visual distortion, but a vast number do undergo blurring of central vision.[1] In some cases, patients are found to develop frank choroidal neovascularisation, which can render the individual with poor central vision, although leaving the peripheral vision unaffected.[1]

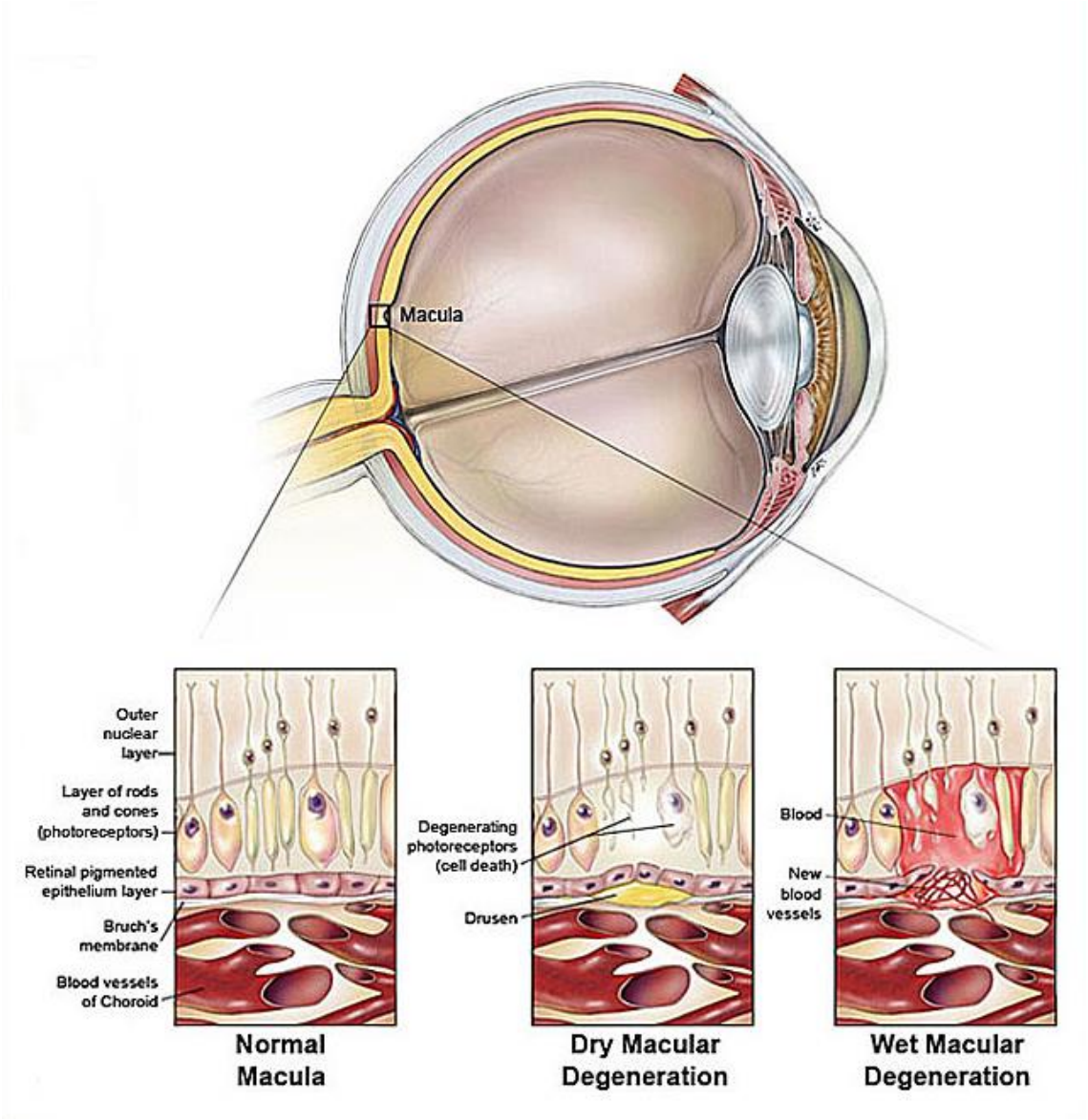

Figure 4: A comparison between a normal human macula and the differences between the dry and wet form of AMD. From this it can be seen that in dry AMD drusen deposit between the Bruch's membrane and the RPE layer, while in wet AMD new blood vessels grow through the Bruch's membrane and RPE layer. Image obtained from http://www.brightfocus.org/macular [4]

No common grading system has yet been compiled to enable easy AMD classification and detection. Epidemiological studies have been carried out in order to develop a classification system for AMD.[12] In this aim The International ARM Epidemiological

Study Group (IAESG) classified the presence, or not, of AMD based primarily on morphological changes seen on colour fundus transparencies.[12] These changes were related to age to obtain a correlation. Visual acuity was found not to be a decisive factor for the presence of AMD, but the presence of white/yellow deposits called drusen was found to be characteristic to confirm AMD.[12]

The IAESG described AMD as a progressive disease consisting of stages. Two categories are given to the two stages of AMD; the first is dry or geographic atrophy, which is characterised by sharply delineated round or oval hypopigmentation or depigmentation or the loss/absence of RPE cells. Wet AMD is called "neovascular", "disciform" or "exudative" AMD and is characterised by the detachment of RPE and subretinal neovascular membrane. Further characteristics include scarring under the RPE and haemorrhaging; which could be subretinal, into the retina, or into the vitreous body.[12]

Although the cause of AMD is still unknown, there have been a number of risk factors associated with the disease. Age is the biggest risk factor, followed by race, with a lower prevalence of the disease in Black people (but this again is confounded by life expectancy) and family history, leading to links to genetic factors.[8]

Four main risk factor definitions were compiled by the age-related eye disease study (AREDS) research group with the following categories: demographic, medical history, use of medication and ocular disease. Any associated assumed causal factors which could be changed or controlled; one being diet and the other smoking, were also discussed. A higher prevalence of signs of AMD in those who smoked was found compared to those who had never smoked.[15]

McCarty *et al.* also compiled a list of possible risk factors that could be controlled by intervention and attempted to see the prevalence of AMD in people who were attributable to those risk factors.[16] No links between vascular disease, such as hypertension, and AMD

were found. Ding *et al*. took the molecular approach giving a high emphasis on the oxidative processes and the effects of inflammation in causes of AMD, with smoking as a risk factor that leads to an increase in oxidative compounds which increase the risk of oxidising stress on the BM.[17] Interestingly a positive correlation between smoking and AMD prevalence was highlighted.[16,17]

1.3.3 Mechanisms of Wet & Dry AMD

Suggestions that the BM altering consequently has direct impact on vision have led to investigations into what changes are in fact occurring and how they affect the RPE. Guymer *et al*. looked at the changes that occur in the BM with age.[18] Various characteristics linked with age that can lead to retinal disease. The surface charge of the BM is affected by the pH of its surroundings. At physiological pH there is a negative charge on the BM, which may cause lack of diffusion of negatively charged molecules. If the characteristics of the BM affect the permeability of the membrane for important molecules, ultimately this will affect the overall membrane function of the RPE cells. Accordingly if the BM malfunctions it will affect the overall function of the RPE and ultimately sight.[18]

There are two types of AMD; dry (or central geographic atrophy) and wet (or neovascular/exudative/disciform). Dry is the more prevalent form and is due to atrophy of the RPE.[1,12] Wet AMD involves unusual vascular growth that occurs through the BM. This leads to leakage of proteins and blood below the macula followed by loss of photoreceptors if left untreated.[1]

1.3.3.1 Wet AMD

Wet AMD, also referred to as choroidal neovascularization (CNV), is the least prevalent form of AMD, causing 10-15 % of all AMD cases.[19] Wet AMD involves the formation of new vascular processes, which can grow through the BM and RPE into the subretinal space

causing bleeding (Figure 5).[20] It is initiated by an increase in vascular endothelial growth factor (VEGF), causing migration and proliferation of choroidal endothelial cells.[21]

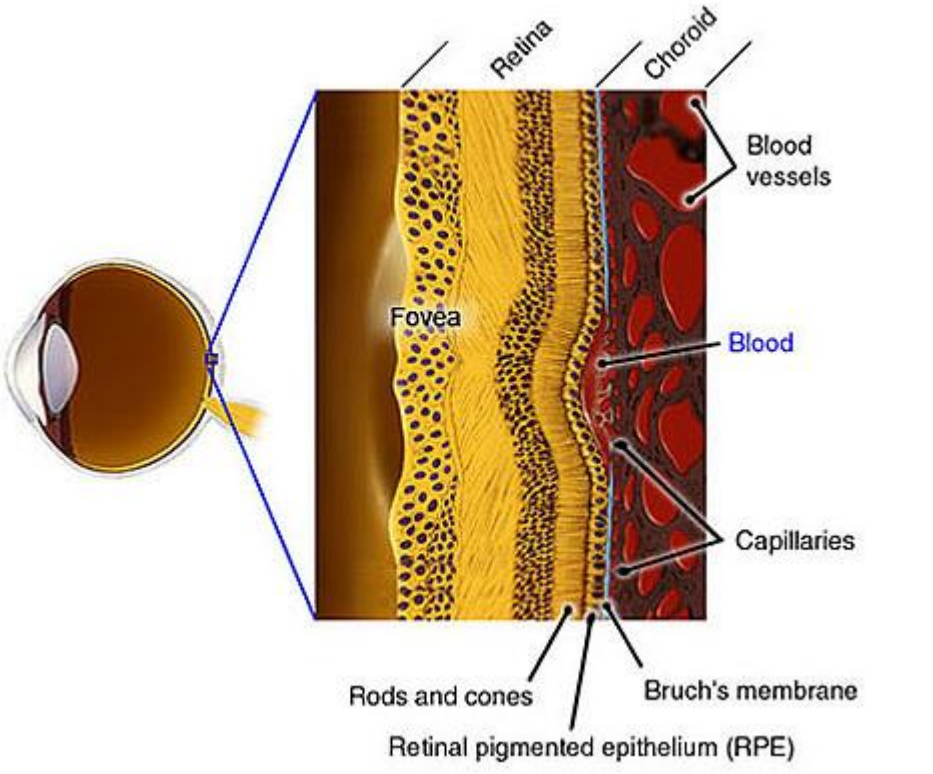

Figure 5: Cross section of a macula depicting what happens during wet AMD. From this it can be seen that capillaries have grown through the Bruch's membrane causing bleeding underneath and disruption of the RPE layer. Image obtained from http://www.brightfocus.org/macular [4]

1.3.3.2 Dry AMD

Dry AMD is thought to occur due to damage of RPE and causes loss of macula photoreceptors.[19] The RPE sits on the BM, age is said to cause thickening of the BM, which in turn prevents efficient diffusion of nutrients and removal of waste products to and from the RPE.[18] Since the RPE continually produces metabolic waste and debris for removal this can cause build up, exacerbating the problem. With age, contact with the choriocapillary area is reduced, and because this is thought to be the main source of

nutrients and route for removal of waste and debris, this loss can cause further problems. A linear regression relationship between BM thickness and RPE function has been found.[22] An efficiently permeable membrane is important in order to allow good nutrient/waste exchange to occur.[22] If this exchange fails, it can lead to deposits and eventually drusen on the BM (Figure 6).[22] Drusen are considered to be the most important symptom of AMD.[23]

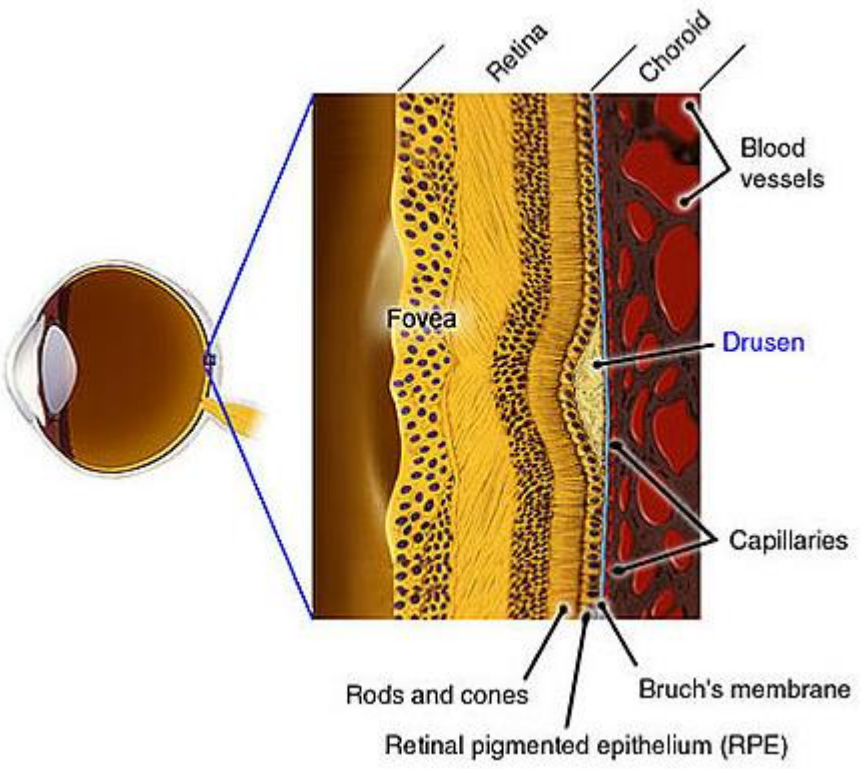

Figure 6: Cross section of a macula depicting what happens during dry AMD. From this it can be seen that drusen deposit on the Bruch's membrane underneath the RPE layer causing and disruption of the RPE layer. Image obtained from http://www.brightfocus.org/macular [4]

Drusen are described as yellow-white deposits that are 30-300 μm in diameter, labelled as hard or soft dependent on the appearance of their borders.[7] There have been a number of descriptions of drusen formation. One being cross-linkage of proteins in the BM thought to be initiated by oxidative stress.[19] A strong emphasis has been put on the link between

smoking, drusen formation and ultimately the development of AMD. A strong prominence has been made on the fact that defence against anti-oxidative stress progressively reduces with age, eventually causing crosslinks to form between the protein hence preventing correct removal of deposits from the RPE.[19] Drusen are also thought to be from left over lipids which are hydrophobic debris due to incomplete breakdown and improper removal of RPE and photoreceptors,[23] with the RPE being described as containing all the necessary molecules to allow the formation of drusen.[7]

Another describes drusen as lipid-containing aggregates that deposit on the BM, whereas in other instances it is believed that drusen may be lipoproteins that act as a means of transport of lipophilic nutrients (carotenoids, vitamin E, cholesterol) to the photoreceptors by RPE, which contain receptors for high and low density lipoproteins (HDL and LDL). Once the nutrients have been stripped from the lipoproteins, it is secreted back into the BM, where it is thought to accumulate.[7] All drusen consist of lipoproteins (esterified cholesterol and unesterified cholesterol), phosphatidylcholine and other phospholipids (apolipoproteins, specifically apolipoprotein B, which is indicated to have been assembled by the RPE), and ceramides (fatty acids found in high concentrations of cell membranes).[7] The non-lipid components of drusen include amyloid vesicles (fibrous protein aggregates), and melanin/lipofuscin granules (pigment), which are indicators of cellular origin. Other components include crystallin (water-soluble protein), ubiquitin (regulatory protein), carbohydrates, and zinc.[7]

The lipoproteins have been described as arising from several sources including outer segments, remnant components from photoreceptor nutrients supply (cholesterol), and endogenous synthesis. Detections of lipids that are rich in esterified cholesterol, triglyceride and fatty acid have been investigated, and these lipids were not found below the age of 30 years, variably present between 30-60 years of age, and were found most abundantly in samples above the age of 61 years.[7]

1.4: Treatments Available

To date, there is no known cure for AMD. Various holistic treatments have been tested, such as treatment with antioxidants or treatment with vitamins.[8,24,25] The AREDS suggest that the only viable medical treatment to date for AMD is very high doses of vitamins and antioxidants, which slow the oxidation process.[24,25]

Many of these holistic treatments are based on the theory that the BM is no longer able to withstand oxidative stress. Therefore, much treatment has been based on diet and inclusion of antioxidants, in order to essentially reverse the effects of oxidative stress on the eye. However no tangible treatments are widely available to date.

1.4.1 Treating Wet AMD

Wet AMD is the least prevalent (10-15 % of total cases) type of AMD but is the most easily treatable.[19,26] Primary US Food and Drug Administration (FDA) approved treatments include photodynamic therapies, laser treatment and surgical procedures that showed modest improvement in vision.[27] Drugs called anti-vascular endothelial growth factor (anti-VEGF) have shown improvement in vision. These drugs are administered via injection through the sclera into the vitreous humour. They are successful in being able to prevent the growth of new vessels when the protein synthesis for the vessels is active; but if the stage of wet AMD is late and vessels are in the mature state, the drugs will be ineffective. Therefore although easily treatable, it is essential to detect the signs of wet AMD early enough to enable drugs to work efficiently.[27]

1.4.2 Treating Dry AMD

Dry AMD is the most prevalent form of AMD, with 90% of registered cases being of this form.[26] Despite being the most prevalent form of AMD, there is to date no known treatment. Many of the treatments suggested have been holistic forms, such as altering diet and lifestyle, in order to reduce possible risk factors of this disease.

1.4.2.1 The Holistic Approach

Various holistic treatments have been tested as aforementioned with antioxidants[24] or vitamins.[8] Antioxidants have been suggested as a treatment in patients that do not have the advanced stage of dry AMD, which has the potential of progressing into wet AMD.[25] The use of vitamins together with antioxidants and zinc are thought to help stop development of dry AMD and may even prevent progression into wet AMD.[25]

The holistic approach, albeit an extensively researched method, often give varied results that are very much dependent upon the stage of the disease. Sight restoration is never achieved, although some visual acuity improvement has been reported.[15] However it should also be noted that poor visual acuity is not a factor when considering the onset of AMD.[12,15]

1.4.2.2 The Clinical Approach

In conjunction with the suggested holistic approach for AMD treatment, there have been many potential clinical treatments. Drusen deposition, for example, could be prevented if the definite mechanism of their formation is understood. The following discusses the investigated routes for potential dry AMD treatment.

1.4.2.2.1 Improvement of Blood Circulation to the Membrane

One suggested treatment was to improve circulation of blood to the RPE since it was found that with age, the increased thickness of the BM means that blood contact with the RPE would decrease.[3]

This process alters blood flow characteristics by altering blood composition allowing perfusion into tissues and is termed rheopheresis.[28] Dry AMD in particular has been suggested to have links with disruption of microcirculation, which supplies blood, ultimately affecting oxygen and nutrient access to the BM and the removal of metabolic products and cellular waste. Reduction in blood circulation to the BM may induce the

deposition of drusen on the membrane.[28] Consequently treating dry AMD was investigated, which was understood to have the potential to progress to wet AMD, as a purely vascular disease. Oxidation products cross-link in the BM forming a barrier called advanced macular oxidation products (AMOPS). AMOPS thicken with age and prevent nutrients diffusing through the BM causing drusen deposition and then RPE deterioration. Improving blood flow to the BM may help remove AMOPS, leaving a clear route for nutrient passage and may prevent drusen deposition.[28]

1.4.2.2.2 Replacing the Host's RPE cells

One suggestion involves the replacement of damaged RPE cells on the patient's BM.

Investigations have been undertaken in order to see how cell transplantation may help retinal disease and various methods of RPE replacement have been undertaken. Some methods involve injecting the cells as a suspension into the back of the eye while the patient maintains a single position for a certain amount of time to allow the settling of the cells onto the retina. It has been suggested that a monolayer of RPE cells inserted into the eye may allow the cells to adhere to the retina better than compared to injection of a suspension of RPE cells.[29]

Wang *et al.* investigated inserting a monolayer of RPE cells obtained from male cats sandwiched between two layers of gelatine, into female cats.[30] It was found that following transplant of the monolayer, folding had occurred during the study. This was because the gelatine substrate had melted away due to the warm environment in the eye thereby allowing the cell monolayer to fold in on itself. Therefore gelatine was not considered a good carrier substrate for the monolayer of cells.[30]

Interest was then turned to RPE monolayer transplants without substrates.[31] The RPE cells were able to attach to the BM, junctions between cells were indicative of being tight and cells were able to survive for a week.[31] The lack of carrier substrate avoids the risk of

inflammation as would be the case with foreign implants. It also avoids the need for sterilisation of carriers and avoids the risk of cross-species infection, as would be a possibility when using animal derived substrates, like gelatine.[32] However, lack of carrier substrate made it difficult in handling the RPE monolayer, with the sheet sometimes not maintaining the desired position. The difficulty in handling the delicate sheet of RPE cells and the folding of the monolayer reinforces the need for a suitable carrier substrate.[32]

1.4.2.2.3 Reconstructing the Macula

The ability of transplanted RPE cells to survive in the aged macula also has implications as to the success of the procedure.[18] If RPE cells are no longer viable due to a poorly structured or defected BM, then transplantation of fresh cells on to this degenerated membrane may cause the new cells to also be non-viable. Therefore attention has been turned to reconstructing the BM in order to allow a new base for the RPE to be transplanted. This procedure is termed "maculoplasty".[8]

Tezel *et al.* investigated whether the native BM could be repopulated by measuring cell survival on various layers of the BM.[33] There were three layers to the BM: basal lamina (BL), inner collagenous layer (ICL) and elastin layer (EL) upon which cells were cultured. Cell count was found to be highest on the uppermost layer, the BL, and cell count decreased the lower the layers got. Cells on the BL were able to attach and reach confluence in 14 days, whereas the cells on the ICL and EL did not reach this stage and eventually died.[33] Del Priore *et al.* found RPE cell proliferation was significantly higher on the upper layers of the BM rather than on the deeper layers and cell apoptosis was found to increase as the deeper layer of BM were exposed.[9] The BM can hence be readily repopulated with RPE cells, but this depends on the ultrastructure that is presented to the cells.[33]

Efficient cell coverage is thought to be dependent on the age of the recipient membrane.[34] Investigations have been undertaken into whether the age of the recipient's BM affected

the ability of the RPE cells to attach and maintain viability on three surfaces; the basement membrane, the superficial ICL and the deep ICL, which were either 18 weeks gestation or 88 years old.[33,34] Cells were also cultured on bovine corneal endothelial extra-cellular matrix (BCE-ECM) coated dishes as a comparison. The BCE-ECM throughout the investigation showed good monolayer coverage by the RPE cells, which exhibited flat morphology, eventually reaching complete coverage by culture day fourteen. The aged (older than 30 years) BM basement membrane exhibited decreasing cell numbers with large defects in the cell monolayer on the basement membrane with culture time, with successive decrease in cell number the deeper the layers got. AMD suffering BM increasingly exhibited extreme defects in cell coverage and morphology throughout the culture time, therefore AMD suffering eyes are not ideal for cell adhesion.[34] Although, it must be noted that re-engineering the native BM by carefully washing out the age-related changes and recoating the surface with ECM improve cell survival.[8,9] However, more recently it has been reported that a cell carrier substrate, either degradable or non-degradable, would be advantageous, as it would protect the cells being implanted from the diseased BM and enable the transplantation of a complete monolayer of RPE cells.[35]

Therefore if the structure of the BM, a membrane of randomly orientated fibres,[8,9] could be mimicked in order to allow the growth of RPE cells then this could allow the replacement of the macula to be undertaken. A wide range of studies have been undertaken in order to realise the potential of polymers for use in regenerative medicine and tissue engineering. However, a wide range of factors must be identified if a viable material is able to be fabricated, such as biocompatibility, prevention of rejection and longevity of the transplant: for example degradability.[29]

1.5: Tissue Engineering

Tissue engineering was developed due to the demand for organ transplants far exceeding the available donors.[36] Although this particular field is relatively young, it has already made much progress including tissue replacements such as skin grafts. However, whole prosthetic organ transplants require much more research. Progress has already been made in heart valve replacements, but can be problematic due to the possible risk of infection and rejection. These factors, hypothetically, can be removed by essentially growing a new, non-faulty organ by using the host's cells (allograft) or donor cells (xenograft) and manipulating them in order to confer functionality similar to that of the native organ that it will replace.[36,37]

1.5.1 Polymers as Biomaterials

Biodegradable polymers have been researched extensively because degradable polymers that exhibit biocompatibility are ideal for use as biomaterials.[38,39] Biopolymers such as collagen and elastin have been used in medicine for tissue engineering constructs, such as resorbable vascular grafts.[40]

Functional groups determine the ability of polymers to biodegrade, can improve biocompatibility, and are responsible for their toxicity or the therapeutic effects exhibited by the polymers.[38]

Biodegradability is a very much desired trait as this allows the host's cells to eventually completely replace the synthetic material, because the scaffold degrades into non-toxic metabolites, which are easily excreted by the body.[38,39] For example, synthetic polymers such as polylactic acid or polyglycolic acid degrade to give the metabolites of lactic acid and glycolic acid. These by-products are synthesised in the body naturally, and are easily removed via natural mechanisms.[41]

Many studies have been pursued to determine the biocompatibility of polymers. Some polymers have gained FDA approval to be allowed to be used in drug delivery mechanisms.[42] Polyesters such as polyglycolic acid and polylactic acid are biodegradable and have been used in resorbable sutures, plates, and fixtures for fractures.[42] Other polymers available are the polylactones such as polycaprolactone, which is considered a non-toxic and tissue compatible material. Polypropylenefumerate is used as an injectable polymer for deep bone treatment. Polyanhydride has shown good use in drug delivery systems because of its surface erosion degradation process. A wide range of degradable and non-degradable polymers enable good mechanical properties and easier handling once inside the body and good in vivo viability. One such polymer is polyurethane (PU), which has demonstrated very good mechanical stability inside the body.[43,44] One problem with this particular polymer is that it exhibits hydrophobicity and therefore requires surface treatment to allow good cell adhesion.[42]

1.5.2 Fundamental Interactions

When considering the possible use of certain materials in humans, it is imperative that the interactive forces within the material are understood in order to explain how the chemical structure affects the overall and surface structure, and how this would affect the material's interactions with its surrounding environment. From this it can be possible to extrapolate a hypothesis as to the stability the material may convey when transplanted into the environment for which it is intended.

Other than understanding the reasons for stability, interactive forces can also be used to explain reasons for why certain materials are unfit for human use. It is important to understand the reason why a substance does not interact with another substance in the way that it was hypothetically supposed to. Functional groups or a certain orientation of functional groups may cause an unwanted response.[38] A material that is deemed to have biocompatible properties can also induce inflammatory response.[45] It has been found that

biological material found in blood serum can cause an inflammatory response; even by those materials originally thought to be non-thrombogenic.[45,46]

As soon as biomaterials are inserted subcutaneously, they are immediately covered by a bio-layer.[45] It is this layer that may or may not attract macrophages and other inflammation causing proteins. Therefore when considering blood-contact materials it must be taken into account that blood serum contains foreign object coating properties, which is essentially a safety mechanism that is triggered when an unknown material enters the body.[45] This is a form of non-specific interaction and must be considered when a new material is being fabricated.

1.5.2.1 Specific and Non-Specific Interaction

There are two categories of cell-biomaterial surface interaction: specific and non-specific.[47] Specific interactions are induced by surface adsorbed proteins, which contain specific ligands with specific functional groups that are complementary to surface cell proteins and allow positive interaction, rather like the lock and key theory as described for enzymes and substrates, between synthetic surfaces and cells.[47] Non-specific interactions, such as the negative charge of the cell membrane and lipophilic membrane proteins, are uncontrollable since these properties are general to all cells and lead to non-specific cell adhesion to materials.[47] For efficient biomimetic interaction to be successful a wide range of phenomena must be taken into account, these include: the chemical structure, hydrophilicity (or lack thereof) hence ionic groups, and morphology (for example whether the material is amorphous or crystalline). This is particularly important for a multi-component material and the topography (how rough the surface is).[47]

Particularly when considering materials for tissue engineering, the material must have the ability to allow cell adhesion. This can be achieved for materials that have been treated or on materials that may have the ability to allow cell growth without any intervention.[48] Cell interaction with the substrate surface is most important since it is from here the cell has the

ability to adhere to the surface, proliferate, spread and mature for the appropriate function (Figure 7). If good cell interaction can be maintained between the cell and substrate then a monolayer formation is more likely, which is a desirable trait in RPE tissue engineering.

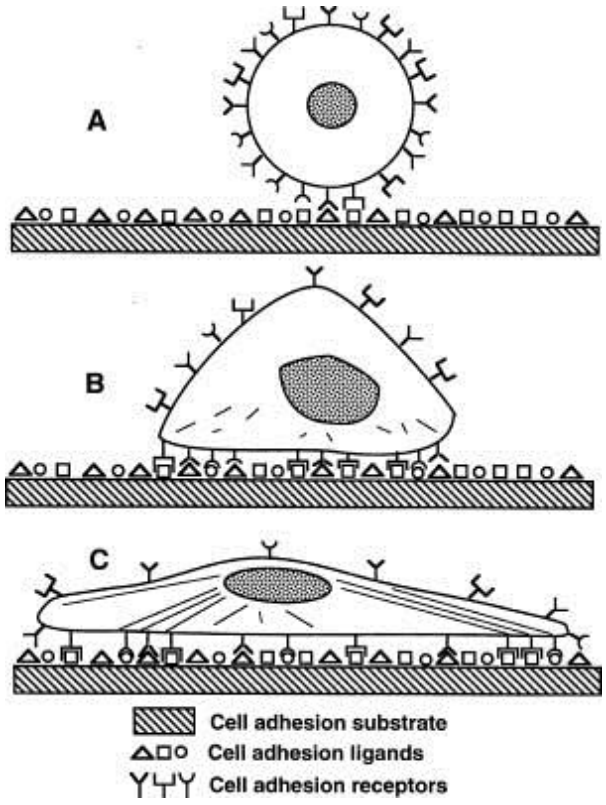

Figure 7: Image depicting the process behind what happens during cell-substrate adhesion. It can be seen that for good cell attachment, substrate surfaces contain cell adhesion ligands, which are complementary to cell adhesion receptors present on the cell membrane. These allow the cell to attach and spread across the substrate. Image obtained from Massia 1999.[48]

1.5.3 The Extracellular Matrix

The extracellular matrix (ECM) is the structure that surrounds and supports all cells in mammalian bodies. Its fibrous meshwork structure[49,50] is based on three macro-components: structural proteins such as collagen and laminin, specialised proteins, and

proteoglycans.[49] The ECM is also a biological process modulator for example in development regeneration, differentiation, and repair.[39] The ECM is a desired moiety for biomaterials and has been used in tissue engineering scaffolds since it naturally exhibits biocompatibility and promotes cell adhesion, proliferation, spreading, and ultimately new tissue formation.[49,51] However, due to its lack of structure and form, cell line derived ECM has been found to be difficult to utilise.[49] Therefore it would be desirable to be able to fabricate a scaffold that can mimic the aforementioned advantageous properties of the natural ECM, together with providing structure for cells to grow on.

The natural ECM also plays a role in the foreign body response, hence rejection.[38,51] The inserted implant undergoes collagenous encapsulation thus preventing any other interaction with other biological molecules, and is essentially isolated from other tissues.[38,39] Although there is no adverse harmful reaction when encapsulation occurs, this is counter-productive to tissue engineering since interactions with the body are hindered.[38] Therefore a scaffold which emulates some, rather than all characteristics of the ECM, for example promotion of cell adhesion and proliferation, rather than encapsulation and isolation, would be a more valued material.

1.5.4 Biocompatibility

In general biocompatibility is the capability of something to coexist with living tissues or organisms, without causing harm. The ambiguity of this term makes it very difficult to be able to define in a singular way. There are various definitions of this term including: the ability of the material to grow cells on its surface, being non-cytotoxic (ie cytocompatible), must not induce an inflammatory response, being non-thrombogenic when it is introduced into a blood-contact environment (does not cause blood clots or induce blood coagulation), must not destroy blood elements, must be resistant to infection, must not cause rejection, being hydrophilic, and being able to function with the host's biochemistry without any non-specific interaction.[37-39,51-53] Essentially, the scaffold must be able to function *in vivo*

as it was hypothetically intended to when it was being fabricated.[38,40,53] This is usually very hard to achieve.

Response towards and behaviour of a material is very much influenced by the functional groups in and on the surface of the polymer. Usually oxygen containing species, such as alcohols and carboxylic acids, will confer degradability well.[38] The rate with which deterioration occurs will depend on the environment in which it is placed, with a range of variables affecting the process; such as temperature, moisture, abrasion, and pH of the environment. These parameters together with susceptibility to chemical attack of the polymer will determine the degree with which the polymer breaks down. Polymers degrade through a variation of mechanistic routes; however the usual mechanism of degradation is by hydrolysis. This is normally because the polymerisation route is a condensation reaction between monomer units, thus hydrolysis is required to break these polymer bonds.

Functional groups that confer the intended desirable response can also be responsible for the unwanted toxicity and inflammatory response of implants.[38] Wettability and inflammatory response of degradable poly-L-lactic acid (PLLA) and non-degradable polytetrafluoroethylene (PTFE) as porous and non-porous subcutaneous implants have been investigated.[52] PLLA was found to be more wettable and invoked a higher inflammatory response compared to PTFE. Higher wettability and degradability exhibited a higher inflammatory response since these characteristics provoke an enhanced biological interaction with the surface of the polymer.[52] The porosity and morphology of the surface can also cause an inflammatory response, but there must be a high enough degree of hydrophilicity for this to occur.[39,52]

1.5.5 Functionalising Scaffold Surfaces

A range of studies have looked at how to induce or improve the biocompatibility of materials using various methodologies. This is usually done by physical means: alteration

of the morphology or topography of the scaffold surface, or by chemical means: hydrolysing the surface of the scaffold or attachment of chemicals or macromolecules to the surface. Physical modification of the surfaces: as exemplified by putting grooves in the surface of scaffolds as opposed to just pores, and chemical modification: as exemplified by surface hydrolysis with sodium hydroxide (NaOH) have been explored. Treatment with NaOH makes the surface rough due to polymer scaffold surface degradation and also can expose advantageous carboxylate and hydroxyl functional groups by chemically reacting with the surfaces of the polymer, thereby improving cell adhesion.[47]

Immobilising biological compounds onto the surface of materials have been found to improve hydrophilicity and cell adherence.[47] There are a variety of methods by which this can be done, one being photoinduced grafting of monomers such as vinyl acetate, acrylamide or acrylic acid. Another is surface plasma treatment, whereby moieties are used as plasma to treat the surface. Poly-lactic-glycolic-acid (PLGA) treatment with O_2 improves cell adherence greatly, whereas PLLA treated with ammonia (NH_3) improves cell interaction on the surface. Biomacromolecular modification of the surface is another technique for improving cell attachment. It is essentially a form of chemical grafting of proteins or peptides to the polymer surface and it can also be termed covalent grafting.[47,54] PLGA-chitosan or PLA-heparin modified surfaces tested by culturing osteoblasts on them implied that adherence of polyester surfaces could be improved using this technique.[47]

Protein adsorption can also help to improve cell adhesion. However it depends on a range of factors including charge of the protein, effect of diffusion, size of the protein, and the concentration of the protein. The charge of the protein affects a list of interactions including electrostatic forces, hydrogen bonding, hydrophobic interaction, and charge transfer interactions/pi orbital electron delocalisation. The overall charge of the proteins exhibited is dependent on the pH of the protein environment. At very high pH

environments the charge on the protein will be positive and at low pH environments the charge will be negative.[55]

The higher concentration of protein will mean that it is able to come in contact with the surface of the substrate more often, so it will have a higher chance of adsorbing to the substrate surface. However it should be able to travel fast enough through the medium to be able to reach the substrate surface, which is normally achieved when the size of the protein is much smaller. Smaller proteins are then eventually replaced by slower moving, larger proteins that are able to make more contact with the surface of the substrate.[55]

Therefore, protein adsorption involves the competitive replacement of proteins that have higher mobility, and so arrive first to the substrate surface in a certain environment, with proteins that have a higher affinity for that particular surface. This is called the Vroman effect.[56,57] It can result in an undesired layer forming on the surface of functionalised biomaterials, however it is described as being a natural result of protein reorganisation.[56]

There are two general interpretations for the protein exchange process that exist. The first involves the desorption of one protein that leaves a space for a second protein to adsorb.[57] The second involves the formation of a layer of one lot of proteins, followed by a second lot of proteins arriving later at the surface forming a complex with the first layer of proteins. This complex turns exposing the first protein layer away from the surface of the substrate, displacing it by the second protein because the second protein has a higher affinity for the surface.[57]

It must be noted that with protein adsorption, the proteins can undergo conformational changes that can affect the way they interact with ligands/antigens. The secondary/tertiary/quaternary structures can change, which can result in change of the orientation/shape of the binding site. These can result in denaturation of the protein so it does not function in the way it was initially intended.[55] Therefore if protein adsorption is

being used to improve cell-substrate interaction, protein conformational changes that may occur following protein adsorption can affect the function of the substrate, and must be taken into account.

Another issue with whole protein attachment is that even though it would first appear to give specific interactions, they in reality have the potential for non-specific interactions too, since proteins contain many different binding sites or motifs.[54] Therefore a method of avoiding this and promoting specific interaction would be to utilise peptides, which provide singular binding motifs and would hence be specific for certain cell adhesion molecules.[54]

Alongside the above discussed variables, substrate surface topography can affect protein adsorption, similar to cell-substrate interaction being enhanced by surface roughness. Not only surface topography, but the overall structure of the substrate can play a key role in protein adsorption, and more emphasis is put on being able to fabricate substrates that closely resemble those found in nature,[55] therefore ECM mimicry is important when considering biomaterials. One aspect of the ECM that can be imitated is the air-water interface.[47] Electrostatic assembly is one such surface modification technique that makes deposits on the surface of the material, and is termed surface mineralisation. This method is exemplified by the deposition of bone like minerals on the surface of either PLLA or PLGA.[47] Another method is the Langmuir-Blodgett technique that fabricates a block copolymer that is ampiphilic in the form AB, where A is water soluble and B is hydrophobic.[47]

The ECM is not only known to allow efficient cell adhesion, but is also important for molecular dynamics across the BM.[39] Surface modification should be such that normal molecular movement is maintained. It is therefore important to understand the natural movement of macromolecules across a healthy membrane. Particularly in regards to biomaterials for the potential treatment for AMD, it is important to understand the

movement of molecules across BM and how the dynamics are affected by the onset and progress of AMD.

1.6: Dynamic Molecular Movement in the RPE

All biological systems undergo constant dynamic molecular movement for the introduction of required nutrients such as sugars, fatty acids and proteins, and for the removal of metabolites, oxidised moieties and other debris between blood vessels and cells. These species have particular characteristics, which allow their movement through blood vessel membrane epithelium.[58] Together with this, the blood vessel membrane also contains certain traits that enable entry for the aforementioned molecules. One of these traits is fenestrated membrane endothelium, which allow fluid movement out of the vessel and into the surrounding tissue; this movement is dependent on blood pressure.[58]

There are a number of transport mechanisms used by nature to allow the migration of required nutrients or fluids into the needed tissue. Much of this transport is dependent upon the intricate structure of the cell membrane. The simplest is diffusion, such as osmosis: the movement of water along a diffusion gradient, which occurs across the phospholipid bilayer of the cell surface membrane, without the need for carrier or channel proteins. No energy is needed for diffusion and the movement of water soluble molecules can occur. The next is facilitated diffusion, which is still a form of passive transport that also works along a diffusion gradient, but utilises protein carriers/channels that allows the movement of molecules, which cannot do so otherwise through the membrane. The reasons for not being able to diffuse without the use of proteins may be because of the inability of the molecules to pass through the lipid layer of the cell membrane freely due to charge, and they are unable to dissolve into the fatty acid "tails" layer of the membrane so cannot pass by simple diffusion.[58]

The other form is active transport, which uses ATP to move substances against a diffusion gradient utilising proteins for this specific process. There are two types of active transport;

the primary that carries a single type of moiety, and secondary, which moves a single moiety creating a concentration gradient, triggering the movement of another substance.[58]

Hussain *et al.* looked at the decline of molecular movement across the BM with age, and successfully found a linear regression in the ability of sugars to move across the BM with age.[59] The overall transport mechanism alters if the BM thickens and the movement of the metal ions, sugars, and lipids are altered, since the proteins that carry them across the BM cannot function correctly.[59] These changes are a normal progression with age, however these findings have also led to the belief that this can cause fluid to build up beneath the RPE, which can lead to RPE detachment.[60]

Olaf Strauss investigated the movement of macromolecules and the various transport cycles in the human RPE (Table 1).[23] A variety of different moieties travel across the RPE membrane, and the movement of these entities are vital for normal function of the RPE. Ions of salts exhibit transepithelial movement via proteins, and their movement is usually dependent upon a diffusion gradient formed by other electrolytes in the blood or subretinal space.

Table 1: Table shows the macromolecule, mode of transport and bulk movement across the RPE. All the macromolecules are regulated by movement of other macromolecules and are important for normal function of the retina. Information obtained from Strauss 2005.[23]

Macromolecule	Mode of transport	Regulated by	Type of moeity	Movement from & to	Notes
Water	Muller cells	Intraocular pressure due to Cl^- and K^+ ions (diffusion gradient produced)	Metabolic product	Subretinal space to blood	Movement of water important for close structural interaction of retina to allow good adhesion between the RPE and retina
Glucose	Glucose transporters located throughout the RPE	Glucose transporters: GLUT1 and GLUT3 highly expressed throughout the RPE to promote efficeint glucose transport	Sugar (nutrient)	blood to photoreceptors	GLUT3 mediates basic glucose movemet into the RPE. GLUT1 induces (actively transports) glucose movement into the RPE.
Retinol/Retinal	Transported as all-trans-retinol (vitamin A) and binds to specific proteins which isomerised to 11-cis retinal	Binding of retinal to specific regulating proteins	nutrient	blood to photoreceptors	Important to regulate movement to allow constant bulk transport of retinal to the photoreceptors for the visual cycle
Dicosohexaenoic acid		Movement along a concentration gradient	nutrient: fatty acid	blood to photoreceptors	This fatty acid is stored in the RPE membrane by incorportation into glycerolipids
Na^+	proteins, transepithelially	ATPase	Electrolyte	Subretinal space to blood & Blood to subretinal space	Movement of this ion dependant upon a concentration gradient produced by K^+ ions
K^+	proteins, transepithelially	ATPase	Electrolyte	Subretinal space to blood & Blood to subretinal space	A concentration gradient is produced by continuous movement throught membrane. Promotes movement of Na^+ and Cl^-
Cl^-	Via Cl^- channel proteins	ATP (active transport)	Electrolyte	Subretinal space to blood	Movement of Cl^- is dependant on Na^+ ion movement. Needs a diffusion gradient to allow efficient transport
Pigment epithelium derived factor	secretion	via activation of transepithelial channels by Ca^{2+} ions	growth factor	From the RPE to the subretinal space	Secreted by the apical (closer to the subretinal space) side of the RPE
Vascular epithelium derived growth factor	secretion	via activation of transepithelial channels by Ca^{2+} ions	growth factor	From the RPE to the extracellular matrix	Is secreted from the basal (closer to the blood vessels) membrane of the RPE and aids stabilisation of choriocapillaries and helps to maintain the fenestrations.

Nutrients required for growth and repair such as glucose and fatty acids are transported via either carrier or channel proteins from the choriocapillaries towards the photoreceptors. Vitamin A (retinol) undergoes structural change upon binding to specific proteins in the basolateral membrane and is converted to retinal. Glucose, fatty acids, and retinal are

important for the visual cycle and are transported in bulk towards the photoreceptors. Growth factors for the photoreceptors are termed pigment epithelium derived factor (PEDF) and are secreted from the RPE's apical side towards the subretinal space. Growth factors for blood vessels are termed vascular endothelium growth factor (VEGF) and are secreted from the RPE's basolateral side towards the ECM.[23] Water is a metabolic product due to breakdown of nutrients and other processes that produce water as a by-product of reaction. This water is removed by Müller cells, which are placed across the RPE monolayer, from the subretinal space to blood. Water movement is regulated by intraocular pressure and a concentration gradient created by salt ion diffusion to promote osmosis.[23]

Channel proteins are essentially what make membranes porous and have specific diameters, known as the size exclusion limit, that allow molecules to travel. Therefore a prerequisite must be that these molecules must have a diameter equal to or lower than the specific size exclusion limit exhibited by the membrane, and hence will not allow molecules larger than the diameter of the pore size to pass through. The size exclusion limit exhibited specifically by the retina is called the retinal exclusion limit (REL).[61]

1.6.1 Retinal Exclusion Limit

The retinal exclusion limit (REL) determines the maximum value for the size of the molecule that will easily transport across a membrane. Jackson *et al.* determined the REL for human retina and compared the value found to other animals. It has been found that the REL for humans is 77 kDa, from analysis of fixed retina.[61] This value has been given as a relative as opposed to absolute value since experiments were carried out on fixed human samples as opposed to being able to obtain fresh animal samples, due to setbacks in obtaining fresh retina from humans.[61] However measurements in animal samples for fresh retina showed similar values, suggesting that animal studies can be a reliable source for analysis.[61]

Moore *et al.* investigated how age affects the movement of macromolecules through the BM, by measuring the permeability of the BM to serum proteins.[62] A general finding was that the permeability of the BM to serum proteins decreased throughout life, decreasing by a factor of 10 between the first two decades of life and the ninth decade of life. However, it should be noted that recording results for the changes occurring in the membrane between these extreme age ranges was difficult due to lack of donors. It was found that younger BMs allowed bigger proteins (200 kDa) to travel across and had a lower exclusion limit, therefore allowed more proteins to pass through the young BM. Whereas the older BMs allowed smaller sized proteins across (100 kDa) while preventing the bigger proteins from passing through, exhibiting a higher exclusion limit, therefore allowing fewer proteins through the older BM.[62]

1.6.2 Biomaterial Pore Size & Leukocyte Migration

Scaffolds for tissue engineering must have appropriately sized pores which allow the needed macromolecules to pass freely, but prevent unwanted species. Another important consideration for tissue engineering scaffold porosity is cell penetration, which is often a desirable trait for tissue engineering scaffolds, in which cells must populate the scaffold to make a three-dimensional tissue. However a BM replacement substrate that supports the RPE must not allow cell invasion. Porosity in this substrate, therefore, must only allow macromolecule penetration and prevent unwanted species, such as immune cells or vascular endothelial cells (VEC) from passing.

White blood cell (WBC) migration is another issue to be thought about when fabricating biomaterials. WBCs have long been known to have the ability to move through pores towards tissues which exhibit inflammation or sites where foreign cells/biological debris remain. They are a defence mechanism to protect the body from harm.

Hence even though materials implanted into the body may be intended for healing purposes, the body may recognise them as a foreign object and attack it in the similar way

to a bacterium protein. Inflammatory response and severe rejection can be reduced by the use of functional groups, which are specific to certain cell binding sites.[38]

Leukocytes are able to move through fenestrations and pores. WBC migration through fabricated membranes has been investigated. Synthetic fabricated membranes of varying materials: collagen, polycarbonate, polyester, poly(ethylene terephthalate) (PET), and Transparent Biopore® of varying pore size, either treated or untreated with fibronectin before culturing an endothelial monolayer have been investigated to specify the limit of the pore size through which leukocytes are able to migrate. The surface charge of the membranes was not mentioned. It has been found that pore sizes through which leukocytes are able to migrate ranged from 0.4 μm to 3 μm.[63-65]

1.7: Methods for Film/Mat Fabrication

1.7.1 Solvent Casting

Solvent casting is the simplest method of obtaining films of polymer substrates and is dependent upon the degree of solubility of the polymer in various solvents. Thorough mixing of the polymer solution is imperative to allow uniform distribution of the polymer through the solvent, usual practice is to allow overnight mixing to ensure this.[66]

1.7.1.1 Why Use Solvent Casting?

This method is easy, cheap and allows films of polymers to be fabricated relatively quickly. Films made by solvent casting are described as being free from pinholes, which have good optical properties and clarity, exhibit uniform strength and have low strains.[66] However a disadvantage of this method is the fact that the films produced are relatively thick (approximately 50 µm to 100 µm) when looked at on a molecular scale and are not porous, therefore is not suitable as a BM mimic.

1.7.2 Electrospinning

This procedure has very strong links with electrospraying, which was first described over 100 years ago, has taken a surge in interest in recent times.[67] Conventional extrusion techniques yield fibres that have relatively large diameters (within the range of 10 – 100 µm). Electrospinning allows for the diameter of the obtained fibres to be reduced significantly down to the scale of a few hundred nanometers, provides large surface area, allows for efficient surface functionalisation, and bestows high mechanical stability.[67,68] These are highly desirable traits for fibres that are to be used in the field of tissue engineering and regenerative medicine.

Electrospinning works by the extrusion of a semi-liquid jet of a polymer solution from a syringe needle onto a grounded collection plate via an electrostatic gradient (Figure 8). As the polymer solution moves through the air it solidifies as the solvent evaporates, forming

a filament.[67-69] For a jet to form the diameter of the jet must be above a critical value.[67,69] If the jet diameter drops below the critical value then surface tension forces become strong enough to overcome the jet and revert back to droplets returning to an electrospray.[67] The distance between the jet and electroplate must be so that a continual jet is extruded and to prevent jet instability.[67,69,70] Electrospinning results in obtaining a mat comprised of randomly placed fibres (Figure 9).

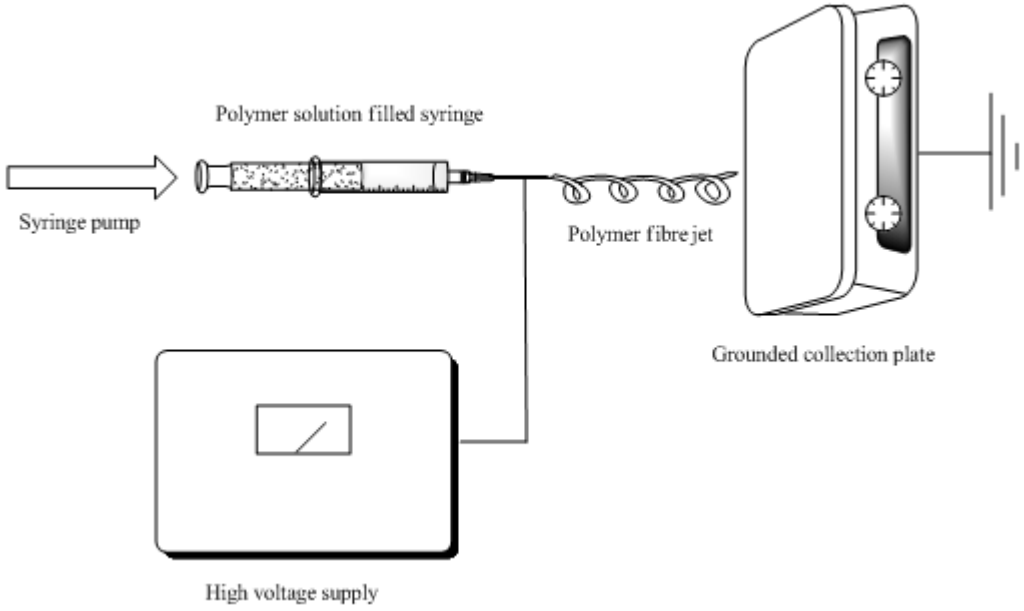

Figure 8: Schematic of the electrospinning apparatus, as it was set up during fabrication of the fibrous polymer mats (polymer jet and distance of syringe from the collection plate is not to scale). Schematic was drawn using ChemDraw11 (CambridgeSoft Corporation).

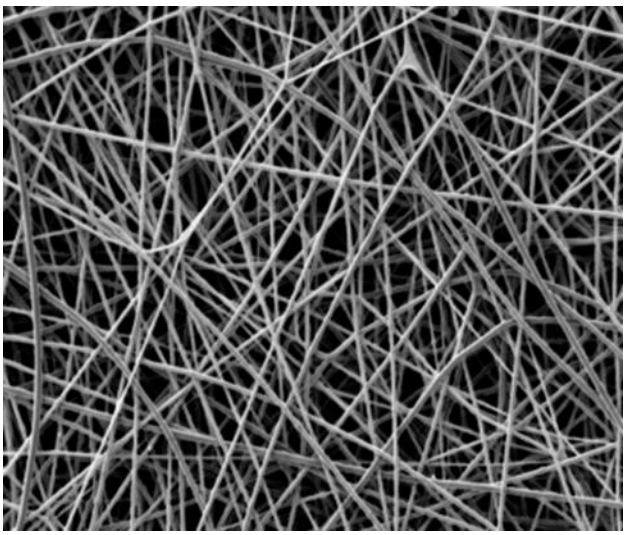

Figure 9: Scanning electron microscope (SEM) image of randomly orientated poly(ethylene terephthalate) (PET) fibres fabricated by electrospinning, with 1,1,1,-3,3,3-hexafluoroisopropanol (HFIP) as solvent.

1.7.2.1 Characterising Electrospun Substrates

Mechanical testing of electrospun materials is carried out with a few factors taken in to account when analysing the results. When tensile strength is measured, especially in mats that contain fibres that are randomly orientated, the fibres will not break uniformly, but anywhere in the structure of the mat depending on its orientation and position. Therefore a wide variation in tensile properties can be recorded.[71-73]

Water contact angle (WCA) gives a depiction of the wettability of a surface, and entails placing a drop of water on the surface of a substrate. WCA of fibrous mats are dependent on the morphology of the fibres. It has been found that not only the diameter of the fibres, but the topography of the fibres also can affect the way the drop of water sits on the surface of the fibrous mats. Bigger fibres have been reported to give significantly lower WCA measurement, smooth fibres gave lower WCA measurements, and with increased surface roughness the WCA increased.[74] This was attributed to more air being trapped in the voids of the smaller and rougher fibres compared to the bigger smoother fibres.[74] Therefore

topography of the substrates must be taken into account, and care must be taken when measuring the planar surface of a polymer as comparison of what the WCA should be like for an electrospun surface since the topography of the two surfaces are completely different and would not be a fair comparison.

Also surface chemistry post surface treatment/grafting are reported to have a big influence on the WCA, since electrospun PET which initially gave high WCA, has been reported to give zero WCA post grafting with gelatin as the water drop was sucked into the fibrous mat too quickly for measurement.[74] Not only surface treatment but the orientation of the functional groups on the unaltered surface of the material also influences the WCA measurement since, obviously, if hydrophilic components on the bulk material are exposed, then lower WCA will be measured due to favourable hydrogen bonding interactions occurring between the drop of water and the hydrophilic functional groups, as opposed to when hydrophobic functional groups are exposed.[74]

Setting aside the surface chemistry and physical properties of the surface substrate, the WCA has also been reported to be dependent on the size of the water drop being used.[75,76] Since other forces may begin to take toll, such as hydrogen bonding within the drop of water, interaction between air-water interface and water-solid interface, which would all give varying WCA measurements.[74-76] Therefore, not only do both surface chemistry and physical characteristics such as topography and surface charge play an influential role in WCA, but also the size of the water droplet being measured, hence it is important that these factors be measured and reported in order to make a complete comparison between data.

1.7.2.2 Why Use Electrospinning?

One of the advantages of electrospinning is that the submicron dimensions of the fibres yielded resemble that of the natural ECM,[49,50,67,68,77,78] therefore there is great interest in electrospinning for tissue engineering. The growth of cells can be enhanced by exploiting

the dimensions of the fibres, which are of nanoscale, therefore provide a large surface area for cell adhesion. Also the voids left between the randomly placed fibres give the mats an enhanced porous structure.[67,68]

Electrospinning has cell culturing implications as exemplified by poly-L-lactic acid (PLLA) electrospun using dichloromethane (DCM)/dioxane mixture as a solvent. Osteoblasts were cultured on these mats and the researchers found higher cell growth on the electrospun material compared to denser material.[79] Advantageously, having a scaffold of a fibrous structure allows cells to give more *in vivo* like morphologies than compared to when cultured on planar surfaces.[50,78,80,81]

In addition, electrospun fibres are recognised as having potential in wound dressing and healing applications such as antibacterial dressing.[82] Electrospun synthetic polymer mats such as polyurethane (PU) and poly-lactic acid-glycolic acid (PLAGA), and natural electrospun mats, such as collagen, are used commonly as wound dressings because they enable good cell support, have good anti-adhesion effects, and prevent infection, loss of fluid and proteins in healing wounds.[77,83-85] PU particularly has shown good cell alignment in epithelialisation in rat dermis, and provided good support for wound healing.[83] Polytetrafluoroethylene (PTFE) electrospun mats have been suggested for use in vascular grafts, because of tensile strength and small diameter, but lack functionality, since there is no muscular interaction. It is currently being investigated, in order to confer possible functionality into the grafts by not only culturing the epithelial cells, but also smooth muscle cells.[77] Other electrospun polymers currently being investigated for tendons/nerve grafts are PLAGA, polycaprolactone (PCL) and PLLA.

Electrospinning utilises a lot of fluorinated solvents for efficient fibre formation, so replacing organic solvents with aqueous solvents has been suggested.[77] This can be problematic since aqueous solvents mainly include acids and alcohols; which means the polymers must have good miscibility with water. This can be challenging when fabricating

potential biomaterials, since high water solubility will mean the scaffold will not remain structured for long enough once put in the body, to allow sufficient cell ingrowth or tissue reconstitution.[77] An example of the use of aqueous solvents for use in electrospinning was shown by Han *et al.* who used a solvent mix of acetic acid/water to form cellulose acetate nanofibres (CA). As acetic acid composition was increased, the nanofibre diameter also increased. Deacetylation was done successfully while maintaining the nanofibre morphology. However it must also be taken into account that they are investigating a biopolymer: cellulose, which has good water miscibility, and degrades well with time.[86]

Bognitzki *et al.* found that different combinations of polymer and solvents give different fibre morphologies.[87] PLLA, polyvinylcarbazole (PVC), and polycarbonate (PC) were electrospun using DCM with constant spinning parameters, all resulted in fibres within 100 nm diameter.[87] Differences were more noted in fibre surface topography; PLLA presented pores in the 100 nm range, PC exhibited pores in the 200 nm range, whereas PVC gave regular pits rather than pores. Structure formation is controlled by phase separation when solvent evaporation occurs as the jet is expelled during the electrospinning process, therefore it is important that the appropriate solvent is utilised in order to underpin the correct morphology/topography for potential scaffolds.[87]

Following findings that electrospun fibres' morphology can be changed, investigations have been carried out in order to evaluate the effects that changes in the polymer solution can have on fibre morphology. The following discusses such investigations.

1.8: Variables to Consider in Electrospinning

A large variety of parameters that can affect electrospinning have been explored (Table 2) such as solvents, spinning (working) distance, and needle diameter.[69] There are a plethora of variables to take into account when carrying out electrospinning. The main variables considered are: polymer solubility, solvent polarity, concentration of polymer solution, solvent characteristics and spinning parameters.

Table 2: The table is showing results from previous papers that have also explored various electrospinning parameters with a range of different polymers.[43,82,87-99]

Polymer	Solvent	Electrospun?	Has this polymer undergone surface treatment for cell attachment?	Used in body?	Application	Notes	Reference
Polystyrene	DMF, THF, DMF/THF	yes	n/a	yes - surgical sutures	solvent conductivity effect, effect of solvent on morphology	Fibres formed with increased solution concentration	T Uyar et al 2008, J Zheng at al 2006
Polyurethane	DMF, THF, DMF/THF, Chloroform	yes	NaCl added in polymer solution pre-spinning (Barakat et al 2009), plasma treatment with hexyfluoropropylene (neutral surface), N,N-dimethylaminoethyl methacrylate (positive surface) and methacrylic acid (negative surface) post spinning (JE Sanders et al 2004). Ketoprofen entrapped on surface pre-spinning (Kenawy et al 2009)	Yes - cervical disc space replacement (Patented)	Nanotechnology (Barakat et al 2009), Effect of surface charge on tissue response (JE Sanders et al 2004), Wound dressing (Khil et al 2003). To test the shape memory effect of electrospun PU (Zhuo et al 2007). Drug delivery systems (Kenawy et al 2009)	THF used to dissolve PU DMF added to obtain electrospinnable solution (Barakat et al 2009). Found no significant difference in surface charge and cell nuclei density (JE Sanders et al 2004). Very good epithelial cell regrowth exhibited, fluid not retained, allows good oxygen diffusion (Khil et al 2003). Used a PCL based shape-memoryPU (Zhuo et al 2007). Higher drug release versus solvent cast films, better visual mechanical property when blended (Kenawy et al 2008).	Barakat et al 2009, JE Sanders et al 2005, Khil et al 2003, Zhuo et al 2007, Kenawy et al 2009
Polyethylene terephthalate	trifluroacetic acid (TFA) (Z Ma et al 2005)	yes	yes - gelatine grafting (Z Ma et al 2005), covalently attaching RGD (Chollet et al 2009)	yes	vascular graft (Z Ma et al 2005). Intraocular lens fixation support (Patented) (Peyman et al 1978). To improve cellular adhesion and proliferation (Chollet et al 2009)	Good cell adhesion and cell phenotype preservation exhibited (Z Ma et al 2005). Remains in eye as a permanent fixture on which iris cells grow and adhere (Peyman et al 1978). Good cell adhesion shown by treated PET, none treated PET showed that cells became detached after initial adhesion (Chollet et al 2009)	Z Ma et al 2005, Peyman et al 1978, Chollet et al 2009
polypyrrole/polyetheylene oxide	deionized water/DMF	yes	n/a	n/a	conductive polymer fibres	Morphology of the fibres was dependant upon PEO content	Charonakis et al 2006
Nylon6	acetic acid/formic acid	yes	NaCl added in polymer solution pre-spinning (Barakat et al 2009)	---	nanotechnology (Barakat et al 2009)	Improved surface wettability and mechanistic characteristics, amphiphilic mat obtained	Barakat et al 2009
Polymethylmethacrylate	acetone	yes	n/a	n/a	---	Increase in PMMA concentration yields better fibres	S. Piperno et al 2006
polyvinylpyrrolidone-iodine	water/EtOH	yes	photo-mediated cross-linking post spinning	wound dressing	anti-microbial dressing	Strong bacteriocidal properties against Staphyloccocus aureus and exhibit stability against aqueous media	M Ignatova et al 2007
PEO/PVP-Iodine							
Poly3-hexyl thiophene/PCBM	choloroform / toluene	yes	n/a	n/a	solar cloth, photovoltaic cloth	PCBM is phenyl-C61-butyric acid methyl ester	S. Sundarajjan et al 2010
polyethersulfone	DMF	yes	plasma treatment with NHS/EDC then collagen grafted post spinning	working towards	improving unrestricted somatic stem cell adhesion	Ideal for 3D tissue eng grafts, collagen greatly enhanced cell adhesion	Shabani et al 2009
polyvinylcarbazole	DCM	yes	n/a	---	biofunctional nanotubes	regular pitting exhibited	Bognitzki et al 2001
polycarbonate						regular pores exhibited	
polydimethylsiloxane		yes - as block tricolpolymer		yes	blood contact medical materials - such as artificial hearts	requires surface enhancement to improve mechanical strength	RW Hergenrother 1994

1.8.1 Degree of Polymer Solubility

Polymer solubility is the most obvious of all the variables to consider. The polymer must be able to disperse in the solvent enough to allow a homogeneous solution to be produced.

This usually occurs when the solvent and polymer have compatible characteristics; for example exploiting the fact that polar functional groups exist in the polymer and in the solvent, which can hence interact with each other, or accounting for dispersion forces. A good polymer solution would be one that, when seen on a molecular level, has molecules of the solvent completely surrounding the polymer molecules. Dipoles within the polymer and the solvent allow for good interaction between the two, hence allowing good solvation of polymer molecules forming a true solvent, this will form a homogeneous mixture that will be optimal for spinning.

Luo *et al.* investigated the solubility of polymethylsilsesquioxane (PMSQ) in various solvents in order to determine the optimal solvent for electrospinning.[100] Pure solvents and solvent mixtures were used and the degree of polymer solubility was monitored, and how well the solutions electrospun was also determined. Fibre morphology was greatly affected by solubility: with partial solubility leading to spinning, and high solubility leading to spraying.[100] Another example investigated by Lee *et al.* is PCL electrospun in; methylene chloride (MC) and then MC/dimethyl formamide (DMF) in various ratios 100/0, 85/15, 75/15 and 40/60, and MC/Toluene 40/60 and 85/15.[101] It was found that PCL dissolved in neat MC, a good solvent for PCL, giving fibres of 5.5 μm in diameter. The addition of DMF, a poor solvent for PCL, decreased the fibre diameter by 200 nm and electrospinning also became easier, whereas addition of toluene, a non-solvent for PCL, prevented electrospinning due to high viscosity and poor conductivity.[101]

This suggests partial solubility may be advantageous over high solubility. The addition of a nonsolvent can aid electrospinning, however the polymer solution viscosity must be such that it is able to be manipulated by an applied potential difference.

1.8.2 Solvent Polarity

Solvent polarity allows polymer solutions to hold together strongly enough to form a continuous jet of polymer solution when spinning. Surface tension must not be so weak as

to cause a break in the continuous flow of the polymer jet. Solvent polarity can be imparted from the solvent or polymer, and can affect the surface charge density. Since the electric potential applied exploits the fact that the polymer solution contains a charge density, it hence determines how well the fibres will form.[69]

1.8.3 Concentration of Polymer Solution and Solvent Characteristics

Consideration of how the concentration of the polymer solution affects the resulting fibres once spun have been made. Son *et al.* investigated various solvents and the effect of concentration of each solvent on fibre diameter and morphology.[70] It was found that generally the higher the percentage weight concentration of the polymer solution the thinner the fibres. The higher the dielectric constant of the solvent, the thinner the fibres formed. They also found that voltage applied, the tip-to-collector distance, and solution flow rate did not vary the fibre diameter for all types of solvents investigated. The addition of polyelectrolytes was investigated to determine their effects on fibre morphology; it was found that the addition of more electrolytes conferred more charge density on to the surface of the polymer solutions, and allowed for thinner fibre formation. It also showed the optimal electrospinning concentration of the polymer to be lowered, therefore the polymer solution did not have to be as concentrated in order to form fibres.[70]

Concentration of the polymer solution affects the morphology of the fibres, as exemplified by polymethylmethacrylate (PMMA):acetone solution.[97] Increasing PMMA:acetone concentrations increased homogeneity in fibre formation, whereas lower concentrations exhibited bead formation. Conversely to Son *et al.*'s findings, it must be noted that fibre diameter increased with polymer concentration.[70]

1.8.4 Polymer Molecular Weight

Molecular weight of polymers being electrospun would have an effect on fabricated fibres, since the molecular weight would essentially determine the solution viscosity,[102] and has been investigated. Koski *et al.* found that for polyvinylalcohol (PVA), fibre diameter

increased with molecular weight, and that at low molecular weight the fibres exhibited a circular cross section, whereas at high molecular weight flat fibres were observed.[103]

1.8.5 Salt Addition

Another variable that can be used is salt[81,90] or polyelectrolytes[70] addition, which has been found to decrease the diameter of the nanofibres.[81] Barakat *et al.* investigated the formation of fibres exhibited when Nylon 6 (N6) was dissolved in an acetic acid/formic acid mixture, polyvinyl alcohol (PVA) was dissolved in water only, and PU was dissolved in tetrahydrofuran (THF) with gradual addition of DMF to adjust viscosity and obtain an electrospinnable solution.[90] Complete salt dissolution required long stirring times otherwise the salt crystals were visible in the nanofibres. To test this stirring at 0.5/3/24 hrs were carried out. Only the 24 hr stirred solutions exhibited no salt crystals on the fibres. Mechanical properties of the fibres were also altered upon addition of the salt, N6 exhibited higher tensile strength with addition of salt. It has also been found that hydrophilicity of surface increased and better control over fibre formation in electrospinning is exhibited with salt addition.[70,81,90]

In summary, fibre morphology is known to be affected by the concentration of the polymer solution, with a minimum optimal concentration allowing the formation of fibres as opposed to beads, or beads with tails, or beads on a string. In addition, the solvent used is also important. A broad range of polymers and solvent combinations have been used in electrospinning, not necessarily for the purposes of biomedical materials, however they have highlighted how electrospinning can help improve fabrication of materials for application in tissue engineering.

1.8.6 Spinning Parameters & Environmental Factors

Spinning parameters include all the variables that can be applied to the electrospinning apparatus, these include: the voltage applied, the tip-to-collector distance, which has been found to affect volume charge density exponentially, solution flow rate (governing how

much of the solution is available at the tip of the needle), and whether electrospinning is carried out in a controlled environment or laboratory conditions. Son *et al.* found that these parameters had no particular effect on the fibre diameter.[70] Conversely, Theron *et al.* found that the flow rate decreased the surface charge density of the polymer solution, which was attributed to low residence time at the tip of the needle where the electrode is present; the drop does not remain at the tip of the needle long enough for the voltage applied to take effect. It was also found that as the tip to collector plate distance increased, the surface charge density decreased and is caused by the weakening of the electric field strength due to increased distance between electrode and grounded collector plate.[69] Chen *et al.* found that if the applied voltage was decreased during electrospinning, the effect of solvent cohesion would decrease and fibres would devolve to beading. They also found that fibre diameter would increase slightly with increasing voltage.[79]

Environmental factors such as humidity and temperature have had an effect on fibres also.[104,105] Humidity can lead to pores in fibres,[104] but overall both of these variables have differing effects on fibre diameter, depending on the type of polymer being investigated, as found by Vreize *et al.*, that found for cellulose acetate (CA) fibre diameter increased with increased humidity, whereas poly(vinylpyrrolidone) (PVP) fibre diameter decreased.[105] Literature therefore suggests that humidity and temperature have a large effect on fibre diameter.

However these parameters vary between the polymer and solvent combination used, therefore absolute parameters for any one particular polymer or solvent is difficult to ascertain.

1.8.7 Polymers Investigated for AMD Application

Many polymers (Table 3) have been electrospun specifically to address the issue of lack of viable treatment of dry AMD.[27] Biopolymers such as collagen,[106] the lens capsule[107] and the Descemet's membrane[108] have been explored for the application of AMD. Traits such

as surgical handling, permeability and RPE cell survival were also explored. Bhatt *et al*. compared crosslinked and non-crosslinked collagen and found that non-crosslinked collagen allowed good RPE monolayer formation and eyes receiving the non-crosslinked collagen sheet showed no signs of rejection.[106] The lens capsule exhibited good surgical handling, but was found to be non-permeable in its native state and caused retinal damage,[107] contrastingly the Descemet's membrane was found to be permeable and supported RPE cells well.[108]

Synthetic polymers have also been extensively explored. For example bio-degradable PLGA and PLLA were investigated due to their good surgical handling, but their acidic metabolites are thought to cause cell damage which is an undesirable characteristic.[109-111] Commercially available polyurethanes such as Pellethane®, Tecoflex® and Zytar® were investigated due to their good surgical handling, but were non-permeable.[112]

Comparisons between planar and fibrous surfaces in response to RPE cell survival have also been explored. Stanzel *et al.* compared porous PET transwell inserts and commercial electrospun polyamide nanofibres (EPN) for RPE cell survival. EPN was in two forms: mounted on an impermeable plastic or free and permeable. PET transwells exhibited good surgical handling and successfully grew and maintained RPE cells over three months. Impermeable EPN showed better RPE differentiation compared to PET, whereas the free and permeable EPN was found to not support RPE very well. The fibrous topography of the EPN was found to improve RPE cell replication in comparison to the planar PET surface.[113]

More recently, Li *et al.* have compared RPE cell growth on EPN and etch pore polyester (EPP) and also subretinally implanted strips of EPN, EPP and EPP coated with EPN in rats for two weeks to ascertain subretinal tolerance of the materials.[114] It was found that both EPP and EPN were able to maintain RPE cells in monolayer well and both materials exhibited gross tolerance towards subretinal implantation. Stanzel *et al.* have also found

that subretinal implantation of planar PET, both with and without gelatine coating, showed good tolerance with no suggestions of inflammation or overt toxicity to the retina or choroid.[115] Interestingly, both Stanzel *et al.* and Li *et al.* described EPN as being especially good as a possible candidate for a synthetic BM since its topography matched that of the native BM.[9,113,114] Therefore electrospinning a fibrous synthetic BM would be desirable.

Polymers that are known to be used in medical applications will have obtained approval from the US Food and Drug Administration (FDA) for use in humans. Therefore these polymers may then be potentially useful for AMD applications and give a faster route to market, if they have already been approved. PET, commercial name Dacron©, is one such polyester which has gained FDA approval. It is used as surgical sutures and large vascular prostheses due to its biostability.[116] Therefore since it is a FDA approved polymer which has been known to support RPE cells well and has exhibited tolerance toward subretinal implantation,[113-115] it was chosen to be taken forward for this study.

Polystyrene was chosen for comparison, since this polymer has been used as commercial tissue culture plastic (TCP) universally to grow many different cell types since about 1965.[117] Commercial TCP is corona discharge surface treated which involves the oxidation of the polymer surface with plasma that grafts high energy oxygen ions on to the surface of polystyrene, this confers a negative charge on the surface, in turn making it hydrophilic and so better for cell attachment and spreading.[117,118]

As a third comparison, polyurethane was chosen since it has been previously reported to be medically relevant,[83] has exhibited good surgical handling[112] and would provide an elastic, soft material with excellent biocompatibility.[112] However polyurethanes exhibit hydrophobic surfaces.[112] Polyurethane can be made favourable for good cell growth with the correct surface treatment. Sanders *et al.* found that plasma treatment with methacrylic acid in order to confer a negative charge on the surface of polyurethane favoured cell

growth.[119] Dennes *et al*. found that RGD-modified polyurethane, Tecoflex®, exhibited significant improvement in hydrophilicity and cell attachment compared to untreated polyurethane.[120] Similarly, Williams *et al.* found that UV/Ozone treatment of polyurethane films conferred hydrophilicity and allowed RPE cells to reach a confluent monolayer, whereas untreated polyurethane prevented RPE cell attachment and spreading.[112] However these membranes were non-permeable,[112] therefore a permeable membrane would be more desirable as a replacement BM, and hence electrospinning may prove to be a beneficial method of fabricating permeable polyurethane membranes. Also UV/Ozone treatment has been described as a good surface functionalization method for polyurethane.[112]

A known technology that exists is Coffey *et al*.'s patented technology which describes the use of a film with pores of a known number and diameter that may be made out of a broad variety of degradable and non-degradable polymers, preferring PET from the list, have described their membrane as being "substantially non-biodegradable".[121] They have also included, amongst other surface treatment methods, UV/Ozone treatment as an option for the porous film, and have also described that ideally a layer of cells on the surface of the membrane would be required if it were to be used for the application of the treatment of AMD.[121]

This research intended to work on previously known polymers that have been able to be functionalised using UV/Ozone treatment, and have been chosen because they have been shown to be relevant to this particular field of research as described above. However fabricating fibrous membranes using electrospinning was preferred over fabricating planar membranes with pores of a known dimension because of the ability to obtain sub-micron scale structures, and also because of the nature of its fabrication which would provide a permeable membrane to work with.

Table 3: The table summarises results from previous papers that have investigated various polymers for application in addressing treatment for AMD.[119,107-112]

Polymer	Electrospun / Solvent Cast	Treatment of Surface?	Solvent	Reference	Notes
Pellethane®	Used as bought 1mm thick films.	Air Plasma Treatment	N/A	Williams et al 2005	All are types of commercially available polyurethane. Exhibited good surgical handling, but are not permeable.
Tecoflex®	Solvent cast to give 200µm thick films.		Dimethylacetimide and methyl ethyl ketone		
Zytar®	Used as bought, 100µm films.	None	N/A		
PLGA & PLLA	Solvent Cast.		Chloroform	Hadlock et al 1999 Lu et al 2001 Thomson et al 1996	Thought to cause cell damage due to acidic metabolites: lactic acid and glycolic acid. Exhibit good surgical handling.
Polyurethane	Electrospun.	Plasma Treatment with hexafluoropropylene (HF) (neutral charge), N,N-dimethylaminoetheyl methacrylate (NN) (positive charge) or methacrylic acid (MA) negative charge and one was left untreated.	N/A. Fibres were fabricated from molten polymer	JE Sanders et al 2005	Coating with different plasmas were to determine whether charge would affect the fibrous capsule growth once implanted subcutaneously. Results showed cell growth is more favourable for negatively charged surfaces as opposed to positive.
Polyester	Obtained as polyester transwell culture inserts	None	N/A	Stanzel et al 2007	Permeable, porous (0.4µm), good surgical handling and successfully allowed RPE cells to grow and differentiate for two weeks.
Polyamide	Obtained as electospun nanofibres, which were stuck to non-permeable base. For some samples the impermeable base was removed for comparison	None	N/A		RPE cells were able to be cultured successfully on the impermeable polyamide scaffold. Whereas the permeable polyamide scaffold is unable to maintain a monolayer.
Lens Capsule	N/A	None	N/A	Turowski et al 2004	Not permable in native state, good surgical handling, causes retinal damage
Descemet's Membrane	N/A	None	N/A	Thumann et al 2007	RPE is well supported and is permeable
Crosslinked and Non-Crosslinked Collagen	Sheets	None	N/A	Bhatt et al 1994	Eyes receiving the non-crosslinked collagen sheets exhibited a good donor RPE layer, with a normal appearing retina and no evidence of rejection.

Chapter 2: Clinical Relevance & Aims of the Research Project

2.1 Clinical Relevance

This research was carried out with the endeavour that it would address a much needed niche area of ophthalmic treatment. Literature and discussions with ophthalmic surgeons at length on this subject highlighted that there is no current treatment in place for dry AMD, and since the life expectancy of the population is increasing the prevalence of this disease is predicted to increase too.[122] Therefore, the demand for treatment is high.

2.2 Implications & Development in Translational Medicine

Although, much debate remains as to whether or not the cell transplantation substrate needs to be non-degradable or biodegradable,[35] we believe that a non-degradable cell substrate would be beneficial, since it would remove the possibility of RPE cell detachment, which may occur as the substrate begins to break down, and would also remove the potential for side-effects from metabolic waste-products from materials such as PLLA or PLGA which have the potential to create acidic microenvironments, therefore potentially causing damage to the cells.[109-111] Not only this, but a fibrous membrane directly mimics the native BM,[9,113,115] and fibrous membranes have been reported to allow better *in vivo* cell morphology.[50,78,80,81] A fibrous membrane fabricated using electrospinning would provide a three dimensional structure with an open network of voids, potentially allowing an unlimited number of routes of transport for nutrients and waste products alike. Comparing this to a planar membrane with pores of a certain dimension, there is a likelihood of said pores blocking and therefore preventing the cell, which may be positioned directly on top of this pore, from obtaining its required nutrients, and similarly preventing waste removal. This in turn may cause cell damage or detachment, leading back to where the problem started. With an open network of voids, if potentially a blockage somewhere in the membrane occurs, then there will always be another route of transport available. Of course some blockage in the open network of

voids may occur, but it is with the intention that if a blockage may occur then it will be happening slowly over a much longer period of time, allowing the substrate to be functional during the lifespan of the patient for which it would be intended for use in.

Ideally a direct BM mimic would be described as one with randomly orientated fibres equal to or less than 70 nm in diameter, or a meshwork of fibres with interfibre voids of at least 1 μm or less in diameter, so as to be porous enough, but to also prevent cell invasion into the membrane and to mimic the RPE-BL and ICL of the native healthy BM.[7] Also the thickness of the ideal synthetic BM would be to match the 4.7 μm thickness of the native BM,[5,6] however thicknesses of 10-14 μm for synthetic BMs have been reported as being suitable.[123] Therefore, considering the potential to directly mimic the fibrous structure of the native BM, and the potentially unlimited routes of transport an open network of voids could provide, this research concentrated on developing a fibrous cell carrier substrate.

2.3 Aims of Research

One of the objectives of this research was to identify a suitable polymer and the required variables (polymer concentration, solvent type, electrospinning parameters (voltage, flow rate and working distance) and the effects of temperature, humidity and salt addition) to easily fabricate a mat of randomly orientated fibres that would mimic the native healthy BM in topography and morphology.

The second objective was to investigate a range of variables (effect of UV/ozone treatment on surface chemistry of the mats, cell morphology and monolayer formation, tensile strength, thickness of the mats, and porosity) in order to determine the suitability of the fabricated mats as cell carrier substrates.

The aim of this research was to shortlist a polymer from polystyrene (PS), PET, and PU, so as to identify a candidate that could potentially be used for subsequent implantation in application for the treatment of dry AMD.

Chapter 3: Materials & Methods

All chemicals and reagents were purchased from Sigma-Aldrich Ltd. (Dorset, UK) unless otherwise stated. In all instances the polymer solution was stirred overnight on a magnetic stirrer plate to give a homogeneous mixture. In all instances a 21G hypodermic needle (BD Microlance, Ref 304432) with the sharp tip shaved down to a blunt end was used. The homogeneous polymer solution was introduced into a 10 ml plastic syringe and the blunt-tip hypodermic needle attached. Any air-bubbles were removed and the filled syringe was fixed in a mechanical syringe pump. All experiments were repeated twice in order to verify results and each sample was placed in triplicate for each condition (n=3).

3.1 Investigation of the Fabrication of Electrospun Mats

The following experiments were carried out to find a suitable non-degradable polymer, which would be easy to fabricate fibres from, give good fibre morphology and good handling in order to take forward for cell culture. A range of parameters was investigated including varying solvents, varying polymer concentration, electrospinning with the addition of salt and carrying out the electrospinning in a controlled environment. Both qualitative and quantitative mechanical properties were tested on the fabricated mats in order to address the issue of ease of handling for surgeons.

3.1.1 Material Fabrication

Electrospinning involves the application of a potential gradient on a needle tip with a syringe attached that contains a polymer solution. The premise of this method involves the application of a high enough voltage to allow the electrostatic repulsion to overcome the surface tension of the polymer solution droplet at the end of the needle tip. The droplet elongates into what is called a Taylor cone from which a fine jet of polymer solution is ejected. A working distance, the length between the needle tip and a grounded collection plate, is set at a distance in which the ejected polymer jet has enough time to be able to dry and then land on the collection plate. The grounded plate can be a static collection plate or

a moving rotating drum, depending on whether the resultant fibrous mat is desired to be a meshwork of randomly orientated fibres, or aligned fibres. Electrospinning has a range of variables that need to be accounted for, including: properties of the polymer (molecular weight, chemical structure), properties of the solution (chemical structure, polarity, volatility), electrospinning parameters (voltage, flow rate, working distance), environmental parameters (humidity, temperature, air velocity), and needle gauge. All variables were closely noted throughout experiments.[124,125]

3.1.1.1 Varying Solvents, Polymer Concentration & Electrospinning Parameters

Using a previously reported method as a guide[88] PS pellets (Mw ≈ 192,000) were dissolved in neat tetrahydrofuran (THF) (BDH), neat dichloromethane (DCM) (BDH), DCM:THF at a 1:1 (v/v) solvent mixture in the following polymer (w/v) concentrations: 15 %, 20 %, 25 %, 30 % and 35 %, and THF:ethanol (EtOH) (Fisher) at a 2:1 (v/v) solvent mixture in the following polymer (w/v) concentrations: 20 %, 25 %, 26.7 % and 30 %.

Using a previously reported method as a guide[126] (PET pellets (Mw ≈ 10,215) were dissolved in neat 1,1,1-3,3,3-hexafluoroisopropanol (HFIP) (Apollo Scientific Ltd.) and neat trifluoroacetic acid (TFA) in the following polymer (w/v) concentrations: 15 %, 20 %, 25 % and 30 %.

Using a previously reported method as a guide[83] PU or Tecoflex® was dissolved in neat THF, neat DCM, THF/DCM at a 1:1 (v/v) solvent mixture at concentrations of 2 %, 2.5 % and 3 % (w/v) and THF:EtOH at a 1:1 (v/v) solvent mixture in the following polymer (w/v) concentrations: 5 %, 7.5 % and 15 %.

The fibres were collected for 1 hour under laboratory conditions on a grounded plate covered with aluminium foil. Working distances ranged from 5-10 cm, the flow rate ranged from 0.5-5 ml/hr and the voltage ranged from 15-25 kV.

3.1.1.2 Salt Addition, Temperature & Humidity

PS pellets were dissolved in THF:EtOH at a 2:1 (v/v) solvent mixture to an end concentration of 26.7 % (w/v), with and without 1 % (w/v) NaCl, since 1 % NaCl has been reported as ideal to reduce fibre variation and fibre diameter.[81] PS was electrospun using the following parameters: voltage 20 kV, working distance 10 cm, flow rate 2 ml/hr and was collected for 1 hour, under laboratory conditions and a controlled environment.

PET pellets were dissolved in neat HFIP to an end concentration of 30 % (w/v), with and without 1 % (w/v) sodium chloride (NaCl). PET was electrospun using the following parameters: voltage 15 kV, working distance 15 cm, flow rate 1 ml/hr and was collected for 1 hour, under laboratory conditions and a controlled environment.

The controlled environment maintained a steady 22 °C temperature and 50 % humidity during electrospinning within a closed custom made environmental chamber (Vindon Scientific Ltd., Rochdale, UK, Serial No: 17456). For PS it must be noted that the needle tip frequently became blocked, hence the chamber was opened only to clean the needle tip and then closed for collection.

3.1.1.3 Compression & Varying Collection Time

PS pellets were dissolved in THF:EtOH at a 2:1 (v/v) solvent mixture to an end concentration of 26.7 % (w/v). Electrospun mats were collected as per the variables described in sections 3.1.2 under laboratory conditions. The mats were cut into 1 cm by 1 cm squares, placed between two clean acetate sheets and compressed to the pressure of 4.982×10^{8} Nm^{-2} using a compression moulder (30 ton press, Research Industrial Instruments Company, London, England). (n=3).

PET pellets were dissolved in neat HFIP to an end concentration of 25 % (w/v). PET was electrospun using the parameters as described in section 3.1.2 under laboratory conditions, collected for the following times: 1, 2, 3, 4, 5, 10, 15 and 60 minutes. (n=3).

3.1.2 Material Characterisation

3.1.2.1 Topographical Analysis

Scanning electron microscopy (SEM) uses electron beams to obtain highly detailed images of nanoscale objects, a trait that is beyond the scope of optical microscopy. The resolution of the image that should be possible to obtain is half the wavelength of the source, therefore since the wavelength of electrons is much smaller than visible light much smaller images can be resolved with SEM. SEM is carried out under vacuum. The electron source emits electrons which are highly energetic and are focussed into beams using magnets and electromagnetic lenses. Images are obtained when high energy incident electrons knock out sample electrons (secondary electrons), which are then detected and an image is formed. Backscatter electrons are also emitted from the sample and this information can be used to measure the elemental distribution, density, and topography of the sample. High atomic weight elements will emit more backscattered electrons compared to those of a low atomic weight; similarly fewer electrons are emitted from deeper within the sample, than electrons on higher up on the sample. Therefore SEM is a good method of obtaining detailed images of the samples fabricated.[127,128]

3.1.2.1.1 Scanning Electron Microscopy (SEM)

Fibre morphology was determined by obtaining SEM images (Zeiss EVO60 serial number: EVO 60-02-88. Software with which images were obtained: SmartSEM V05.02.05 from Carl Zeiss SMT Ltd.). Small mat samples (n=3) were cut and mounted on sticky carbon pads (Agar), placed on aluminium stubs (Agar) and gold sputter coated (Edwards, Sussex, UK). Images were obtained using a SEM at an EHT value of 5 kV (VPSEM, Zeiss, EVO60; Carl Zeiss Ltd., Hertfordshire, UK).

3.1.2.1.2 Fibre Diameter Measurement

Fibre diameters were analysed from the SEM images obtained using ImageJ (National Institutes of Health, MN, USA). Upon opening the image with ImageJ the image was

zoomed in on, a line drawn across the scale bar, clicking “analyse” the scale was set by putting in the scale bar distance in the “known distance” and clicking “ok”. The image was now calibrated to the whole image in order to give a true measurement of the fibres. Keeping the same magnification, the fibres were then measured across the whole SEM image by randomly picking fibres, drawing a line across the diameter of the fibres and clicking “control+m” giving a tabulated measurement of fibres. The results were graphed using GraphPad Prism5 (GraphPad Software Inc). (n=3).

3.1.2.2 Mechanical Testing & Handling

Tensile testing is an easy way of understanding the strength of the mats. It directly measures the ultimate tensile strength: the maximum stress the material is able to take when being pulled before failing. The sample is mounted on to the machine into a static grip with the other end attached to a moving grip which is set to elongate the sample at a constant rate. The load versus elongation is graphically presented from which the stress-strain curve can be obtained. Care must be taken when measuring the tensile strength of the samples, since orientation of the fibres can affect the results. Therefore, for viable results the orientation of the collection plate was noted during electrospinning, so as to mount and measure the samples in the orientation in which they were collected.[125,128]

3.1.2.2.1 Qualitative Analysis: Handling

Mats were tested by hand to determine practicality of handling each type of electrospun polymer. Strips of electrospun PS and PET mats underwent folding, pulling, twisting and rolling. (n=3).

3.1.2.2.1 Quantitative Analysis: Tensile Testing

Tensile testing of the electrospun mats were measured using Instron 1122 (Instron series 1x Automated Materials Tester). Strips of the PET mats were cut into 1 cm by 2 cm strips and mounted onto a paper frame and held down with tape. The mats were tested until failure. (n=3).

3.1.2.3 Mat Thickness & Porosity

The thickness of the collected mats was measured using a digital micrometer (HITEC, 190-00, Farnell). Mats were cut to approximately 11 mm by 11 mm squares placed in the micrometer, so that the centre of the mat was placed between the measuring surfaces. The measuring surfaces were brought closer together until the mat could not be removed from the device, taking care as to not crush the mat and the measurement recorded. The weighed mats then had the porosity calculated using the following equation:

Porosity (%) = [1 – (apparent density/bulk density)] x 100

Where apparent density (g/cm^3) = [mat mass (g)/mat thickness (cm)] x mat area (cm^2)

Bulk density of PET was taken as 1.4 g/cm^3.[129] and the bulk density of PS was taken as 1.05 g/cm^3.[71] (n=3).

3.2 Electrospun Mat UV/Ozone Surface Treatment & Cell Survival

3.2.1 Material Fabrication

PS pellets (Mw ≈ 192,000) were dissolved in tetrahydrofuran:ethanol (THF:EtOH) (BDH and Fisher) at a ratio of 2:1 (v/v) at a final concentration of 26.7 % (w/v). PS electrospinning parameters: 25 kV, 10 cm working distance, 1 ml/h flow rate and collected for 1 hour on an aluminium foil on a grounded plate under laboratory conditions.

PET pellets (Mw ≈ 10,215) were dissolved in 1,1,1,3,3,3-hexafluoroisopropanol (HFIP) (Apollo Scientific Ltd) at a final concentration of 25 % (w/v).

3.2.2 Surface Treatment

UV/ozone is likened to corona discharge ozone generation in which oxygen molecules homogeneously split to obtain to highly energetic oxygen radicals in which they go on to react with other oxygen molecules to form ozone, which then goes on to react with the material surface. The difference between the two methods however is that corona

discharge involves oxygen being passed through an electrical field, whereas UV/ozone uses UV light to split the oxygen molecules. Corona discharge is used in industry because there is a higher throughput production of ozone, which can be used to efficiently clean and treat surfaces in large bulk production, for example tissue culture plastic. UV/ozone was used in this research because the same process is achieved in a simpler way.[130,131]

Mats were cut into approximately 11 mm by 11 mm squares and placed in a UV/ozone chamber (Novascan, Digital UV Ozone System, model number PSD-UV4). A pure oxygen flow was allowed to fill the chamber for 5 minutes. The UV light was turned on for the allocated times. After the lapsed time the UV light was switched off, oxygen flow turned off and the chamber was allowed to empty for 5 minutes in a fume hood under extraction fan flow.

3.2.3 Material Characterisation

3.2.3.1 Topographical Analysis

3.2.3.1.1 Scanning Electron Microscopy

As in section 3.1.2.1.1

3.2.3.2 Water Contact Angle (WCA) Measurement

Wettability was measured using the static sessile drop method, by placing a drop of liquid on the surface of the material, where the contact angle measured was at the liquid/solid interface. A high contact angle denoted poor wettability and low contact angle denoted good wettability. Multiple samples were measured in order to obtain viable results and to account for surface treatment and polymer.[125,128,133]

Wettability tests were undertaken on untreated and treated PET and PS electrospun mats. Samples were treated in pure oxygen flow for 0 s, 150 s and 300 s at room temperature at 0.5 cm and 10.1 cm away from the UV lamp for PET, and 2.8 cm and 0.5 cm away from the UV lamp for PS. Water contact angle (WCA) was measured using a contact angle

analyser (DSA100, Kruss, Hamburg, Germany). Three drops of 3 µl distilled water were placed on the mat surface (n=9) and the sessile drop contact angle measured using Kruss Drop Shape Analysis software (Kruss, Hamburg, Germany).

Untreated, 300 s treated and 450 s treated mats were used for the purpose of cell culture. These times were chosen because 300 s was found to give the desired approximately 60° water contact angle, which has been previously reported to be the ideal contact angle for protein adsorption.[132] The untreated and 450 s treated samples provided a comparison for higher and lower water contact angles, respectively.

3.2.3.3 X-ray Photoelectron Spectroscopy (XPS) for Surface Chemistry Analysis

X-ray photoelectron spectroscopy (XPS) is a way of analysing elemental composition of the surface of the materials. Samples are irradiated with X-rays, which ejects photoelectrons that go on to be detected. Dependent on the kinetic energies of the emitted photoelectrons, the binding energies can be determined since the wavelength energy of the X-ray will be known, and therefore give information of the elements and also the bond environments (through chemical shift values) present on the surface of the material.[128,134]

Analyses of the elements present on the surfaces of the scaffolds were carried out using XPS (Axis Ultra, Kratos). Electrospun PET and PS mats were cut to approximately 4 mm x 6 mm strips and then exposed to the following conditions:

Untreated, 300 s UV/ozone treated and 450 s UV/ozone treated.

After treatments, a selection of mats were incubated in cell culture media for 1 hour. After the elapsed time media was removed and the samples washed twice in distilled water before allowing to air dry. Taking care as to not touch the surface of the samples, the mats were wrapped in clean, dry foil, and then stored in a sterile plastic screw-top jar to be able to transport to the XPS equipment. XPS was performed by Professor Sven Schroeder (University of Manchester) and an initial explanation in labelling and analysis of peaks

was given by Dr Joanna Stevens (University of Manchester). All data was analysed by me using CasaXPS (CasaXPS MFC Application, Casa Software Ltd).

3.2.4 *In vitro* Cell Culture

3.2.4.1 Passaging Cells

Dulbecco's modified Eagle's medium (DMEM) – low glucose (1 g/l) with L-glutamine (PAA laboratories, UK) and F12-HAM nutrient mixture with $NaHCO_3$ and L-glutamine (PAA laboratories, UK) were mixed with 10 % (v/v) foetal bovine serum (FBS) (PAA laboratories, A15-151), 1 % (v/v) aliquot of antibiotic/antimycotic (AB) mixture of streptomycin sulphate (1 %), amphotericin B (0.0025 %), penicillin G (0.63 %) (PAA laboratories, P11-002) and 1 % (v/v) aliquot of 200 mM L-glutamine (L-gluts) (PAA laboratories, M11-004) under sterile conditions. A 50:50 mix of the aliquoted DMEM: F12-HAM was used for cell culture media.

Spontaneously arising retinal pigment epithelial (ARPE-19) cells (ATCC-LGC, CRL-2302) were cultured on TCP T-75 flasks (Nunclon Surface –Nunc) to allow a sufficient number of cells to be used for cell culture with the electrospun polymer mats. Frozen ARPE-19 cells were quickly defrosted and suspended into 10 ml of warmed media in a T-75 flask under sterile conditions and incubated at 37 ˚C, 5 % CO_2, 98-99 % humidity. The media was changed on the third day of incubation and cells were found to be confluent by day four.

In order to passage cells, the confluent flasks had existing media removed and cells washed twice with warmed, sterile Dulbecco's phosphate buffered saline (PBS) without Ca and Mg (PAA laboratories, UK). Trypsin-EDTA solution (2 ml of 0.05 % (w/v)) (Sigma, T4422) was added and the flasks incubated at 37 ˚C, 5 % CO_2, 98-99 % humidity for 3-5 minutes to detach cells from flasks. Fresh, warmed media (4 ml) added (totalling to a volume of 6 ml) to quench and collect the cells by pumping the suspension up and down

multiple times. This cell suspension (2 ml) was added to three new T-75 flasks containing 10 ml fresh media and incubated at 37 ˚C, 5 % CO_2, 98-99 % humidity. The emptied T-75 flasks were filled with Virkon® and left overnight before discarding.

3.2.4.2 Material Preparation for Cell Culture

Mats were cut into approximately 11 mm by 11 mm squares and placed in a UV/ozone chamber (Novascan, Digital UV Ozone System, model number PSD-UV4). A pure oxygen flow was allowed to fill the chamber for 5 minutes. The UV light was turned on and samples treated in pure oxygen flow for 300 s, 450 s at room temperature at 0.5 cm away from the UV lamp. After the lapsed time the UV light was switched off, oxygen flow turned off and the chamber was allowed to empty for 5 minutes in a fume hood under extraction fan flow. Untreated mats were exempt from this step.

To sterilise the mats, they were mounted onto Scaffdex® crowns and immersed into 70 % ethanol and soaked for 2 x 3 hours, changing the ethanol wash in between and finally were soaked overnight in 70 % ethanol. To clear them of ethanol they were washed three times in fresh distilled water and soaked overnight in distilled water.

3.2.4.3 Counting Cells for Seeding

Confluent flasks of cells (passage number ranging from 22 to 35) had the existing media removed, washed twice with warmed, sterile PBS and the cells removed from the T-75 flasks by incubating at 37 ˚C, 5 % CO_2, 98-99 % humidity for 3-5 minutes with 2 ml trypsin-EDTA. The trypsin-EDTA was quenched and cells collected with 4 ml fresh, warmed media as described in Section 3.2.4.1. This suspension was then collected and placed into a 15 ml Falcon tube and centrifuged at 1300 rpm for 4 minutes. The supernatant media was removed and the cell pellet resuspended in 5 ml fresh, warmed media. A 10 µl cell suspension using a Gilson pipette was charged into a 15 ml Falcon tube followed by 10 µl trypan blue (Sigma, T8154), mixed thoroughly by pipetting up and

down vigorously. The cell/trypan blue suspension was pipetted on to a haemocytometer in order to count the cells using an optical microscope. The total cell count for the stock cell suspension was found by the following equation:

Total cell count = 10,000 x (2 x Cell Count)

Wanted cell count was calculated as follows:

Dilution Factor = Cell number in stock suspension/cell number wanted

Cell solution volume needed (ml) = volume wanted/dilution factor

Volume media needed (ml) = Total volume – cell solution volume

A 1 ml of the cell suspension was introduced in to each well and incubated for the required time at 37 ˚C, 5 % CO_2, at 98-99 % humidity. The media was changed every three days.

3.2.4.4 Cell Culture

3.2.4.4.1 Initial Assessment

ARPE-19 cells were seeded onto the mounted, sterilised 11 mm by 11 mm mats, at a density of 10,000 cells/cm^2 and incubated at 37 ˚C, 5 % CO_2, 98-99 % humidity for 0, 1, 2, 3, 4 and 5 days. Cell number was deliberately kept low in order to assess how cells reacted initially towards the electrospun mats. Cell culture media was changed every three days. Media consisted of: a 50/50 mix of DMEM and F12-HAM, which had been mixed with 10 % FBS, 1 % AB and 1 % L-gluts. The positive control was 11 mm borosilicate discs (Scientific Laboratory Supplies, MIC3302) and the negative control was low attachment 24-well plates (Corning® Costar®). (n=3).

3.2.4.4.2 Long Term Culture

As in section 3.2.4.4.1, but cultured at a density of 50,000 cells/cm^2 for 0, 14, 28 and 56 days. Cell count was increased for long term culture to assess monolayer formation and cell survival. (n=3).

3.2.4.5 Proliferation Assessment & Cell Morphology

3.2.4.5.1 Alamar Blue

Alamar blue is a dye that is used in cell culture assays to determine cell metabolism and can be used to determine cell growth. Resazurin is a weakly fluorescent blue dye, which is irreversibly reduced to the pink, highly fluorescent resorufin when cells carry out aerobic respiration. When the pink dye is exposed to green light it fluoresces. This is measured using a detector, with the amount of fluorescence proportional to cell metabolism, and hence cell number. This method is an easy way of measuring cell metabolism, but is dependent on incubation time and so must have a calibration carried out to determine the incubation time required in order to obtain reliable results.[135]

Calibration of the assay was carried out for known number of cells, to be able to determine for how long the experimental cells should be incubated with Alamar blue in order to obtain accurate results.

3.2.4.5.1.1 Calibration

ARPE-19 cells were cultured, collected and a stock cell suspension prepared as mentioned in section 3.2.4.3. Six different cell suspensions were prepared using the stock cell suspension at the following cell densities: 10,000 cells/ml, 20,000 cells/ml, 40,000 cells/ml, 100,000 cells/ml, 150,000 cells/ml and 200,000 cells/ml. Each cell suspension (1 ml) was placed in triplicate in an adherent 24-well plate. After 15 minutes, to allow time for cells to attach, 100 µl Alamar blue solution (5 mg resazurin sodium salt (Sigma, 62758-13-8) in 40 ml PBS) was placed into each well (assuming 1 ml of media in each well) and

incubated at 37 ˚C, 5 % CO_2, at 98-99 % humidity. After increasing time intervals (2 hrs, 2.5 hrs, 3 hr, 3.5 hrs and 4 hrs) 200 µl of each sample (triplicate of triplicate) was place in a black bottomed 96-well plate (Nunclon Surface-Nunc). Fluorescence was measured at 530-510 nm excitation and 590 nm emission with a fluorescence reader (FLUOstar OPTIMA, BMG LABTECH, serial number: 413-0959, model FLUOSTAR, software version 1.32, supplied by JENCONS-PLS). After measurement, the samples were returned to the original wells and re-incubated until the next time point. Once all time points were measured, the measurements were blanked (fluorescence values of the empty controls were taken away from the values that contained cells), plotted fluorescence versus cell number to obtain a straight-line graph (Microsoft Excel and GraphPad Prism 5). The time point plot that gave the R^2 value closest to 1 was utilised as the incubation time for Alamar blue assay for all further experiments.

3.2.4.5.1.2 Experimental

Alamar blue solution was added to each sample to give 100 µl of Alamar blue solution per 1 ml media. Samples were returned to the incubator for the time dictated by the calibration curve. A 200 µl aliquot of media was taken from each sample and transferred into a black bottomed 96-well plate. Fluorescence was measured at 530-510 nm excitation and 590 nm emission using a fluorescence reader. (n=9).

3.2.4.5.2 DAPI/Phalloidin Fluorescence Staining

DAPI/Phalloidin staining is used to visualise cell cytoskeleton morphology. It is useful to determine how the cells react towards the material. DAPI is used to stain the nucleus; it is able to pass through the cell membrane intact, attaches to the A-T rich segments of DNA, and fluoresces at a short wavelength of 460 nm (note that it can also bind to RNA, however does not fluoresce as strongly at a longer wavelength of 500 nm). Phalloidin binds to the actin filaments (specifically at the interface between F-actin subunits) in the cell cytoskeleton. The phalloidin itself is conjugated with a fluorophore (several combined

aromatic groups that contain pi-bonds that emit photons when excited) eosin in the dye fluoresein, which intensely fluoresces.[136,137]

At the relevant time points, well plates were removed from the incubator, cell media removed and cells washed twice, gently with PBS. Samples were fixed with 3.7 % Formalin for 10 minutes at room temperature then washed twice with PBS. After soaking in ICC buffer [50 ml PBS, 500 µl goat serum, 50 µl of 0.1 % Triton X-100 in PBS and 5 mg/ml bovine serum albumin] for 30 minutes at room temperature the ICC buffer was removed and samples stained with Fluoresein Phalloidin (Invitrogen) (1:40 from stock Phalloidin: ICC buffer [50 µl: 2 ml]) for 20 minutes at room temperature. A double washing with PBS followed before mounting samples onto glass slides with DAPI Prolong Gold antifade (Invitrogen). The samples were left at 4 ˚C in the dark overnight to cure. Images were obtained with a fluorescence microscope (Nikon eclipse 50i JENCONS-PLS). (n=3).

3.2.4.5.3 SEM Fixation

SEM for cell culture samples have to firstly be dried since SEM imaging is carried out under high vacuum. Therefore the cells are fixed to stop all biological reactions that may be occurring within the cell. Crosslinking fixatives, such as formaldehyde/glutaraldehyde, are commonly used as this creates covalent chemical bonds between proteins in the tissue and anchors proteins to the cytoskeleton. Glutaraldehyde is a bigger molecule therefore is able to link proteins over a greater distance than formaldehyde, and gives good nuclear and cytoplasmic detail. The samples are then dried to maintain their morphology using graded ethanol and finally hexamethyldisilazane (HMDS) to ensure complete dehydration.[127,128]

At the relevant time points, well plates were removed from the incubator, cell media removed and cells washed gently, twice with PBS. Samples were fixed with 1.5 % glutaraldehyde (Fluka, 85191) in PBS for at least 30 minutes at 4 ˚C, washed twice with PBS and then dehydrated using graded EtOH: 2 x 3 minutes 50 %, 2 x 3 minutes 70 %, 2 x

3 minutes at 90 % and 2 x 5 minutes at 100 %. Samples were then soaked in fresh HMDS (Fluka, 999-97-3) for 2 x 5 minutes, in a fume cupboard. Excess HMDS was removed and samples were left to evaporate to dryness in the fume cupboard. SEM samples were mounted as described in section 3.2.3.1.1, and images were obtained using Phenom Pro Desktop SEM (Phenom World) at an EHT value of 5 kV. (n=3).

3.2.4.6 Monolayer Formation Assessment

3.2.4.6.1 Transepithelial electrical resistance (TEER) measurement

TEER is a way of quantitatively measuring cell confluence. It involves electrodes that are attached to a probe that allows easy measurement of epithelial resistance. The shorter tip of the probe is placed inside the Scaffdex® crown, immersed in the media but not touching the surface of the membrane that has the cells on it, and the longer tip is placed outside the Scaffdex® immersed in the media, just touching the bottom of the well plate. A blank (the mounted membrane in media with no cells) was also set up. The blank values were subtracted from the experimental values to give a true measurement. Resistance is inversely proportional to surface area (the bigger the area the lower the resistance), so the true measurement is multiplied by the membrane area to give the resistance of the unit area. The unit area resistance is independent of the area of the membrane, therefore allows comparison of data between membranes of different sizes. The higher resistance values denote more resistance, and indicate growth of a monolayer.[138]

PET mats were prepared as mentioned in section 3.2.4.2. Samples were set up in Scaffdex® with the electrospun mats such that the gap was fully covered leaving no voids and sterilised as described in section 3.2.4.2. Samples were then transferred to well plates, immersing them into 1 ml complete media, allowing space around the perimeter of Scaffdex® in order to allow the TEER measurer (EVOM2, epithelial voltohmmeter, World Precision Instruments) probe to fit with ease. Cells were counted and seeded as described in section 3.2.4.4.2 into the Scaffdex® onto the PET mats, taking care to not spill any cell

containing media into the outer perimeter of the Scaffdex®. TEER was measured from day 7 to 56, every 7 days in ohms. (n=3).

3.2.4.6.2 DAPI/Phalloidin Fluorescence Staining & SEM Fixation

As described in sections 3.2.4.5.2 and 3.2.4.5.3. This allowed the cell monolayer morphology to be assessed.

3.2.5 Statistical Analysis

Standard deviation (SD) shows the spread of the data about the mean and how much variance there is within the data. The larger the SD the more variation there is within a data set, the smaller the SD the less variation and the more uniform the values are. The SD has the same units as the data. There are two kinds of standard deviation: one that is calculated for the population mean, and another that is calculated for the sample mean. The difference between the two is the denominator (ie the total number of values you are working with) used in the SD calculation equations. In population SD the denominator is n, whereas in sample SD the denominator is n-1. This is because in statistics there is n-1 degrees of freedom for sample data that must be accounted for.[139] This was used for fibre diameter size distribution graphs.

As further statistical support, the p-value is noted to denote significance in data that was collected in order to determine the effect of a certain variable. A one-way ANOVA with Tukey's multiple post-test compares multiple means between all data sets to determine whether or not there is a significant difference between them, and how significant (or not) that difference is.[139] Statistical analysis for the Alamar blue assays was carried out using one way ANOVA, with Tukey's multiple comparisons post-test to measure the differences between each treatment condition on each day of cell culture using GraphPad Prism 5 (GraphPad Software Inc.). Significant difference in data is denoted by: $P<0.05$. High significant difference is denoted by: *** = $P<0.001$, good significant difference is denoted

by: ** = $0.001 \leq P \leq 0.01$, significant difference is denoted by: * = $0.01 \leq P \leq 0.05$ and no significant difference is denoted by: ns = $P > 0.05$.

Chapter 4: Objectives and Background of Published Material

The following papers discussed the development process behind the selection of a suitable polymer, and fabrication of a fibrous mat that could be taken forward for cell culture, and investigated long term RPE cell survival.

The first paper investigated the development process behind selection of a suitable polymer, suitable solvent, and ideal fabrication conditions of a fibrous structure that could be taken forward for cell culture. A suitable polymer, for the purposes of this research, was a non-degradable polymer that could be electrospun with ease, to give a fibrous mat of nanoscale fibres with no beading which exhibited good handling. Discussion with ophthalmic clinicians emphasised the desire to use FDA approved polymers, which was also realised by literature research. By the end of this part of the research, two potential substrates of PET and PS from the initial three investigated polymers of PET, PS and PU were selected to be taken forward for cell culture, and the optimal electrospinning parameters were identified.

The premise of the second paper involved identifying which of the substrates shortlisted from the previous investigation allowed good cell survival and morphology, and whether or not UV/ozone surface treatment would be necessary for cell proliferation on the identified substrates. A short term cell culture was carried out, with a low cell seeding density, to ascertain the initial reaction of the cells to both materials, and how the surface treatment of the materials affected the growth of the cells, if at all. The short term study identified the substrate that exhibited good cell proliferation and cell morphology, and whether surface treatment affected these factors. It was found that RPE cells reacted well to PET, with cells beginning to form monolayers in patches, regardless of surface treatment. PS was found to be unsuitable with undesirable cell morphology, as cells wrapped around fibres instead of forming monolayers, however surface treatment was necessary for cell survival on PS. On-going discussion with ophthalmic surgeons stressed

the importance of being able to work with the eventual cell substrate with ease. Thickness of the substrate was also identified as being an important factor when considering the implant. Since the native healthy BM has a thickness of 4.7 μm,[5,6] it was important that the implant could match this thickness as closely as possible, without losing the robustness of the substrate. Both qualitative and quantitative handling was measured throughout the study. These tests identified PET as exhibiting the best handling during experimental processing, and through tensile testing. PS exhibited loss of some of the substrate during experimental processing and was not suitable to be taken forward for tensile testing, due to its fragility. Therefore, since PET exhibited good initial cell culture results and good mechanical properties, it was deemed eligible for long term cell culture, to evaluate the ability of the RPE cells to form and maintain a complete monolayer over a period of two months, and PS was rejected as unsuitable. The effects of UV/ozone treatment on the growth of cells was evaluated through proliferation assays and TEER over two months. It showed that surface treatment affected the speed with which cells formed a monolayer, but eventually cell growth plateaued regardless of surface treatment. In conclusion, PET was identified as the best candidate as cell carrier substrate as a replacement BM.

A third publication was a patent application (Synthetic Membrane; GB12009863.8), which was filed but not commercialised. The patent application can be referred to in the appendix.

Chapter 5: Publication Title: Controlling fiber morphology and scaffold design for treatment of dry age-related macular degeneration.

Publication DOI: 10.1080/00914037.2014.886231

Available at: http://dx.doi.org/10.1080/00914037.2014.886231

Journal: International Journal of Polymeric Materials and Polymeric Biomaterials

Page Number of Thesis: 86

Controlling fiber morphology and scaffold design for treatment of dry age-related macular degeneration.

Atikah Shahid Haneef[a*] and Sandra Downes[a]

[a]School of Materials, Materials Science Centre, Department of Engineering and Physical Sciences, The University of Manchester, Grosvenor Street, Manchester, M1 7HS, United Kingdom.

*Corresponding author: atikah.haneef@postgrad.manchester.ac.uk

Abstract

Polystyrene (PS), poly(ethylene terephthalate) (PET), and polyurethane (PU) was electrospun in various solvents, to ascertain the ideal conditions for reproducible scaffold production, in order to develop a synthetic BM. Effect of different environmental factors under laboratory conditions and controlled conditions, with and without 1% NaCl were investigated.

For PS, environmental conditions were more important than NaCl addition in fibre diameter reduction, however NaCl addition showed reduced fibre size variation. For PET, reduction in fibre diameter on addition of NaCl compared to controlled environmental conditions was observed. Fibre size variation for PET was unaffected by NaCl addition or controlled conditions.

Key words: AMD, electrospinning, PET, fibres, Bruch's membrane.

1. Introduction

In this work, we have attempted to find the most suitable non-degradable, biocompatible, synthetic polymer for use as a scaffold to replace the damaged Bruch's membrane (BM) for patients suffering from dry age-related macular degeneration (AMD). The idea is to electrospin such polymers to create a nanofibrous mat. Electrospinning is the method of

fibre extrusion from a needle tip on to a grounded plate via an electrostatic gradient. It differs from conventional extrusion methods since the fibre diameters that can be achieved are of submicron-scale, which bestow larger surface area that allow for efficient surface functionality and high mechanical stability.[1,2,3] Nano-scale fibres yielded from electrospinning resemble that of the natural extra-cellular matrix[1,4] and are therefore of great interest for application in tissue engineering.[5,6]

The nature of this method is such that the parameters must be controlled closely, in order to obtain fibres rather than spraying, and to form the required fibre diameter reproducibly.[2,7,8] For a fibre to be produced, a stable polymer solution jet needs to be ejected from the tip of the droplet on the polymer solution that forms a Taylor cone on the end of the needle. The jet diameter must be above a critical value,[2] in order to overcome surface tension forces in the polymer solution, for a fibre to be extruded. If surface tension forces are high enough to overcome the critical diameter value, then the jet will break and spraying will occur.[2,7]

Variables that have been explored include polymer solubility,[9,10,11] solvent polarity,[2] concentration of polymer solution[3,7,12,13] and spinning parameters such as applied voltage, tip-to-collector distance (working distance) and flow rate.[2,7,8] Various results have been reported such as none of the aforementioned parameters making a difference to fibre diameter[7] to increased voltage increasing the fibre diameter and decreased voltage resulting in beading.[14] Theron *et al.* found that higher flow rates resulted in low residence time for the drop at the end of the needle, so voltage did not have enough time to take effect and increasing the working distance resulted in weakening of the applied electric field.[2] Therefore the parameters can have different effects on fibre diameters and also vary with the polymer/solvent combination used.

Addition of polyelectrolytes[7] or salt[15,16] have been reported to allow for thinner fibres with increased surface hydrophilicity and better control over fibre formation.[7,15,16]

Environmental factors such as humidity and temperature have had an effect on fibres also.[17,18,19] Humidity can lead to pores in fibres,[17,19] but overall both of these variables have differing effects on fibre diameter, depending on the type of polymer being investigated, as found by Vreize *et al.*, that found for cellulose acetate (CA) fibre diameter increased with increased humidity, whereas poly(vinylpyrrolidone) (PVP) fibre diameter decreased.[18] Literature therefore suggests that salt presence, humidity and temperature have a large effect on fibre diameter in electrospinning.

Our aim for the following study was to determine the appropriate requirements to fabricate a synthetic BM, which mimicked the native healthy BM in topography and morphology for application in the treatment of dry AMD. The main variables investigated were polymer concentration, solvent type, electrospinning parameters (voltage, flow rate and working distance) and the effects of temperature, humidity and salt addition for polystyrene (PS), poly(ethylene terephthalate) (PET) and poly(urethane) (PU).

2. Materials and Methods

2.1 Materials

All chemicals and reagents were ordered from Sigma-Aldrich, Dorset unless otherwise stated. In all instances the polymer solution was stirred overnight on a magnetic stirrer plate to give a homogeneous mixture. In all instances a 21G hypodermic needle (BD Microlance, Ref 304432) with the sharp tip shaved down to a blunt end was used. The homogeneous polymer solution was introduced into a 10 ml plastic syringe and the blunt-tip hypodermic needle attached. Any air-bubbles were removed and the filled syringe was fixed in a mechanical syringe pump. All experiments were repeated twice.

2.2 Methods

2.2.1 Effect of Solvents, Polymer Concentration & Electrospinning Parameters

Using a previously reported method as reference,[20] PS pellets (Mw ≈ 192,000) were dissolved in neat tetrahydrofuran (THF) (BDH), neat dichloromethane (DCM) (BDH), DCM:THF at a 1:1 (v/v) solvent mixture in the following polymer (w/v) concentrations: 15 %, 20 %, 25 %, 30 % and 35 %, and THF:ethanol (EtOH) (Fisher) at a 2:1 (v/v) solvent mixture in the following polymer concentrations: 20 %, 25 %, 26.7 % and 30 % (w/v).

Using a previously reported method as a reference,[21] PET pellets (Mw ≈ 10,215) were dissolved in neat 1,1,1-3,3,3-hexafluoroisopropanol (HFIP) (Apollo Scientific Ltd.) and neat trifluoroacetic acid (TFA) in the following polymer concentrations: 15 %, 20 %, 25 % and 30 % (w/v).

Using a previously reported method as a reference,[22] PU or Tecoflex® was dissolved in neat THF, neat DCM, THF/DCM at a 1:1 (v/v) solvent mixture at concentrations of 2 %, 2.5 % and 3 % (w/v) and THF:EtOH at a 1:1 (v/v) solvent mixture in the following polymer concentrations: 5 %, 7.5 % and 15 % (w/v).

The fibres were collected for 1 hour under laboratory conditions on a grounded plate covered with aluminium foil. Working distances ranged from 5-10 cm, the flow rate ranged from 0.5-5 ml/hr and the voltage ranged from 15-25 kV.

2.2.2 Effect of Salt Addition, Temperature and Humidity

PS pellets were dissolved in THF:EtOH at a 2:1 (v/v) solvent mixture to an end concentration of 26.7 % (w/v), with and without 1 % (w/v) NaCl. PS was electrospun using the following parameters: voltage 20 kV, working distance 10 cm, flow rate 2 ml/hr and was collected for 1 hour, under laboratory conditions and a controlled environment.

PET pellets were dissolved in neat HFIP to an end concentration of 30 % (w/v), with and without 1 % (w/v) sodium chloride (NaCl). PET was electrospun using the following

parameters: voltage 15 kV, working distance 15 cm, flow rate 1 ml/hr and was collected for 1 hour, under laboratory conditions and a controlled environment.

The controlled environment maintained a steady 22 °C temperature and 50 % humidity during electrospinning within a closed custom made environmental chamber (Vindon Scientific Ltd., Rochdale, UK, Serial No: 17456). For PS it must be noted that the needle tip frequently became blocked, hence the chamber was opened only to clean the needle tip and then closed for collection.

2.3 Material Characterisation

2.3.1 Topographical Analysis: Scanning Electron Microscopy (SEM)

Fibre morphology was determined by obtaining SEM images (EVO®60 serial number: EVO 60-02-88. Software with which images were obtained: SmartSEM V05.02.05 from Carl Zeiss SMT Ltd.). Small mat samples (n=3) were cut and mounted on sticky carbon pads (Agar), placed on aluminium stubs (Agar) and gold sputter coated (Edwards, Sussex, UK). Images were obtained using a SEM at an EHT value of 5 kV (VPSEM, Zeiss, EVO60; Carl Zeiss Ltd., Hertfordshire, UK). Fibre diameters were analysed using ImageJ (National Institutes of Health, MN, USA). (n=3).

3 Results & Discussion

3.1 Fibre Morphology & Fibre Diameter

3.1.1 Effect of Solvents, Polymer Concentration & Electrospinning Parameters

For all polymers, fibre diameter was found to increase with polymer concentration, since a higher output of polymer is ejected with higher polymer concentrations.

The solvents used for electrospinning have an electric dipole, an ideal trait which allows a charge to be carried. The solvents also have high volatility, which is useful for electrospinning since fibres form as the solvent evaporates from the polymer solution jet.

Fibre formation and diameter may be dependent on the solvent's electric dipole.[2,7] There were some fibre morphological differences exhibited between polymers and between the solvents used.

Polystyrene dissolved in neat THF, neat DCM, THF/DCM and THF/EtOH solvent mixtures. The polymer-solvent interactions in these mixtures are such that the organic chemical structure of polystyrene interacts with the organic structure of the solvent to produce a homogeneous polymer solution. Both THF and EtOH contain a lone pair of electrons in their structures and DCM contains two chloride atoms which are rich in electron density, therefore the electron rich phenyl ring in polystyrene can interact.

All PS fibres had ribbon-like morphology, which may be due to the high molecular weight of the polymer.[23] In neat THF, beading was present at 15 % and 20 % (w/v). Fibres formed at concentrations above and including 25 % (w/v) (Figure 1 [A,B,C,D,E]). In neat DCM, beading was present up to and including 25 % (w/v) and fibres only formed at 30 % and 35 % (w/v) (Figure 1 [F,G,H,I,J]). In the THF/DCM mixture beading was present up to 25 % (w/v) with fibres present at 30 % (w/v) (Figure 1 [K,L,M]).

In neat THF the mean fibre diameter (FD) and standard deviation (SD) for PS increased with polymer solution concentration: in 15 % (w/v) FD = 1.845 µm, SD = 0.592 µm, in 25 % (w/v) FD = 3.607 µm, SD = 1.907 µm, in 30 % (w/v) FD = 4.940 µm, SD = 2.592 µm and in 35 % FD = 6.446 µm, SD = 3.083 µm (Figure 2 [A,B,C,D]). In neat DCM the mean FD and SD increased with polymer solution concentration: in 15 % (w/v) FD = 0.937 µm, SD = 0.330 µm, in 25 % (w/v) FD = 1.512 µm, SD = 0.508 µm, in 30 % (w/v) FD = 8.30 µm, SD = 4.357 µm and in 35 % (w/v) FD = 7.15 µm, SD = 2.961 µm (Figure 2 [E,F,G,H]).

As exhibited by PS, fibres formed at a lower polymer concentration in neat THF (25 %) compared to neat DCM (30 %). PS fibres also had a lower mean diameter when spun in

THF than DCM. THF has a dielectric constant of 7.52 and a dipole moment of 1.750,[24] whereas DCM has a dielectric constant of 8.93 and a dipole moment of 1.600.[25] Higher dipole moment may mean a better charge is able to be carried with THF allowing better discrimination by an applied potential difference, therefore extruded finer fibres and allowed fibres to form at lower polymer concentrations. On a qualitative perspective, THF was found to be a better solvent compared to DCM as it required less cleaning and unblocking of the needle during experiments. It was eventually found that PS at 25 % (w/v) in neat THF did not reproducibly form fibres. Concentrations including 30 % (w/v) and above would block the needle, making collection of fibres difficult. At the instances fibres were obtained at 25 % (w/v), at other instances beading would be exhibited at the same concentration. Therefore the solvent mixture was changed to THF/EtOH in order to predictably produce fibres.

The collection of fibres was made easier with reproducible results; some cleaning of the needle was required, but not as frequently as with neat THF. In the THF/EtOH mixture beading was present up to 25 % (w/v) and fibres only formed at 26.7 % (w/v) and above (Figure 1 [N,O,P,Q]). To make collection of fibres more efficient, since ease of spinning was reduced as at 30 % a lot of cleaning of the needle tip was required; the polymer concentration was altered to concentrations of 26.7 % (w/v) and 28.3 % (w/v). Optimal parameters for electrospinning PS were: voltage 24 kV, working distance 10 cm, flow rate 2 ml/hr (Table 1). Fibres were obtained at both instances, but collection was slightly better at 26.7 % (w/v). Interestingly, these findings agree with literature[9,10] that better fibres/electrospinning occurs when solvents that do not allow complete dissolution of the polymer are used. This may suggest that a polymer suspension may be better, with the solvent being used as a polymer holding medium only and not allowing the polymer to become completely homogeneous, as is the case with true solutions. As shown by our data, neat ethanol did not allow PS to dissolve completely into solution, whereas THF did.

Therefore the addition of ethanol to THF would make the solvent mixture such that PS dispersed within the medium, but did not completely homogeneously, leaning slightly more towards being a suspension, and hence allowed more stability to fibre formation for PS.

PET dissolved well in HFIP and TFA, but not in THF, DCM, THF/DCM or THF/EtOH solvent mixtures. Good polymer-solvent interaction for PET was achieved through solvents which contained highly electronegative species in their structures (fluoride) that are able to interact through dipole-dipole forces with the dipoles created in PET by the ester functional group. Another structural difference in solvents was that HFIP contains an alcohol functional group and TFA contains a carboxylate functional group. These functional groups are able to interact with the oxygen containing ester group in PET, via hydrogen bonding. THF was unable to provide good chemical interaction with PET, the lone pair of electrons were not enough to allow PET to dissolve. It was also noted that although DCM contains electronegative species in its structure too (chloride), it was not able to dissolve PET. This is since chloride ions are much larger than fluoride ions, which means that chloride is not as electronegative as fluoride and so the pull of electrons by chloride is not as strong as in fluoride, therefore the dipole created by fluoride is much stronger than with chloride, which in turn provides a better means of interaction with PET.

All PET fibres had a wire-like morphology, which may be due to the low molecular weight of the polymer.[23] In neat HFIP, beading was present at 15 % (w/v), fibres formed at concentrations above and including 20 % (w/v) (Figure 3 [A,B,C,D]). In neat TFA, beading was exhibited up to and including 20 % (w/v) and fibres only formed at concentrations above and including 25 % (w/v) (Figure 3 [E,F,G,H]). Both solvents proved easy to use for spinning PET, with no blocking of the needle. Optimal parameters for spinning were: voltage 15 kV, working distance 15 cm and flow rate 1 ml/hr (Table 2).

In neat HFIP an increase in the mean FD and SD with increase in polymer solution concentration was exhibited: in 15 % (w/v) FD = 3.285 µm, SD = 1.306 µm, in 20 % (w/v) FD = 0.150 µm, SD = 0.050 µm, in 25 % (w/v) FD = 0.277 µm, SD = 0.095 µm and in 30 % (w/v) FD = 0.423 µm, SD = 0.117 µm (Figure 4 [A,B,C,D]). In neat TFA an increase in the mean FD and SD with increase in polymer solution concentration was exhibited: in 15 % (w/v) FD = 0.118 µm, SD = 0.047 µm, in 20 % (w/v) FD = 0.136 µm, in 25 % (w/v) FD = 0.146 µm, SD = 0.053 µm and in 30 % (w/v) FD = 0.231 µm, SD = 0.087 µm (Figure 4 [E,F,G,H]).

PET fibres were obtained at 25 % (w/v) in HFIP and 20 % (w/v) in TFA. Fibres spun from HFIP were generally thicker, although still nanoscale, than compared to fibres spun from TFA. This may be because TFA contains the carboxylate functional group in its structure, which is able to interact with the ester functional group in PET via hydrogen bonding and dipole-dipole interaction. Whereas, HFIP contains hydroxide groups only, this can interact with PET via hydrogen bonding, but does not provide dipole-dipole interaction. Qualitatively, both solvents were extremely good for electrospinning, polymer deposits did not block the needle and did not require cleaning. But for further experiments HFIP was used since it was slightly better for handling.

PU fibres had a web-like morphology, with some of the fibres merged into the other, giving a sticky look to the fibres. In neat THF and THF/DCM solvent mixture PU was not electrospinnable. In neat DCM, PU exhibited spraying at 2 % (w/v), 2.5 % (w/v) and 3 % (w/v) concentrations (Figure 5 [A,B,C]). Higher concentrations were not able to be electrospun in DCM due to high viscosity of the PU solutions. Therefore a mixture of THF/EtOH was used at higher concentrations. Beading was exhibited at 5 % (w/v) and fibres were achieved at concentrations of 7.5 % (w/v) and above (Figure 5 [D,E,F]). Optimal parameters for electrospinning PU were: voltage 20 kV, working distance 10 cm and flow rate 1 ml/hr (Table 3).

Fibres were only obtained from spinning PU dissolved in the THF/EtOH solvent mixture. An increase in the mean FD and SD with polymer solution concentration was exhibited: in 5 % (w/v) FD = 0.388 µm, SD = 0.143 µm, in 7.5 % (w/v) FD = 1.170 µm, SD = 0.520 µm and in 15 % (w/v) FD = 1.403 µm, SD = 0.719 µm (Figure 6 [A,B,C]).

PU dissolved well in THF/EtOH mixture. Although the chemical structure of the commercial PU used Tecoflex® is not known, all polyurethanes contain the urethane (or carbamate) link: R-NH-COOR'. The THF/EtOH solvent mixture interacts well with these urethane links via hydrogen bonding.

Spraying was exhibited for PU in neat THF and neat DCM. An increase in polymer concentration formed a very thick polymer solution that could not be introduced into the syringe. Fibres of PU were formed with THF/EtOH solvent mixture at 7.5 % (w/v), for which the voltage had to be adjusted to 25 kV as initial voltage used gave a slight bulge in some fibres. Increase of voltage provided a higher current that allowed a better potential difference to be applied while maintaining polymer solution surface tension, which allowed the fibres to be extruded more smoothly. The ethanol in the solution may have provided the polarity required to allow a current to be carried. Also ethanol has a lower volatility compared to THF and so may have provided longer residence time for the polymer at the needle tip for the voltage applied to take effect for fibre extrusion.

3.2 Overall Mat Morphology

PS mats resembled cotton wool, which could be lightly flattened by hand pressure to smooth out somewhat, whereas PET mats had a tape-like morphology with a smooth appearance (Figure 7). PS mats were fragile and although could withstand experimental processing, some loss of sample did occur. PET mats were very robust and were able to undergo all experimental processing without any loss of sample. The most difficult to handle was PU, since its sticky trait, caused the mat to intertwine, which proved difficult to resolve, often leading to mat destruction (Figure 8).

PU mats were very problematic in handling. While PS mats were fluffy and brittle, the PU mats were elastic and sticky. Initially the elastic nature of PU was thought of as an advantageous characteristic however during processing the mat would entwine and could not be detached without damaging the scaffold. Handling PU was frustrating and difficult and therefore would not hold well in practice. For these reasons PU was deemed unsuitable for further testing.

In view of the described findings, only PET and PS were decided to be taken forward since they showed the most promise. PS was used at 26.7 % (w/v) in THF/EtOH and PET was used at 30 % (w/v) in neat HFIP.

3.3 Effect of Salt Addition, Temperature and Humidity

Under both laboratory conditions and controlled conditions PS gave ribbon like fibre morphology. PS fibre diameters were smaller when electrospun with the addition of salt than compared to when electrospun without salt, this agrees with literature.[15] The largest PS fibre diameter was found in the batch electrospun in laboratory conditions without salt.

Under laboratory conditions and no salt FD = 5.500 µm, SD = 2.840 µm, in an environmental chamber and no salt FD = 4.317 µm, SD = 1.598 µm, under laboratory conditions and 1 % NaCl FD = 5.028 µm, SD = 2.374 µm and in an environmental chamber and 1 % NaCl FD = 4.775 µm, SD = 1.616 µm (Figure 9 [A,B,C,D]).

Addition of salt and carrying out the experiments in a controlled environment had varying effects on the polymers and the fibre morphology.[19] A controlled environment had the largest effect on the fibres of PS. It can be noted with both the presence and absence of 1 % salt, when spun under laboratory conditions, the standard deviation for the fibre size are large for PS. SEM images also show this as under laboratory conditions a wide variety of fibre sizes can be seen, whereas when spun in a controlled environment the fibre sizes look similar and the standard deviation is also smaller. This may be because the controlled

environment allowed the control of the evaporation rate of the very volatile solvent mixture, allowing a smaller variation in fibre size. The rate at which the solvent evaporates in normal laboratory conditions may be erratic enough to cause wide distribution of fibre size. Qualitatively the salt allowed the collection of fibres much more easily than when no salt was added. The needle needed to be cleaned less frequently as it did not block as often. This may be because the salt allowed the current of the voltage applied to be carried well and so fibres extruded much more easily, due to the ionic nature of NaCl. These findings are also in agreement with previously reported literature.[16,18]

PET gave fibres of wire-like morphology when electrospun under both laboratory conditions and in an environmental chamber, with and without salt. Salt addition lowered the fibre diameter when electrospun in both laboratory conditions and an environmental chamber. The smallest fibre diameter was achieved when electrospun in an environmental chamber with the addition of 1 % NaCl. However it was noted that when PET was electrospun in an environmental chamber, regardless of whether salt was added or not, bumps formed throughout the mat.

Under laboratory conditions and no salt FD = 0.412 µm, SD = 0.129 µm, in an environmental chamber and no salt FD = 0.412 µm, SD = 0.132 µm, under laboratory conditions and 1 % NaCl FD = 0.363 µm, SD = 0.138 µm and in an environmental chamber and 1 % NaCl FD = 0.356 µm, SD = 0.128 µm (Figure 10 [A,B,C,D]).

Contrasting to PS, the addition of salt to PET/HFIP reduced the average fibre size more than electrospinning in a controlled environment. The smallest fibre size was found when PET was electrospun with the addition of salt in an environmental chamber. This again can be attributed to the ionic nature of HFIP in conjunction with the ionic nature of salt, which would increase the overall ionic value of the polymer solution, therefore allowing better discrimination of an applied potential difference.[15,16] Under all conditions the standard deviation in fibre size was not significantly affected. Interestingly,

electrospinning PET in a controlled environment, regardless of salt addition, caused bumping to occur in the mat structure. Although addition of salt reduced the amount of bumping in the mat, this is still an undesirable trait for a Bruch's membrane mimic. This may be attributed to the higher humidity in the environmental chamber, which would reduce the speed of evaporation of the solvent from the polymer solution causing drops of polymer solution to remain in the structure. In lieu of this, it was decided that the optimal parameters for electrospinning PET would be under laboratory conditions.

4. Conclusion

Following the investigation, we found that various solvents can have varying effects on the polymer. We also showed that concentration of the polymer solution and varying the electrospinning parameters can also lead to varying effects. Salt addition and environmental factors do have an effect on the gross morphology of the electrospun mats and also on the fibre size, however these effects vary depending on the solvent/polymer combination utilised.

For PS electrospinning in a controlled environment reduced the fibre size more than with the addition of salt, similarly the addition of salt reduced the variation of fibre size within a single batch of produced fibres. Therefore, for PS, the use of salt in conjunction with spinning in a controlled environment proved advantageous; providing smaller fibres with less fibre size variation. Contrastingly for PET salt addition reduced the fibre size whereas a controlled environment did little in changing fibre size. Neither of the conditions was able to alter the fibre size variation within a batch of PET fibres. Unexpectedly electrospinning PET in a controlled environment, regardless of the addition of salt, disrupted the gross morphology causing bumping throughout the mat, which is an undesirable characteristic for a replacement BM. Therefore, although the addition of salt may prove advantageous in reducing the fibre size slightly, electrospinning PET within a controlled environment was not beneficial in order to form a mat of fibres.

In terms of a scaffold for a synthetic replacement BM, PET is the most suitable in terms of fibre dimension, gross morphology, handling and ease of production. Electrospun polystyrene was found to be unsuitable due to its fragility and polyurethane was excluded due to very difficult handling traits. Surprisingly, there were no advantages in the use of changing the environmental conditions during the electrospinning process of PET. The fibres were easily electrospun in ambient conditions, room temperature and normal humidity. Electrospun PET would make an ideal candidate for a scaffold as a synthetic BM replacement.

References

1. Agarwal, S., Wendorff, J.H., and Greiner, A., Polymer. 49 (2008).

2. Theron, S.A., Zussman, E., and Yarin, A.L., Polymer. 45 (2004).

3. Aytimur, A., Kocyigit, S., and Uslu I., Polym-Plast Technol. 52 (2013).

4. Kumbar, S.G., James R., Nukavarapu, S.P., and Lairencin, C.T., Biomed. Mater. 3 (2008).

5. Jiang, S., and Liao, G., Polym-Plast Technol. 51 (2012).

6. Shadi, L., Karimi M., Asadpour-Zeynali, K., Entezami, A.A., and Safa, K.D., Polym-Plast Technol. DOI: 10.1080/03602559.2013.844237 (2013).

7. Son, W.K., Youk, J.H., Lee, T.S., and Park, W.H., Polymer. 45 (2004).

8. Senthil, T., George, G., and Anandhan, S., Polym-Plast Technol. 53 (2013).

9. Luo, C.J., Nangrejo, M., and Edirisinghe, M., Polymer. 51 (2010).

10. Lee, K.H., Kim, H.Y., Khil, M.S., Ra, Y.M., and Lee, D.R., Polymer. 44 (2003).

11. Koysuren, O., Karaman, M., Yildiz, H.B., Koysuren, H.N., and Dinc, H., Int. J. Polym. Mater. DOI: 10.1080/00914037.2013.845188 (2013).

12. Piperno, S., Lozzi, L., Rastelli, R., Passacantando, M., and Santucci, S., Appl. Surf. Sci. 252 (2006).

13. Aghdam, R.M., Shakhesi, S., Najarian, S., Mohammadi, M.M., Tafti, S.H.A., and Mirzadeh, H., Int. J. Polym. Mater. DOI: 10.1080/00914037.2013.800983 (2013).

14. Chen, J.W., Tseng, K.F., Delimartin, S., Lee, C.K., and Ho, M.H., Desalination. 233 (2008).

15. Barakat, N.A.M., Kanjwal, M.A., Sheikh, F.A., and Kim, H.Y., Polymer. 50 (2009).

16. Jean-Gilles, R., Soscia, D., Sequeira, S., Melfi, M., Gadre, A., Castracane, J., and Larsen, M., J. Nanotechnol. Eng. Med.-T. ASME. 1 (2010).

17. Casper, C.L., Stephens, J.S., Tassi, N.G., Chase, D.B., and Rabolt, J.F., Macromolecules. 37 (2004).

18. De Vrieze, S., Van Camp, T., Nelvig, A., Hagström, B., Westbroek, P., and De Clerck, K., J. Mater. Sci. 44 (2009).

19. Abadi, F.J.H., Tehran, M.A., Zamani, F., Nematollahi, M., Mobarakeh, L.G., and Nasr-Esfahani M.H., Int. J. Polym. Mater. 63 (2013).

20. Uyar, T., and Besenbacher, F., Polymer. 49 (2008).

21. Ma, Q., Mao, B., and Cebe, P. Proceedings of the 38th Annual Conference of North American Thermal Analysis Society (2010).

22. Khil, M.S., Cha, D.I., Kim, H.Y., Kim, I.S., and Bhattarai, N., J. Biomed. Mater. Res. Part B: Appl. Biomater. 67, B (2003).

23. Koski, A., Yim, K., and Shivkumar, S., Mater. Lett. 58 (2004).

24. Sigmaaldrich.com [Internet]. United States: Sigma-Aldrich Co LLC; c2013 [cited 2013 Sep 11]. Available from: http://www.sigmaaldrich.com/chemistry/solvents/tetrahydrofuran-center/physical-properties.html

25. Sigmaaldrich.com [Internet]. United States: Sigma-Aldrich Co LLC; c2013 [cited 2013 Sep 11]. Available from: http://www.sigmaaldrich.com/chemistry/solvents/dichloromethane-center/physical-properties.html

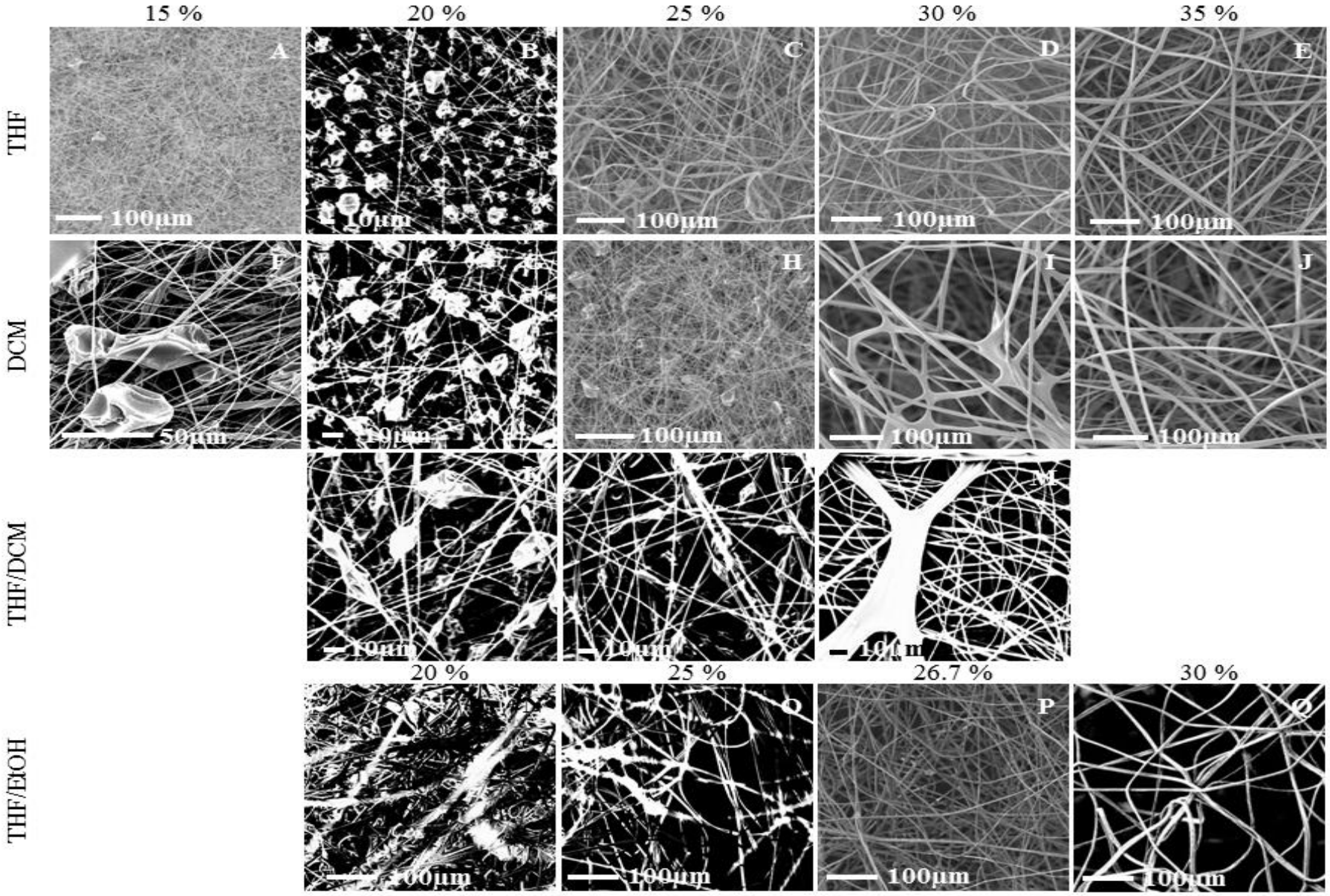

Figure 1: SEM images of electrospun PS fibres when dissolved in neat THF (A,B,C,D,E), neat DCM (F,G,H,I,J), THF/DCM solvent mix (K,L,M) and THF/EtOH solvent mix (N,O,P,Q) at concentrations of 15%, 20%, 25%, 26.7%,30% and 35% (w/v).

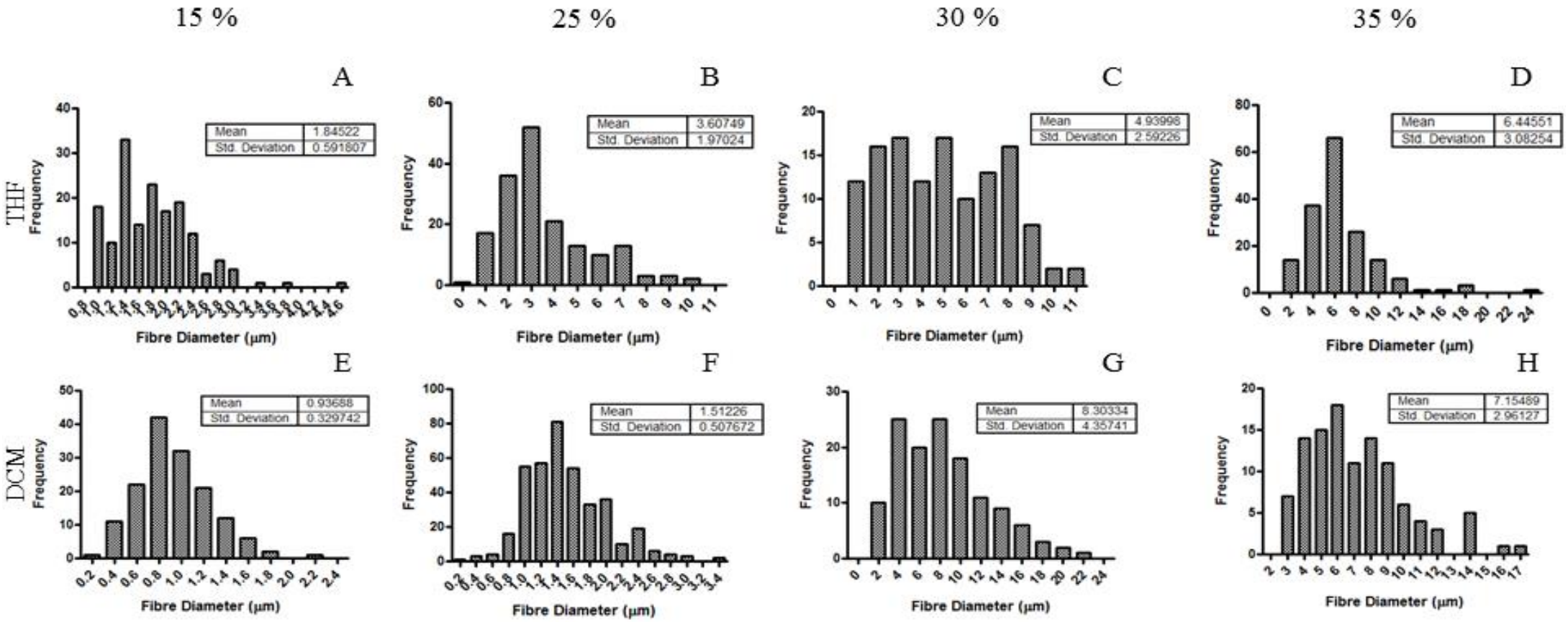

Figure 2: Frequency distribution graphs of electrospun PS fibre diameter when dissolved in neat THF (A,B,C,D) and neat DCM (E,F,G,H) at concentrations of 15%, 25%, 30% and 35% (w/v).

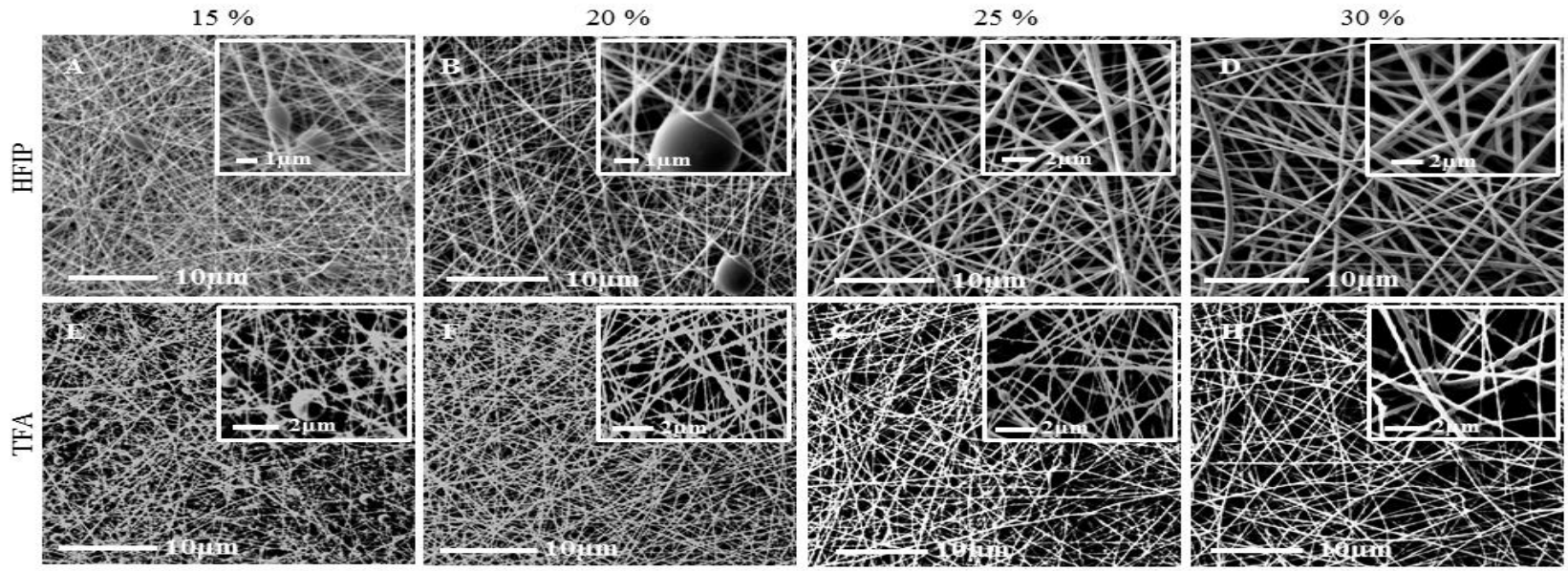

Figure 3: SEM images of elctrospun PET fibres when dissolved in neat HFIP (A,B,C,D) and neat TFA (E,F,G,H) at concentrations of 15%, 20%, 25% and 30% (w/v).

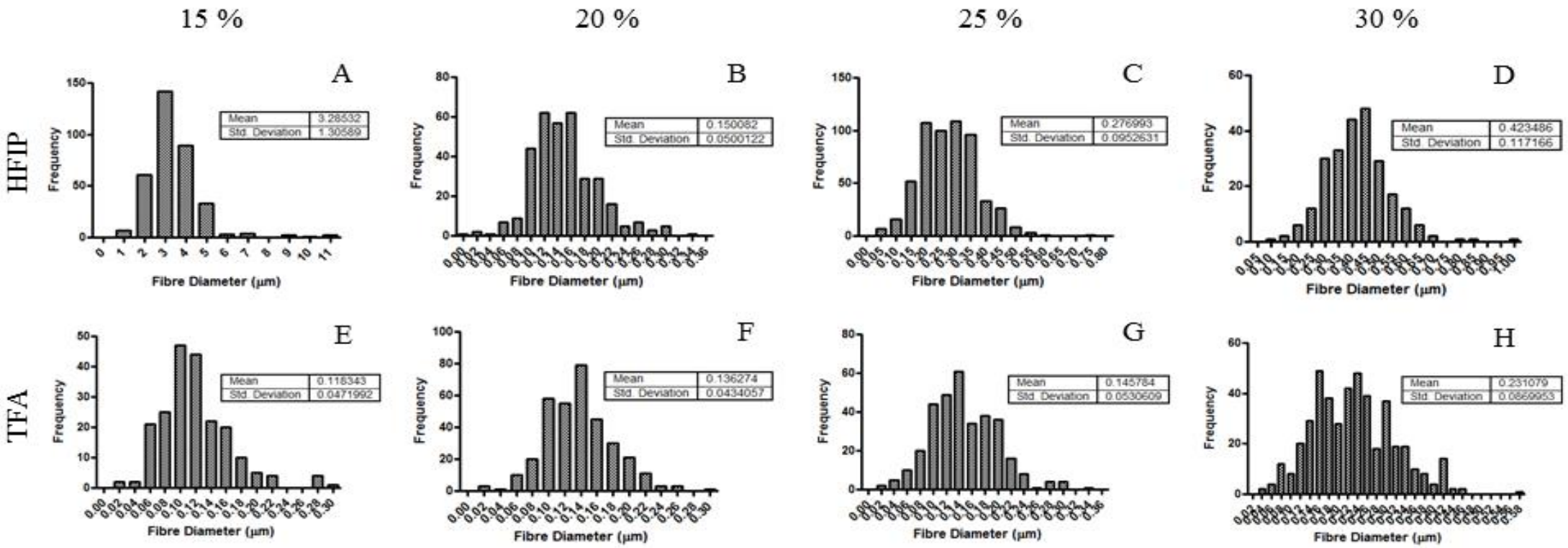

Figure 4: Frequency distribution graphs of electrospun PET fibre diameter when dissolved in neat HFIP (A,B,C,D) and neat TFA (E,F,G,H) at concentrations of 15%, 20%, 25% and 30% (w/v).

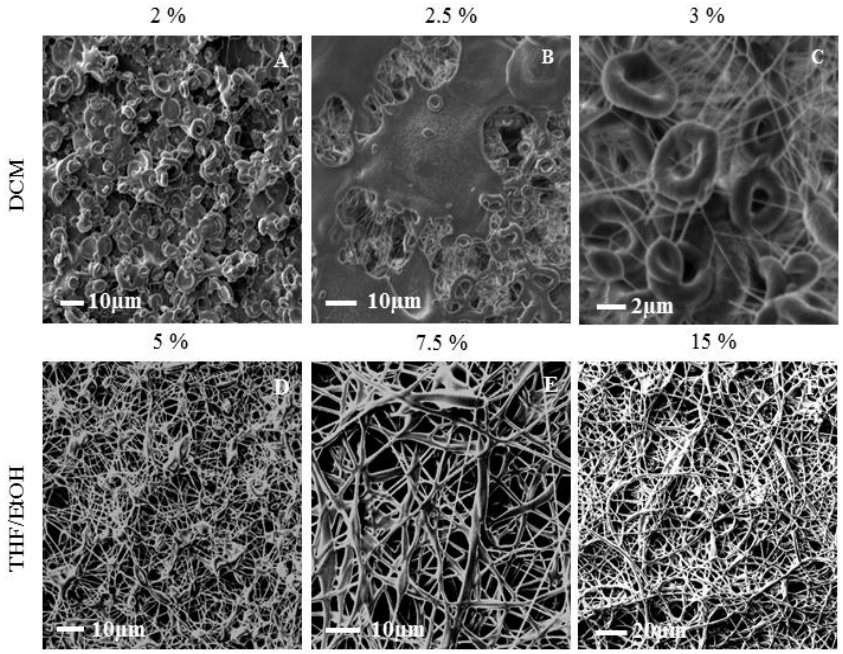

Figure 5: SEM images of electrospun PU fibres when dissolved in neat DCM (A,B,C) at concentrations of 2%, 2.5% and 3% (w/v) and when dissolved in THF/EtOH solvent mix (D,E,F) at concentrations of 5%, 7.5% and 15% (w/v).

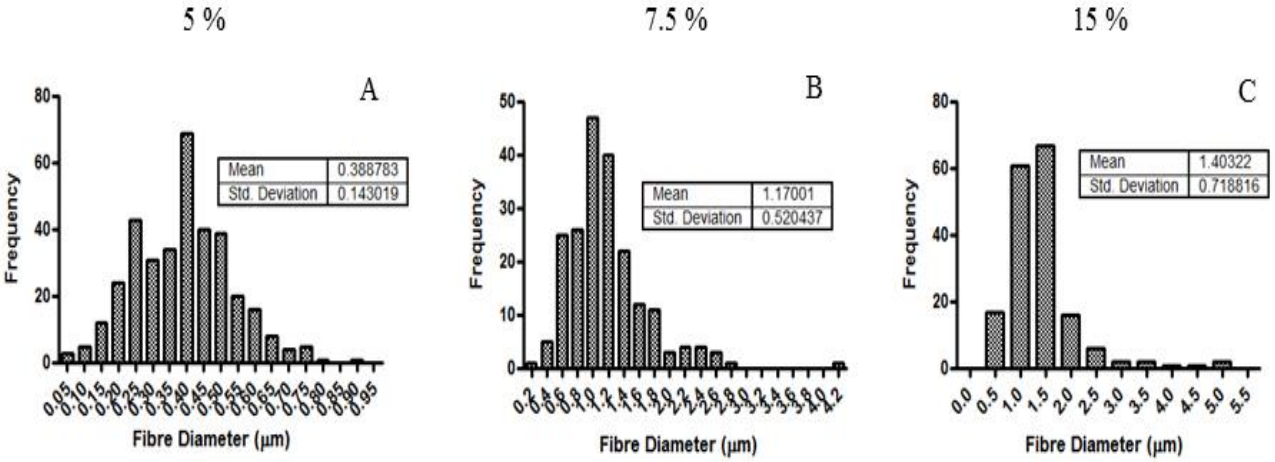

Figure 6: Frequency distribution graphs of electrospun PU fibre diameter when dissolved in THF/EtOH solvent mix (A,B,C) at concentrations of 5%, 7.5% and 15%

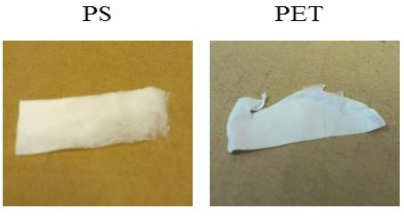

Figure 7: Photographs of PS and PET electrospun mats.

Figure 8: Photograph of intertwined PU electrospun mats.

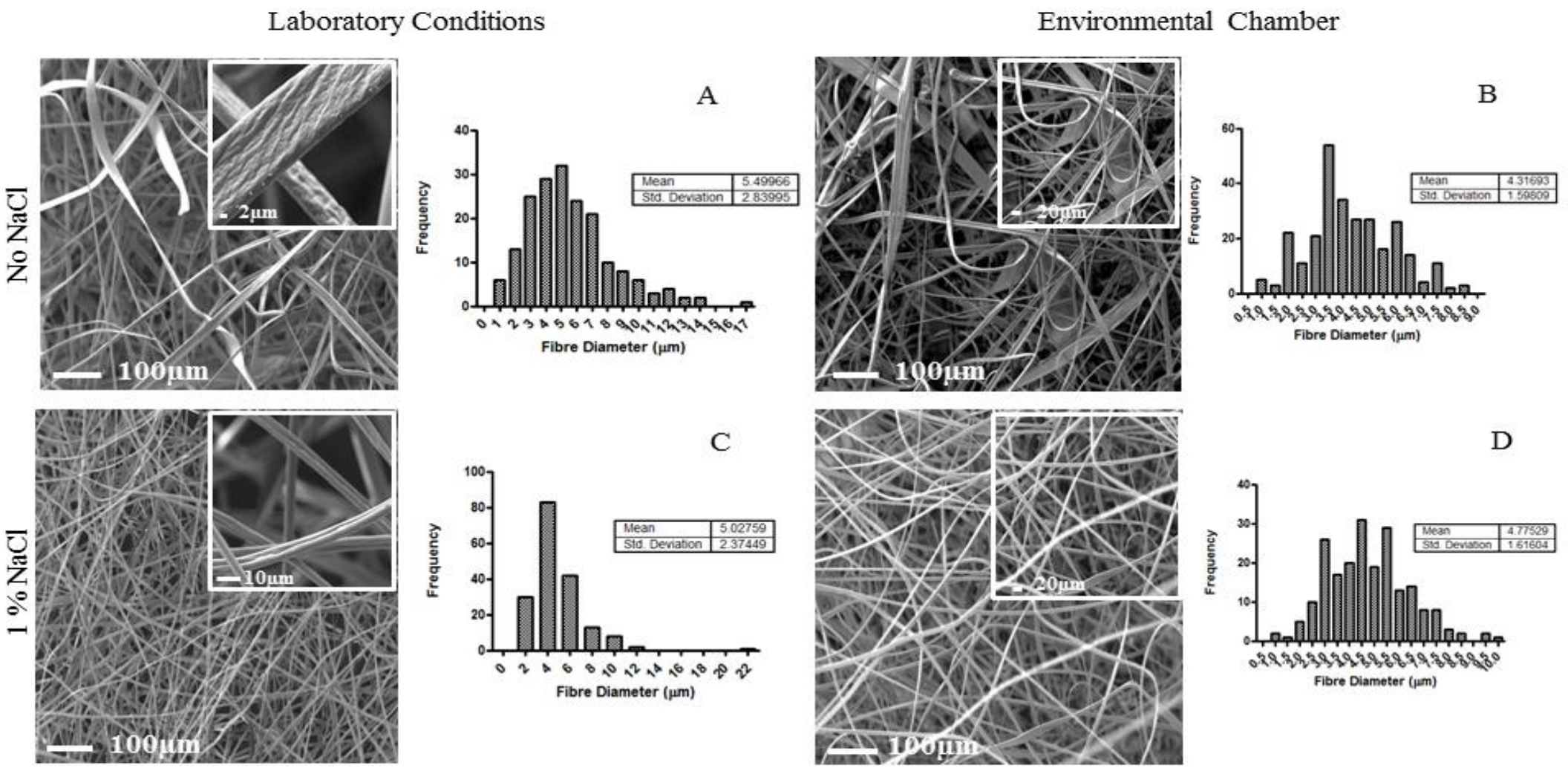

Figure 9: SEM images and frequency distribution graphs of fibre diameter of 26.7% (w/v) PS dissolved in THF/EtOH solvent mix and electrospun with no salt under laboratory conditions (A), no salt in an environmental chamber (B), 1% (w/v) NaCl in laboratory conditions (C) and 1% (w/v) NaCl in an environmental chamber (D).

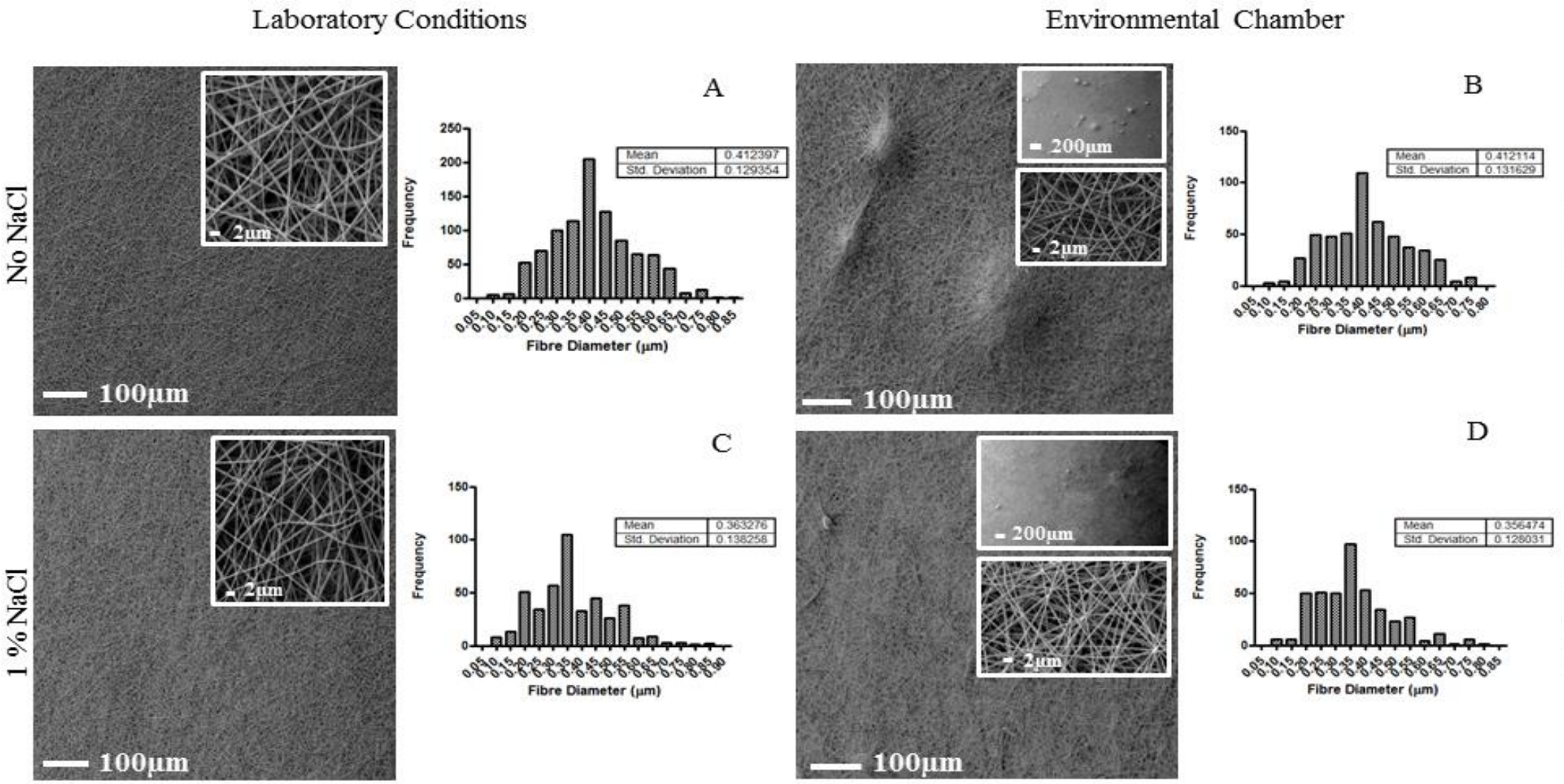

Figure 10: SEM images and frequency distribution graphs of fibre diameter of 30% (w/v) PET dissolved in neat HFIP and electrospun with no salt under laboratory conditions (A), no salt in an environmental chamber (B), 1% (w/v) NaCl in laboratory conditions (C) and 1% (w/v) NaCl in an environmental chamber (D).

Polymer	Conc (%w/v)	Solvent	Working Distance (cm)	Voltage (kV)	Flow Rate (mL/h)	Fibre Quality	Notes
PS	35	DCM	10	20	1	Fibres	Transition between beads on a string and fibres was exhibited for both solvents within the range of 20% to 30% w/v concentrations. Therefore further tests were carried out for polymer concentrations within this concentration range. A mixture of solvents was tried to attempt to use the ease of spinning with DCM together with the fact that fibres were exhibited at a lower concentration of polymer solution in THF.
	30			25			
	25		5	20		Beading	
	20		10	16			
	15			20	2		
	35	THF	10	15	2	Fibres	
	30			25			
	25						
	20			16	1	Beading	
	15			25	5		
	30	DCM/THF	10	16	1	Fibres	
	25			20		Beading	
	20						
PS	30	THF/EtOH	5	24	5	Fibres	Fibre formation was easily disrupted with neat THF. Solvent combination of THF/EtOH used in the ratio 20mL:10mL THF:EtOH, or 66.67%:33.33% (v/v). Although PS does not dissolve in neat EtOH, PS dissolved well in this solvent mixture. Electrospinning was carried out with ease, giving reproducibly good fibre collection.
	28.3		10		3		
	26.7				3		
	25				5	Beading	
	20						
	20				1		

Table 1: Table showing the electrospinning parameter changes, the solvent combinations used and the resulting fibre quality for PS.

Polymer	Conc (% w/v)	Solvent	Working Distance (cm)	Voltage (kV)	Flow Rate (mL/h)	Fibre Quality	Notes
PET	30	HFIP	15	15	1	Fibres	PET did not dissolve in acetone, THF, DCM, chloroform or m-Cresol. The only solvents found suitable for PET were HFIP and TFA. They are also highly toxic and corrosive, so ensuring removal of all the solvent would be ideal pre-cell culture.
	25						
	20						
	15					Beading	
	30	TFA	10	15	0.5	Fibres	
	25						
	20					Beading	
	15						

Table 2: Table showing the electrospinning parameter changes, the solvent combinations used and the resulting fibre quality for PET.

Polymer	Conc (% w/v)	Solvent	Working Distance (cm)	Voltage (kV)	Flow Rate (mL/h)	Fibre Quality	Notes
PU	3	DCM	10	18	1	Beading	First attempts (following Khil et al 2003) at spinning PU were problematic. Very low concentrations exhibited spraying as opposed to spinning. Higher concentrations with DCM/THF gave very viscous polymer solutions, which could not be introduced to the syringe for spinning. Another paper followed (S.A. Theron et al 2004) solvent mix was changed.
	2.5						
	2						
	3	THF	10	18	1	Not spinnable.	
	2.5			23			
	2		8	25	2		
	3	DCM/THF	8	18	2	Not spinnable.	
	2.5						
	2						
	15	THF/EtOH	10	20	1	Fibres	
	7.5						
	5					Beading	

Table 3: Table showing the electrospinning parameter changes, the solvent combinations used and the resulting fibre quality for PU.

Chapter 6: Publication Title: Assessing the suitability of electrospun poly(ethylene terephthalate) and polystyrene as cell carrier substrates for potential subsequent implantation as a synthetic Bruch's membrane.

Publication DOI: 10.1080/00914037.2014.945206

Available at: http://dx.doi.org/10.1080/00914037.2014.945206

Journal: International Journal of Polymeric Materials and Polymeric Biomaterials

Page Number in Thesis: 87

Assessing the suitability of electrospun poly(ethylene terephthalate) and polystyrene as cell carrier substrates for potential subsequent implantation as a synthetic Bruch's membrane.

Atikah Shahid Haneef[a*] and Sandra Downes[a]

[a]School of Materials, Materials Science Centre, Department of Engineering and Physical Sciences, The University of Manchester, Grosvenor Street, Manchester, M1 7HS, United Kingdom.

*Corresponding author: atikah.haneef@postgrad.manchester.ac.uk

Abstract

Electrospun poly(ethylene terephthalate) (PET) and polystyrene (PS) were tested for suitability as cell carrier substrates. Membranes were UV/ozone treated, which improved protein adsorption, with aminolysis observed on PET. PET demonstrated greater handling and durability compared to PS.

Treated and untreated PET supported cell proliferation, with cells exhibiting the desired monolayer morphology. Untreated PS did not support cell proliferation and although treated PS did, the resultant RPE cell morphology was undesirable.

Preliminary tests investigating thickness of mats were also undertaken, with PET exhibiting better results. Electrospun PET exhibited cytocompatibility, and could prove to be a suitable candidate for potential subsequent implantation.

Key words: AMD, cytocompatibility, electrospinning, cell carrier substrate, Bruch's membrane.

1. Introduction

Age-related macular degeneration (AMD) is the primary registered cause of blindness in the Western world.[1] Currently 182-300 thousand people are affected in the United Kingdom alone, with 20-25 million affected worldwide[2] and due to an increase in life

expectancy, clinicians predict this value to triple in the next three decades.[3] AMD is a disorder of the retina, in particular the macula region, which arises due to degeneration of the retinal pigment epithelium (RPE). The basement membrane of the RPE forms the inner most layer of the Bruch's membrane (BM), which together separate the neurosensory retina from the underlying highly vascularised choroid layer of the eye. In dry AMD (the most common form) it is thought that the BM thickens because oxidation products cross-link in the BM, forming a barrier called advanced macular oxidation products (AMOPS) which thicken over time, blocking exchange of nutrients and waste across the membrane.[4] The RPE monolayer is therefore not able to obtain nutrients and may be exposed to waste products, ultimately causing RPE cell death, monolayer disruption, and photoreceptor death, in turn causing central blindness.

Investigations looking at seeding cells on various layers of the native BM showed that the lower the layers got, the more cell death occurred[5,6] and that AMD afflicted eyes did not allow RPE cells to resurface well,[6] although promise has been reported through re-engineering of the native BM by slowly washing out the age-related changes from the BM followed by extracellular matrix coating.[7,8] Much discussion has been placed on whether a degradable or non-degradable membrane should be used.[9] It has been suggested it may be advantageous to employ the use of a cell carrier substrate, whether degradable, non-degradable or degradable over a needed time period, since it would provide protection to the transplanted cells from the diseased BM as well as enable a complete monolayer of RPE cells to be transplanted.[9]

Comparisons between the planar surface of poly(ethylene terephthalate) (PET) transwell inserts and commercially available, fibrous surface of electrospun polyamide nanofibres (EPN) in response to RPE cell survival and tolerance to sub-retinal insertion have been explored.[10-12] Both polymers have been reported to allow good RPE cell growth and survival and also exhibit gross tolerance towards sub-retinal implantation, with no

suggestions of inflammation or overt toxicity to the choroid or retina.[11,12] Although both PET and EPN showed very good cell response, EPN has been described as being a better surface for RPE cell replication, due to its fibrous structure.[10,12] Fibrous surfaces have been previously reported to allow cells to exhibit a more *in vivo*-like morphology than compared to when grown on planar surfaces[13-16] and since the native BM is fibrous[8] it would be ideal if the cell carrier substrate were to also mimic this fibrous structure.

The native BM is 2-4.7 μm thick[17,18] and is comprised of five distinct layers consisting of the basement layer that RPE cells attach to, an inner fibrous collagen layer, a fibrous elastic sheet, an outer collagen fibre layer and a basement layer upon which capillary endothelial cells of the choroid attach to.[8,18] Therefore a fibrous cell carrier substrate would be advantageous, since it would give a truer reflection of the native BM. The synthetic cell carrier substrate should also show good mechanical stability, robustness and some degree of elasticity, since the native BM contains an elastic layer, and to allow for good surgical handling.

Previous investigations have looked at using electrospun methacrylate based co-polymer scaffolds as a permanent BM replacement.[19] PET has been investigated as a material for cell transplantation[20] and has been electrospun to form fibrous scaffolds for large vascular replacements due to its biostability.[21] UV/ozone treatment has also been investigated for PET films.[22]

In the present study we aimed to assess the suitability of electrospun PET and PS as cell carrier substrates, for eventual implantation in application for the treatment of dry AMD. Mats were fabricated by electrospinning non-degradable polymers PET, which has been previously reported as being good for RPE cell survival and has shown good tolerance to sub-retinal insertion,[10-12] and polystyrene (PS), which is a universally used polymer in tissue culture plastic for cell culture. Variables investigated were tensile strength,

thickness, porosity, effect of UV/ozone treatment on surface chemistry, cell morphology and monolayer formation.

2. Materials and Methods

All chemicals and reagents were purchased from Sigma-Aldrich Ltd. (Dorset, UK) unless otherwise stated.

2.1 Substrate Fabrication

In all instances the polymer solution was stirred overnight on a magnetic stirrer plate to give a homogeneous mixture. In all instances a 21G hypodermic needle (BD Microlance, Ref 304432) with the sharp tip shaved down to a blunt end was used. The homogeneous polymer solution was introduced into a 10 ml plastic syringe and the blunt-tip hypodermic needle attached. Any air-bubbles were removed and the filled syringe was fixed in a mechanical syringe pump. All experiments were repeated twice. Using a previously published paper as reference,[23] the following parameters were used:

PET 25 % (w/v), voltage 15 kV, working distance 15 cm, flow rate 1 ml/hr, and collection time 60 minutes.

PS 26.7 % (w/v), voltage 25 kV, working distance 10 cm, flow rate 2 ml/hr, and collection time 60 minutes.

2.2 Characterisation

2.2.1 Surface Treatment & Water Contact Angle (WCA) Measurement

Mats were cut into approximately 1 cm^2 squares and placed in a UV/ozone chamber (Novascan, Digital UV Ozone System, model number PSD-UV4). A pure oxygen flow was allowed to fill the chamber for 5 minutes. Samples were treated in a pure oxygen flow for 300 s and 450 s at room temperature at 10.1 cm and 0.5 cm away from the UV lamp for PET, and at 2.8 cm and 0.5 cm away from the UV lamp for PS. After the lapsed time the UV light was switched off, oxygen flow turned off and the chamber was allowed to empty for 5 minutes in a fume hood under extraction fan flow. Water contact angle (WCA) was

measured using a contact angle analyser (DSA100, Kruss, Hamburg, Germany). Three drops of 3 µl distilled water were placed on the mat surface and the sessile drop contact angle measured using Kruss Drop Shape Analysis software (Kruss, Hamburg, Germany). (n=9).

2.2.2 X-ray Photon Spectroscopy (XPS) for Surface Chemistry Analysis

Analyses of the elements present on the mat surfaces, after UV/ozone treatment, and after UV/ozone treatment followed by immersion in complete media [50/50 mix of Dulbecco's modified Eagle's medium (DMEM) (PAA laboratories, UK) and Ham's F12 nutrients (PAA laboratories, UK), with 10 % foetal bovine serum (PAA laboratories, UK), 1 % penicillin/streptomycin antibiotic mixture (PAA laboratories, UK) and 1 % L-glutamine (PAA laboratories, UK)], was carried out using X-ray Photon Spectroscopy (XPS) (Axis Ultra, Kratos) with analysis carried out using CasaXPS (CasaXPS MCF Application, Casa Software Ltd). Electrospun PET and PS mats were cut to approximately 4 mm by 6 mm strips and then UV/ozone treated. Samples immersed in media following UV/ozone treatment were incubated, without cells, for 1 hour at 37˚c, 5 % CO_2, 98-99 % humidity, and then washed twice in distilled water before allowing to air dry.

2.2.3 Tensile Testing & Handling

Qualitative testing was carried out by hand. Mats were cut into 1 cm by 2 cm strips, and underwent folding, rolling, and twisting. (n=3).

Quantitative tensile testing of the electrospun mats were measured using Instron 1122 (Instron series 1x Automated Materials Tester) equipped with a 5N load cell at a displacement rate of 5 mm/minute. Mats were cut into 1 cm by 2 cm strips, mounted onto a paper frame, and fixed with tape. The mats were tested until failure. (n=3).

2.2.4 Thickness & Porosity

Mats were cut into approximately 1 cm^2 squares and thickness measured using a digital micrometer (HITEC, 190-00, Farnell), which were then weighed and the porosity calculated using the following equation:

Porosity (%) = [1 – (apparent density/bulk density)] x 100

Where apparent density (g/cm^3) = [mat mass (g)/mat thickness (cm)] x mat area (cm^2)

Bulk density of PET was taken as 1.4 g/cm^3 [24] and the bulk density of PS was taken as 1.05 g/cm^3.[25] (n=3).

2.3 Cell Culture

ARPE-19 cells (ATCC-LGC, CRL-2302) were seeded at a density of 10,000 cells/cm^2 for the 5 day study and 50,000 cells/cm^2 for the 2 month study and incubated at 37˚c, 5 % CO_2, 98-99 % humidity. Media was changed every three days. The positive control was 11 mm borosilicate discs (Scientific Laboratory Supplies, MIC3302) and the negative control was low attachment 24-well plates (Corning® Costar®).

2.3.2 Proliferation: Alamar Blue

Alamar blue solution [5 mg resazurin salt in 40 ml Dulbecco's phosphate buffered saline (PBS) (PAA laboratories)] was added to each sample to give 100 µl of Alamar blue solution per 1 ml media, and returned to the incubator for the time dictated by the calibration curve. A 200 µl aliquot of media was taken from each sample and transferred into a black bottomed 96-well plate. Fluorescence was measured at 530-510 nm excitation and 590 nm emission using a fluorescence reader (FLUOstar OPTIMA, BMG LABTECH). (n=9). (See appendix for method for cell counting using Alamar blue).

Statistical analysis was carried out using one way ANOVA, with Tukey's multiple comparisons post-test to measure the differences between each condition on each day of cell culture using GraphPad Prism 5 (GraphPad Software Inc.). Significant difference in

data is denoted by: $P<0.05$. High significant difference is denoted by: *** = $P<0.001$, good significant difference is denoted by: ** = $0.001 \leq P \leq 0.01$, significant difference is denoted by: * = $0.01 \leq P \leq 0.05$ and no significant difference is denoted by: ns = $P>0.05$.

2.3.3 Morphology & Monolayer Formation: DAPI/Phalloidin & SEM

Samples were fixed with 3.7 % Formalin for 10 minutes at room temperature then washed twice with PBS. After soaking in ICC buffer [50 ml PBS, 500 µl goat serum, 50 µl of 0.1 % Triton X-100 in PBS and 5 mg/ml bovine serum albumin] for 30 minutes at room temperature, the ICC buffer was removed and samples stained with Fluoresein Phalloidin (Invitrogen) (1:40 from stock Phalloidin: ICC buffer [50 µl: 2 ml]) for 20 minutes at room temperature. Samples were washed twice with PBS, mounted onto glass slides with DAPI Prolong Gold antifade (Invitrogen), and left at 4˚C in the dark overnight to cure. Images were obtained with a fluorescence microscope (Nikon eclipse 50i JENCONS-PLS). (n=3).

For SEM, samples were removed from the incubator at relevant time points and washed twice with PBS, fixed with 1.5 % glutaraldehyde (Fluka, 85191) in PBS for 30 minutes at 4˚C, washed twice with PBS, dehydrated using graded ethanol: 2 x 3 minutes 50 %, 2 x 3 minutes 70 %, 2 x 3 minutes at 90 % and 2 x 5 minutes at 100 %, soaked in fresh hexamethyldisilazane (HMDS) (Fluka, 999-97-3) for 2 x 5 minutes, left to evaporate to dryness in a fume cupboard. Dried samples were mounted on sticky carbon pads (Agar), placed on aluminium stubs (Agar), and gold sputter coated (Edwards, Sussex, UK). Images were obtained using Phenom Pro Desktop SEM (Phenom World) at an EHT value of 5 kV. (n=3).

Monolayer formation was measured using a transepithelial electrical resistance (TEER) measurer (EVOM2, epithelial voltohmmeter, World Precision Instruments). Samples were set up in Scaffdex® and placed in a well containing 1 ml complete media only. Media with cells (1 ml) were seeded at a density of 50,000 cells/cm^2 onto the surface of the sample. TEER measurements were taken, in ohms, every 7 days up to 56 days. All

measured values were blanked by removing background TEER values of the membrane immersed in complete media only. Higher resistance values denote formation of monolayer.

2.4 Preliminary Experiment on Varying PET and PS mat thickness

The natural BM is between 2-4.7 μm thick,[17,18] so it would be ideal if the membrane investigated could also match this thickness. As discussed in a previous publication[23] PET exhibited a desirable flatter overall mat morphology, similar to tape, and so to investigate thickness, collection times were altered. PET mats were collected for: 1, 2, 3, 4, 5, 10, 15 and 60 minutes.

Contrastingly, PS mats exhibited an unwanted fluffy overall mat morphology as discussed previously.[23] So to investigate thickness, PS mats were compressed instead of varying collection times, since 60 minutes was found to allow a good collection of fibres for PS to be taken forward for further experiments. PS mats were cut into 1 cm^2 squares, placed between two clean acetate sheets and compressed to the pressure of 4.982 x 10^8 Nm^{-2} using a press (30 ton press, Research Industrial Instruments Company, London, England). Thickness and porosity measurements were taken for these mats as aforementioned. (n=3).

3. Results & Discussion

3.1 Characterisation

3.1.1 Surface Treatment & Water Contact Angle (WCA) Measurement

Water contact angles (WCA) for PET and PS decreased as treatment times increased (Table 1), indicating that oxygen modification of the surfaces had taken place.[26,27] Treatment times of 300 s was found to give the desired approximately 60° water contact angle, which is reported to be the ideal contact angle for protein adsorption.[28] The untreated and 450 s treated samples provided a comparison for higher and lower water contact angles, respectively. For comparison on PS 2.8 cm away from the UV source was used as 10.1 cm away from the UV source had no effect on WCA for PS (data not shown).

It was also found that high treatment times caused discolouration on PS mats, an indication of oxygen incorporation and degradation.[29]

3.1.2 X-ray Photon Spectroscopy (XPS) for Surface Chemistry Analysis

XPS analysis showed that PS was more susceptible to surface oxidation,[30] as oxygen groups were added to PS but not PET following UV/ozone treatment (Figure 1, Table 2, Table 3). Examination of treated PS spectra showed one new carbon species and two new oxygen species after UV/ozone treatment, exhibiting phenolic oxygen peaks at 284.92 eV and carboxylic oxygen peaks at 285.16 eV respectively. Little difference in oxygen incorporation between 300 s and 450 s treated PS was observed. The low amount of oxygen observed on untreated PS is due to residual THF and ethanol, which contain oxygen in their chemical structures. No fluorine peaks were observed in PET, suggesting no residual HFIP was left in PET fibres. Closer evaluation of the PET spectra showed three peaks for carbon and two peaks for oxygen present at all treatment times, therefore the change in WCA for PET may be due to effects of mat handling, giving an appearance of WCA reduction.

After incubation in cell culture media, however, XPS spectra showed nitrogen was introduced onto the surface of the PET mats regardless of UV/ozone treatment, whereas on PS nitrogen was only introduced after treatment (Figure 2 Table 4, Table 5). Closer evaluation of incubated PET spectra showed an increase in the number of carbon environments and a shift in the position of the oxygen peaks, as well as the presence of nitrogen peaks, suggesting that the N-terminal of the proteins were able to undergo aminolysis, opening the ester bond in PET (Figure 3).[31] The two new carbon peaks found at 287.67 eV and 285.84 eV are -C(O)N and C-OH peaks respectively, the nitrogen peak present is the nylon-like -C(O)N peak at 399.96 eV, which coincides with the suggestion of aminolysis occurring in the ester, and also explains why nitrogen was detected on untreated PET. This is further backed up by the observation that the ratio of aliphatic and carboxylic

carbon, and C-O-C oxygen species was reduced on incubated PET compared to the ratio found on PET that had not been immersed in media (Table 3, Table 5). Our results are in agreement with Atthoff *et al.* who found that surface activation of PET would be preferred over untreated as more protein was found on surface activated PET.[31]

Incubated UV/ozone treated PS spectra also showed an increase in the number of carbon and oxygen environments. There was only one new carbon peak detected on 450 s treated PS at 284.07 eV, which denoted the –C-N bond. There were three new oxygen peaks present on 300 s and 450 s treated PS found at 527.02 eV, 528.08 eV and 528.98 eV indicating –C-OH, -COOH and –C(O)N respectively. The nitrogen peaks found only on treated PS were at 395.79 eV and 3.95.53 eV respectively and denoted the presence of –C(O)N bonds, an aramide (aromatic amide)-like bond. The lack of nitrogen on untreated PS indicated a lack of protein adsorption, suggesting UV/ozone treatment is necessary for protein adsorption for PS. The presence of chlorine, a common contaminant,[32] was also observed on the surfaces of treated PS, suggesting that UV/ozone treated PS is susceptible to contamination, as this was not present on PET.

3.1.3 Tensile Testing & Handling

Qualitative tests showed that PET was more robust than PS. PET was able to withstand all tests without falling apart. Tensile tests showed that the maximum allowable strain until failure for electrospun PET collected for 60 minutes was 166.06 Nm^{-2}. PS mats were fragile and loss of sample occurred, sometimes leaving a gritty powder (Figure 4). The PS mats were too delicate to undergo tensile tests, therefore tensile properties of electrospun PS could not be ascertained. This is a contrary finding to Baker *et al.*, however comparison is made difficult since a collection time of their mats is not reported.[25]

3.1.4 Thickness & Porosity

PS mats were an average of 180.7 μm (SD ± 25.6) thick with 92 % (SD ± 0.74) porosity, and PET mats were an average of 50.7 μm (SD ± 2.96) thick with 86 % (SD ± 2.26)

porosity. The higher porosity of PS could be due to the looser packing of the fibres, as confirmed by its poor mechanical properties, and due to the larger fibres, which in turn leave larger voids between each fibre. The thinner PET mats exhibited better handling in comparison to PS mats.

As aforementioned, the natural BM consists of layers, one of which is the RPE basal lamina that has been described as a meshwork of fibres, however no fibre diameter is given.[33] The inner collagenous layer is a layer of fibres that are 60-70 nm in diameter.[33,34] Previously reported results showed PS fibres with an average diameter of 550 μm (SD ± 2.84) and PET fibres with an average diameter of 277 nm (SD ± 0.095).[23] We have fabricated the meshwork of fibres to match the natural BM, but further reduction of the fibre diameter would be beneficial.

3.2 Cell Culture

For the purposes of this study, mats collected for 60 minutes at 0 s, 300 s, and 450 s UV/ozone treatment times were taken forward for cell culture. Collection times less than this did not produce a good enough mat of PS fibres (data not shown) that could be taken forward for practical use.

Initially, cell count was deliberately kept low at 10,000 cells/cm^2 in order to ascertain whether cells reacted well to the material, and not just to the presence of other close proximity cells. Once the behaviour of the cells towards each substrate was ascertained, the cell count was increased to 50,000 cells/cm^2 for the two month cell culture in order to assess the formation and maintenance of a complete monolayer.

3.2.1 Proliferation: Alamar blue

Short term Alamar blue results showed that RPE cells grew on both treated and untreated PET (Figure 5). In contrast, untreated PS exhibited lowest cell growth, over time compared to both 300s and 450s treated PS. Overall higher cell number was exhibited on

PS, which may be due to the cells being able to grow on the inner fibres, rather than just on the surface, due to larger voids between fibres in PS.[35]

Long term Alamar blue results for PET showed an increase in the cell number (Figure 6) for all treatment times. Alamar blue also confirmed a significantly lower cell number on the positive controls, than compared to PET. Therefore the long term cell culture suggests that ARPE-19 cells are able to grow and survive on electrospun PET.

3.2.2 Morphology & Monolayer Formation

DAPI/Phalloidin fluorescence staining and SEM demonstrated that for PET, even the untreated samples allowed cell growth (Figure 7, Figure 8). Cells grew in patches[16] starting to form monolayers in the short term culture. Fluorescence images for PS also showed cell presence only on UV/ozone treated surfaces, although not in the monolayer morphology as exhibited on PET, but wrapped around individual fibres due to the larger distance between PS fibres.[35,36] Due to this and the poor handling quality of electrospun PS, it was not taken forward for long term cell culture.

Fluorescence staining images and SEM images confirmed the growth and maintenance of cells on PET up to day 56 (Figure 9, Figure 10). Fluorescence images showed that ARPE-19 cells had a different morphology on the fibrous mats compared to the planar glass control. This can be associated with the obvious difference in surface topography between glass discs and fibrous electrospun PET.[10,12,15,37] Some cracking is visible in the SEM images, which can be associated with the dehydrating step in the SEM sample preparation method, since the phalloidin stain in the fluorescence images exhibit cell to cell contact. By day 56 the positive control exhibited fewer cells on the surface of the glass than compared to PET.

Failure to reach complete monolayer can be attributed to a number of factors. It could be due to low cell count used in experiments, others have used much higher cell densities.[38-40]

Or due to surface roughness which has been reported to exhibit slow cell growth, compared to smooth surfaces.[41] Or it could be a result of high substrate porosity which has been reported to reduce cell proliferation, due to formation of aggregates which inhibit further proliferation because of cell-cell contact.[36]

TEER measurements for PET showed a gradual increase in electrical resistance, which corresponded to monolayer formation (Figure 11). TEER values towards the end of the two month study were similar to human RPE-choroid resistance of 36-148 Ωcm^2.[42] Initially, 300 s and 450 s UV/ozone treated PET exhibited higher TEER readings, compared to untreated PET. By day 56, TEER readings had begun to plateau for all three conditions. Untreated PET also allowed the formation of a monolayer, but at a slower rate. Our results coincide with Dunn *et al.*.[38] However others have reported higher values reached at shorter culture times[40] or lower values throughout culture period,[39,43] some with the use of supplements,[38,39] and others without.[40] Cell densities used in some investigations were much higher than the density used in our investigations,[38-40] whereas others matched ours.[43] Mixed reported results reinforces the advice that caution be exercised when comparing results with others, as ARPE-19 cell behaviour is dependent upon the history of how they were maintained and passaged.[39,40]

3.3 Preliminary Experiment on Varying PET and PS Thickness

Clearly, the mats do not match the 4.7 μm thickness of the native BM,[17,18] so preliminary investigation into altering electrospinning collection time and mat compression were carried out. The collection time was altered for the PET mats, since they already exhibited a flat tape-like gross morphology, whereas compression was undertaken for PS since its uncompressed form was fluffy, and reducing the collection time for PS did not allow an adequate mat to be fabricated.[23]

Tensile properties of the PET mats generally increased with increased collection time, but the thickness and maximum strain before failure varied largely (Figure 12). This variation

could due to the erratic placement of fibres in electrospinning .[23,24] At 15 minutes mats were 16 μm (SD ± 2.31) thick with 65.3 % (SD ± 11.8) porosity, at 10 minutes mats were 19 μm (SD ± 2.6) thick with 70.17 % (SD ± 20.95) porosity, at 5 minutes mats were 11.7 μm (SD ± 1.86) thick with 72.77 % (SD ± 8.9) porosity, at 4 minutes mats were 8 μm (SD ± 0) thick with 29.6 % (SD ± 1) porosity, at 3 minutes mats were 4.3 μm (SD ± 0.67) thick with 50.70 % (SD ± 4.16) porosity, at 2 minutes mats were 7.67 μm (SD ± 0.3) thick with 50.70 % (SD ± 4.3) porosity, and at 1 minute mats were 8.67 μm (SD ± 1.45) thick with 71.2 % (SD ± 4.9) porosity. The thicknesses exhibited would be appropriate for subsequent implantation as thicknesses of 10-14 μm have been reported as being suitable for sub-retinal implantation.[34]

After compression, the PS mats measured an average of approximately 38.7 μm (SD ± 1.33) thick with 61.33 % (SD ± 14.04), therefore porosity was reduced after compression. Photographs showed that the mats were flatter post-compression and SEM images showed that fibres post-compression were packed more closely, while still maintaining the fibrous structure (Figure 13). Tensile properties of the compressed PS mats could not be undertaken as the mats became more fragile post-compression.

Although PET has been reported to exhibit gross tolerance to sub-retinal insertion,[11,12] it is endeavoured that eventually *in vivo* testing will be undertaken in order to assess the suitability of electrospun fibrous PET as a replacement BM, since difference in scaffold morphology can cause diverse reactions *in vivo*, due to dissimilarity in scaffold physical properties.[44]

4. Conclusion

We have successfully fabricated nanoscale PET fibres of random orientation that we believe would be the ideal design for a cell carrier substrate with potential for subsequent implantation. It was found that PET allowed the addition of nitrogen without particular intervention making it a desirable candidate, as this represents protein adsorption. We

have also shown that electrospun PS mats would not be a suitable candidate, as they exhibited poor handling and cells were unable to form the correct morphology. Our results agree with previous literature that PET allows RPE cell growth and that electrospun PET has potential as a suitable cell carrier substrate.

Acknowledgements

This report presents independent research commissioned by the National Institute for Health Research (NIHR) under the Invention for Innovation (i4i) Programme. The views expressed in this report are those of the authors and not necessarily those of the NHS, the NIHR or the Department of Health. We would like to thank Professor Sven Schroeder and Dr Joanna Stevens for helping with the XPS equipment and software.

References

1. Resnikoff, S., Pascolini, D., Etya'ale, D., Kocur, I., Pararajasegaram, R., Pokharel, G.P., and Mariotti, S.P., B. World. Health. Organ. 82 (2004).

2. Chopdar, A., Chakravarthy, U., and Verma, D., Brit. Med. J. 326 (2003).

3. Minassian, D.C., Reidy, A., Lightstone, A., and Desai, P., Br. J. Ophthalmol. DOI: 10.1136/bjo.2010.195370 (2011).

4. Pulido, J., Sanders, D., Winter, J.L., and Klingel, R., J. Clin. Apheresis. 20 (2005).

5. Tezel, T.H., Kaplan, H.J., and Del Priore, L.V., Invest. Ophthalmol. Vis. Sci. 40 (1999).

6. Gullapalli, V.K., Sugino, I.K., Patten, Y.V., Shah, S., and Zarbin, M.A., Exp Eye Res. 80 (2005).

7. Tezel, T.H., Del Priore, L.V., and Kaplan, H.J., Invest. Ophthalmol. Vis. Sci. 45 (2004).

8. Del Priore, L.V., Tezel, T.H., and Kaplan, H.J., Prog Retin Eye Res. 25 (2006).

9. Binder, S., Br. J. Ophthalmol. 95 (2011).

10. Stanzel, B.V., Englander, M., Tieltges, F., Strick, D.J., Blumenkranz, M.S., Holz, F.G., Binder, S., and Marmor, M.F., DOG Kong. (2008).

11. Stanzel, B.V., Liu, Z., Brinken, R., Braun, N., Holz, F.G., and Eter, N., Invest. Ophthalmol. Vis. Sci. 53 (2012).

12. Li, Y., and Tang, L., J. Cent. S. Univ. Med. Sci. 37 (2012).

13. Schindler, M., Ahmed, I., Kamal, J., Nur-E-Kamal, A., Grafe, T.H., Chung, H.Y., and Meiners, S., Biomaterials. 26 (2005).

14. Nisbet, D.R., Forsythe, J.S., Shen, W., Finkelstein, D.I., and Horne, M.K., J. Biomater. Appl. 24 (2009).

15. Jean-Gilles, R., Soscia, D., Sequeira, S., Melfi, M., Gadre, A., Castracane, J., and Larsen, M., J. Nanotechnol. Eng. Med.-T. ASME. 1 (2010).

16. Thieltges, F., Stanzel, B.V., Liu, Z., and Holz, F.G., Ophthalmic. Res. 46 (2011).

17. Ramrattan, R.S., van der Schaft, T.L., Mooy, C.M., de Bruijn, W.C., Mulder, P.G.H., and de Jong, P.T.V.M., Invest. Ophthalmol. Vis. Sci. 35 (1994).

18. Booij, J.C., Baas, D.C., Beisekeeva, J., Gorgels, T.G.M.H., and Bergen, A.A.B., Prog. Retin. Eye. Res. 29 (2010).

19. Treharne, A.J., Thomson, H.A.J., Grossel, M.C., and Lotery, A.J., J. Biomed. Mater. Res. A. 100A (2012).

20. Liu, Y., Tao, H., Song, H., and Gao, C., J. Biomed. Mater. Res. A. 81 (2007).

21. Ma, Z., Kotaki, M., Yong, T., He W., and Ramakrishna, S., Biomaterials. 26 (2005).

22. Formosa, F., Anfuso, C.D., Satriano, C., Lupo, G., Giurdanella, G., Ragusa, N., Marletta, G., and Alberghina, M., Microvasc. Res. 75 (2008).

23. Haneef, A.S., and Downes, S., Int. J. Polym. Mater. 63 (2014).

24. Veleirinho, B., Rei, M.F., and Lopes-Da-Silva, J.A., J. Polym. Sci. Pol. Phys. 46 (2008).

25. Baker, S.C., Atkin, N., Gunning, P.A., Granville, N., Wilson, K., Wilson, D., and Southgate, J., Biomaterials. 27 (2006).

26. Gopal, R., Zuwei, M., Kaur, S., Ramakrishna, S. (2007). Surface Modification and Application of Functionalized Polymer Nanofibers. In: Mansoori, G.A., George, T.F., Assoufid, L., Zhang, G., editors. Molecular Building Blocks for Nanotechnology. (Springer, New York), p. 72-91.

27. Keselowsky, B.G., Collard, D.M., Garcia, A.J., J. Biomed. Mater. Res. 66A (2003).

28. Xu, L.-C., and Siedlecki, C.A., Biomaterials. 28 (2007).

29. Gillen, K.T., Wallace, J.S., and Clough, R.L., Radiat. Phys. Chem. 41 (1993).

30. Klein, R.J., Fischer, D.A., and Lenhart, J.L., Langmuir. 24 (2008).

31. Atthoff, B., and Hillborn, J., J. Biomed. Mater. Res. Part B: Appl. Biomater. 80B (2007).

32. xpssimplified.com [Internet]. Thermo Fisher Scientific Inc; c2013 [cited 2014 Jan 29]. Available from: http://www.xpssimplified.com/elements/chlorine.php

33. Curcio, A.C., and Johnson, M. (2013). Structure, Function, and Pathology of Bruch's Membrane. In: Ryan, S.R., Schachat A.P., Wilkinson C.P., Hinton, D.R., Sadda, S., and Wiedemann P., editors. Retina, 5th edition, (Saunders, USA), p. 465-481.

34. Warnke, P.H., Alamein, M., Skabo, S., Stephens, S., Bourke, R., Heiner, P., and Liu, Q., Acta. Biomater. 9 (2013).

35. Nisbet, D.R., Forsythe, J.S., Shen, W., Finkelstein, D.I., and Horne, M.K., J. Biomater. Appl. 24 (2009).

36. Ma, T., Li, Y., and Shang-Tang, Y., Biotechnol. Prog. 15 (1999).

37. Badami, A.S., Kreke, M.R., Thompson, M.S., Riffle, J.S., and Goldstein, A.S., Biomaterials. 27 (2006).

38. Dunn, K.C., Aotaki-Keen, A.E., Putkey F.R., and Hjelmland, L.M., Exp. Eye Res. 62 (1996).

39. Luo, Y., Zhuo, Y., Fukuhara, M., and Rizzolo, L.J., Invest. Ophthalmol. Vis. Sci. 47 (2006).

40. Mannermaa E., Reinisalo, M., Ranta V.-P., Vellonen, K.-S., Kokki, H., Saarikko, A., Kaarniranta, K., and Urtti, A., Eur. J. Pharm. Sci. 40 (2010).

41. Baharloo, B., Textor, M., and Brunette, D.M., J. Biomed. Mater. Res. A., 74A (2005).

42. Quinn, R.H., and Miller, S.S., Invest. Ophthalmol. Vis. Sci., 33 (1992).

43. Nevala, H., Ylikomi, T., and Tahti, H., Hum. Exp. Toxicol., 27 (2008).

44. Christiansen, A.T., Tao, S.L., Smith, M., Wnek, G.E., Prause, J.U., Young, M.J., Klassen, H., Kaplan, H.J., la Cour, M., and Kiilgaard, J.F., Stem Cells Int. DOI:10.1155/2012/454295 (2012).

Appendix

Six known cell suspensions were prepared using the stock cell suspension at the following cell densities: 10,000 cells/ml, 20,000 cells/ml, 40,000 cells/ml, 100,000 cells/ml, 150,000 cells/ml and 200,000 cells/ml. Each cell suspension (1 ml) was placed in triplicate in an adherent 24-well plate. After 15 minutes, to allow time for cells to attach, 100 µl Alamar blue solution was placed into each well (assuming 1ml of media in each well) and incubated at 37 ˚C, 5 % CO_2, at 98-99% humidity. At time interval (2 hrs, 2.5 hrs, 3 hr, 3.5 hrs and 4 hrs) 200 µl of each sample (triplicate of triplicate) was placed in a black bottomed 96-well plate. Fluorescence was measured at 530-510 nm excitation and 590 nm emission with a fluorescence reader. After measurement, the samples were returned to the original wells and re-incubated until the next time point. Measurements were blanked and the fluorescence versus cell number was plotted to obtain a straight-line graph (GraphPad Prism 5). The time plot that gave the R^2 value closest to 1 (the incubation time that would provide the most accurate readings) was used as the incubation time for Alamar blue assay for all further experiments. Cell numbers from fluorescence values of the experimental data were calculated using the straight line equation of the plot that gave the R^2 value closest to 1.

Since the straight line equation is: $y = mx + c$

Fluorescence = (gradient x cell number) + intercept

Cell number from the blanked fluorescence experimental data was obtained by rearranging the equation as follows:

$x = (y - c) / m$

Cell number = (fluorescence - intercept) / gradient

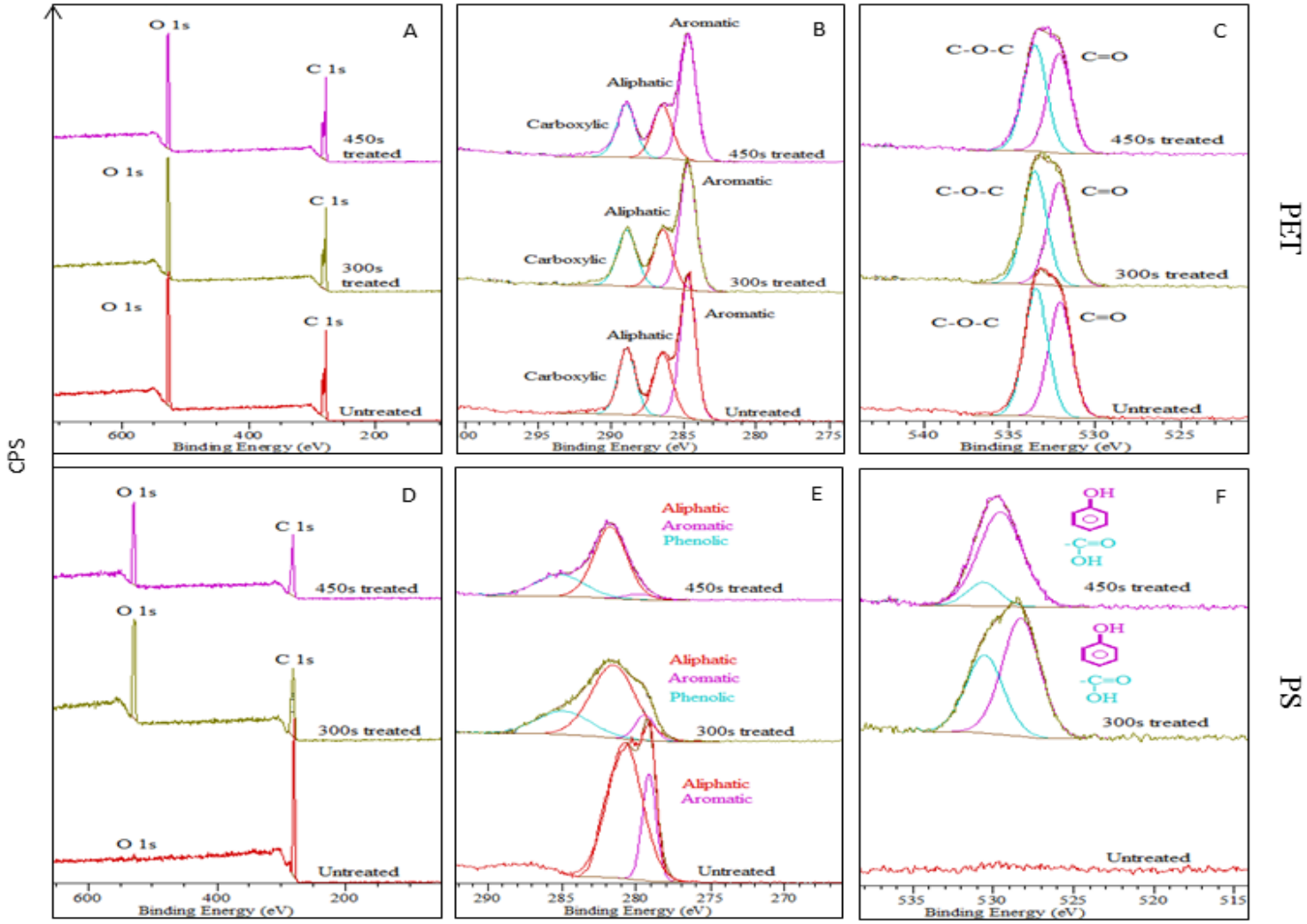

Figure 1: XPS spectra of PET: overview (A), carbon (B), and oxygen (C), after UV/ozone treatment. XPS spectra of PS: overview (D), carbon (E), and oxygen (F), after UV/ozone treatment.

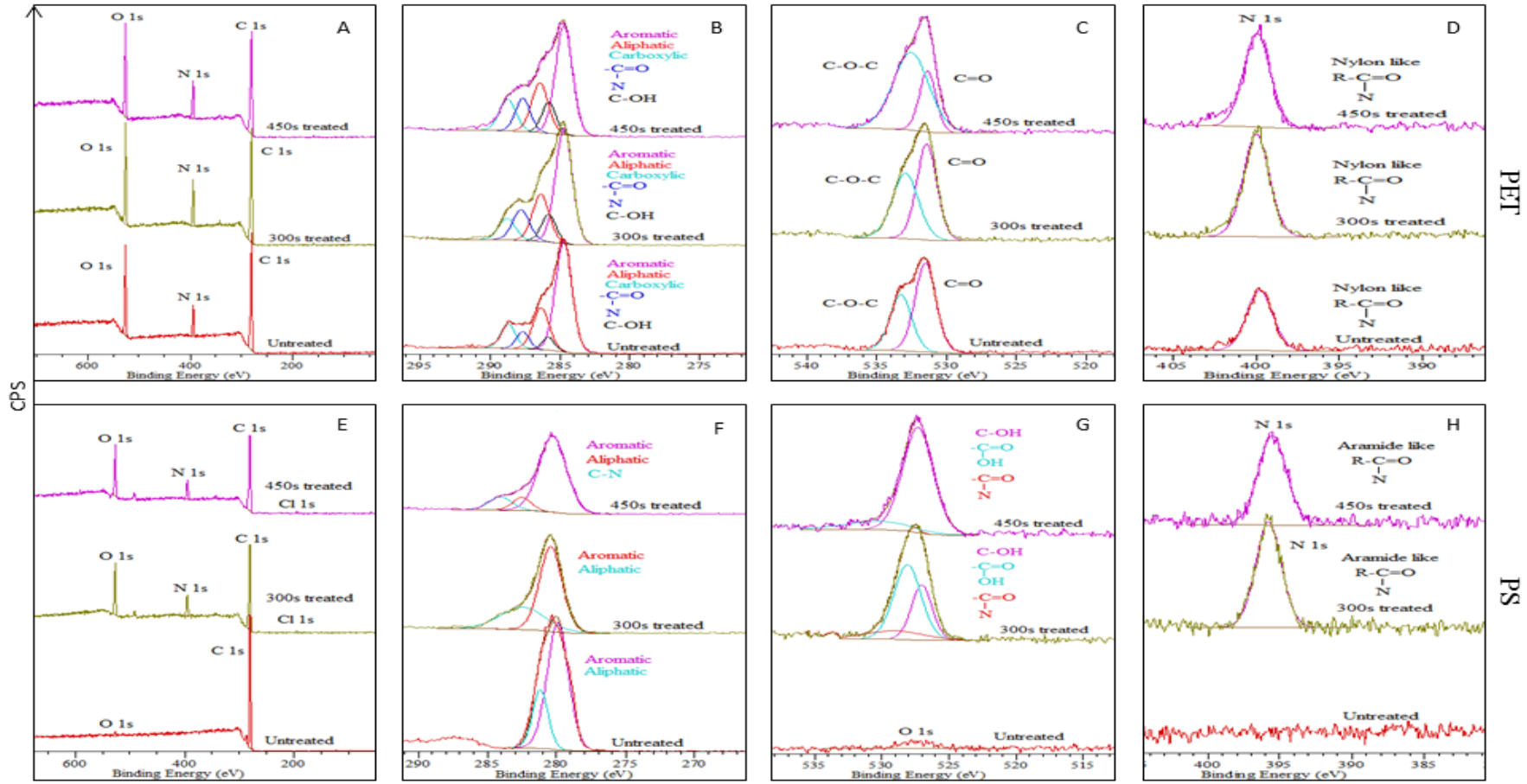

Figure 2: XPS spectra of PET: overview (A), carbon (B), oxygen (C), and nitrogen (D), after UV/ozone treatment and incubation with cell culture media. XPS spectra for PS: overview (E), carbon (F), oxygen (G), and nitrogen (H) after UV/ozone treatment and incubation with cell culture media.

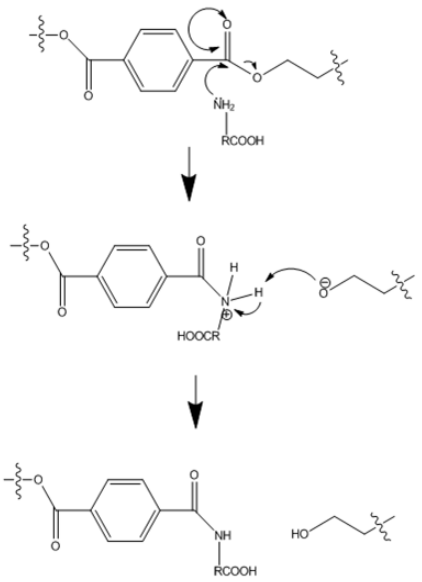

Figure 3: Schematic showing the possible route of aminolysis of the ester bond in PET. This is a possible explanation of the presence of nitrogen on the surface of PET. Schematic drawn using ChemDraw11 (CambridgeSoft Corporation).

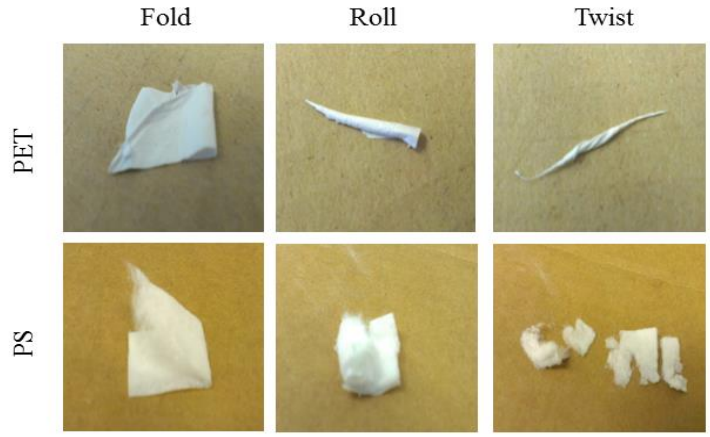

Test	PET	PS
Fold	Yes	Yes
Roll	Yes	Yes
Twist	Yes	No

Figure 4: Photographs of PS and PET before and after undergoing folding, rolling and twisting.

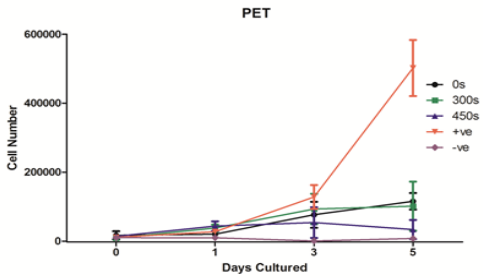

Average cell number

PET	Day 0	Day 1	Day 3	Day 5
0s	38251	108739	2962	19436
300s	34066	66878	11657	1049
450s	33568	56861	12200	8552

Satistical analysis

PET	Day 0	Day 1	Day 3	Day 5
0s vs 300s	ns	***	ns	ns
0s vs 450s	ns	***	ns	**
300s vs 450s	ns	ns	**	*

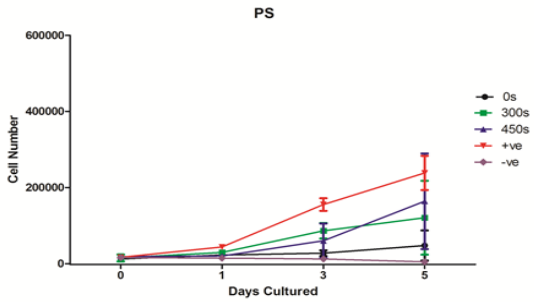

Average cell number

PS	Day 0	Day 1	Day 3	Day 5
0s	12643	22887	27737	47860
300s	15177	29827	86615	120807
450s	18707	20383	60350	164038

Satistical analysis

PS	Day 0	Day 1	Day 3	Day 5
0s vs 300s	ns	***	***	ns
0s vs 450s	ns	ns	*	*
300s vs 450s	ns	***	ns	ns

Figure 5: Graph showing the trend in cell metabolism, hence cell number over 5 days in culture using Alamar blue assay for untreated, 300s and 450s UV/ozone treated PET and PS, compared to positive glass control and negative low attachment culture plates control, at a starting cell seeding density of 10,000 cells/cm^2, with corresponding statistical analysis.

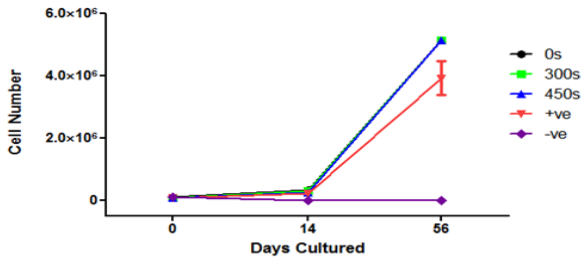

Average cell number

PET	Day 0	Day 14	Day 56
0s	114566	321911	5130843
300s	82475	303405	5130843
450s	62392	248342	5130843
Positive	85679	215226	3927412

Satistical analysis

PET	Day 0	Day 14	Day 56
0s vs 300s	*	ns	ns
0s vs 450s	**	*	ns
300s vs 450s	ns	ns	ns
0s vs +ve	ns	***	***
300s vs +ve	ns	**	***
450s vs +ve	ns	ns	***

Figure 6: Graph showing the trend in cell metabolism, hence cell number over 56 days in culture using Alamar blue assay for untreated, 300s and 450s UV/ozone treated PET, compared to positive glass control and negative low attachment culture plates control, at a starting cell seeding density of 50,000 cells/cm^2, with corresponding statistical analysis.

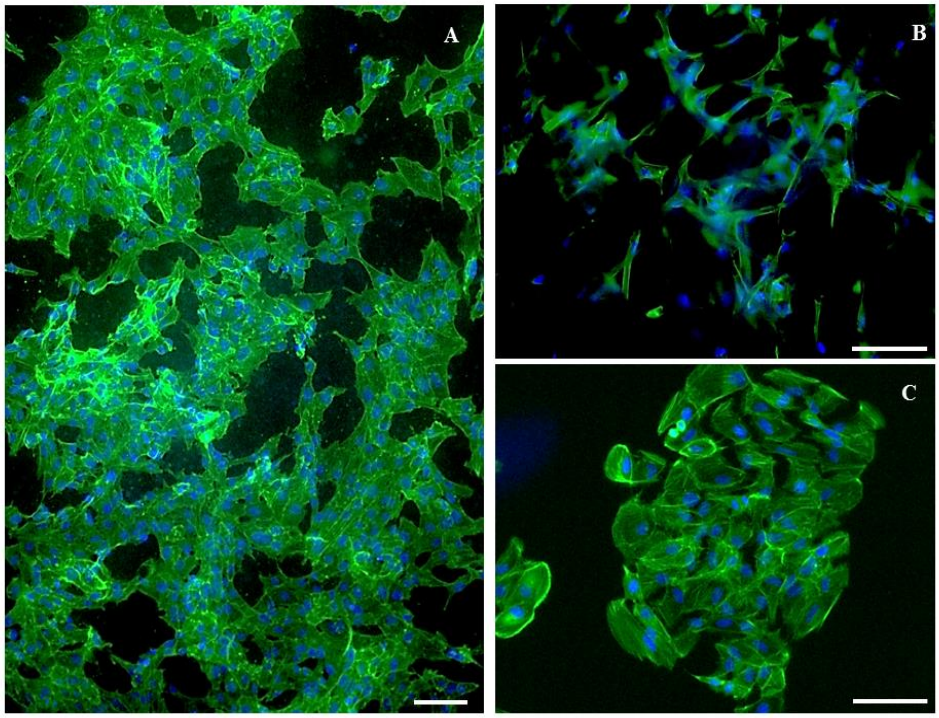

Figure 7: DAPI/phalloidin stained fluorescence images of cells grown on 300 s treated PET after 4 days culture (A), 300 s treated PS after 5 days culture, and positive glass control after 3 days culture (C). Starting cell seeding density at 10,000 cells/cm^2, scale bars 100 µm. Difference in cell morphology is exhibited between PET and PS, with cells wrapping around individual fibres on PS. Cells grew in patches on PET and the positive control.

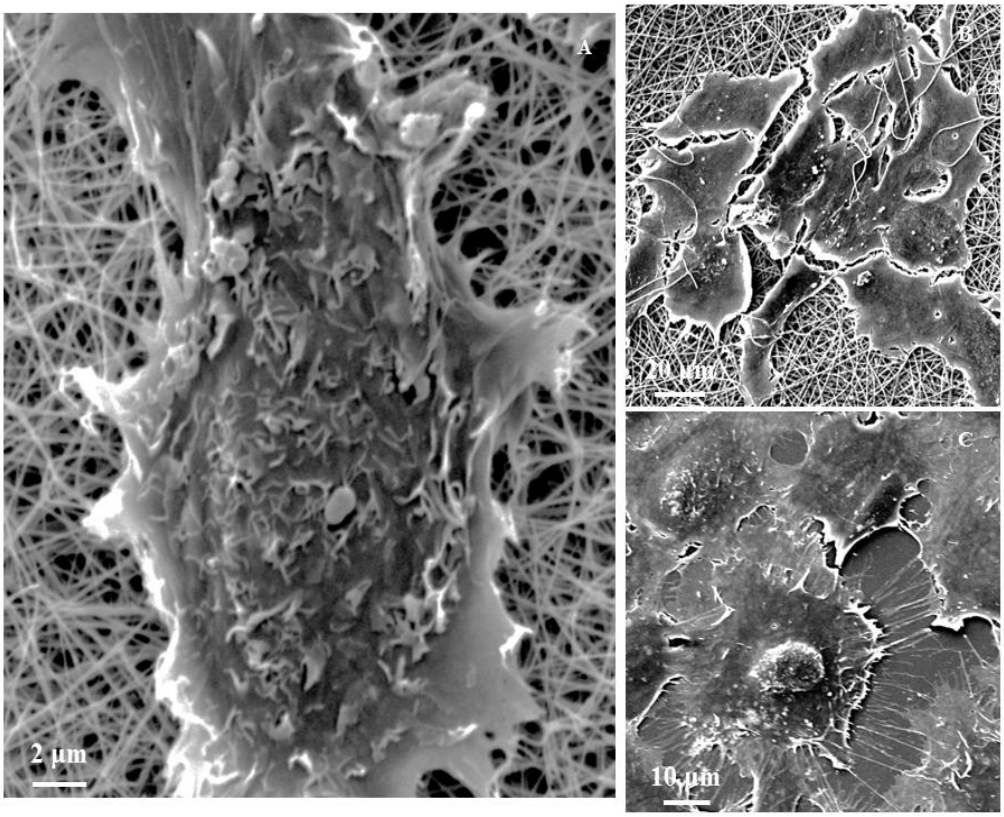

Figure 8: SEM images of cells on 300 s PET after 2 days culture (A), 450 s treated PET after 4 days culture, and positive glass control after 5 days culture (C). Starting cell seeding density at 10,000 cells/cm^2. Patch growth of cells exhibited.

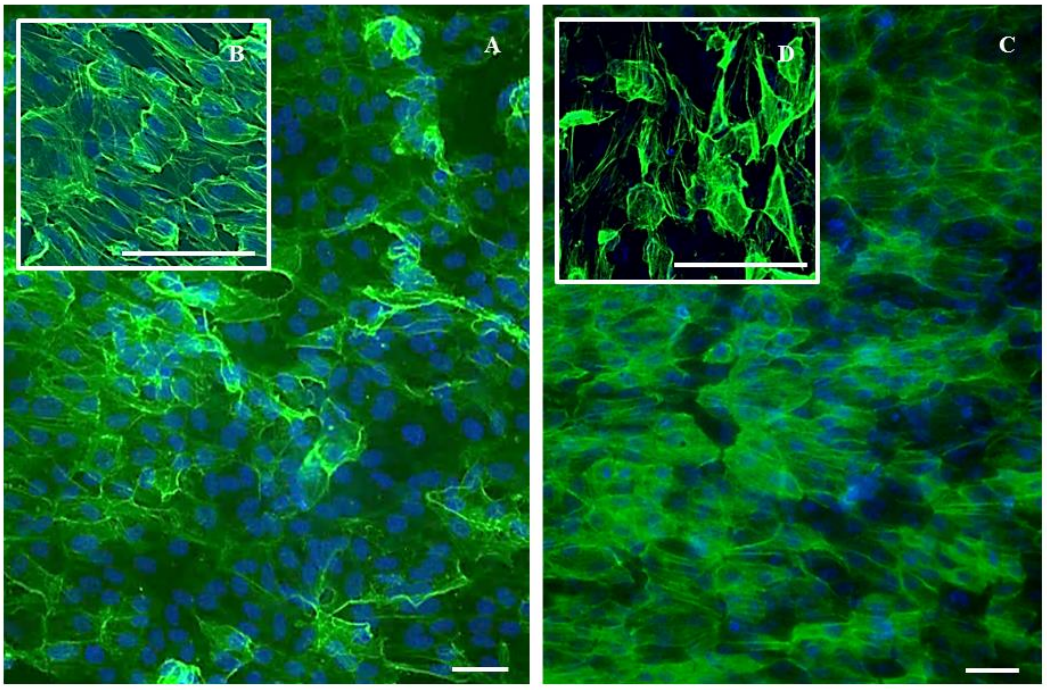

Figure 9: DAPI/phalloidin stained fluorescence images of cells grown on untreated PET after 14 days culture (A), positive glass control after 14 days culture (B), untreated PET after 56 days culture (C), and positive glass control after 56 days culture (D). Starting cell seeding density at 50,000 cells/cm^2, scale bars 100 µm.

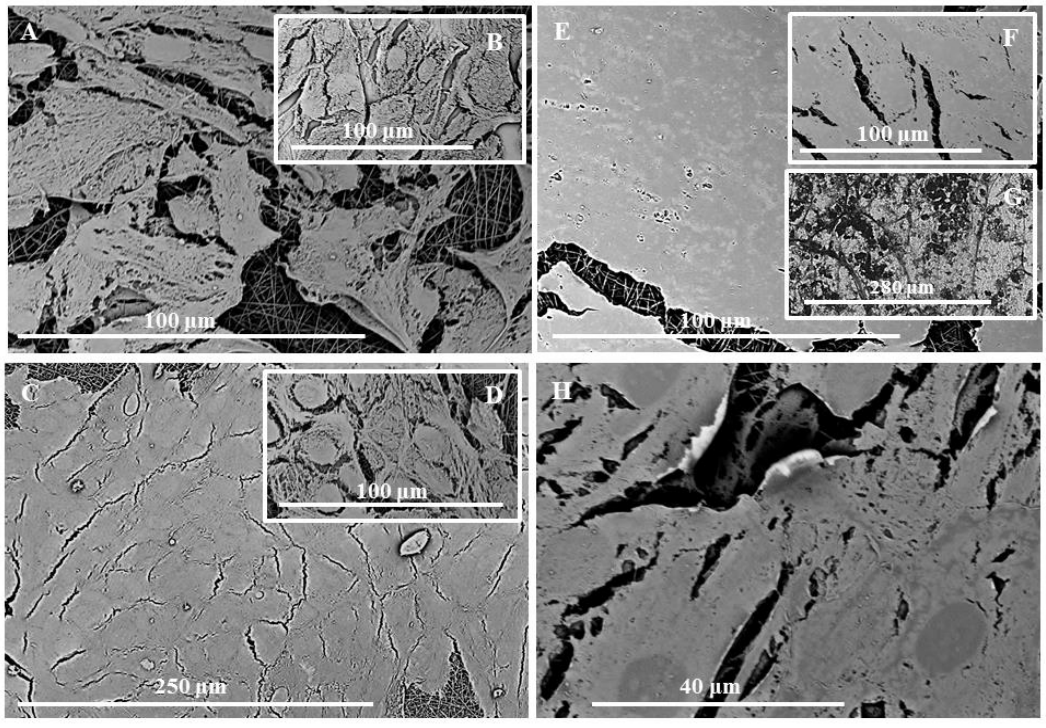

Figure 10: SEM images of cells grown on untreated PET after 14 days culture (A), positive control after 14 days culture (B), 450 s treated PET after 14 days culture (C), 300 s treated PET after 14 days culture (D), untreated PET after 56 days culture (E), 450 s treated PET after 56 days culture (F), positive control after 56 days culture (G), and 300s treated PET after 56 days culture (H). Starting cell seeding density at 50,000 cells/cm^2. Monolayer morphology of cells exhibited on PET. Loss of cells exhibited on the positive glass control after 56 days.

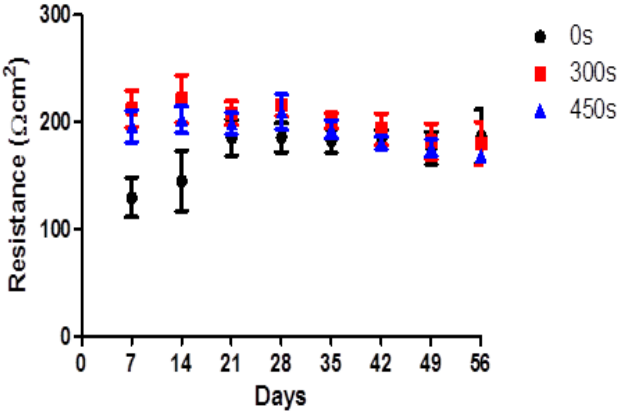

Figure 11: TEER measurements of ARPE-19 cells grown on untreated, 300 s treated and 450 s treated PET over 56 days of cell culture, with starting cell seeding density at 50,000 cells/cm^2.

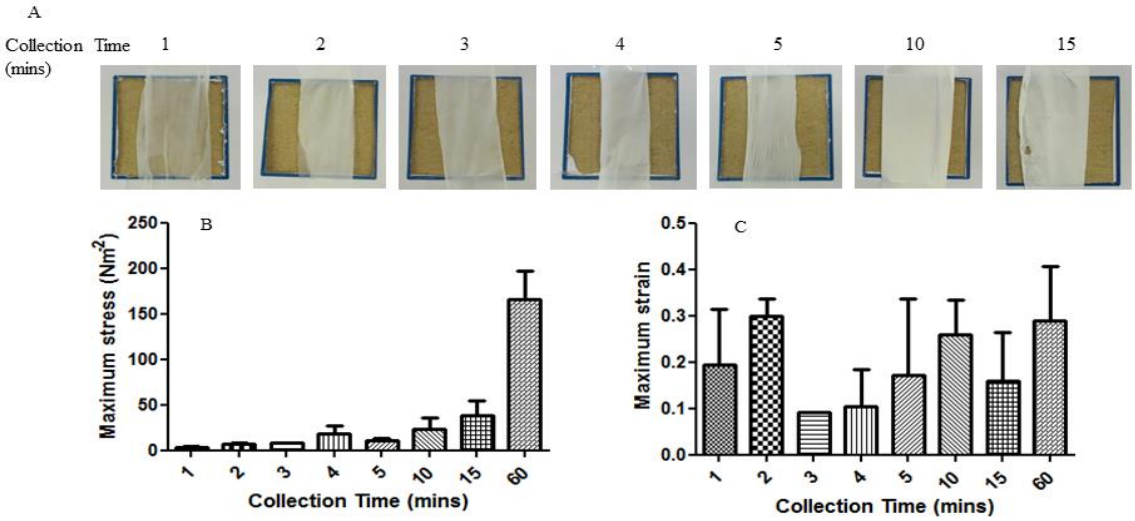

Figure 12: Photographs of electrospun PET mats collected at increasing times (A), graphs showing the variation of maximum stress with increased collection time (B), and the maximum strain with increased collection time (C).

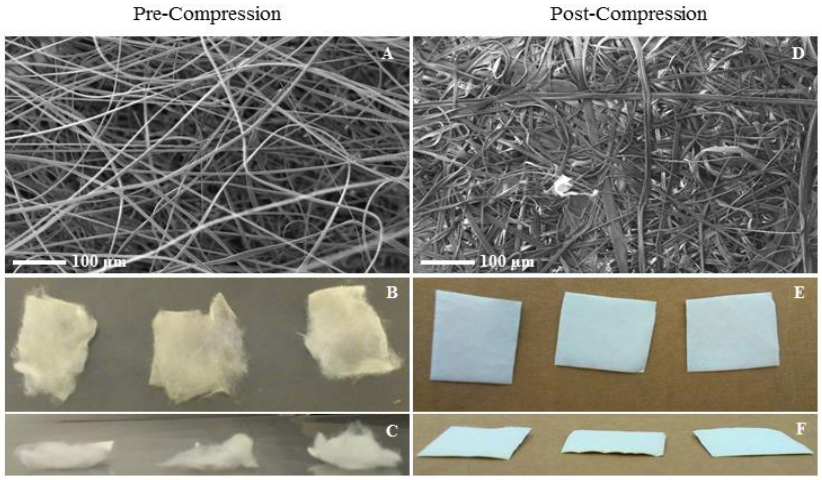

Figure 13: SEM images of PS before (A) and after (D) compression and photographs of the PS mats bird's eye view and side view before (B,C) and after (E,F) compression.

Treatment times (s)	PET WCA (°)		PS WCA (°)	
	10.1 cm away	0.5 cm away	2.8 cm away	0.5 cm away
0	135.9	135.9	130.1	130.1
150	49.5	37.4	120.55	77.8
300	53.9	23.6	99.5	56.3

Table 1: WCA of PET before and after 150 s and 300 s UV/ozone treatment at 10.1 cm and 2.8 cm away from the UV lamp in pure oxygen, and WCA of PS before and after 150 s and 300 s UV/ozone treatment at 2.8 cm and 0.5 cm away from the UV lamp in pure oxygen.

PET	0s		300s		450s	
Element	Position	Atomic %	Position	Atomic %	Position	Atomic %
Carbon (1s)	279.5	67.15	279.5	68.65	279.5	68.67
Oxygen (1s)	527.5	32.85	527.5	31.35	527.5	31.33

PS	0s		300s		450s	
Element	Position	Atomic %	Position	Atomic %	Position	Atomic %
Carbon (1s)	279	99.29	281	70.31	281.5	71.22
Oxygen (1s)	529.5	0.71	529	29.69	529.5	28.78

Table 2: Table showing the results from the XPS analysis of the composition of carbon and oxygen on the surface of the electrospun PET and PS mats before and after UV/ozone treatment.

PET		0s		300s		450s	
Element	Species	Position	Atomic %	Position	Atomic %	Position	Atomic %
Carbon (1s)	Aromatic	284.7	48.35	284.7	48.8	284.7	50.79
	Aliphatic	286.43	26.24	286.42	25.85	286.42	25.07
	Carboxylic	288.43	25.41	288.9	25.35	288.95	24.14
Oxygen (1s)	Ester C=O	532.02	47.37	532.07	47.66	532.08	48.36
	Ester C-O-C	533.43	52.63	533.51	52.34	533.5	51.64

PS		0s		300s		450s	
Element	Species	Position	Atomic %	Position	Atomic %	Position	Atomic %
Carbon (1s)	Aromatic	280.77	76.05	281.53	64.57	281.74	65.67
	Aliphatic	279.13	23.95	279.42	10.01	279.78	4.48
	Phenolic C-OH	na	na	284.92	25.42	285.16	29.85
Oxygen (1s)	Phenolic C-OH	na	na	528.25	60.34	529.53	84.49
	Aromatic C(OH)=O	na	na	530.53	39.66	530.6	15.51

Table 3: Table showing the results from the XPS analysis of the detailed composition of carbon and oxygen on the surface of the electrospun PET and PS mats before and after UV/ozone treatment.

PET	0s		300s		450s	
Element	Position	Atomic %	Position	Atomic %	Position	Atomic %
Carbon (1s)	279.5	71.73	279.5	69.88	279.5	69.93
Oxygen (1s)	526.5	20.68	526	20.46	526.5	20.62
Nitrogen (1s)	394.5	7.59	394.5	9.66	394.5	9.44

PS	0s		300s		450s	
Element	Position	Atomic %	Position	Atomic%	Position	Atomic %
Carbon (1s)	280	98.34	280	76.07	280	74.47
Oxygen (1s)	527	1.66	527.5	15.54	527	16.87
Nitrogen (1s)	na	na	395.5	7.68	395	7.59
Chlorine (2p)	na	na	193.5	0.71	194	1.07

Table 4: Table showing the results from the XPS analysis of the composition of the elements found on the surface of electrospun PET and PS mats before and after UV/ozone treatment followed by incubation with cell culture media.

PET		0s		300s		450s	
Element	Species	Position	Atomic %	Position	Atomic %	Position	Atomic %
Carbon (1s)	Aromatic	284.73	56.11	284.72	48.35	284.72	44.57
	Aliphatic	286.35	21.26	286.37	19.76	286.44	20.24
	Carboxylic	288.7	11.05	288.79	9.03	288.74	12.8
	C(N)=O	287.67	6.76	287.79	12.84	287.65	11.83
	C-OH	285.84	4.83	285.8	10.01	285.8	10.56
Oxygen (1s)	Ester C=O	531.51	60.64	531.41	53.11	531.36	26.42
	Ester C-O-C	533.27	39.36	532.94	46.89	532.54	73.58
Nitrogen (1s)	R-C(N)=O	399.18	100	399.99	100	399.95	100

PS		0s		300s		450s	
Element	Species	Position	Atomic %	Position	Atomic %	Position	Atomic %
Carbon (1s)	Aromatic	279.92	75	280.42	65.2	280.28	79.18
	Aliphatic	281.18	25	282.44	34.8	282.51	9.24
	C-N	na	na	na	na	284.07	11.59
Oxygen (1s)	C-OH	na	na	527.02	30.78	527.3	84.31
	C(OH)=O	na	na	528.08	55.33	530.22	14.55
	C(N)=O	na	na	528.98	13.88	527.47	1.13
Nitrogen (1s)	C(N)=O	na	na	395.79	100	395.53	100

Table 5: Table showing the results from the XPS analysis of the detailed composition of the elements found on the surface of electrospun PET and PS mats before and after UV/ozone treatment followed by incubation with cell culture media.

Chapter 7: Summary of Published Material

The research has identified the polymer and the fabrication parameters for developing a cell carrier substrate for application as a replacement BM in treatment for AMD. The substrate developed was a PET mat of bead-free fibres, which could be reproducibly fabricated (see Appendix 2). The fabricated substrate allowed growth and maintained a monolayer of RPE cells over two months, and it had appropriate qualitative (handleability) and quantitative mechanical (tensile) properties. Although untreated PET allowed growth of a monolayer of cells, it was concluded that UV/ozone treatment was beneficial and would aid in speeding the growth of the monolayer. Thicknesses of 10-14 μm exhibited in the preliminary tests carried out have been reported to be suitable for subretinal insertion.[123]

The substrate was presented to ophthalmic clinicians and validation as to the handling properties was gained. One criticism mentioned was the relatively large size of the prototype presented, with an area of 1 cm^2. This would be easily rectified by cutting the substrate to the desired size and shape.

In summary the aforementioned published material described the process behind developing a cell carrier substrate, with the end user and application in mind throughout. The ultimate aim of fabricating a cell carrier substrate that could potentially be used for eventual subretinal insertion has been achieved and verification from ophthalmic clinicians further supports the work.

Chapter 8: Discussion

8.1 Polymer Solubility

The solvents used for electrospinning have an electric dipole, an ideal trait which allows a charge to be carried. The solvents also have high volatility, which is useful for electrospinning since fibres form as the solvent evaporates from the polymer solution jet. Fibre formation and diameter may be dependent on the solvent's electric dipole.[69,77] Polystyrene dissolved in neat THF, neat DCM, THF/DCM and THF/EtOH solvent mixtures. The polymer-solvent interactions in these mixtures are such that the organic chemical structure of polystyrene (Figure 10) interacts with the organic structure of the solvent to produce a homogeneous polymer solution. Both THF and EtOH contain a lone pair of electrons in their structures and DCM contains two chloride atoms which are rich in electron density, therefore the electron rich phenyl ring in polystyrene can interact, thus allowing the PS to dissolve (Figure 11).[140,141]

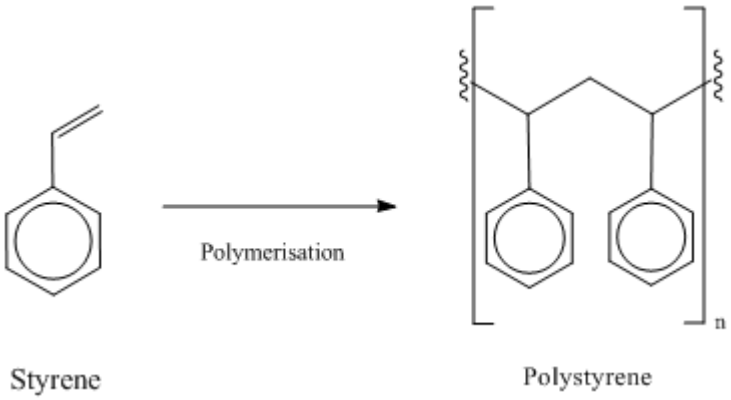

Figure 10: Simple carbon backbone structure of styrene and polystyrene. The double bond breaks to form single bonds with other styrene monomers during polymerisation, forming the polymer. Drawn using ChemDraw11 (CambridgeSoft Corporation).

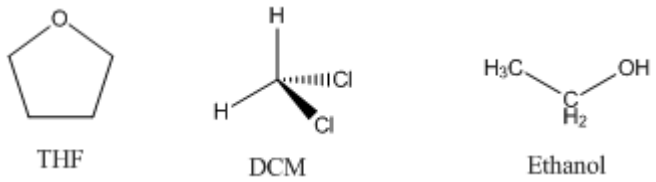

THF DCM Ethanol

Figure 11: Simple structures of THF, DCM and EtOH. Each of the structures contains electron rich species, which are able to interact well with the electron rich phenyl ring in polystyrene, allowing it to dissolve. Drawn using ChemDraw11 (CambridgeSoft Corporation).

PET dissolved well in HFIP and TFA, but not in THF, DCM, THF/DCM or THF/EtOH solvent mixtures. Good polymer-solvent interaction for PET was achieved through solvents which contained highly electronegative species in their structures (fluoride) that are able to interact through dipole-dipole forces with the dipoles created in PET by the ester functional group (Figure 12).[140,141] Another structural difference in solvents was that HFIP contains an alcohol functional group and TFA contains a carboxylate functional group (Figure 13). These functional groups are able to interact with the oxygen containing ester group in PET, via hydrogen bonding. THF was unable to provide good chemical interaction with PET since the lone pair of electrons was not enough to allow PET to dissolve. It was also noted that although DCM contains electronegative species in its structure too (chloride), it was not able to dissolve PET. This is since chloride ions are much larger than fluoride ions, which means that chloride is not as electronegative as fluoride and so the pull of electrons by chloride is not as strong as in fluoride, therefore the dipole created by fluoride is much stronger than with chloride, which in turn provides a better means of interaction with PET.[140,141]

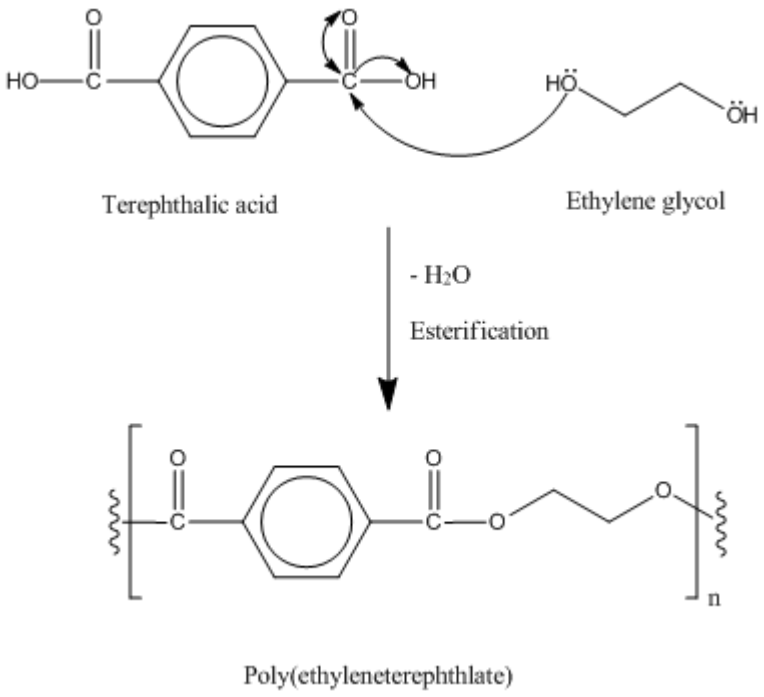

Figure 12: Schematic showing the structures of the monomers that react during polymerisation to form PET, with arrows depicting electron movement between the monomers. Drawn using ChemDraw11 (CambridgeSoft Corporation).

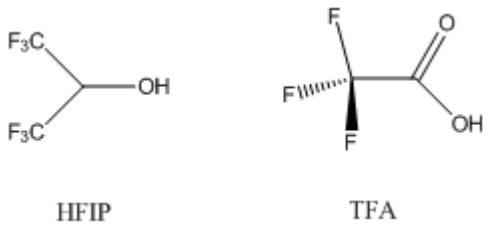

Figure 13: Simple structure of HFIP and TFA depicting the electron rich species contained within their chemical structures. These electron rich species were able to interact with the electron rich groups in PET, which allowed it to dissolve. Drawn using ChemDraw11 (CambridgeSoft Corporation).

PU dissolved well in THF/EtOH mixture. Although the chemical structure of the commercial PU used Tecoflex® is not known, all polyurethanes contain the urethane (or

carbamate) link: R-NH-COOR' (Figure 14). The THF/EtOH solvent mixture interacts well with these urethane links via hydrogen bonding.[141]

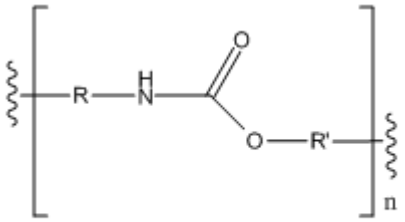

Urethane link repeating unit

Figure 14: Chemical structure of the repeating unit in polyurethane. The complete structure of the commercially available Tecoflex® is not known. Drawn using ChemDraw11 (CambridgeSoft Corporation).

8.2 Electrospinning & Fibre Morphology

8.2.1 Effect of Solvent Type & Polymer Concentration

Electrospinning theory dictates, as mentioned in the introduction, that in order for the polymer solution to spin as opposed to spray depends on a threshold value, that lies within a range of an upper and lower limit: a balance between the polymer solution surface tension and the strength of the electrostatic potential applied, which must be maintained in a steady manner for a continuous jet of polymer solution to be ejected from the needle tip.[67,69,70] If this threshold value is not met, then the polymer solution will not be ejected from the needle tip, since a strong enough potential difference between the charged needle tip and the collection plate is not made. If this threshold value is exceeded then the jet is broken and a spray is given.[67] This value is dependent on the polymer/solvent combinations used, as well as the concentrations of the polymer solutions. Fibre formation may also be dependent on the working distance between the needle tip and collection plate,

as this dictates how long the solvent has to evaporate before landing on the collection plate, and also dictates the strength of the electric field applied between needle tip and collection plate.[67,69,70] Experimental observation showed that if the distance was too short the polymer solution accumulated on the collection plate, since the solvent did not have enough distance and time to evaporate, and if the distance was too high then fibres were not ejected. Therefore, in order to improve spinning, the working distance was adjusted accordingly. Also, the voltage applied may affect fibre morphology, since it dictates the strength of the potential difference applied.[79] If the voltage is too low a polymer solution jet will not eject and if the voltage is too high, surface tension in the polymer solution is exceeded past the point of fibre formation, and consequently gives spray.[79] Experimental observation agreed with literature and thus voltages were adjusted to improve fibre collection.

For all polymers, fibre diameter was found to increase with polymer concentration, since a higher output of polymer is ejected with higher polymer concentrations. All PS fibres had ribbon-like morphology, which may be due to the high molecular weight of the polymer.[103] In neat THF, beading was present at 15 % and 20 % (w/v). Fibres formed at concentrations above and including 25 % (w/v). In neat DCM, beading was present up to and including 25 % (w/v) and fibres only formed at 30 % and 35 % (w/v). In the THF/DCM mixture beading was present up to 25 % (w/v) with fibres present at 30 % (w/v). As exhibited by PS, fibres formed at a lower polymer concentration in neat THF (25 %) compared to neat DCM (30 %). PS fibres also had a lower mean diameter when spun in THF than DCM. THF has a dielectric constant of 7.52 and a dipole moment of 1.750,[142] whereas DCM has a dielectric constant of 8.93 and a dipole moment of 1.600.[143] Higher dipole moment may mean a better charge is able to be carried with THF allowing better discrimination by an applied potential difference, therefore extruded finer fibres and allowed fibres to form at lower polymer concentrations. On a qualitative perspective, THF

was found to be a better solvent compared to DCM as it required less cleaning and unblocking of the needle during experiments. It was eventually found that PS at 25 % (w/v) in neat THF did not reproducibly form fibres. Concentrations including 30 % (w/v) and above would frequently block the needle, making collection of fibres difficult. At the instances fibres were obtained at 25 % (w/v), at other instances beading would be exhibited at the same concentration. Therefore the solvent mixture was changed to THF/EtOH in order to predictably produce fibres (see Appendix 2).

The collection of fibres was made easier with reproducible results; some cleaning of the needle was required, but not as frequently as with neat THF. In the THF/EtOH mixture beading was present up to 25 % (w/v) and fibres only formed at 26.7 % (w/v) and above. To make collection of fibres more efficient, since ease of spinning was reduced as at 30 % a lot of cleaning of the needle tip was required; the polymer concentration was altered to concentrations of 26.7 % (w/v) and 28.3 % (w/v). Optimal parameters for electrospinning PS were: voltage 24 kV, working distance 10 cm, flow rate 2 ml/hr. Fibres were obtained at both instances, but collection was slightly better at 26.7 % (w/v) hence this concentration was used throughout further experiments. Interestingly, the findings agree with literature that better fibres/electrospinning occurs when solvents that do not allow complete dissolution of the polymer are used.[100,101] This may suggest that a polymer suspension may be better, with the solvent being used as a polymer holding medium only and not allowing the polymer to become completely homogeneous, as is the case with true solutions. Experimental observation showed that neat ethanol did not allow PS to dissolve completely into solution, whereas THF did. Therefore the addition of ethanol to THF would make the solvent mixture such that PS dispersed within the medium, but not truly homogeneously, leaning slightly more towards being a suspension, and hence allowed more stability to fibre formation for PS.

All PET fibres had a wire-like morphology, which may be due to the low molecular weight of the polymer.[103] In neat HFIP, beading was present at 15 % (w/v), fibres formed at concentrations above and including 20 % (w/v). In neat TFA, beading was exhibited up to and including 20 % (w/v) and fibres only formed at concentrations above and including 25 % (w/v). Both solvents proved easy to use for spinning PET, with no blocking of the needle. Optimal parameters for spinning were: voltage 15 kV, working distance 15 cm and flow rate 1 ml/hr. PET fibres were obtained at 25 % (w/v) in HFIP and 20 % (w/v) in TFA. Fibres spun from HFIP were generally thicker, although still nanoscale, than compared to fibres spun from TFA. This may be because TFA contains the carboxylate functional group in its structure, which is able to interact with the ester functional group in PET via hydrogen bonding and dipole-dipole interaction. Whereas, HFIP contains hydroxide groups only, this can interact with PET via hydrogen bonding, but does not provide dipole-dipole interaction. Qualitatively, both solvents were extremely good for electrospinning, polymer deposits did not block the needle and did not require cleaning. But for further experiments, PET at 25 % (w/v) in neat HFIP was used since it was slightly better for handling. This can be explained using the acid dissociation constant ($_pK_a$) for each solvent. The $_pK_a$ gives an idea of the strength of the acid. An acid (HA) is described as something which dissociates to give an H^+ ion and its conjugate base A^-: $HA \leftrightharpoons H^+ + A^-$. The dissociation constant is calculated as: $K_a = \frac{[A-][H+]}{[HA]}$ using the concentrations of each moiety. The logarithmic dissociation constant is more commonly used and is calculated as follows: $_pK_a = -\log_{10} K_a$. The bigger the $_pK_a$ value, the less the acid has dissociated, which means it is the weaker acid. For HFIP $_pK_a = 9.3$ and for TFA $_pK_a = 0.23$, therefore HFIP was better for handling during experiments.[140,142,143]

Fibres were only obtained from spinning PU dissolved in the THF/EtOH solvent mixture. PU fibres had a web-like morphology, with some of the fibres merged into the other, giving a sticky look to the fibres. In neat THF and THF/DCM solvent mixture PU was not

electrospinnable. In neat DCM, PU exhibited spraying at 2 % (w/v), 2.5 % (w/v) and 3 % (w/v) concentrations. Higher concentrations were not able to be electrospun in DCM due to high viscosity of the PU solutions. Therefore a mixture of THF/EtOH was used at higher concentrations. Beading was exhibited at 5 % (w/v) and fibres were achieved at concentrations of 7.5 % (w/v) and above. Optimal parameters for electrospinning PU were: voltage 20 kV, working distance 10 cm and flow rate 1 ml/hr. The voltage had to be adjusted to 25 kV as initial voltage used gave a slight bulge in some fibres. Increase of voltage provided a higher current that allowed a better potential difference to be applied while maintaining polymer solution surface tension, which allowed the fibres to be extruded more smoothly.[79] The ethanol in the solution may have provided the polarity required to allow a current to be carried. Also, ethanol has a lower volatility compared to THF and so may have provided longer residence time for the polymer at the needle tip for the voltage applied to take effect for fibre extrusion.

8.2.2 Effect of Salt Addition, Temperature & Humidity

Addition of salt and carrying out the experiments in a controlled environment had varying effects on the fibre diameter and on the variation of sizes of fibres within a mat. A controlled environment had the largest effect on the fibres of PS. Although, fibre morphology was unaffected by salt addition or electrospinning under controlled conditions, and PS fibres still had a ribbon-like morphology when spun under controlled temperature and humidity, fibre diameters were smaller when electrospun with the addition of salt than compared to when electrospun without salt, this agrees with literature.[90] The largest PS fibre diameter was found when PS was electrospun under laboratory conditions without salt. It too can be noted that even with the presence of salt, when spun under laboratory conditions, the standard deviation for the fibre size is large for PS, whereas when spun in a controlled environment the fibre sizes look similar and the standard deviation is also smaller. This may be because the controlled environment allowed the control of the

evaporation rate of the very volatile solvent mixture, allowing a smaller variation in fibre size. The rate at which the solvent evaporates in normal laboratory conditions may be erratic enough to cause a wide distribution of fibre size.

On a qualitative perspective, salt allowed the collection of PS fibres much more easily than when no salt was added, under both laboratory conditions and in a controlled environment. The needle needed to be cleaned less frequently as it did not block as often. This may be because the salt allowed the current of the voltage applied to be carried well and so fibres extruded much more easily, due to the ionic nature of NaCl. These findings are also in agreement with previously reported literature, which described 1 % NaCl as improving fibre uniformity and morphology significantly, and allowing electrospinning to go through with ease when added to the spinning solution.[81] Also, fibre size has been reported to alter significantly when electrospinning is carried out under controlled temperature and humidity, due to having effect on the rate of solvent evaporation.[105]

Similar to PS, the PET fibre morphology was not affected by the change in electrospinning conditions, and PET gave fibres of wire-like morphology when electrospun under both laboratory conditions and in an environmental chamber, with and without salt. Contrastingly, it was found that the addition of salt to PET/HFIP reduced the average fibre size more than electrospinning in a controlled environment. The smallest fibre size was found when PET was electrospun with the addition of salt in an environmental chamber. This again can be attributed to the ionic nature of HFIP in conjunction with the ionic nature of salt, which would increase the overall ionic value of the polymer solution, therefore allowing better discrimination of an applied potential difference.[81,90] Under all conditions the standard deviation in fibre size was not significantly affected. Interestingly, electrospinning PET in a controlled environment, regardless of salt addition, caused bumping to occur in the mat structure. Although addition of salt reduced the amount of bumping in the mat, this is still an undesirable trait for a BM mimic. This may be

attributed to the higher humidity in the environmental chamber, which would reduce the speed of evaporation of the solvent from the polymer solution, causing drops of polymer solution to remain in the structure. In lieu of this, it was decided that the optimal parameters for electrospinning PET would be under laboratory conditions. No change in the quality of the electrospinning PET procedure was observed.

8.3 Substrate Characteristics

8.3.1 Gross Morphology & Tensile Properties

PS mats resembled cotton wool, which could be lightly flattened by hand pressure to smooth out somewhat, whereas PET mats had a tape-like morphology with a smooth appearance. PS mats were fragile and although could withstand experimental processing, some loss of sample did occur. PET mats were very robust and were able to undergo all experimental processing without any loss of sample. The most difficult to handle was PU, since its sticky trait caused the mat to intertwine. Initially the elastic nature of PU was thought of as an advantageous characteristic, however during processing the mat would entwine and could not be detached without damaging the scaffold. Handling PU was frustrating and difficult, and therefore would not hold well in practice for application as a cell carrier substrate for AMD treatment. For these reasons, PU was deemed unsuitable for further testing. PS and PET were taken further since they showed the most promise due to their ease of fabrication.

Qualitative tests showed that PET was more robust than PS. PET was able to withstand all tests without falling apart, whereas PS was not able to maintain its structure and fell apart quite easily, sometimes leaving a gritty powder. The delicacy of the PS mats was such that it could not withstand tensile tests, therefore the quantitative tensile properties of electrospun PS could not be ascertained. This is a contrary finding to Baker *et al.*, however the comparison is made difficult since a collection time of their mats is not reported.[71] PET was robust enough to undergo tensile testing. The maximum allowable

strain until failure varied throughout testing. This can be attributed to random fibre breakage of randomly placed[129] fibres within the mat, which is difficult to control on a static collection plate, since the whipping action of fibres during electrospinning cannot be controlled.[124,125] The orientation of the mats was noted during fabrication, to ensure that tensile tests were undergone on the mats in the same direction as the mats were set during fabrication, since orientation of fibres can affect fibre breakage.[125,128]. The tensile strength of the mat perpendicular to the fabrication direction could also have been measured to test whether there was any difference in tensile strength.

8.3.2 Thickness & Porosity

PS mats at 60 minutes collection time were an average of 180.7 μm thick with 92 % porosity and PET mats at 60 minutes collection times were an average of 50.7 μm thick with 86 % porosity. The higher porosity of PS could be due to the looser packing of the fibres, as confirmed by its poor mechanical properties, and due to the larger fibres, which in turn leave larger voids between each fibre. The thinner PET mats exhibited better handling. Although the PET mats collected for 60 minutes did not match the 4.7 μm thickness of the native BM,[5,6] collection times of 5 minutes and under exhibited potential. It is anticipated that further investigation into mat fabrication will provide both the correct thickness and good mechanical properties for a cell carrier substrate.

The thickness of the PET mats generally increased with increased collection time, as expected. However, variation was expected and exhibited during measurement due to the uncontrollable nature of electrospinning and the erratic placement of fibres. Nonetheless the thicknesses of 10-14 μm exhibited in the preliminary thickness tests have been reported to be suitable for subretinal insertion.[123] Therefore with some further experimentation a suitable collection time in order to fabricate a substrate of an appropriate thickness can be evaluated.

After compression, the PS mats measured an average of approximately 38.7 µm thick with 61.33 % porosity. Photographs showed that the mats were flatter post-compression and SEM images of pre and post compression showed that fibres post-compression were packed more closely, while still maintaining the fibrous structure. Therefore 4.982 x 10^8 Nm^{-2} of pressure was able to maintain the fibre morphology well. However compression did not improve the handling properties for the PS substrate, rather it became more fragile post-compression and could not undergo tensile tests.

8.4 Surface Treatment

8.4.1 Hydrophilicity

Hydrophilic character can be described by interactive forces between polar functional groups in the polymer surface with the polar water molecules[74,140] or because of the overall scaffold structure and morphology, which may alter the way the water droplet is able to sit on the surface on the scaffold.[74]

All untreated polymers were found to be hydrophobic and results showed that surface chemistry affected the WCA on the substrates, especially polystyrene and this was backed up with the XPS results. However, for PET no surface chemistry changes were exhibited but still the WCA reduced with higher treatment times, backing up the suggestion that WCA is affected by the texture of the surface of the substrate.[74]

Rougher surfaces give higher WCA compared to smoother surfaces.[74] The roughness of the substrate is dependent on its topography following fabrication and by how much it has been handled; for example if it may have come into contact with abrasive surfaces, if it may have been stretched while processing, if it had maybe been handled a bit more roughly than intended. One method that could have been investigated was to test the WCA of substrates after being handled (ie folded, rolled) for increasing times, both pre and post-UV/ozone treatment, to see if the WCA was altered with increased handling. This would

distinguish between the effect of chemistry, which is known to have strong effects on WCA,[74] and the effect of physical properties of the substrate.

Untreated PS exhibited hydrophobic character, which could be due to its entire chemical structure lacking in polar functional groups containing oxygen or nitrogen, which can provide hydrogen bonding interaction with polar water molecules.[140,141] It could also be due to the morphology of the scaffold, since the surface of the polystyrene scaffold was very fluffy in appearance and not planar, preventing the water droplet from sitting flatly on the surface.[74] The fluffy appearance of the PS mats may be due to repulsive forces between the polymer fibres caused by electron rich phenyl rings exhibiting repulsion from one another.[140,141] The strong carbon-carbon backbone of PS gives the polymer its hard structure, making the rigid fibres unable to sit to give a flat surface (Figure 15).

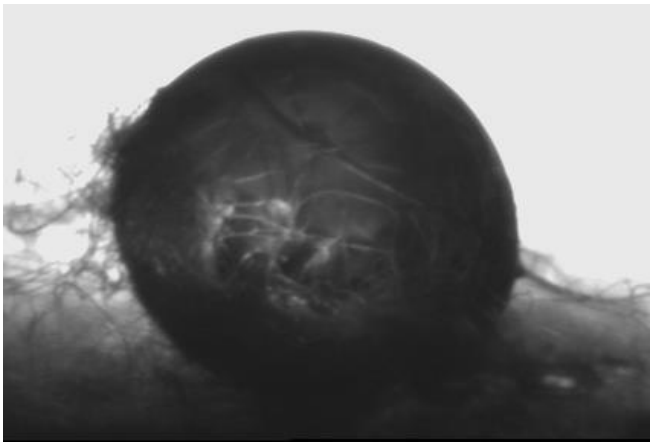

Figure 15: Image of a 3 µl drop of water on the surface of untreated, electrospun PS mat. The fluffy nature of the mat is distorting the water droplet.

Untreated PET exhibited hydrophobic character, even though ester functional groups are present in the chemical structure, which should be ideal for good hydrogen bonding with polar water molecules.[140,141] Repulsive forces could be acting between the electron rich

phenyl ring present in PET and the electronegative oxygen in the water molecule,[140,141] or the fibrous surface of the mat may be preventing the water droplet from sitting flatly as it would on a planar surface, due to air being trapped in the voids between the fibres.[74,75] A flatter surface in PET compared to PS was exhibited. This flattening may be due to good dipole-dipole interaction between the ester functional groups in the polymer.[140,141] However the wire-like morphology of the fibres, which are randomly placed throughout the PET mat, do not allow for a planar surface to be achieved, therefore preventing the water droplet from sitting on the surface flatly, giving characteristically hydrophobic WCAs.[74]

Untreated PU also showed hydrophobicity, even though a nitrogen atom and two oxygen atoms, electronegative atoms that are ideal for hydrogen bonding interaction with polar water molecules, are present in the urethane link.[140,141] The other functional groups present in the commercial PU (Tecoflex®) are unknown, therefore the hydrophobic character could be due to other functional groups which are hydrophobic or exhibit repulsive forces.[140,141] One observation that can help with understanding of what other functional groups may be present, is the fact that the PU mats discoloured with exposure to white light, going from white through to a pink or red-brown colour. This gives evidence for the presence of chromophores, which can include double bonds, triple bonds, lone pair of electrons and delocalised systems such as phenyl rings or long chains with alternating double and single bonds (Figure 16).[140,141]

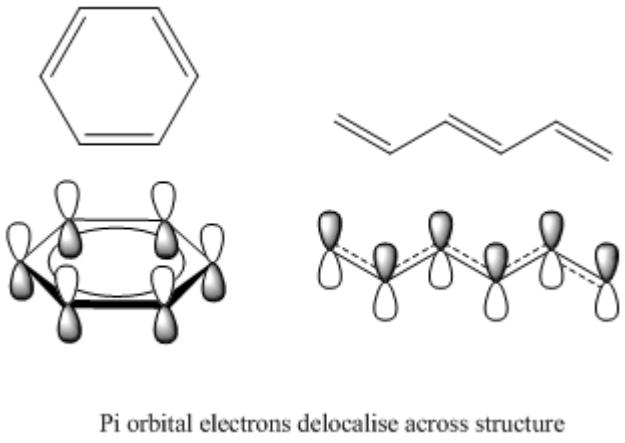

Figure 16: Simple structure of an example of double bonds in aromatic and long chains, alongside the depiction of pi orbitals. The electrons delocalise across each structure. Drawn using ChemDraw11 (CambridgeSoft Corporation).

These bonds contain conjugated pi-orbitals containing electrons, which can be promoted from a lower energy orbital to an empty, higher energy orbital by the energy absorbed from white light. When the molecule is exposed to the correct wavelength of radiation, an electron from the highest occupied molecular orbital (HOMO) is excited to the lowest unoccupied molecular orbital (LUMO). As the promoted electron relaxes a photon is emitted (Figure 17).[140] This photon has the wavelength of the energy difference between the two orbitals, which lies in the visible radiation wavelength range, hence a red-brown discolouration of PU is seen (data not shown). This was tested by treating PU for 300 s under UV light and no discolouration was observed. This observation that this discolouration was not caused by treatment in UV light further provides evidence of a highly conjugated system, as opposed to a system containing single bonds. The energy of orbitals is lowered due to delocalised electrons, therefore lower energy is required to promote electrons to higher energy orbitals and a longer wavelength of radiation (visible) is absorbed.[140] The energy of the photon released, as the electron relaxes, is equal to the energy required to promote it to a higher orbital, which has wavelength in the visible

radiation range, hence colour change is seen.[140] UV radiation has a shorter wavelength, therefore does not provide the correct energy to promote electrons, hence colour change was not seen when PU was exposed to UV light (data not shown).

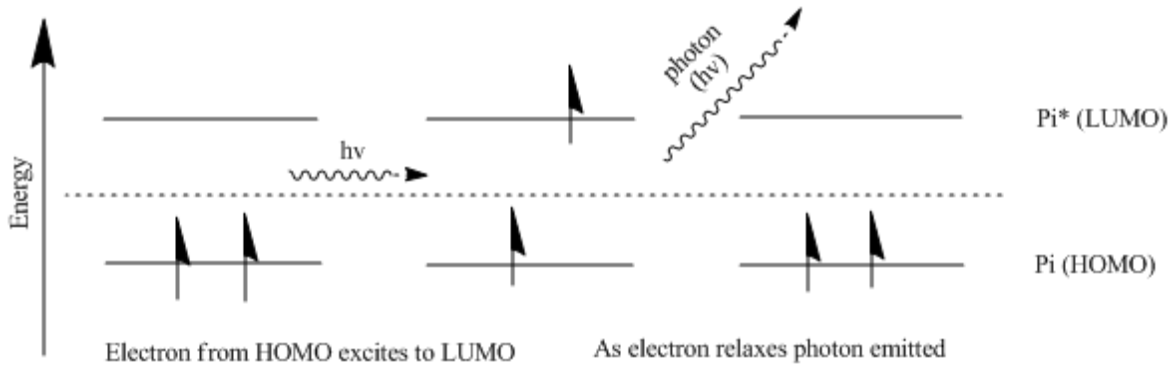

Figure 17: Schematic of what happens during electron excitation and relaxation, and the release of a photon between the HOMO and LUMO. Drawn using ChemDraw11 (CambridgeSoft Corporation).

Therefore the presence of hydrocarbons, that contain lots of double bonds, contribute to the hydrophobic character of PU. Interestingly, untreated PU exhibited lower hydrophobic WCA than compared to untreated PET and untreated PS. PU exhibited an average WCA of 126.18˚, PET exhibited an average WCA of 135.85˚ and PS exhibited an average WCA of 130.11˚. The lower WCA in PU may be due to the fibres exhibiting tape like morphology, as opposed to ribbon-like or wire-like morphology as seen in PS and PET. The flatter fibre morphology in PU allows a flatter overall scaffold surface morphology to be obtained and therefore the water droplet sits on the surface more flatly giving lower WCA. Nonetheless, untreated PU still exhibited hydrophobic character.[74]

Oxidising the surface of polymers via oxygen-plasma treatment, or UV/ozone treatment introduces oxygen containing species on to the surface of the polymer. These oxygen

containing species can interact with water molecules, making the polymers more hydrophilic. The mechanism of oxygen species introduction in both plasma treatment and UV/ozone treatment is by the formation of oxygen containing radicals that attack the surface of the polymer.[130,131]

Firstly molecular oxygen undergoes homolysis in UV light to give oxide radicals, these oxide radicals go on to react with molecular oxygen to form ozone. Ozone is a highly unstable molecule that forms and reacts very quickly: it can abstract hydrogen from water present in the atmosphere to form hydroxide radical and molecular oxygen. This hydroxide radical can then go on to attack the surface of a polymer resulting in an alkyl radical formation. Radicals formed on the surface of polymers can react by various routes: quenching by other radicals (this is rare, since radicals usually form in very small quantities so the likelihood of two radicals coming together would be very little) or radical attack on other oxygen or ozone molecules followed by hydrogen abstraction from water molecules to introduce alcohol groups to the polymer surface (Figure 18).[140]

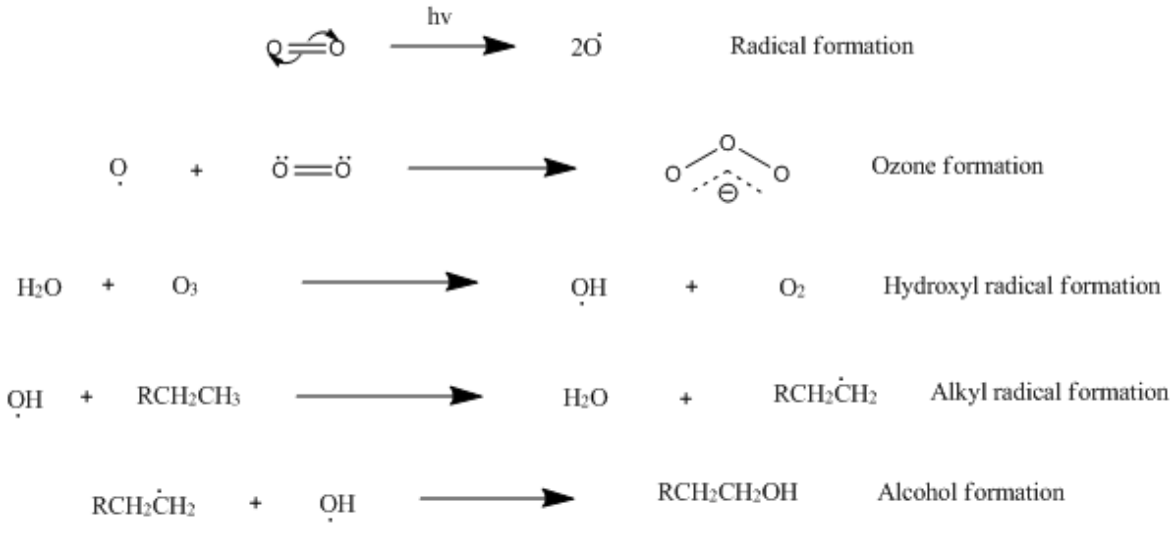

Figure 18: Reaction scheme of one of many possible routes of oxidation that can occur during UV/Ozone treatment. Drawn using ChemDraw11 (CambridgeSoft Corporation).

Short oxidation treatment times give low oxidation species on the surface of the polymer such as alcohols, aldehydes or ketones whereas long oxidation treatment times lead to high oxidation species, such as carboxylic acids or esters.[140,141] Plasma treatment is more complicated and a more expensive method of surface modification, however both methods have the same effect. Therefore UV/ozone treatment was utilised as the surface treatment method for this work.[130,131]

WCA for PET and PS decreased as treatment times increased, indicating that oxygen modification of the surfaces had taken place, therefore improving the hydrophilicity of the surface of polymers to allow cell attachment. This finding is in agreement with literature.[144,145] For both PET and PS mats, lower WCA measurements were observed for samples treated at 0.5 cm away from the UV lamp, compared to those treated at a distance of 10.1 cm from the UV lamp for PET and 2.8 cm from the UV lamp for PS at the same treatment times, indicating that proximity to the UV source also impacted on oxygen incorporation into the polymer mats. The distance of 2.8 cm was used as comparison for PS since 10.1 cm for PS did not have any effect on WCA on PS (data not shown). At high treatment times, increasing discolouration was noticed on PS mats, which indicated oxygen incorporation into the mats.[146] This discolouration was also an indication that the PS mats were starting to degrade.[146]

Determining the WCA of treated electrospun mats in general was difficult, since voids produced due to the randomly placed fibres make the mats porous, which allow water to seep through the voids during a WCA measurement.[74] These voids may result in the materials feigning hydrophilic behaviour in materials that may actually be hydrophobic. In order to account for this and for statistical accountability, the WCA of six different samples were measured in each condition.

To summarise, the surface treatment conditions for PET and PS taken forward for cell culture were untreated, 300 s treated, and 450 s treated in a pure oxygen atmosphere, at a

distance of 0.5 cm away from the UV lamp. These times were chosen because 300 s was found to give the desired approximately 60° water contact angle, which has been previously reported to be the ideal contact angle for protein adsorption.[132] The untreated and 450 s treated samples provided a comparison for higher and lower water contact angles, respectively.

8.4.2 Chemical Composition

XPS analysis showed that UV/ozone treatment did not add any additional oxygen groups to the surface of PET, whereas oxygen groups were added to PS. Closer evaluation of the PET spectra showed that three peaks for carbon and two peaks for oxygen were present at all treatment times, thus UV/ozone treatment had no effect on PET surface chemistry. Contrastingly, closer examination of treated PS mats showed that the number of oxygen and carbon environments increased with increasing treatment times. PS specifically showed one new carbon species and two new oxygen species after UV/ozone treatment, highlighting an obvious addition of oxygen to the PS mats. Both 300 s and 450 s treated PS mats exhibited phenolic oxygen peaks at 284.92 eV and carboxylic oxygen peaks at 285.16 eV respectively.

Little difference in oxygen incorporation between PS treated for 300 s and 450 s was observed. The low amount of oxygen observed in the untreated PS can be explained by residual solvent in the fibrous mats, since the solvents THF and ethanol contain oxygen in their chemical structures. Additionally, no fluorine peaks were observed in PET, suggesting that no residual HFIP was left in the PET fibres.

These results demonstrate that, at the times investigated, PS was more susceptible to the introduction of oxygen on its surface, which is also in agreement with literature that have identified oxygen incorporation on to PS in as little as 1 minute UV/Ozone exposure.[147]

8.4.3 Protein Adsorption

After being incubated in cell culture media, XPS spectra revealed that nitrogen was introduced onto the surface of the PET mats regardless of UV/ozone treatment times, whereas, on PS nitrogen was only introduced when the scaffolds were treated. The presence of chlorine, a common contaminant, was also observed on the surfaces of treated PS, suggesting that UV/ozone treated PS is susceptible to contamination.

Detailed carbon and oxygen XPS spectra of incubated PET showed an increase in the number of carbon environments and a shift in the position of the oxygen peaks, as well as the presence of nitrogen peaks in the samples. The two new carbon peaks found at 287.67 eV and 285.84 eV are -C(O)N and C-OH peaks respectively, the nitrogen peak present is the nylon-like -C(O)N peak at 399.96 eV.

Detailed carbon and oxygen XPS spectra for PS showed an increase in the number of carbon and oxygen environments only on UV/ozone treated PS, suggesting the introduction of nitrogen. There was only one new carbon peak detected on 450 s treated PS at 284.07 eV, which denoted the –C-N bond. There were three new oxygen peaks present on 300 s and 450 s treated PS found at 527.02 eV, 528.08 eV and 528.98 eV indicating –C-OH, -COOH and –C(O)N respectively. The nitrogen peaks found only on the 300 s and 450 s treated PS were at 395.79 eV and 3.95.53 eV respectively and denoted the presence of –C(O)N bonds, an aramide (aromatic amide)-like bond.

Nitrogen is hypothesised to be included onto mat surfaces as a result of protein adsorption from cell culture media onto the surfaces of the PET and treated PS mats. Where nitrogen was present, it remained following washing of the polymer surfaces with distilled water. This observation suggests strong interactions between protein and the surfaces of the PET (both treated and untreated) and treated PS. In addition there is a possibility that the N-terminal of the proteins were able to undergo aminolysis, opening the ester bond and forming a chemical covalent bond between the protein and polymer substrate.[140,141]

Detailed analysis of PET showed two new carbon species being formed following incubation of UV/ozone treated PET in media, which coincides with the suggestion of aminolysis occurring in the ester. This is further backed up by the interesting observation that the ratio of aliphatic and carboxylic carbon and the C-O-C oxygen species was generally reduced compared to the ratio found in the PET analysed after UV/ozone treatment without incubation with media. The lack of nitrogen on untreated PS indicated a lack of protein adsorption. These results strongly suggest that UV/ozone treatment is necessary for protein addition to PS, but not for PET.

XPS analysis showed interesting results, especially for the samples incubated in cell culture media. The nitrogen based groups, which could have only been introduced to the polymers by the culturing media, showed that proteins in the media were attaching to the polymer surfaces in both treated PET and PS. For PET, however, even the untreated surface showed the presence of nitrogen groups. The functional groups added to the surface of both the polymers did not wash off, which suggests strong bonding. For example the N-terminal of protein present in the media may be able to aminolyse the ester groups in the polyester PET and therefore aid the attachment and proliferation of ARPE-19 cells.[148] Since PET contains esters throughout its chemical structure, it also explains why the cells are able to attach and proliferate even on the untreated PET surface. Atthoff *et al.* have investigated surface activation of PET where they found that surface activation would be preferred over untreated as more protein adsorption was found on surface activated PET.[148] Our results are in agreement with this and demonstrate that surface treatment using UV/ozone enhances protein adsorption onto the mat surfaces, thus potentially improving cell attachment.

8.5 Cell Culture

A short term cell culture was carried out because it was necessary to ascertain which of the two substrates the cells would react better towards initially, and whether or not the RPE

cells would eventually be able to form the ideal monolayer. The short term culture also allowed a further shortlisting of the substrates to a final substrate, which could be taken forward to the longer cell culture time. The long term cell culture was necessary in order to see whether the cells were able to form and maintain a monolayer over a long period of time, for the instance of this research two months, and whether or not the surface treatment of the substrate affected the cell growth.

8.5.1 Short Term

Alamar blue results showed that RPE cells grew on both treated and untreated PET. In contrast, untreated PS exhibited lowest cell growth, over time compared to both 300 s and 450 s treated PS.

DAPI/Phalloidin fluorescence staining for PET confirmed Alamar blue results and showed growth of RPE cells in each condition as comparable. Interestingly the results shown in our investigations demonstrated that for PET, even the untreated samples allowed successful cell growth that was comparable to cell growth on positive glass controls. Cells grew in patches, which is in agreement with literature that describe RPE cell growth in a colony-like manner,[80] starting to form monolayers in the short term culture. Fluorescence images for PS also showed cell presence only on the UV/ozone treated surfaces, although not in the desired monolayer morphology as cells exhibited on PET, but rather wrapped around individual fibres. This may be because the PS mat was 'fluffy', in the sense that the fibres were much more distanced from each other compared to the flatter PET fibres, therefore the cells could not achieve the correct distance required to achieve cell to cell interaction, hence could not begin to form a monolayer.[149,150] Following this and together with the poor handling quality of the electrospun PS, it was decided that PS would not be taken forward for long term cell culture and was rejected as an option as a cell carrier substrate in the application for AMD treatment.

The failure to reach complete monolayer by day 5 of culture on PET can be attributed to the low cell count, others have used much higher cell densities,[151,152,153] or due to surface roughness,[154] or because of high substrate porosity, which causes cell aggregates to form and due to cell-cell contact which inhibits further proliferation.[150]

Initially, cell count was deliberately kept low at 10,000 cells/cm^2 in order to ascertain whether cells reacted well to the surface of the material, and not just to the presence of other close proximity cells.

8.5.2 Long Term

Once the behaviour of the cells towards PET was ascertained, the cell count for the two month cell culture was increased to 50,000 cells/cm^2 in order to assess the ability of the cells to form and maintain of a complete monolayer on the fibrous PET substrate.

Alamar blue assay on the long term cell culture, showed an increase in the cell number for all treatment times. Fluorescence staining images and SEM images also confirmed the growth and maintenance of a monolayer on PET up to day 56. Fluorescence images also showed that ARPE-19 cells had a different morphology on the fibrous mats compared to the planar glass control. This can be associated with the obvious difference in surface topography between glass discs and fibrous electrospun PET. [81,113,114,155] Cell morphology difference in planar compared to fibrous surfaces has also been previously reported, which describe fibrous mats allowing self-organized cell aggregates to form in a typical three-dimensional morphology compared to planar surfaces,[81] and others which describe fibrous surfaces as being a mimic of the native BM and therefore allowing better RPE cell differentiation and morphology.[113,114] Some cracking in the cell monolayer is visible in the SEM images; this can be associated with the dehydrating preparation step in the SEM method, since the phalloidin stain in the fluorescence images exhibit good cell to cell contact. Interestingly, by day 56 the positive control exhibited fewer cells on the surface of the glass than compared to all the PET mats. Alamar blue also confirmed a significantly

lower cell number, than compared to all the PET mats. Therefore the long term cell culture suggests that ARPE-19 cells are able to grow and survive well on electrospun PET.

TEER measurements for PET showed a gradual increase in electrical resistance, which corresponded to the formation of a monolayer. Initially, 300 s and 450 s UV/ozone treated PET exhibited higher TEER readings, compared to untreated PET. By day 56, TEER readings had begun to plateau for all three conditions. This showed that untreated PET allows the formation of a monolayer, but at a slower rate. Towards the end of the two month study, TEER values were similar to the human RPE-choroid resistance of 36-148 Ωcm^2.[156] Other studies have reported varying results including higher TEER values obtained at shorter culture times,[153] or lower values throughout the culture period.[152,157] However there are dissimilarities in experimental design between them, for example some used supplements,[151,152] others did not,[153] some used higher cell densities compared to our work,[151-153] others matched ours.[157] It has been reported that ARPE-19 cell behaviour is dependent on the history of how they were maintained and passaged, therefore caution must be exercised when comparing results to others findings.[152,153]

It has been previously reported that commercially available PET as etched pore polyester (EPP) allow good growth of RPE cells, which are maintained over three months.[113,114] As aforementioned, planar sheets of PET, with and without a gelatine coating,[115] have been reported to show gross tolerance to subretinal insertion, with no suggestions of inflammation or overt toxicity to the retina or choroid.[114,115,158] The fibre size of 200 nm, or within that range, has been reported as being beneficial in order to acquire typical RPE cell features and enhanced subretinal space tolerance.[159] In Liu *et al.*'s report they compared electrospun PET and poly(L-lactide-co-ε-caprolactone) (PLCL), and found that RPE cells exhibited similar features on both substrates, and concluded that the cell characteristics were due to the fibres that were within a 200 nm fibre diameter range.[159] The fibre diameters for the substrates in my research coincide with this.

It was noted that these electrospun fibres were mounted on porous rigid-elastic carriers for ease of subretinal insertion.[159] Certainly this would make a difference to how the body would react towards the substrate.[160] Therefore it is endeavoured that eventually *in vivo* testing will still be undertaken for the developed substrates from my research in order to assess the suitability of electrospun fibrous PET as a replacement BM, since difference in scaffold morphology can cause diverse reactions *in vivo*, due to dissimilarity in scaffold physical properties.[160]

Chapter 9: Conclusion

From this research it was found that various solvents had varying effects in terms of polymer fibre morphology and ease of electrospinning. Concentration of the polymer solution and varying the electrospinning parameters can also lead to varying effects. Salt addition and environmental factors affected the gross morphology of the electrospun mats and also the fibre size, however these effects varied depending on the solvent/polymer combination. In terms of a substrate for a synthetic replacement BM, PET was found to be the most suitable in terms of gross morphology, handling, and ease of production. Electrospun PS was found to be unsuitable due to its fragility and PU was excluded due it being too sticky which made it difficult to undergo experimental processing.

Electrospinning PS in a controlled environment reduced the fibre size more than with the addition of salt. Addition of salt also reduced the variation of fibre sizes within a single batch of produced fibres, with a smaller standard deviation given when electrospun with the addition of salt. For PS, the use of salt in conjunction with electrospinning in a controlled environment proved advantageous; providing smaller fibres with less fibre size variation. PS mats were too fragile, even more so post-compression, and could not undergo experimental processing without crumbling. It was also found that even with optimal surface chemistry, the cells were unable to form the correct monolayer morphology due to the PS fibres being too far apart and instead wrapped around single fibres. Therefore electrospun PS would not make a suitable cell carrier substrate.

Contrastingly for PET, there were no advantages observed from controlling the environmental conditions during the electrospinning process. PET fibres were easily electrospun in ambient conditions, room temperature and normal humidity. Salt addition reduced the fibre size, whereas a controlled environment did little in changing fibre size. Neither of the conditions were able to alter the fibre size variation within a batch of PET fibres, with similar standard deviations found for both conditions. Unexpectedly,

electrospinning PET in a controlled environment, regardless of the addition of salt, disrupted the gross morphology causing bumping throughout the mat, which is an undesirable characteristic for a replacement BM. Therefore, although the addition of salt may prove advantageous in reducing the fibre size slightly, electrospinning PET within a controlled environment was not beneficial in order to form a mat of only fibres. Although cell culture was carried out on much thicker PET mats, thicknesses of 10-14 μm that are suitable for subretinal insertion are obtainable as exhibited by the preliminary thickness tests, and they also demonstrate tolerable tensile strength.

Short term cell culture results showed that cells were able to grow on the electrospun PET with correct morphology, regardless of UV/ozone treatment, and so were taken forward to long term culture. Long term culture results showed that ARPE-19 cells were able to form and maintain a monolayer. Our results agree with previous literature that PET is a suitable polymer for RPE cell growth and results also show that electrospun PET provides an adequate surface topography for cell monolayer growth and maintenance. Surface treatment, such as UV/ozone treatment and the adsorption of proteins, can be used to confer cytocompatibility to the substrate surfaces. However even without surface treatment, adequate cytocompatibility was exhibited by untreated PET, and a monolayer of RPE cells formed and was maintained over two months, with TEER results exhibiting resistance values between 36-148 Ωcm^2, similar to those found in the human RPE-choroid.

In conclusion, a porous mat of electrospun PET fibres of random orientation have been successfully fabricated, that can be UV/ozone treated to enhance cytocompatibility. This substrate exhibits potential for eventual application as cell carrier substrate as a synthetic BM replacement to address the treatment of dry AMD.

The substrates fabricated in my research satisfy the preference of fibrous structures over planar structures when considering RPE cell replication, in conjunction with the use of PET which has been reported to be grossly tolerant to subretinal insertion.[113-115,158] Not

only this but the substrates developed in my research also are within the 200 nm range, which have been reported to be beneficial in order to acquire typical RPE cell features in culture and enhance subretinal insertion tolerance.[159]

Chapter 10: Future Work

Immediate future work would entail carrying out the long term cell culture experiments over a longer period of time, for example six to seven months. This would enable us to measure how long the cells would take to polarise and pigment, which are an essential trait of RPE cells.[158] Live/dead assays, tight junction protein staining (ZO-1, RPE65) and confocal microscopy of the long term culture would be beneficial as an additional assessment of cell monolayer viability. The live/dead assay would allow a visual analysis to be obtained alongside the metabolic activity of Alamar blue assays, and the tight junction staining would visualise an important aspect of RPE cell monolayer function. The confocal microscopy would enable us to see whether or not cells have invaded the fibrous substrate, and would also help us to ascertain the presence of a monolayer of cells and not multiple layering of cells. Also RPE cell culture, alongside the range of biochemical assays aforementioned, on the thinner PET membranes would need to be carried out to ascertain how well the cells are able to grow on thinner membranes.

The hydraulic conductance of the substrate should be measured because it is linked to the porosity. The hydraulic conductance is the ease with which fluids flow across a vessel wall.[7] The hydraulic conductance of a healthy young human's BM/choroid ranges between 20-100 x 10^{-10} $ms^{-1}Pa^{-1}$, and it has been found that it can reduce to 0.52 x 10^{-10} $ms^{-1}Pa^{-1}$ in old age, because of lipid accumulation in the BM, which leads to the requirement of higher pressures being needed to push fluid towards the choriocapillaries that can lead to RPE-BL detachment from the ICL as is presented in 12-20 % of AMD cases.[7] Therefore the evaluation of the hydraulic conductance of the substrate, with and without a cell monolayer would be important, so as to prevent RPE detachment.

Since the percentage porosity of the substrates has been evaluated, it would too be beneficial to measure the substrate exclusion limit, similar to a retinal exclusion limit.[61,62] The native healthy BM allows solutes, such as inorganic ions and glucose molecules, to

pass freely through, but prevents passage of RPE cells and vascular endothelial cells (VECs), similarly the substrate should also exhibit such filtration. If the movement of various solutes of known diameter is confirmed as either being able to pass or be excluded by the membrane, then this would correspond to membrane pore size and hence a substrate exclusion limit. One way of measuring this would be by setting up a concentration gradient with the electrospun polymer acting as a permeable barrier, the solute would be allowed to diffuse for a set amount of time and then the charge difference measured on either side of the membrane.

Migration of cells could be measured using a similar technique, but using fluorescent staining instead.[63] An interesting investigation would be to cut the mats after cell culture to determine whether cells have invaded the three-dimensionally porous substrate structure. Finally, in cell penetration/migration investigations, as well as observing behaviour of RPE cells and VECs, it would also be beneficial to observe leukocyte activity on the electrospun substrates both with and without a RPE cell monolayer on the substrate surface. This would show how well the tight junctions on the RPE monolayer function and would also give an insight into how the leukocytes react towards the functional groups on the treated substrates.[38]

Discussion with ophthalmic surgeons realised that the native BM would need to be removed. The BM is located such that it cannot be excised from the eye as this would cause considerable damage. One possibility would be to use the electrospraying technique and spray the untreated side of the substrate (basement layer for the choriocapillaries) with a biodegradable polymer which would contain enzymes. The premise is that the degradable polymer would slowly degrade, in turn releasing the enzymes that would slowly digest the native diseased BM, once implanted into the eye. The natural filtering and waste disposal method of the eye would enable the removal of metabolic waste. The most important factors would be to ensure that the degradation was a slow enough process

in order to prevent damage to both the patient to ensure recovery, and the substrate with the monolayer of cells to ensure monolayer viability, but still work as per its intended function. Initial tests would include optimisation of the electrospraying method to measure the ideal size of the droplets and the ideal frequency of the spray to cover the substrate. The rate of degradation, the effects of degradation on the substrate and the RPE monolayer of cells, would also need to be investigated. This would include measuring what metabolic products are released (infra-red spectroscopy to determine what functional groups are present) and what effects, if any, the metabolic products would have on the overall substrate (SEM to image any possible substrate morphological changes) and the cell monolayer; for example whether cell morphology alters (DAPI/phalloidin staining followed by fluorescence microscopy/SEM, to image any possible cell morphological changes), whether the tight junctions remain (protein staining), or whether the enzymes cause cell death (live/dead assay, or Alamar blue assay). Further to this eventual tests to measure how long it would be required to enable complete removal of the diseased BM would be needed. One method could be to determine *in vitro* how long a sample of macula tissue takes to be digested; this could be done by attaching the substrate with the enzymes (without cells in the first instance) to a macula tissue sample, and determine how long it may take to digest. After the length of time required to digest the macula tissue has been evaluated and the effects of the presence of enzymes on the cell monolayer has been determined, then a further experiment with the cell monolayer on the substrate with the enzymes on the macula tissue could be carried out. In lieu of this, it is important that the complete dimensions of the substrate required for implantation are determined. This would require further discussion with ophthalmic clinicians and experts to determine what size and shape exactly the implant should be, in order to satisfy their requirements.

It is with the intention that further work would eventually include *in vivo* animal investigation, to ascertain the tolerance towards the fibrous structure of the substrate, even

though planar PET sheets and PET fibres mounted on porous rigid-elastic carriers have been reported as exhibiting good tolerance towards subretinal insertion.[113-115,158,159] This is because substrate morphology can have varying effects *in vivo*, as found by Christiansen *et al.*[160] therefore, it is imperative to evaluate whether good tolerance will be exhibited towards a fibrous PET structure in the first instance. Then depending on these results and the enzyme activity results described above, a further experiment would need to be set up involving the substrate with a cell monolayer that has enzymes patterned on the underside of the substrate, to evaluate tolerance *in vivo*.

References

1. Harries M, Vaz F, Verma S. The special senses. In: Kumar P, Clark M, editors. Clinical medicine, 6th edition. London: Elsevier Ltd.; 2005. p. 1171-1172.
2. Virtualmedicalcentre.org [Internet]. Australia: Virtual Medical Centre; c2002-13 [updated 2013 Sept 17; cited 2013 Sept 17]. Available from: http://www.virtualmedicalcentre.com/anatomy/the-eye-and-vision/28
3. Sumita R. The fine structure of Bruch's Membrane of the human choroid as revealed by electron microscopy. J Electron Microsc. 1961, Jun, 20;10(2):111-118.
4. Brightfocus.org [Internet]. USA: BrightFocus Foundation; c2000-13 [updated 2013 Aug; cited 2013 Sep 6]. Available from: http://www.brightfocus.org/macular/about/understanding/medical_illustrations.html
5. Ramrattan RS, van der Schaft TL, Mooy CM, de Bruijn WC, Mulder PGH, de Jong PTVM. Morphometric analysis of Bruch's membrane, the choriocapillaries, and the choroid in aging. Invest Ophthalmol Vis Sci. 1994, May, 14;35(6):2857-2864.
6. Booij JC, Baas DC, Beisekeeva J, Gorgels TGMH, Bergen AAB. The dynamic nature of Bruch's membrane. Prog Retin Eye Res. 2010;29:1-18.
7. Curcio CA, Johnson M. Structure, Function and Pathology of Bruch's Membrane. In Ryan SJ, Schachat AP, Wilkinson CP, Hinton DR, Sadda SVR, Wiedermann P, editors. Retina 5th Edition. Elsevier Saunders; 2013. P. 465-481.
8. Tezel TH, Del Priore LV, Kaplan HJ. Reengineering of aged Bruch's membrane to enhance pigment epithelium repopulation. Invest Ophthalmol Vis Sci. 2004, Sep;45(9):3337-3348.
9. Del Priore LV, Tezel TH, Kaplan HJ. Maculoplasty for age-related macular degeneration: Reengineering Bruch's membrane and the human macula. Prog Retin Eye Res. 2006;25:539-562.
10. Resnikoff S, Pascolini D, Etya'ale D, Kocur I, Pararajasegaram R, Pokharel GP, Mariotti SP. Global data on visual impairment in the year 2002. B World Health Organ. 2004, Nov;82(11):844-852.
11. Owen CG, Fletcher AE, Donoghue M, Rudnicka AR. How big is the burden of visual loss caused by age related macular degeneration in the United Kingdom? Br J Ophthalmol. 2003;87:312-317.
12. Bird AC, Bressler NM, Bressler SB, Chisholm IH, Coscas G, Davis MD, de Jong PTVM, Klaver CCW, Klein BEK, Klein R, Mitchell P, Sarks JP, Sarks SH, Soubrane G, Taylor HR, Vingerling JR (The international ARM epidemiological study group). An international classification and grading system for age-related maculopathy and age-related macular degeneration. Surv Ophthalmol. 1995, Mar-Apr;39(5):367-374.
13. Rosenberg T, Klie F. The incidence of registered blindness caused by age-related macular degeneration. Acta Ophthalmol Scand. 1996;74:399-402.
14. Cousins SW, Marin-Castano ME, Csaky KG. Pathogenesis of Early Age-Related Macular Degeneration (AMD): A New Hypothesis. In: Ioselini OR, editor. Focus on eye research. New York: Nova Science Publishers Inc.; 2005. p. 39-80.
15. Age-Related Eye Disease Study Research Group. Risk factors associated with age-related macular degeneration. A case-control study in the age-related eye disease

study: Age-related eye disease study report number 3. Ophthalmology. 2000, Jul;107:2224-2232.
16. McCarty CA, Mukesh BN, Fu CL, Mitchell P, Wang JJ, Taylor HR. Risk factors for age-related maculopathy. The visual impairment project. Arch Ophthalmol. 2001, Oct;119:1455-1462.
17. Ding X, Patel M, Chan CC. Molecular pathology of age-related macular degeneration. Prog Retin Eye Res. 2009;28:1-18.
18. Guymer R, Luther P, Bird A. Changes in Bruch's membrane and related structures with age. Prog Retin Eye Res. 1998;18(1):59-90.
19. Crabb JW, Miyagi M, Gu X, Shadrach K, West KA, Sakaguchi H, Kamei M, Hasan A, Yan L, Rayborn ME, Salomon RG, Hollyfield JG. Drusen proteome analysis: An approach to the etiology of age-related macular degeneration. P Natl Acad Sci USA. 2002;99(23):14682-14687.
20. Ambati J, Ambati BK, Yoo SH, Ianchulev S, Adamis AP. Age-related macular degeneration: etiology, pathogenesis, and therapeutic strategies. Surv Ophthalmol, 2003, May-Jun;48(3):257-293.
21. Binder S, Stanzel BV, Krebs I, Glittenberg C. Transplantation of the RPE in AMD. Prog Retin Eye Res. 2007;26:516-554.
22. Okubo A, Rosa Jr RH, Bunce CV, Alexander RA, Fan JT, Bird AC, Luthert PJ. The relationship of age changes in retinal pigment epithelium and Bruch's membrane. Invest Ophthalmol Vis Sci. 1999, Feb;40(2):443-449.
23. Strauss O. The retinal pigment epithelium in visual function. Physiol Rev. 2005, July;85:845-881.
24. Cangemani FE. TOZAL study: An open case control study of an oral antioxidant and omega-3 supplement for dry AMD. BMC Ophthalmology. [Internet] 2007 [cited 17 Sep 2013];7(3):1471-2415. Available from: doi: 10.1186/1471-2415-7-3
25. Age-Related Eye Disease Study Research Group. A randomized, placebo-controlled, clinical trial of high-dose supplementation with vitamins C and E, beta carotene, and zinc for age-related macular degeneration and vision loss: AREDS report No. 8. Arch Ophthalmol. 2001, Oct;119(10):1417-1436.
26. Rnib.org.uk [Internet]. UK: Royal National Institute of Blind People; c2013[updated 2013 Sep 12; cited 2013 Sep 17]. Available from http://www.rnib.org.uk/eyehealth/eyeconditions/conditionsac/Pages/amd.aspx
27. Englebert M, Klancknik Jr JM. The coming boom in dry AMD therapies. Retinal Physician. [Internet] 2009 [cited 17 Sep 2013]. Available from: http://www.retinalphysician.com/articleviewer.aspx?articleid=103061
28. Pulido J, Sanders D, Winter JL, Klingel R. Clinical outcomes and mechanism of action of rheopheresis treatment of age-related macular degeneration (AMD). J Clin Apheresis. 2005;20:185-194.
29. Lund RD, Kwan ASL, Keegan DJ, Sauve Y, Coffey PJ, Lawrence JM. Cell transplantation as a treatment for retinal disease. Prog Retin Eye Res. 2001;20(4):415-449.
30. Wang H, Yagi F, Cheewatrakoolpong N, Sugino IK, Zarbin MA. Short-term study of retinal pigment epithelium sheet transplants on Bruch's membrane. Exp Eye Res. 2004;78:53-65.

31. Yaji N, Yamato M, Yang J, Okano T, Sadao H. Transplantation of tissue-engineered retinal pigment epithelial cell sheets in a rabbit model. Biomaterials. 2009;30:797-803.
32. Hsiue GH, Lai JY, L PK. Absorbable sandwich-like membrane for retinal-sheet transplantation. J Biomed Mater Res. 2002;61:19-25.
33. Tezel TH, Kaplan HJ, Del Priore LVD. Fate of human retinal pigment epithelial cells seeded onto layers of human Bruch's membrane. Invest Ophthalmol Vis Sci. 1999, Feb;40(2):467-476.
34. Gullapalli VK, Sugino IK, Patten YV, Shah S, Zarbin M.A. Impaired RPE survival on aged submacular human Bruch's membrane. Exp Eye Res. 2005;80:235-248.
35. Binder S. Scaffolds for Retinal Pigment Epithelium (RPE) Replacement Therapy. Br J Ophthalmol. 2011;95:441-442.
36. Langer R, Vacanti JP. Tissue engineering. Science. 1993, May, 14;260:920-926.
37. Fuchs JR, Nasseri BA, Vacanti JP. Tissue engineering: A 21st century solution to surgical reconstruction. Ann Thorac Surg. 2001;72:577-591.
38. Jagur-Grodzinski J. Biomedical application of functional polymers. React Funct Polym. 1999;39:99-138.
39. Morais JM, Papadimitrakopoulos F, Burgess DJ. Biomaterials/tissue interaction: possible solutions to overcome foreign body response. AAPS J. 2010, June;12(2):188-196.
40. Sell SA, McClure MJ, Garg K, Wolfe PS, Bowlin GL. Electrospinning of collagen/biopolymers for regenerative medicine and cardiovascular tissue engineering. Adv Drug Deliver Rev. 2009, Aug, 3;61:1007-1019.
41. Lavik E, Langer R. Tissue engineering: current state and perspectives. Appl Microbiol Biotechnol. 2004, Feb, 20;65:1-8.
42. Gunatillake PA, Adhikari R. Biodegradable synthetic polymers for tissue engineering. Eur Cells Mater. 2003;5:1-16.
43. Hergenrother RW, Yu XH, Cooper SL. Blood-contacting properties of polydimethylsiloxane polyurethanes. Biomaterials. 1992;15(8):635-640.
44. Werkmeister JA, Adhikari R, White JF, Tebb TA, Le TPT, Taing HC, Mayadunne R, Gunatillake PA, Danon SJ, Ramshaw JAM. Biodegradable and injectable cure-on-demand polyurethane scaffolds for regeneration of articular cartilage. Acta Biomater. 2010, Mar, 7;6:3471-3481.
45. Eaton JW. Molecular determinants of acute inflammatory responses to biomaterials. J Vasc Interv Radiol. 1998, Jul-Aug;9(4):703-705.
46. Courtney JM, Lamba NMK, Sundaram S, Forbes CD. Biomaterials. 1994;15(10):737-744.
47. Jiao YP, Cui FZ. Surface modification of polyester biomaterials for tissue engineering. Biomed Mater. 2007, Nov, 26;2:24-37.
48. Massia SP, Zilla P, editor. Tissue engineering of vascular prosthetic grafts [Internet]. Texas: Landes Bioscience; 1999 [cited 2010 Nov 10]. Available from: http://www.landesbioscience.com/curie/chapter/281/
49. Narayanan K, Leck KJ, Gao S, Wan ACA. Three-dimensional reconstituted extracellular matrix scaffolds for tissue engineering. Biomaterials. 2009, May, 28;30:4309-4317.

50. Nisbet DR, Forsythe JS, Shen W, Finkelstein DI, Horne MK. Review paper: A review of the cellular response on electrospun nanofibers for tissue engineering. J Biomater Appl. 2009, Jul;24:7-29.
51. Ma PX. Biomimetic materials for tissue engineering. Adv Drug Deliver Rev. 2008, Nov, 28;60:184-198.
52. Lam KH, Schakenraad JM, Grown H, Esselbrugge H, Dijkstra PJ, Feijen J, Nieuwenhuis P. The influence of surface morphology and wettability on the inflammatory response against poly(l-lactic acid): A semi-quantitative study using monoclonal antibodies. J Biomed Mater Res. 1995;29:929-942.
53. Harken DE, Taylor WJ, Lefemine AA, Lunzer ST, Low HBC, Cohen ML, Jacobey JA. Aortic valve replacement with a caged ball valve. Am J Cardiol. 1962, Feb:292-299.
54. Hersel U, Dahmen C, Kessler H. RGD modified polymer: biomaterials for stimulated cell adhesion and beyond. Biomaterials. 2003;24:4385-4415.
55. Ratner BD, Hoffman AS, Schoen FJ, Lemons JE. Biomaterials Science: An Introduction to Materials in Medicine. California: Academic Press; 1996.
56. Krishnan A, Siedlecki CA, Vogler EA. Mixology of protein solutions and the Vroman effect. Langmuir. 2004, Apr, 1;20:5071-5078.
57. Hirsh SL, McKenzie DR, Nosworthy NJ, Denman JA, Sezerman OU, Bilek MMM. The Vroman effect: competitive protein exchange with dynamic multilayer protein aggregates. Colloid Surface B. 2013;103:395-404.
58. Concord.org [Internet]. Massachusetts: The Concord Consortium; c2013 [updated 2010 Sep 10; cited 2013 Sep 17]. Available from: http://concord.org/stem-resources/diffusion-osmosis-andactive-transport
59. Hussain AA, Starit C, Hodgets A, Marshall J. Macromolecular diffusion characteristics of ageing human Bruch's membrane: Implication for age-related macular degeneration (AMD). Exp Eye Res. 2010, Mar, 3;703-710.
60. Bird AC, Marshall J. Retinal pigment epithelial detachments in the elderly. T Ophthal Soc UK. 1986;105(6):674-682.
61. Jackson TL, Antcliff RJ, Hillenkamp J, Marshall J. Human retinal molecular weight exclusion limit and estimate of species variation. Invest Ophthalmol Vis Sci. 2003, May;44(5):2141-2146.
62. Moore DJ, Clover GM. The effects of age on the macromolecular permeability of human Bruch's membrane. Invest Ophthalmol Vis Sci. 2001;42(12):2970-2975.
63. Sunder-Plassmann G, Hofbauer R, Sengoelge G, Horl WH. Quantification of leukocyte migration: Improvement of a method. Immunol invest. 1996:25(1&2):49-63.
64. Egger G. A noninvasive membrane filter method for in vivo determination of leukocyte migration in man. Inflammation. 1980;4(2):215-231.
65. Persidsky Y. Model systems for studies of leukocyte migration across the blood-brain barrier. J Neurovirol. 1999;5:579-590.
66. Rosato DV, Rosato DV, Rosato MV. Plastic product materials and process selection handbook. Oxford: Elsevier Advanced Technology; 2004.
67. Vasita R, Katti DS. Nanofibers and their applications in tissue engineering. Int J Nanomed. 2006;1(1):15-30.

68. Agarwal S, Wendorff JH, Greiner A. Use of electrospinning technique for biomedical applications. Polymer. 2008, Sep, 24;49:5603-5621.
69. Theron SA, Zussman E, Yarin AL. Experimental investigation of the governing parameters in the electrospinning of polymer solutions. Polymer. 2004;45:2017-2030.
70. Son WK, Youk JH, Lee TS, Park WH. The effects of solution properties and polyelectrolyte on electrospinning of ultrafine poly(ethylene oxide) fibers. Polymer. 2004;45:2959-2966.
71. Baker SC, Atkin N, Gunning PA, Granville N, Wilson K, Wilson D, Southgate J. Characterisation of electrospun polystyrene scaffolds for three-dimensional in vitro biological studies. Biomaterials. 2006;27:3136-3146.
72. Boland ED, Wnek GE, Simpson DG, Pawlowski KJ, Bowlin GL. Tailoring tissue engineering scaffolds using electrostatic processing techniques: A study of poly(glycolic acid) electrospinning. J Macromol Sci – Pure Appl Chem. 2001;A38(12):1231-1243.
73. Boland ED, Coleman BD, Barnes CP, Simpson DG, Wnek GE, Bowlin GL. Electrospinning polydioxanone for biomedical applications. Acta Biomater. 2005;1:115-123.
74. Cui W, Li X, Zhou S, Weng J. Degradation patterns and surface wettability of electrospun fibrous mats. Polym Degrad Stabil. 2008;93:731-738.
75. Brandon S, Haimovich N, Yeger E, Marmur A. Partial wetting of chemically patterned surfaces: the effects of drop size. J Colloid Interf Sci. 2003;263:237-243.
76. Meiron TS, Marmur A, Saguy IS. Contact angle measurement on rough surfaces. J Colloid Interf Sci. 2004;274:637-644.
77. Kumbar SG, James R, Nukavarapu SP, Lairencin CT. Electrospun nanofiber scaffolds: Engineering soft tissues. Biomed Mater. 2008, Aug, 8;3:1-15.
78. Schindler M, Ahmed I, Kamal J, Nur-E-Kamal A, Grafe TH, Chung HY, Meiner S. Biomaterials. 2005, Apr, 18;26:5624-5631.
79. Chen JW, Tseng KF, Delimartin S, Lee CK, Ho MH. Preparation of biocompatible membranes by electrospinning. Desalination. 2008;233:48-54.
80. Thieltges F, Stanzel BV, Liu Zengping, Holz FG. A nanofibrillar surface promotes superior growth characteristics in cultured human retinal pigment epithelium. Ophthal Res. 2011, Feb, 18;46:133-140.
81. Jean-Gilles R, Soscia D, Sequeira S, Melfi M, Gadre A, Castracane J, Larsen M. Novel modeling approach to generate a polymeric nanofiber scaffold for salivary gland cells. J Nanotechnol Eng Med-T ASME. 2010, Aug;1:1-9.
82. Ignatova M, Manolova N, Rashkov I. Electrospinning of poly(vinyl pyrrolidone)-iodine complex and poly(ethylene) oxide/poly(vinyl pyrrolidone)-iodine complex – a prospective route to antimicrobial wound dressing materials. Eur Polym J. 2007, Feb, 25;43:1609-1623.
83. Khil MS, Cha DI, Kim HY, Kim IS, Bhattarai N. Electrospun nanofibrous polyurethane membrane as wound dressing. J Biomed Mater Res Part B: Appl Biomater. 2003;67B:675-679.
84. Zhong S, Teo WE, Zhu X, Beuerman RW, Ramakrishna S, Yung LYL. An aligned nanofibrous collagen scaffold by electrospinning and its effects on invitro fibroblast culture. J Biomed Mater Res. 2006, Jun, 2;79A:456-463.

85. Zhang J, Qi H, Wang H, Hu P, Ou L, Guo S, Li J, Che Y, Yu Y, Kong D. Engineering of vascular grafts with genetically modified bone marrow mesenchymal stem cells on poly(propylene carbonate) graft. Artif Organs. 2006;30(12):898-905.
86. Han SO, Youk JH, Min KD, Kang YO, Park WH. Electrospinning of cellulose acetate nanofibers using a mixed solvent of acetic acid/water: Effects of solvent composition on the fiber diameter. Mater Lett. 2008, Jun, 30;62:759-762.
87. Bognitzki M, Czado W, Frese T, Schaper A, Hellwig M, Steinhart M, Greiner A, Wendorff JH. Nanostructure fibers via electrospinning. Adv Mater. 2001, Jan, 5;13(1):70-72.
88. Uyar T, Besenbacher F. Electrospinning of uniform polystyrene fibers: The effect of solvent conductivity. Polymer. 2008, Sep, 28;49:5336-5343.
89. Zheng J, He A, Li J, Xu J, Han CC. Studies on the controlled morphology and wettability of polystyrene surfaces by electrospinning or electrospraying. Polymer. 2006, Aug, 30;47:7095-7102.
90. Barakat NAM, Kanjwal MA, Sheikh FA, Kim HY. Spider-net within the N6, PVA and PU electrospun nanofiber mats using salt addition: Novel strategy in the electrospinning process. Polymer. 2009, Jul, 8;50:4389-4396.
91. Zhuo H, Hu J, Chen S. Electrospun polyurethane nanofibers having shape memory effect. Mater Lett. 2008;62:2074-2076.
92. Kenaway ER, Abdel-Hay FI, El-Newehy MH, Wnek GE. Processing of polymer nanofibers through electrospinning as drug delivery systems. Mater Chem Phys. 2009;113:296-302.
93. Ma Z, Kotaki M, Yong T, He W, Ramakrishna S. Surface engineering of electrospun polyethylene terephthalate (PET) nanofibers towards development of a new material for blood vessel engineering. Biomaterials. 2005;26:2527-2536.
94. Peyman GA, Koziol JE. Artificial intraocular lens attachment. United States patent 4,073,015, 1978, Feb, 14.
95. Chollet C, Chanseau C, Remy M, Guignandon A, Bareille R, Labrugere C, Bordenave L, Durrieu MC. The effect of RGD density on osteoblast and endothelial cell behavior on RGD-grafted polyethylene terephthalate surfaces. Biomaterials. 2009;30:711-720.
96. Charonakis IS, Grapenson S, Jakob A. Conductive polypyrrole nanofibers via electrospinning: Electrical and morphological properties. Polymer. 2006;47:1597-1603.
97. Piperno S, Lozzi L, Rastelli R, Passacantando M, Santucci S. PMMA nanofibers production by electrospinning. Appl Surf Sci. 2006;252:5583-5586.
98. Sundarrajan S, Murugan R, Nair AS, Ramakrishna S. Fabrication of P3HT/PCBM solar cloth by electrospinning technique. Mater Lett. 2010, Aug, 3;64:2369-2372.
99. Shabani I, Haddadi-Asl V, Seyedjafari E, Babaeijandaghi F, Soleimani M. Improved infiltration of stem cells on electrospun nanofibers. Biochem Bioph Res Co. 2009, Mar, 3;382:129-133.
100. Luo CJ, Nangrejo M, Edirisinghe M. A novel method of selecting solvents for polymer electrospinning. Polymer. 2010;51:1654-1662.

101. Lee KH, Kim HY, Khil MS, Ra YM, Lee DR. Characterization of nano-structured poly(ε-caprolactone) nonwoven mats via electrospinning. Polymer. 2003;44:1287-1294.
102. Li Z, Wang C. One-dimensional nanostructures: electrospinning technique and unique nanofibers. London: Springer London, Limited; 2013.
103. Koski A, Yim K, Shivkumar S. Effect of molecular weight on fibrous PVA produced by electrospinning. Mater Lett. 2004;58:493-497.
104. Casper CL, Stephens JS, Tassi NG, Chase DB, Rabolt JF. Controlling surface morphology of electrospun polystyrene fibers: Effect of humidity and molecular weight in the electrospinning process. Macromolecules. 2004;37:573-578.
105. De Vrieze S, Van Camp T, Nelvig A, Hagström B, Westbroek P, De Clerck K. The effect of temperature and humidity on electrospinning. J Mater Sci. 2009;44:1357-1362.
106. Bhatt NS, Newsome DA, French T, Hessberg TP, Diamond JG, Miceli MV, Kratz KE, Oliver PD. Experimental transplantation of human retinal pigment epithelial cells on collagen substrates. Am J Ophthalmol. 1994, Feb, 15;117(2):214-221.
107. Turowski P, Adamson P, Sathia J, Zhang JJ, Moss SE, Aylward GW, Hayes MJ, Kanuga N, Greenwood J. Basement membrane-dependent modification of phenotype and gene expression in human retinal pigment epithelial ARPE-19 cells. Invest Ophthalmol Vis Sci. 2004;45:2786-2794.
108. Thumann G, Schraermeyer U, Bartz-Schmidt KU, Heimann K. Descemet's membrane as membranous support in RPE/IPE transplantation. Curr Eye Res. 1997, Dec;16(12):1236-1238.
109. Thomson RC, Giordano GG, Collier JH, Ishaug SL, Mikos AG, Lahiri-Munir D, Garcia CA. Manufacture and characterization of poly(α-hydroxy ester) thin films as temporary substrates for retinal pigment epithelium cells. Biomaterials. 1996;17(3):321-327.
110. Hadlock T, Singh S, Vacanti JP, McLaughlin BJ. Ocular cell monolayers cultured on biodegradable substrates. Tissue Eng. 1999;5(3)187-196.
111. Lu L, Yaszemski MJ, Mikos AG. Retinal pigment epithelium engineering using synthetic biodegradable polymer. Biomaterials. 2001;22:3345-3355.
112. Williams RL, Krishna Y, Dixon S, Haridas A, Grierson I, Sheridan C. Polyurethanes as potential substrates for sub-retinal retinal pigment epithelial cell transplantation. J Mater Sci-Mater M 2005;16:1087-1092.
113. Stanzel BV, Englander M, Tieltges F, Strick DJ, Blumenkranz MS, Holz FG, Binder S, Marmor MF. Towards prosthetic replacement of Bruch's membrane: comparison of polyester and electrospun nanofiber substrates. Deutsche Ophthalmologische Gesellschaft Kongress; 2008 Sep 18-21; Berlin.
114. Li Y, Tang L. Comparison of growth of human fetal RPE cells on electrospun nanofibers and etched pore polyester membranes. J Cent S Univ Med Sci. 2012, May;37(5):433-440.
115. Stanzel BV, Liu Z, Brinken R, Braun N, Holz FG, Eter N. Subretinal delivery of ultrathin rigid-elastic cell carriers using a metallic shooter instrument and biodegradable hydrogel encapsulation. Invest Ophthalmol Vis Sci. 2012, Jan;53(1):490-500.

116. Hadjizadeh A, Ajji A, Bureau MN. Nano/micro electro-spun polyethylene terephthalate fibrous mat preparation and characterization. J Mech Behav Biomed. 2011;4:340-351.
117. Curtis ASG, Forrester JV, McInnes C, Lawrie F. Adhesion of cells to polystyrene surfaces. J Cell Biol. 1983;97:1500-1506.
118. Corning.com [Internet]. New York: Corning Incorporated; c1994-2013 [updated 2013 Feb 25; cited 2013 Jun 19]. Available from: http://www.corning.com/lifesciences/us_canada/en/technical_resources/surfaces/culture/stc_treated_polystyrene.aspx
119. Sanders JE, Lamont SE, Karhin A, Golledge SL, Ratner BD. Fibro-porous meshes made from polyurethane micro-fibers: Effects of surface charge on tissue response. Biomaterials. 2005, May, 12;26:813-818.
120. Dennes TJ, Schwartz J. Controlling cell adhesion on polyurethanes. Soft Matter. 2008;4:86-89.
121. Coffey P, Da Cruz L, Cheetham K. Membrane. US20110236464A1 (Patent). 2011.
122. Minassian DC, Reidy A, Lightstone A, Desai P. Modelling the prevalence of age-related macular degeneration (2010-2020) in the UK: Expected impact of anti-vascular endothelial growth factor (VEGF) therapy. Br J Ophthalmol. 2011 [cited 18 Jan 2012]. 1-4. Available: doi: 10.1136/bjo.2010.195370
123. Warnke PH, Alamein M, Skabo S, Stephens S, Bourke R, Heiner P, Liu Q. Primordium of an artificial Bruch's membrane made of nanofibers for engineering of retinal pigment epithelium monolayers. Acta Biomater. 2013;9:9414-9422.
124. Wendorff JH, Agarwal S, Greiner A. Electrospinning: Materials processing and applications. John Wiley and Sons; 2012.
125. Ramakrishna S, Fujihara K, Too W-E, Tim T-C, Ma Z. An introduction to electrospinning and nanofibers. World Scientific; 2005
126. Ma Q, Mao B, Cebe P. Morphology and phase structure of electrospun nanofibers of PET with silicon dioxide nanoparticles. Proceedings of the 38th Annual Conference of North American Thermal Analysis Society; 2010 Aug 15-18; Philadelphia, Pennsylvania.
127. Reimer L, Hawkes PW, editor. Scanning electron microscopy: Physics of image formation and microanalysis. Springer London, Ltd; 2010.
128. Agarwal CM, Ong JL, Appleford MR, Mani G. Introduction to biomaterials: Basic theory with engineering applications. Cambridge University Press; 2013.
129. Veleirinho B, Rei MF, Lopes-Da-Silva JA. Solvent and concentration effects on the properties of electrospun poly(ethylene terephthalate) nanofiber mats. J Polym Sci Pol Phys. 2008;46:460-471.
130. Mittal KL. Polymer surface modification: Relevance to adhesion, volume 5. BRILL; 2009.
131. Fridman A, Kennedy LA. Plasma physics and engineering. CRC Press; 2004.
132. Xu L-C, Siedlecki CA. Effects of surface wettability and contact time on protein adhesion to biomaterial surfaces. Biomaterials. 2007;28:3273-3283.
133. Mittal KL. Contact angle, wettability and adhesion, volume 6. BRILL; 2009.
134. Watts JF, Wolstenholme J. An introduction to surface analysis by XPS and AES. Wiley; 2003.

135. Chen T. A practical guide to assay development and high-throughput screening in drug discovery. CRC Press; 2009.
136. Hughes D, Mehmet H, editors. Cell proliferation and apoptosis. Garland Science; 2003.
137. Buchwalow IB, Bocker W. Immunohistochemistry: Basics and methods. Springer, 2010.
138. World Precision Instruments, Inc. EN 61326-2-3:2006. EVOM^2 Epithelial Voltohmeter. Sarasota: WPI, Inc; 2009.
139. Harland DJ. STEM student research handbook. USA: NSTA Press; 2011.
140. Housecroft CE, Constable EC. Chemistry. 3rd ed. Essex: Pearson Education Limited; 2006.
141. Clayden J, Greeves N, Warren S, Wothers P. Organic chemistry. New York: Oxford University Press Inc; 2006.
142. Sigmaaldrich.com [Internet]. United States: Sigma-Aldrich Co LLC; c2013 [cited 2013 Sep 11]. Available from: http://www.sigmaaldrich.com/chemistry/solvents/tetrahydrofuran-center/physical-properties.html
143. Sigmaaldrich.com [Internet]. United States: Sigma-Aldrich Co LLC; c2013 [cited 2013 Sep 11]. Available from: http://www.sigmaaldrich.com/chemistry/solvents/dichloromethane-center/physical-properties.html
144. Gopal R, Zuwei M, Kaur S, Ramakrishna S. Surface modification and application of functionalized polymer nanofibers. In: Mansoori GA, George TF, Assoufid L, Zhang G, editors. Molecular building blocks for nanotechnology. New York: Springer; 2007. p. 72-91.
145. Keselowsky BG, Collard DM, Garcia AJ. Surface chemistry modulates fibronectin conformation and directs integrin binding and specificity to control cell adhesion. J Biomed Mater Res. 2003;66A:247-259.
146. Gillen KT, Wallace JS, Clough RL. Dose-rate dependence of the radiation-induced discolouration of polystyrene. Radiat Phys Chem. 1993;41(1/2):101-113.
147. Klein RJ, Fischer DA, Lenhart JL. Systematic oxidation of polystyrene by ultraviolet-ozone, characterized by near-edge X-ray absorption fine structure and contact angle. Langmuir. 2008;24(15):8187-8197.
148. Atthoff B, Hillborn J. Protein adsorption onto polyester surfaces: Is there a need for surface activation. J Biomed Mater Res Part B: Appl Biomater. 2007;80B:121-130.
149. Nisbet DR, Forsythe JS, Shen W, Finkelstein DI, Horne MK. Review paper: A review of the cellular response on electrospun nanofibers for tissue engineering. J Biomater Appl. 2009;24:7-29.
150. Ma T, Li Y, Shang-Tang Y. Tissue engineering human placenta trophoblast cells in 3-D fibrous matrix: Spatial effects on cell proliferation and function. Biotechnol Prog. 1999;15:715-724.
151. Dunn KC, Aotaki-Keen AE, Putkey FR, Hjelmeland LM. ARPE-19, a human retinal pigment epithelial cell line with differentiated properties. Exp Eye Res. 1996;62:155-169.

152. Luo Y, Zhuo Y, Fukuhara M, Rizzolo LJ. Effects of culture conditions on heterogeneity and the apical junction complex of the ARPE-19 cell line. Invest ophthalmol vis sci. 2006;47:3644-3655.
153. Mannermaa E, Reinisalo M, Ranta V-P, Vellonen K-S, Kokki H, Saarikko A, Kaarniranta K, Urtti A. Filter-cultures ARPE-19 cell as outer blood-retinal barrier model. Eur J Pharm Sci. 2010;40:289-296.
154. Baharloo B, Textor M, Brunette DM. Substratum roughness alters the growth, area, and focal adhesions of epithelial cells, and their proximity to titanium surfaces. J Biomed Mater Res A. 2005;74A:12-22.
155. Badami AS, Kreke MR, Thompson MS, Riffle JS, Goldstein AS. Effect of fiber diameter of spreading, proliferation, and differentiation of osteoblastic cells on electrospun poly(lactic acid) substrates. Biomaterials. 2006;27:596-606.
156. Quinn RH, Miller SS. Ion transport mechanisms in native human retinal pigment epithelium. Invest Ophthalmol Vis Sci. 1992;33:3513-3527.
157. Nevala H, Ylikomi T, Tahti H. Evaluation of the selected barrier properties of retinal pigment epithelial cell line ARPE-19 for an in-vitro blood-brain barrier model. Hum Exp Toxicol. 2008;27:741-749.
158. Stanzel BV, Liu Z, Somboonthanakij, Wongsawad W, Brinken R, Eter N, Corneo B, Holz FG, Temple S, Stern JH, Blenkinsop TA. Human RPE stem cell grown into polarized RPE monolayers on a polyester matrix are maintained after grafting into rabbit subretinal space. Stem Cell Reports. [Internet] 2014;In Press [cited 17 Jul 2014]. Available from: http://dx.doi.org/10.1016/j.stemcr.2013.11.005
159. Liu Z, Yu N, Holz FG, Yang F, Stanzel BV. Enhancement of retinal pigment epithelial culture chracteristics and subretinal space tolerance of scaffold with 200 nm fiber topography. Biomaterials. [Internet] 2014;In Press [cited 17 Jul 2014]. Available from: http://dx.doi.org/10.1016/j.biomaterials.2013.12.069
160. Christiansen AT, Tao SL, Smith M, Wnek GE, Prause JU, Young MJ, Klassen H, Kaplan HJ, la Cour M, Kiilgaard JF. Subretinal implantation of electrospun, short nanowire, and smooth poly(ε-caprolactone) scaffolds to the subretinal space of porcine eyes. Stem Cells International. [Internet] 2012 [cited 11 Sep 2013]; 2012:1-8. Available from: doi:10.1155/2012/454295

Appendix 1

Here follows the patent, application number: GB12009863.8, as it was sent.

SYNTHETIC MEMBRANE

FIELD OF THE INVENTION

The present invention relates to synthetic membranes that can be used to replace naturally occurring membranes in the body of humans or animals, especially synthetic basal membranes. In particular, the present invention relates to a synthetic membrane that can be used as a replacement for the Bruch's membrane, for the treatment of age-related macular degeneration.

BACKGROUND

Age-related macular degeneration (AMD) is the primary registered cause of blindness in the West [Resnikoff et al 2004]. Recent estimates suggest that 182,000 to 300,000 people are affected in the United Kingdom alone, and 20 to 25 million are affected worldwide [Chopdar et al 2003]. Furthermore, due to an increase in life expectancy, clinicians predict this value will triple in the next three decades [Minassian et al 2011].

AMD is a disorder of the retina, in particular a region called the macula, which is situated directly behind the lens and is responsible for central vision. The retina is a made up of multiple membranous layers. Of particular relevance to AMD is the Bruch's membrane (BM) whose top-most layer (the basal lamina) serves as a substrate for a monolayer of retinal pigment epithelial cells (RPE) which in turn provides a substrate for the attachment of photoreceptors. The Bruch's membrane is a porous structure, formed from layers of collagen, elastin and laminin, which permits the passage of nutrients to and waste from the RPE and photoreceptor cells, but blocks the passage of larger structures such as blood vessels.

There are two forms of AMD: the wet form, which makes up 10% of all AMD cases and is treatable and the dry form, which makes up 90% of all AMD cases, and has no known cure to date.

In dry AMD it is thought that the BM thickens because of an increase in oxidative stress with age. This leads to the accumulation of oxidation products in the porous BM, which blocks the exchange of nutrients and waste across the membrane. As a result of this blockage, the
RPE monolayer is not able to obtain the nutrients it requires in order to survive and begins to die. This in turn causes the photoreceptors to die, leading to central blindness.

Various treatments for dry AMD have been proposed which seek to address the loss of RPE cells and, in turn, photoreceptor cells.

Some suggested approaches have sought to replace lost RPE cells with fresh cells, either introduced in the form of a suspension or in the form of a cell monolayer placed directly onto
the native BM [Hsiue et al 2002]. However, these approaches have met with limited success because cells introduced as part of a suspension exhibit poor cell survival, and cell monolayers have proved difficult to handle. Moreover, these approaches rely on the fresh cells attaching to the native BM which, because of its diseased state, is not able to effectively support newly-introduced cells.

Other suggested approaches have sought to replace the diseased BM with an alternative BM, either obtained from a donor or created synthetically. Since obtaining healthy BM's from donors is of limited practical value (given the large number of potential patients compared to the number of available donors) recent studies have focussed on synthetic cell-supporting substrates that can be substituted for a diseased BM [Del Priore et al 2006].

Known substrates taking the form of synthetic membranes made from biodegradable polymers such as poly-L-lactic acid or polyglycolic acid [Thomson et al 2011], and substrates where cell monolayers are sandwiched between two layers of gelatine [Wang et al 2004] have a number of drawbacks. For example, the metabolic products of the biodegradable polymer materials are acidic, which could have an adverse impact on cell survival once the polymers begin to degrade [Binder et al 2011].

US 2012/0009159 suggests various synthetic substrates for the replacement of the BM. The substrates may include surfaces for growing cells on or cage-like structures for growing cells in, and allow transfer of material through pores or by the inherent permeability of the material used to make the substrate (which involves optimisation of the thickness of the layer). The substrates may be manufactured by extrusion, drawing, injection moulding, sintering, micro machining, laser machining and/or electrical discharge machining. Pores may also be introduced by photolithography, or dissolving away regions of water-soluble polymer. The substrates may be made from either biodegradable or non-biodegradable polymers (in particular, Parylene™ polymers), or a combination of both.

As mentioned above, a replacement for the Bruch's membrane should allow RPE cells to attach to and grow on the substrate. To promote cell attachment to known synthetic substrates, it is common to functionalise the surface with cell-binding molecules, in particular, nitrogen-containing molecules such as proteins. For long lasting attachment, it is preferable for such molecules to chemically bond to the surface via a reactive group on the surface, instead of relying on weaker physisorption. To this end, it is known to introduce suitable reactive groups to the surface in a separate step; for example, it is known to introduce oxygen-containing moieties on the surface by UV/ozone or plasma treatment. However, such additional surface treatment steps add further complexity and expense to the manufacturing process.

In view of the above, there still exists a need for a synthetic substrate suitable for replacing the Bruch's membrane which addresses the above-mentioned problems. The present inventors have identified that such synthetic substrates should preferably satisfy several criteria. Firstly, the substrate should share the same transfer properties as the Bruch's membrane: allowing nutrients and waste to pass through the membrane whilst blocking the passage of blood vessels. Secondly, the substrate should allow RPE cells to attach to and grow on the substrate. Thirdly, the substrate should not break down into potentially

damaging degradation products. Fourthly, the substrate should have similar mechanical properties to the Bruch's membrane (in particular, flexibility) when engineered to be a similar size to the native membrane.

SUMMARY OF THE INVENTION

To address the above problems, at its most general, the present invention proposes that a suitable replacement for the Bruch's membrane can be created from fibres, especially polyester fibres.

A first aspect of the invention provides a synthetic Bruch's membrane comprising fibres. Suitably the fibres are polymer fibres, preferably polyester fibres.

Embodiments of the present invention satisfy the criteria outlined above, and address problems associated with previously suggested substrates.

The fibres may overlap with one another so as to take the form of a mesh. By "mesh" we mean that the fibres overlap or are overlaid with respect to each other so as to form a network of fibres.

The synthetic membrane suitably comprises, at least in the plane of the membrane (i.e. in the plane parallel to the upper and lower surfaces of the membrane when the membrane is lying on a flat surface), randomly oriented polyester fibres. That is the fibres do not have a specific or ordered orientation relative to one another, and are not aligned with one another. Suitably, the membrane comprises layers of randomly oriented fibres. In embodiments, the fibres are formed or deposited on top of one another but adopt random orientations relative to one another.

Suitably, the membrane (at least prior to insertion in the body) is a planar membrane. Thus, the membrane is suitably substantially flat (e.g., when laid out on a flat surface). In preferred embodiments, the majority of the fibres are oriented approximately parallel to the plane of

the membrane. In other words, the majority of the fibres lay approximately horizontal within the membrane. That is, the fibres do not substantially extend vertically through the thickness of the membrane. For example, 50% or more of the fibres extend in a direction parallel to the plane of the membrane, more preferably 75% or more, more preferably 90% or more, most preferably 95% or more. In embodiments, substantially all of the fibres are parallel to the plane of the membrane. Some or all of the fibres may, however, adopt a shallow angle relative to the plane of the membrane. For example, the fibres may adopt an angle of 15° or less relative to the plane of the membrane, more preferably 10° or less, more preferably still 5° or less.

The synthetic membrane is a biocompatible substrate that can serve as a replacement for some or all of the native BM. The term "biocompatible" as used herein will be familiar to the skilled reader but for completeness it pertains to a substrate which is compatible with natural tissue such that a significant immune response or other rejection response is not observed when the substrate is inserted (e.g., surgically implanted) into the human or animal body. Suitably, the synthetic membrane is made from a biocompatible polymer, preferably a biocompatible polyester.

Membranes of the present invention are suitably configured so that cells can grow in a monolayer on top of the membrane but are unable to substantially infiltrate and grow within the membrane. In other words, the membrane essentially presents a two-dimensional surface for cells to grow on, instead of a three-dimensional scaffold that cells can grow in and around. Thus, suitably, the membrane is substantially impermeable to cells, in particular, substantially impermeable to blood vessels/capillaries.

The synthetic membrane of the present invention has been found by the present inventors to provide an excellent mimic of the fibrous structure of the native Bruch's membrane (which can be seen in Del Priore 2006). The present inventors have found that the synthetic membrane shares similar transfer properties with the Bruch's membrane. The gaps

between fibres define fluid flow paths that are sufficiently large to allow the passage of nutrients and waste but are too small to allow larger structures such as blood vessels/capillaries to infiltrate the membrane. When the fibres are randomly oriented relative to one another, the fluid flow paths can be tortuous paths. The presence of fluid flow paths in synthetic membranes of the present application is advantageous over synthetic membranes which rely on the inherent porosity of the membrane for transfer of material, because the porosity of such membranes is often dependent on the thickness of the membrane, meaning that suitable transfer properties may only be achieved for membranes having a small range of thicknesses.

In terms of cell proliferation, the present inventors have found that polyester fibres in particular provide an excellent surface for cells to attach to and grow upon. The present inventors have found that polyesters fibres are able to chemically bond to proteins and other nitrogen-containing compounds without the need for additional surface groups to be introduced. It is believed that this is due to the presence of the ester moiety, which may react with and bond to nitrogen-containing molecules, a reaction known as aminolysis. Advantageously, this means that synthetic membranes of the present invention can chemically bond to cell-binding molecules without the need for prior surface treatment. This has the potential to decrease the time and expense of creating the synthetic membrane compared to substrates that require surface treatment. Although surface treatment is not necessary, it is still possible for synthetic membranes of the present invention to undergo surface treatments known in the art.

The synthetic membranes can be coated with specific molecules to promote cell attachment including, but not limited to, RGD moieties, PDGF, IKVAV, fibronectin, vitronectin and other adhesive glycoproteins. In addition, it has been found by the present inventors that treatment with standard cell culture medium is sufficient to functionalise membranes of the present invention with molecules that promote cell attachment.

Forming the synthetic membrane from fibres helps to improve the flexibility of the membrane compared to prior art substrates having a comparable thickness. In particular, the membrane is more flexible than a solid sheet of the same material having a comparable thickness. In addition, the fact that the fibres are suitably randomly oriented means that the effort required to flex the membrane should be reasonably independent of the direction in which it is flexed. This is in contrast to substrates having through pores at specific locations, because the effort required to flex the substrate in such instances will be more dependent on the direction in which the substrate is flexed, due to the specific positioning of the through pores. The flexibility of the membranes of the present invention means that it can conform to a chosen surface in the body, such as the back of the eye. In addition, a mesh of fibres is less prone to curling up at the edges than prior art membranes, which decreases the risk of the retina being damaged.

Advantageously, the mechanical properties of the membranes of the present invention allow the membranes to be easily handled and manipulated by surgeons, veterinarians and others.

Synthetic membranes of the present invention can be produced with the micro-porosity, mechanical properties and diffusion properties required for specific medical needs. The shape, size and connectivity of the inter-fibre fluid flow paths can be readily altered. This is a major advantage in developing synthetic membranes because the membranes can be configured so as to have specific exclusion properties. Suitably, the membranes can be configured so that they prevent the infiltration of small capillaries, but allow the diffusion of growth factors, nutrients and gases across the membrane. Suitably, the membranes may encourage tissue repair.

Suitably, the fibres comprise at least 50 wt% of the synthetic membrane based on the total weight of the membrane, preferably at least 60 wt%, more preferably at least 70 wt%, more

preferably at least 80 wt%, more preferably still at least 90 wt% and most preferably about 100 wt%.

Preferably, the fibres comprise at least 50 wt% polyester based on the weight of the fibres, preferably at least 60 wt%, more preferably at least 70 wt%, more preferably at least 80 wt%, more preferably still at least 90 wt% and most preferably about 100 wt%. In embodiments, the fibres may consist essentially of polyester. The polyester may be a homopolymer or a copolymer.

Preferably, the synthetic membrane is made from a non-biodegradable fibre, suitably a non-biodegradable polymer, preferably a non-biodegradable polyester. Advantageously, membranes formed from non-biodegradable polyesters will persist in the body of a patient in which they are inserted. The term "non-biodegradable" as used herein will be familiar to the skilled reader but for completeness pertains to a substance that does not break down and disperse *in vivo*. This means that the membrane does not produce any harmful breakdown products and will persist in the body, so that it is not necessary to replace it by repeat surgery. By contrast, membranes formed from a biodegradable substance may degrade in the body (potentially generating harmful (e.g., acidic) degradation products) to a point where it is necessary to replace them.

Preferably, the polyester used to make the fibres is poly (ethylene terephthalate), henceforth referred to as PET. PET is a biocompatible polymer that is approved for medical use by the US Food and Drug Administration, and is commonly used in medical sutures. Advantageously, PET is a commonly available non-biodegradable polyester. The present inventors have found that PET can be formed into nanoscale fibres to make synthetic membranes of the present invention. In addition, the surface chemistry of PET facilitates the attachment of cells to the substrate. For example, the surface of PET inherently contains oxygen groups which the present inventors have found readily react with nitrogen-containing molecules including proteins. Therefore, no surface treatment (such as UV/ozone treatment

or O_2 plasma treatment) is required to functionalise the surface in order for it to be reactive towards proteins, and other molecules which promote cell attachment. This is advantageous because no surface treatment step is required during the manufacture of the membrane (which would otherwise increase the complexity of the manufacturing). However, surface treatment using methods known in the art is still possible when desired.

In embodiments of the invention in which the fibres comprise polymer, it is preferred that the polymer has a number average molecular weight (MW) of 5×10^5 or less, more preferably 1×10^5 or less, more preferably still 5×10^4 or less. In embodiments of the invention in which the fibres comprise polymer, the MW may be, for example, 1×10^3 or greater, 5×10^3 or greater, or 1×10^4 or greater.

In embodiments of the invention, the gaps between fibres (inter fibre gaps or voids) are smaller than the cells which the membrane is intended to support in order to promote formation of a monolayer. When the gaps between fibres are comparable to or larger than the size of the cells, cells can sit within these gaps. This means that neighbouring cells may be present at different heights on the membrane, or may be “corralled” within separate regions on the membrane, making it difficult to form a monolayer. An advantage of the present invention is that the gaps/voids can be controlled so as to control the topography of the relevant surface(s) of the membrane (typically the upper cell-contacting surface).

The fibres overlay one another so as to form gaps having random shapes in the plane of the membrane. These shapes approximate the form of polygons, sometimes with curved sides (when the fibres themselves are curved within the membrane). In preferred embodiments, on a surface of the membrane that is intended for cell attachment, cell growth or cell support, the maximum distance separating the sides of these inter fibre void shapes is 20 µm or less, more preferably 15 µm or less, more preferably 10 µm or less, more preferably still 5 µm or less. Alternatively or additionally, the mean maximum distance separating the sides of the inter fibre voids, in respect of the surface, is 20 µm or less, 15 µm or less, 10 µm or less, or 5

µm or less. The maximum distance separating the sides of the voids can be measured from SEM images and analysed using a software package such as ImageJ. For example, a user can manually identify inter fibre voids and, with a knowledge of the size of the SEM image, measure the distances between the fibres defining that void to determine the maximum distance.

Generally, and in particular to achieve gaps of the desired size, it is preferable for the fibres to have a mean diameter of about 1 µm or less. Advantageously, fibres having a mean diameter of about 1 µm or less pack together to form a synthetic membrane having gaps which are smaller than the cells which the membrane is intended to support (for example, RPE cells are approximately 20 µm in diameter). This promotes the formation of a monolayer, and avoids cells entering the gaps and wrapping around the fibres. More preferably, the fibres have a mean diameter of about 800 nm or less, more preferably about 600 nm or less and most preferably about 400 nm.

The minimum mean diameter may be, for example, about 100 nm, about 150 nm, about 200 nm, about 250 nm, about 300 nm, about 350 nm, or about 400 nm.

In preferred embodiments, the synthetic membrane has a thickness (i.e. between upper and lower surfaces of the membrane) of about 100 µm or less. For example, the membrane may have a thickness of about 80 µm or less, about 60 µm or less, about 40 µm or less, about 20 µm or less, about 10 µm or less, about 5 µm or less, about 4 µm or less, about 3 µm or less, about 2 µm or less or about 1 µm or less. In particularly preferred embodiments the membrane is about 5 µm or less, more preferably about 4 µm or less. Advantageously, a thickness of about 4 µm reflects the thickness of the native BM in humans, and therefore makes the membrane ideally suited to being used as a replacement for the native BM.

In embodiments, the synthetic membrane may have a thickness of about 1 µm or more. For example, the membrane may have a thickness of about 2 µm or more, 3 µm or more, 4 µm or more, 5 µm or more, 10 µm or more or 20 µm or more.

In preferred embodiments, the membrane has a thickness of between 1 to 4 μm, preferably between 2 to 4 μm and most preferably between 3 to 4 μm. The thickness of the membranes can be measured using methods known in the art. For example, the thickness can be measured using a micrometer, such as a digital electronic micrometer. Alternatively, the thickness may be measured from scanning electron micrographs. Preferably, the thickness of the membrane is relatively uniform across the membrane. For example, the difference between the thinnest and thickest sections of the membrane may be less than 30% of the mean thickness value for the membrane, less than 20% of the mean thickness value, less than 10% of the mean thickness value or less than 5% of the mean thickness value.

In embodiments of the invention, the membranes may take a variety of shapes. For example, the membrane may have a polygonal shape (such as a square or rectangle) or may be circular or elliptical. The shape of the membrane can be chosen according to the particular use it is being put to. For example, the membrane's shape can be configured so as to satisfy specific biological and anatomical requirements.

In preferred embodiments, the membrane has a maximum length and/or width (which may be selected independently) of 10 mm or less. More preferably the membrane has a maximum length and/or width (which may be selected independently) of 5 mm or less. When the membrane is circular, "length" refers to the diameter of the circle.

Preferably, the synthetic membrane has a very small number of bead structures, most preferably, no bead structures. Bead structures are imperfections in the membrane which are formed from globules of polymer that stick to the fibres. These globules can be significantly larger than the diameter of the fibres, and therefore can lead to "lumps" in the membrane. Such lumps can adversely affect the mechanical properties of the membrane, and affect the membrane's ability to support a monolayer of cells. Preferably, the mean number of bead structures per 20 μm^2 (of a surface of the membrane) is less than 10, more

preferably less than 5, more preferably less than 1. Most preferably, the membrane does not contain any bead structures.

Preferably, the distribution of fibre thicknesses is relatively narrow. Advantageously, a narrow distribution of fibre thicknesses improves the packing of fibres, resulting in the substrate having good surface uniformity. For example, when the distribution can be approximated by a normal distribution, it is preferred that the distribution has a standard deviation less than 50% of the distribution's mean, more preferably less than 40%.

In preferred embodiments the fibres have a rounded cross-section, because this leads to improved packing of the fibres. In such embodiments, it is preferred that the fibres have a substantially circular cross-section.

The membranes of the present invention can be used in conjunction with other layers, for example when used as a replacement for the Bruch's membrane. For example, the synthetic membrane of the present invention may be connected to or abut another fibrous or non-fibrous layer. In certain embodiments, the membrane of the present invention forms only the basal layer/lamina of the Bruch's membrane. The other layers may be synthetic, or may be naturally occurring, such as human or animal tissue. Alternatively, the synthetic membranes of the present invention may be used as a replacement for the Bruch's membrane without the addition of other layers.

The present inventors have found that electrospinning provides a particularly effective way of producing the synthetic membrane of the first aspect. Accordingly, it is preferred that synthetic membranes of the present invention are created by electrospinning (and hence the fibres are electrospun fibres). The electrospinning can either be achieved using molten polymer (e.g., polyester) or, more preferably, a polymer-solution (e.g., a polyester-solution). However, it should be appreciated that other methods know in the art may be used to produce the synthetic membranes of the present invention, including melt spinning and fibre extrusion.

Electrospun membranes of the present invention may be produced from polymer solutions containing 15 to 35% w/v polymer (e.g., polyester), using applied voltages of 15 to 25 kV, a needle-to-collection plate distance of 5 to 15 cm, and a flow rate of 0.5 mL/hour to 3 mL/hour.

If the applied voltages are significantly larger than 25 kV then the fibres will tend to be thicker than desired, and if the voltage is significantly lower than 15 kV then beading of the fibres will occur.

If the polymer solution concentration is significantly greater than 35% w/v polymer (e.g., polyester) then the electrospinning will be ineffective, and if the polymer solution concentration is significantly less than 15% w/v polymer (e.g., polyester) then beading of the fibres will occur. Suitable solvents for dissolving the polymer include, for example, acetone, chloroform and 1,1,1,3,3,3-hexafluoroisopropanol.

A second aspect of the invention relates to the use of a synthetic membrane as described above for replacing some or all of the Bruch's membrane of a human or animal. A related aspect is a method of treatment (e.g., of AMD) comprising replacing some or all of the Bruch's membrane).

A third aspect of the invention provides a synthetic membrane according to the first aspect for use in a method of treatment of the human or animal body. In particular, this further aspect provides a synthetic membrane for use in a method of treating dry AMD in a human or animal body. Suitably the method is a method of treatment by surgery.

In this aspect, it is preferred that the method of treatment involves growing a monolayer of RPE cells on the synthetic membrane and subsequently transplanting the cell-bearing membrane into the eye of a patient.

A fourth aspect of the invention provides a method of making a synthetic Bruch's membrane comprising electrospinning a plurality of fibres. In preferred embodiments of this aspect, the

method involves electrospinning a polymer, for example from a polymer-solution. In some embodiments, the method involves a further step of re-sizing (e.g., by cutting or trimming) the membrane for insertion into a human or animal body. In a fifth aspect, the invention provides a synthetic membrane made according to the fourth aspect.

In embodiments, the synthetic membrane of any of the aspects is provided in a sterile enclosure, for example a sterile packet. Suitably the enclosure is hermetically sealed.

Thus, in a sixth aspect the present invention provides a synthetic membrane according to any one of the aspects herein, wherein the membrane is provided in a sterile enclosure.

It is envisaged that the synthetic membrane may be provided in a variety of different sizes and morphologies, for example in a number of "off the shelf" configurations, so as to enable a surgeon or veterinarian to select the most appropriate membrane to suit the human or animal being treated. Thus, in a seventh aspect, the present invention provides a kit comprising a plurality of synthetic membranes, each membrane being a membrane according to any one of the aspects herein, wherein each membrane is provided in a sterile enclosure. Suitably at least some of the membranes are different, e.g. have different dimensions and/or morphologies.

In other aspects, the synthetic membrane is used in applications other than for replacement of a BM. Suitably, in such aspects, the synthetic membrane is for replacement of a naturally occurring/native membrane in a human or animal body other than the BM. For example, the synthetic membrane may be a synthetic basal membrane for replacing a naturally occurring membrane. The aspects relating to making and using the membrane also apply here.

Any one of the aspects of the present invention may be combined with any one or more of the other aspects. Furthermore, any of the optional or preferred features of any one of the aspects may apply to any of the other aspects. In particular, optional features associated with a method or use may apply to a synthetic membrane, and vice versa.

BRIEF DESCRIPTION OF THE DRAWINGS

Embodiments of the invention will now be described, by way of example only, with reference to the accompanying drawings in which:

Figure 1 shows an SEM image of an electrospun PET membrane;

Figure 2 shows an SEM image of an electrospun PS membrane;

Figure 3 shows a histogram of fibre diameters from an SEM image of a PET membrane;

Figure 4 shows a histogram of fibre diameters from an SEM image of a PS membrane;

Figure 5 shows water contact angle data for PET membranes subjected to UV/ozone treatment for different periods of time;

Figure 6 shows water contact angle data for PS membranes subjected to UV/ozone treatment for different periods of time;

Figure 7 shows XPS data for PET membranes, both with and without UV/ozone treatment;

Figure 8 shows the C1s peaks of Figure 7 in greater detail;

Figure 9 shows the O1s peaks of Figure 7 in greater detail;

Figure 10 shows XPS data for PS membranes, both with and without UV/ozone treatment;

Figure 11 shows the C1s peaks of Figure 10 in greater detail;

Figure 12 shows the O1s peaks of Figure 10 in greater detail;

Figures 13 and 14 show XPS data demonstrating the effect of cell culture medium on the PET and PS membranes respectively;

Figure 15 shows fluorescence from ARPE-19 cells, stained with DAPI and Phalloidin, grown on (A) an untreated PET membrane, (B) a 300 seconds UV/ozone treated PET membrane of

the present invention, (C) a 450 seconds UV/ozone treated PET membrane of the present invention and (D) a positive control glass slide;

Figure 16 shows fluorescence from ARPE-19 cells, stained with DAPI and Phalloidin, grown on (A) an untreated PS membrane, (B) a 300 seconds UV/ozone treated PS membrane, (C) a 450 seconds UV/ozone treated PS membrane and (D) a positive control glass slide.

DETAILED DESCRIPTION OF THE INVENTION

A synthetic membrane formed from a mesh of PET was created as described below. In addition a membrane formed from polystyrene (PS) was created to allow a comparison of the properties of a polyester with those of a non-polyester polymer. PS provides a useful comparison because it is the polymer in tissue culture plastic that is used universally to successfully culture various cells.

Production of the synthetic membranes

Fibres were produced by electrospinning. Electrospinning provides a way of generating fibres of controlled diameter. In particular, electrospinning enables the fabrication of long, continuous fibres of controlled diameter. At its simplest, the application of a high voltage to a polymer solution within a syringe causes expulsion of a polymer jet towards an earthed collector.

A number of parameters can be used to control the properties of the fibres formed using electrospinning. The following parameters are mentioned as particularly useful in controlling the collected fibres:

1. Solvent
2. Molecular weight of polymer
3. Concentration of polymer-solvent solution
4. Applied voltage

5. Tip to collector distance
6. Flow rate of polymer-solvent solution

A homogeneous PET solution was created by dissolving PET pellets (MW (Mn) 10,215, Sigma-Aldrich Ltd.) in 1,1,1,3,3,3-hexafluoroisopropanol (HFIP) (Apollo Scientific Ltd.) to a final concentration of 25 % w/v. Similarly, a homogenous PS solution was created by dissolving PS pellets (MW (Mn) 192,000, Sigma-Aldrich Ltd.) in THF/EtOH (BDH and Fisher) 66.66%:33.33% v/v to a final concentration of 26.7% w/v. The mixtures were left to stir overnight to allow the polymers to completely dissolve to give homogeneous polymer solutions.

The homogeneous polymer solutions were electrospun to form an electrospun membrane. Electrospinning was carried out by extruding the polymer solutions from a syringe at a flow rate of 1 mL/hour, with an applied voltage of 20 kV and a working distance of 10 cm. Fibres were collected for 1 hour on a stationary collecting plate, consisting of a sheet of aluminium foil on a grounded plate.

Topography and thickness of the substrates

Investigation of the topography of the untreated and treated PET and PS mats (n=3) was undertaken by mounting the mats on aluminium stubs (Agar Scientific), gold sputter coating (Edwards, Sussex, UK) and analysing using SEM (VPSEM, Zeiss EVO60; Carl Zeiss Ltd, Hertfordshire, UK).

Representative SEM images for the PET and PS membranes are shown in Figures 1 and 2 respectively. Figure 1 shows that the membrane formed from PET consists of a mesh of randomly oriented thread-like and relatively uniform fibres having diameters much less than the 2 µm scale bar shown in the image. Figure 2 shows that PS fibres are larger than the PET fibres (the scale bar is 100 µm), and are much less uniform, with a mixture of large and small fibres. In addition, at least some of the PS fibres appear to have a ribbon-like structure

(i.e., a flattened structure) instead of the thread-like structure (i.e., a rounded structure) displayed by PET fibres.

To quantitate the thickness of the fibres, an SEM image of a randomly selected portion of the membrane was analysed using ImageJ software (National Institute of Health, MN, USA). The SEM image magnification was chosen such that between 100 to 400 fibres appeared in the image, and the thickness of each fibre in the SEM image was determined by measuring the distance between the edges of the intensity profile of a line drawn perpendicularly to the fibre at a random position along the fibre. The mean of the values for all fibres was then calculated. As mentioned above, the PS fibres shown in Figure 2 appeared to be ribbon-like in nature, and occasionally displayed varying thicknesses along their lengths in the SEM image. This could either be due to the fibres having an inhomogeneous diameter, or due to the ribbon-like fibres laying twisted across the surface instead of laying flat. To account for this variation in thickness, diameters were measured at several randomly selected points along each PS fibre, and the mean of this value was taken to be the fibre diameter of that particular fibre. These fibre diameters were subsequently averaged to produce the mean fibre diameter for the sample as a whole.

Figures 3 and 4 show the distribution of fibre diameters from SEM images of PET and PS fibres respectively. The mean diameter of the PET fibres was measured to be approximately 400 nm and that for the PS fibres was measured to be approximately 4 μm. The size of the fibres affects their ability to pack together, so it can be clearly seen that the gaps between fibres in the PET membrane were smaller than those for PS.

The thickness of each membrane was measured using an electronic digital micrometer (Farnell). To conduct this analysis, samples of 1 cm^2 were cut from three areas (top, middle and bottom) of three complete 6 cm^2 PET and PS mats.

Surface chemistry of the membranes

The surface chemistry of the membranes was assessed. In addition, the effect of surface treatment on the membranes was examined.

To examine the effect of surface treatment on the membranes, the above-described membranes were cut into approximately 11 mm by 11 mm squares and placed in a UV/ozone chamber. A pure oxygen flow was allowed to fill the chamber for 5 minutes. The UV light was turned on and samples treated, in a pure oxygen flow, for 300 seconds or 450 seconds at room temperature. After treating for the desired length of time the UV light was switched off, the oxygen flow turned off and the chamber allowed to empty for 5 minutes in a fume hood under extraction fan flow.

The effect of the UV/ozone surface treatment on the surfaces of the membranes was assessed by examining the hydrophilicity of the membranes using water contact angle analysis. Wettability tests were undertaken on untreated, 300 s and 450 s treated PET and PS electrospun membranes by a contact angle analyser (DSA100, Kruss, Hamburg, Germany). Three drops of 3 µL distilled water were placed on each membrane's surface (n=3) and the sessile drop contact angle measured using the software on the apparatus (Kruss Drop Shape Analysis software, Kruss, Hamburg, Germany).

Data from the wettability tests are shown in Figures 5 and 6. For both figures, the top row demonstrates wettability after treatment with atmospheric oxygen and the bottom row demonstrates treatment with pure oxygen. Data labelled with "A" correspond to samples that were placed in closer proximity to the UV lamp than those labelled with "B". The data demonstrate that, for PET, the water contact angle reaches a plateau region within the 300 seconds and 450 seconds of UV/ozone treatment to which the membranes were subjected, indicating that the hydrophilicity of the membranes did not alter significantly with longer UV/ozone treatment times.

Analyses of the elements present on the surfaces of the membranes were subsequently carried out by X-ray Photoelectron Spectrometry (XPS) (Axis Ultra, Kratos). The treated and

non-treated membranes were cut to approximately 4 mm x 6 mm squares (n=1), and subjected to XPS analysis, either without any surface treatment or after 300 seconds or 450 seconds of the above-described UV/ozone treatment.

Figure 7 shows XPS data for untreated PET membranes (bottom row) together with data for PET membranes subjected to UV/ozone treatment for 300 seconds (middle row) or 450 seconds (top row). In all cases the spectra display a peak just below 300 eV, which can be attributed to 1*s* electrons from carbon (C1s), and another peak just above 500 eV, which can be attributed to 1*s* electrons from oxygen (O1s). The data show that the UV/ozone treatment did not noticeably increase the number of oxygen groups on the surface of PET. Figures 8 and 9 show, respectively, the carbon and oxygen peaks in closer detail, together with peaks used to fit the data. These data confirm that there is no significant alteration in the types of oxygen and carbon environments on the surface of the PET substrate that occur with UV/ozone treatment.

These data clearly demonstrate that PET inherently has an oxygen containing surface in the absence of surface treatment, and that UV/ozone treatment does not significantly increase the amount of oxygen at the surface.

Figure 10 shows XPS data for untreated PS membranes (bottom row) together with data for PET membranes subjected to UV/ozone treatment for 300 seconds (middle row) or 450 seconds (top row). Unlike PET, there is no prominent peak corresponding to oxygen for untreated PS. However, oxygen is introduced to the surface upon UV/ozone treatment. Figure 11 shows the carbon peak in the spectra of Figure 10 in greater detail, together with peaks used for fitting the data. The spectra show that there is a change in the carbon environments on the PS membrane surface, with more carbon environments being present after UV/ozone treatment (the data are fitted by three peaks with UV/ozone treatment and two peaks without). Similarly, Figure 12 shows the oxygen peak of Figure 10 and the peaks

used to fit the data, and shows that the oxygen peak is only present after UV/ozone treatment of the surface.

These data clearly demonstrate that PS does not inherently have an oxygen containing surface, but that oxygen functionality is introduced to the surface upon UV/ozone treatment.

To examine the effect of biological fluids on the surface chemistry of the membranes, further XPS analyses were conducted on membranes after they had been treated with cell culture medium. The above-mentioned membranes were treated with cell culture medium (consisting of a 50:50 mixture of Dulbecco's modified Eagle's medium and Ham's F12 nutrients) for 1 hour, after which the media was removed, and the membranes washed twice with distilled water. The membranes were left to air dry before XPS analysis.

Figure 13 presents data for the PET membranes treated with cell culture medium and shows that an additional peak around 400 eV, corresponding to 1*s* electrons from nitrogen (N1s), in addition to the O1s and C1s peaks that were present for untreated and treated surfaces. In contrast, data for PS membranes treated in the same way presented in Figure 14 show that the N1s peak is only present for PS membranes that have been subjected to UV/ozone treatment. This suggests that oxygen is required for nitrogen-containing species to bond to the surface.

The nitrogen groups present in the XPS spectra remained present following washing of the surfaces, which suggests that a strong interaction between one or more proteins in the cell culture medium and the surfaces of the polymers is occurring. This could possibly be due to the N-terminal of the proteins available in the culture media taking part in aminolysis of the ester bond, opening the ester bond and forming a chemical bond.

Cell proliferation studies

Attachment of RPE cells to untreated and treated membranes was measured using ARPE-19 cells (ATCC-LGC, CRL-2302), a spontaneously arising human RPE cell line.

ARPE-19 cells were grown in a 50:50 cell culture media mix of Dulbecco's modified Eagle's medium and Ham's F12 nutrients mixed with 10% foetal bovine serum, L-glutamine and antibiotic and incubated at 37˚C, 5% CO_2, 98 - 99% humidity until cells were confluent. The media was changed every three days. All reagents were from PAA laboratories, UK.

Membranes were cut into approximately 11 mm^2 squares and either not treated with UV/ozone, or treated with UV/ozone for 300 seconds or 450 seconds as described above. The substrates were subsequently sterilised under UV light for 30 minutes on each side, mounted onto sterile Scaffdex clips and put into low-adherent 24-well plates. A cell suspension of ARPE-19 cells was made up having 10,000 cells/mL, and 1 mL of this suspension was placed into each membrane-bearing well-plate. Membranes were incubated for 5 days, with the media changed on the third day.

After five days of growth, cell media was removed and the sample was rinsed twice with PBS (PAA laboratories). Samples were fixed with formalin for 10 minutes at room temperature then washed twice with PBS. Samples were then soaked in ICC buffer (50 mL PBS, 500 µL goat serum, 50 µL (0.1%) Triton X-100 in PBS and 5 mg/mL bovine serum albumin (BSA)- all reagents from Sigma except for PBS) for 30 minutes at room temperature. ICC buffer was removed and samples stained with Phalloidin stain for 20 minutes at room temperature. The Phalloidin stain consisted of 50 µL of a 1:40 dilution of stock fluorescein-tagged Phalloidin (Invitrogen) and 2 mL of ICC buffer together, and also contained DAPI with ProLong® Gold Antifade reagent (Invitrogen). The membranes were then washed twice with PBS, mounted onto glass slides with PBS and left at 4˚C in the dark overnight in order to cure (n=3). Samples were analysed using a fluorescence microscope (Nikon Eclipse 50i JENCONS-PLS).

Figure 15 shows fluorescence images from ARPE-19 cells at 10× magnification (scale bar is 100 µm) for (A) untreated PET, (B) 300 seconds UV/ozone treated PET, (C) 450 seconds UV/ozone treated PET and (D) positive glass control. The figure shows that the cells have a

central fluorescence signal, arising from DAPI bound to the ARPE-19 cells' DNA, surrounded by fluorescence from Phalloidin bound to the cells' F-actin.

Figure 16 shows fluorescence images from ARPE-19 cells at 20× magnification (scale bar is 100 µm) for (A) untreated PS, (B) 300 seconds UV/ozone treated PS, (C) 450 seconds UV/ozone treated PS and (D) positive glass control.

Figure 15 shows that for PET membranes, even the untreated samples allowed successful cell growth that was comparable to cell growth on the positive glass control. By contrast, Figure 16 shows that fewer cells were able to attach to the untreated PS membranes, but that cells attached to UV/ozone treated PS membranes (although not in the desired monolayer morphology). Overall, the number of cells that grew on the PET membranes was greater than the number cells on the PS membranes. Furthermore, cells on the PET membranes displayed morphologies closer to the positive control than those on PS membranes.

To assess whether cell metabolism was affected by the PET and PS membranes, cells grown on these membranes were treated with alamarBlue®: a fluorescent probe that allows the assessment of metabolic activity. To treat the cells, media on samples was replenished and 100 µL of an alamarBlue® solution (5 mg resazurin salt (Sigma) in 40 mL PBS) was added into each well plate (assuming 1 mL media in a 24-well plate). Samples were returned to the incubator for the time dictated by a calibration curve. Each sample (200 µL) was transferred to a black bottomed 96-well plate and fluorescence was measured at 530 - 510nm excitation and 590nm emission (n=3) with a fluorescence reader (FLUOstar OPTIMA, BMG LABTECH). The results indicated that no change in cell metabolism occurred for cells grown on PET and PS membranes compared to those grown on glass.

Data described above show that a synthetic membrane formed from a web of non-biodegradable polyester can be engineered to have both a fibrous structure and a thickness comparable to the BM. Furthermore, such membranes are shown to be capable of being

functionalised with nitrogen-containing molecules and supporting the growth of viable RPE cells without the need for UV/ozone treatment. Therefore, the data indicate that membranes of the present invention are suitable for use as replacements for native BM.

*****

REFERENCES

A number of patents and publications are cited above in order to more fully describe and disclose the invention and the state of the art to which the invention pertains. Full citations for these references are provided below. Each of these references is incorporated herein by reference in its entirety into the present disclosure, to the same extent as if each individual reference was specifically and individually indicated to be incorporated by reference.

Binder, S. (2011) 'Scaffolds for retinal pigment epithelium (RPE) replacement therapy', Br J Opthalmol, vol. 95, pp.441-442, doi: 10.1136/bjo.2009.171926

Chopdar, A., Chakravarthy, U., and Verma, D. (2003) 'Age related macular degeneration', BMJ, vol. 326, pp. 485-488

Del Priore, L.V., Tezel, T.H., and Kaplan, H.J. (2006) 'Maculoplasty for age-related macular degeneration: Reengineering Bruch's membrane and the human macula', Progress in Retinal and Eye Research, vol. 25, pp. 539-562

Hsiue, G.H., Lai, J.Y., Lin, P.K. (2002) 'Absorbable sandwich-like membrane for retinal-sheet transplantation', J Biomed Mater Res, vol. 61, pp 19-25

Minassian, D.C., Reidy A., Lightstone, A., and Desai P. (2011) 'Modelling the prevalence of age-related macular degeneration (2012-2020) in the UK: expected impact of anti-vascular endothelial growth factor (VEGF) therapy', Br J Ophthalmol, doi:10.1136/bjo.2010.195370

Resnikoff, S., Pascolini, D., Etya'ale, D., Kocur, I., Pararajasegaram, R., Pokharel, G.P., and Mariotti, S.P. (2004) 'Global data on visual impairment in the year 2002', Bulletin of the World Health Organisation, vol. 82, pp. 844-852

Thomson, H.A.J., Treharne, A.J., Walker, P., Grossel, M.C., Lotery, A.J. (2011) 'Optimisation of polymer scaffolds for retinal pigment epithelium (RPE) cell transplantation', Br J Opthalmol, vol. 95, pp. 563-568, doi:10.1136/bjo.2009.166728

Wang, H., Yagi, F., Cheewatrakoolpong, N., Sugino, I.K., Zarbin, M.A., (2004) 'Short-term study of retinal pigment epithelium sheet transplants onto Bruch's membrane', Experimental Eye research, vol. 78, pp.53-65.

CLAIMS

1. A synthetic Bruch's membrane comprising fibres.

2. A synthetic Bruch's membrane according to claim 1, wherein the fibres are polymer fibres.

3. A synthetic Bruch's membrane according to claim 2, wherein the fibres are polyester fibres.

4. A synthetic Bruch's membrane according to claim 3, wherein the fibres are poly (ethylene terephthalate) fibres.

4. A synthetic Bruch's membrane according to any one of the preceding claims, wherein the fibres are in the form of a mesh.

5. A synthetic Bruch's membrane according to any one of the preceding claims, wherein the fibres are randomly oriented in the plane of the membrane.

6. A synthetic Bruch's membrane according to any one of the preceding claims, wherein the majority of the fibres lay approximately horizontal within the membrane.

7. A synthetic Bruch's membrane according to any one of the preceding claims, wherein the fibres do not substantially extend vertically through the thickness of the membrane.

8. A synthetic Bruch's membrane according to any one of the preceding claims, wherein the fibres comprise at least 95 wt% of the synthetic membrane based on the total weight of the membrane.

9. A synthetic Bruch's membrane according to any one of the preceding claims, wherein the fibres are non-biodegradable.

10. A synthetic Bruch's membrane according to any one of claims 2 to 9, wherein the fibres are polymer fibres and the polymer has a number average molecular weight of 5×10^5 or less.

11. A synthetic Bruch's membrane according to any one of the preceding claims, wherein the fibres have a mean diameter of 5 µm or less.

12. A synthetic Bruch's membrane according to any one of the preceding claims, wherein the fibres have a mean diameter of 1 µm or less.

13. A synthetic Bruch's membrane according to any one of the preceding claims, wherein the membrane has a thickness of 20 µm or less.

14. A synthetic Bruch's membrane according to any one of the preceding claims, wherein the membrane has a thickness of 10 µm or less.

15. A synthetic Bruch's membrane according to any one of the preceding claims, wherein the membrane has a thickness of 5 µm or less.

16. A synthetic Bruch's membrane according to any one of the preceding claims, wherein the membrane has a length and/or width or 10 mm or less.

17. A synthetic Bruch's membrane according to any one of claims 2 to 16, wherein the fibres are polymer fibres and the average number of bead structures per 20 μm^2 of the membrane surface is fewer than 10.

18. A synthetic Bruch's membrane according to any one of the preceding claims, wherein fibres have a distribution of diameters which can be approximated by a normal distribution having a standard deviation less than 50% of the mean fibre diameter.

19. A synthetic Bruch's membrane according to any one of the preceding claims, wherein the fibres have a rounded cross-section.

20. A synthetic Bruch's membrane according to any one of claims 2 to 19, wherein the fibres are polymer fibres and the membrane is created by electrospinning.

21. A synthetic Bruch's membrane according to any one of the preceding claims, wherein the membrane is provided in a sterile enclosure.

22. A kit comprising a plurality of synthetic Bruch's membranes according to any one of the preceding claims.

23. A synthetic Bruch's membrane of any one of the preceding claims for use in a method of treatment comprising replacing some or all of the Bruch's membrane of a human or animal.

24. A synthetic membrane according to claim 23, wherein the synthetic Bruch's membrane is used in conjunction with other layers.

25. A method of making a synthetic Bruch's membrane comprising electrospinning a plurality of fibres.

26. A method according to claim 25, wherein the method involves electrospinning a polymer from a polymer-solution.

27. A method according to claim 25 or 26, wherein the method involves a further step of re-sizing the membrane for insertion into a human or animal body.

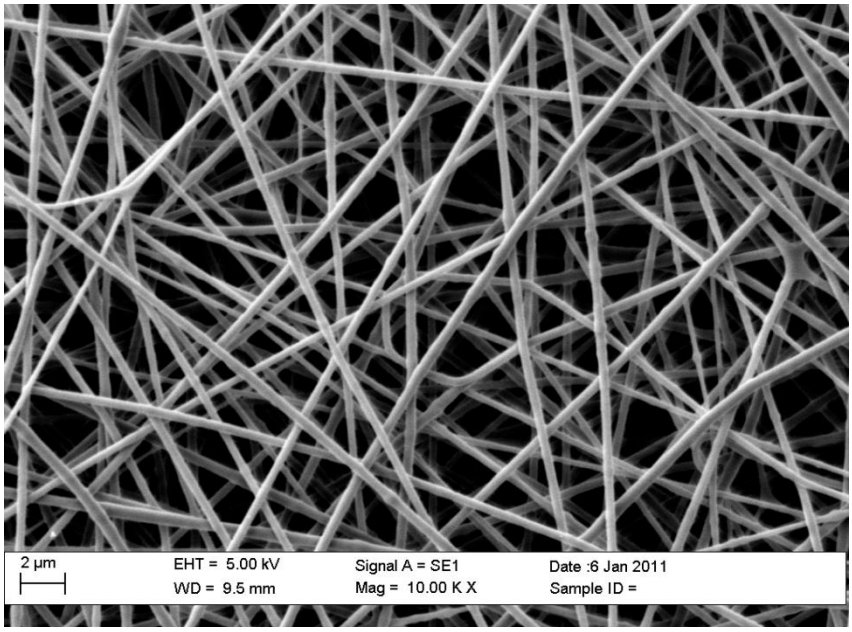

Figure 1

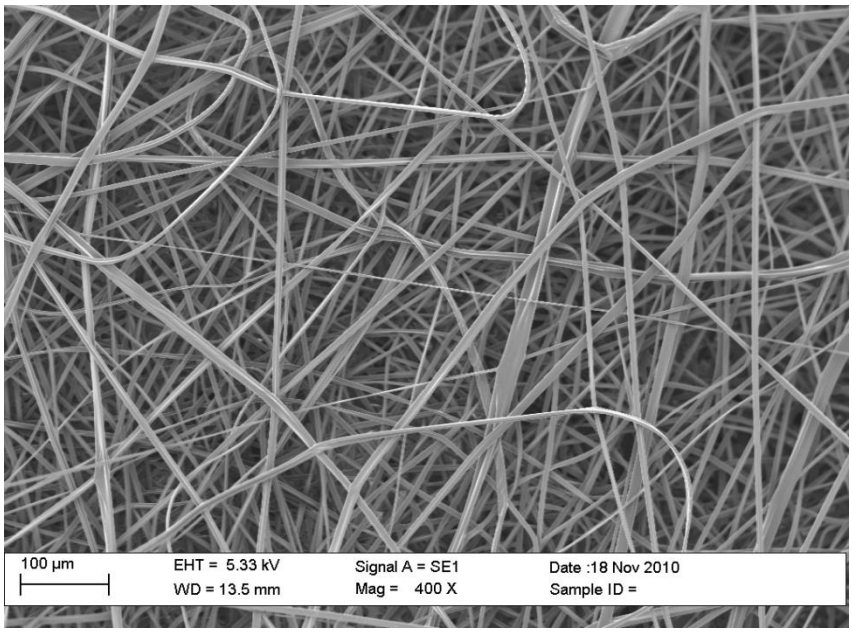

Figure 2

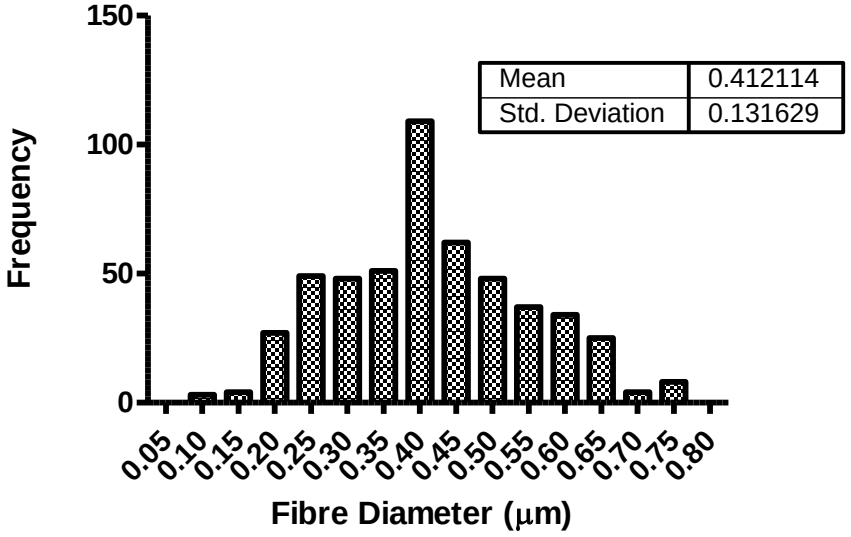

Figure 3

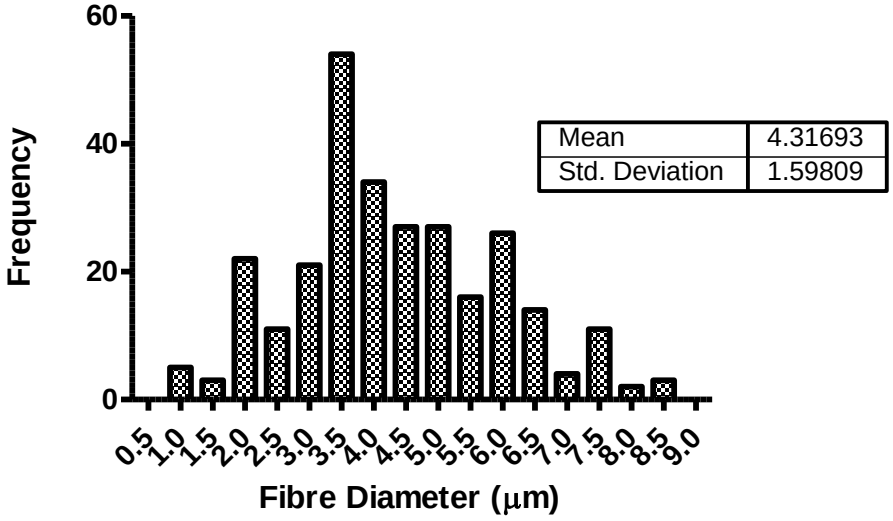

Figure 4

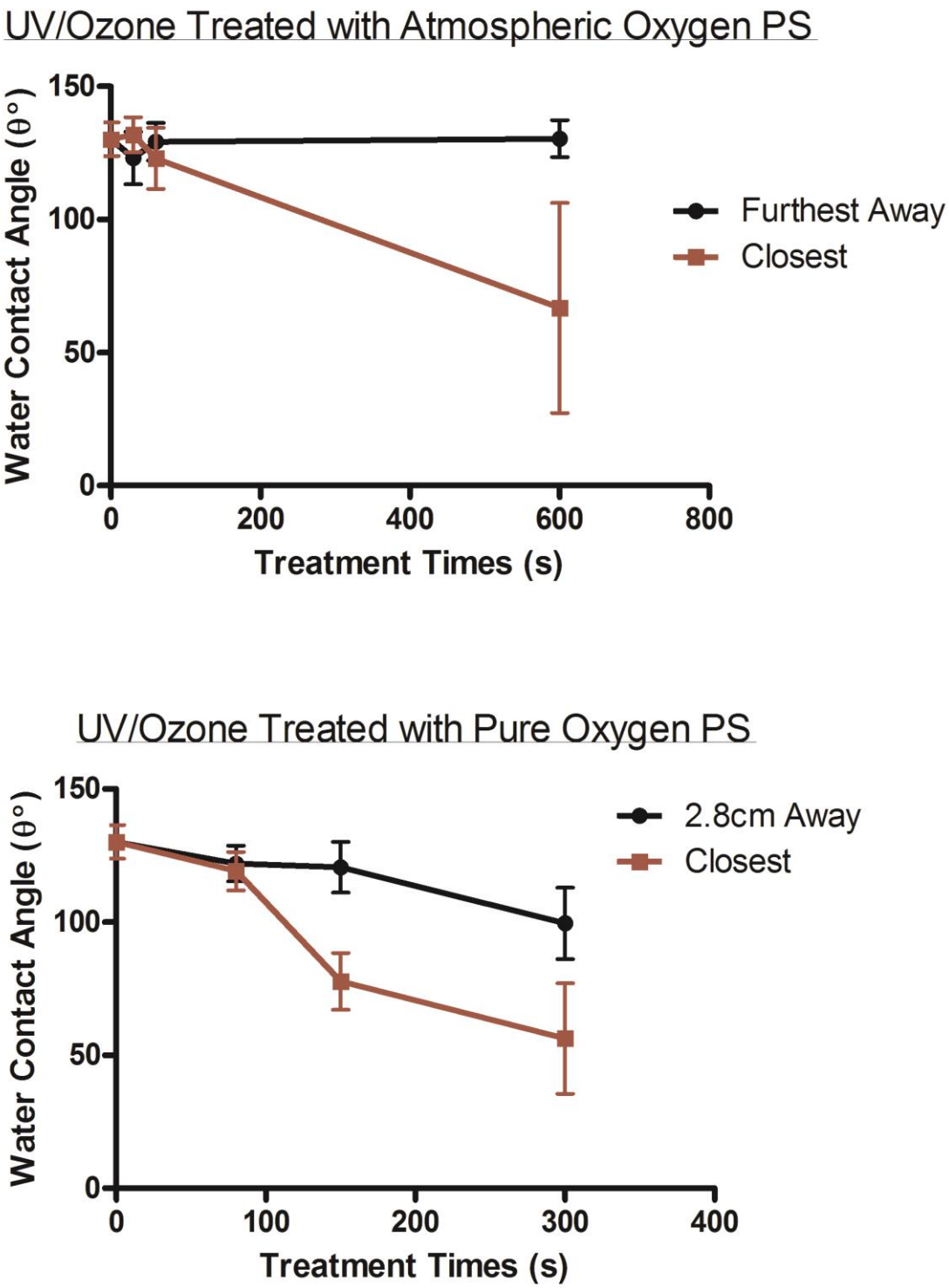
UV/Ozone Treated with Atmospheric Oxygen PS
Water Contact Angle (θ°)
150
100
50
0
0
200
400
600
800
Treatment Times (s)
Furthest Away
Closest
UV/Ozone Treated with Pure Oxygen PS
Water Contact Angle (θ°)
150
100
50
0
0
100
200
300
400
Treatment Times (s)
2.8cm Away
Closest

Figure 5

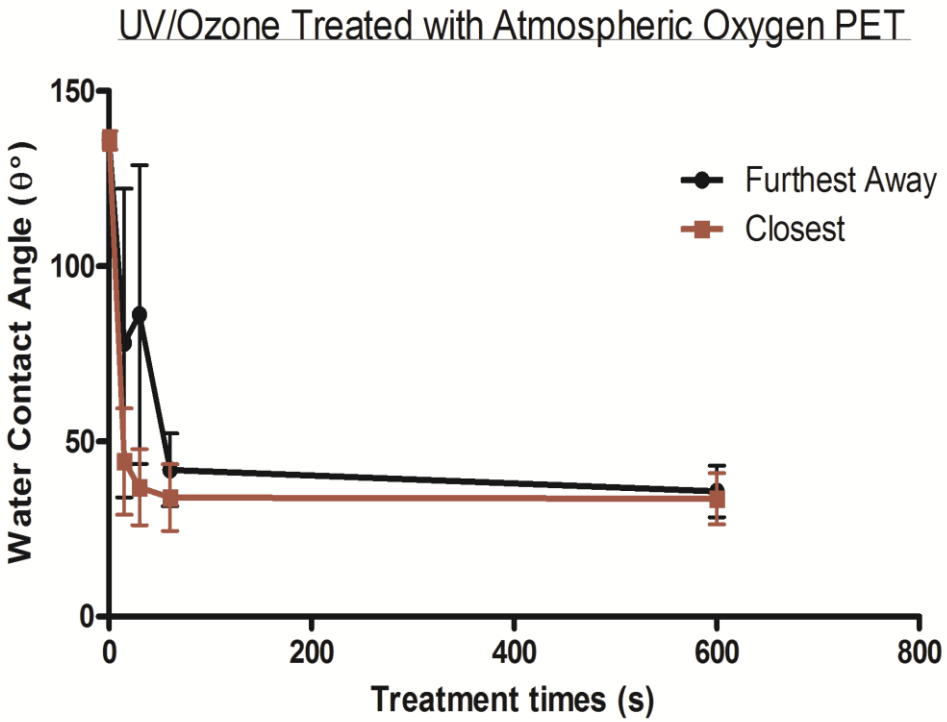
UV/Ozone Treated with Atmospheric Oxygen PET
Water Contact Angle (θ°)
150
100
50
0
0
200
400
600
800
Treatment times (s)
Furthest Away
Closest

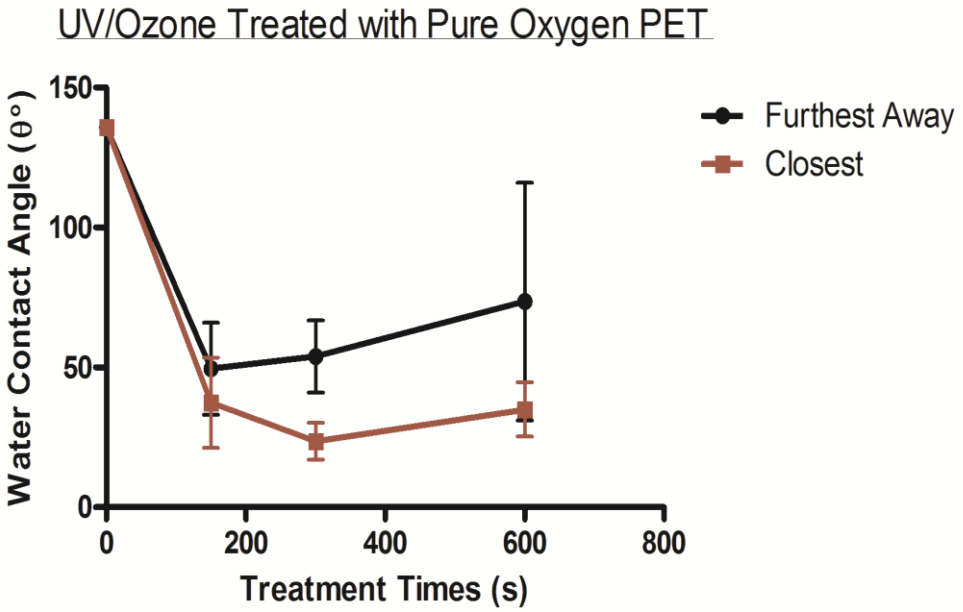
UV/Ozone Treated with Pure Oxygen PET
Water Contact Angle (θ°)
150
100
50
0
0
200
400
600
800
Treatment Times (s)
Furthest Away
Closest

Figure 6

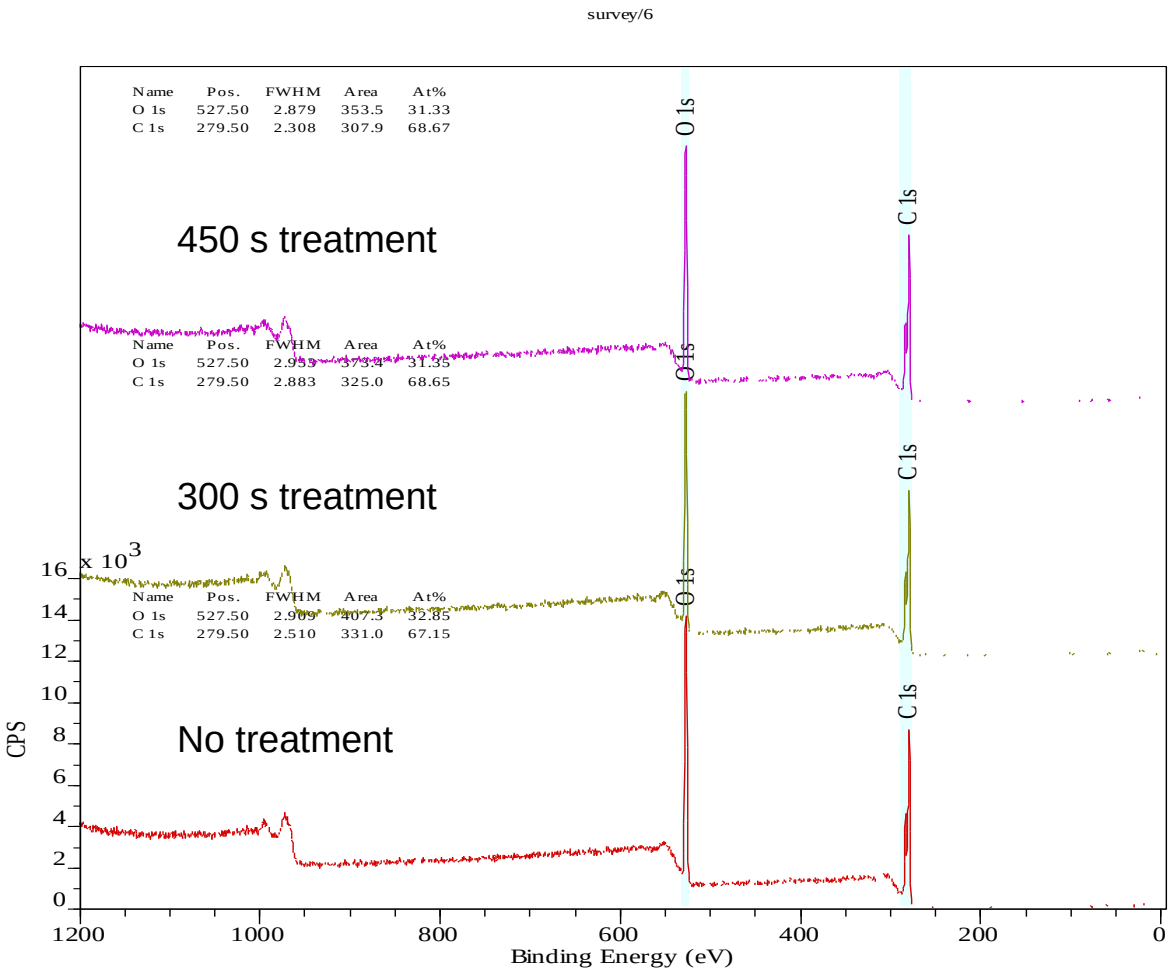
survey/6
Name Pos. FWHM Area At%
O 1s 527.50 2.879 353.5 31.33
C 1s 279.50 2.308 307.9 68.67
450 s treatment
Name Pos. FWHM Area At%
O 1s 527.50 2.959 373.4 31.55
C 1s 279.50 2.883 325.0 68.65
300 s treatment
Name Pos. FWHM Area At%
O 1s 527.50 2.909 407.3 32.85
C 1s 279.50 2.510 331.0 67.15
No treatment
O 1s
C 1s
x 10^3
CPS
16
14
12
10
8
6
4
2
0
1200
1000
800
600
400
200
0
Binding Energy (eV)

Figure 7

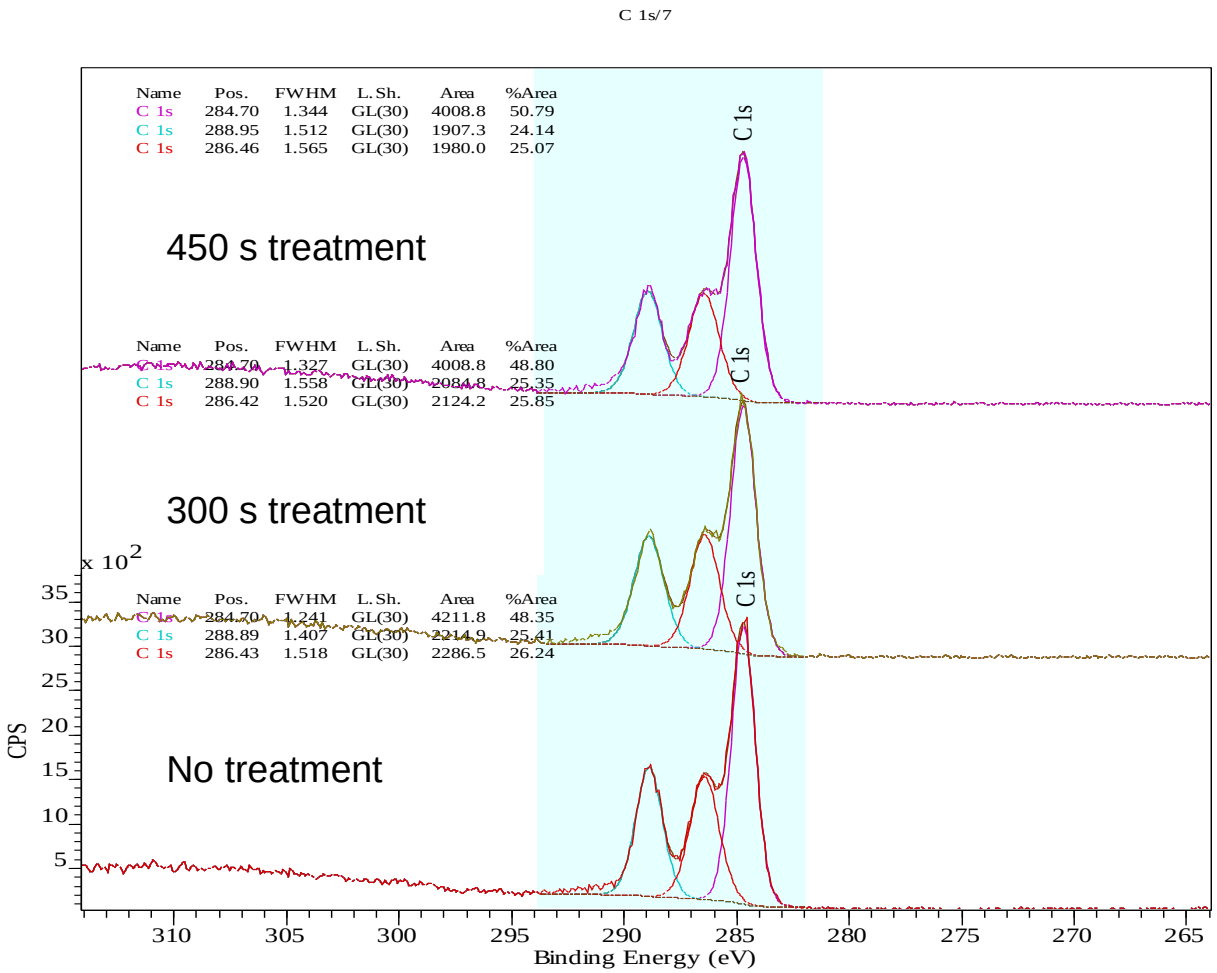
C 1s/7
Name Pos. FWHM L.Sh. Area %Area
C 1s 284.70 1.344 GL(30) 4008.8 50.79
C 1s 288.95 1.512 GL(30) 1907.3 24.14
C 1s 286.46 1.565 GL(30) 1980.0 25.07
450 s treatment
Name Pos. FWHM L.Sh. Area %Area
C 1s 284.70 1.327 GL(30) 4008.8 48.80
C 1s 288.90 1.558 GL(30) 2084.8 25.35
C 1s 286.42 1.520 GL(30) 2124.2 25.85
300 s treatment
x 10^2
Name Pos. FWHM L.Sh. Area %Area
C 1s 284.70 1.241 GL(30) 4211.8 48.35
C 1s 288.89 1.407 GL(30) 2214.9 25.41
C 1s 286.43 1.518 GL(30) 2286.5 26.24
No treatment
C 1s
CPS
35
30
25
20
15
10
5
310
305
300
295
290
285
280
275
270
265
Binding Energy (eV)

Figure 8

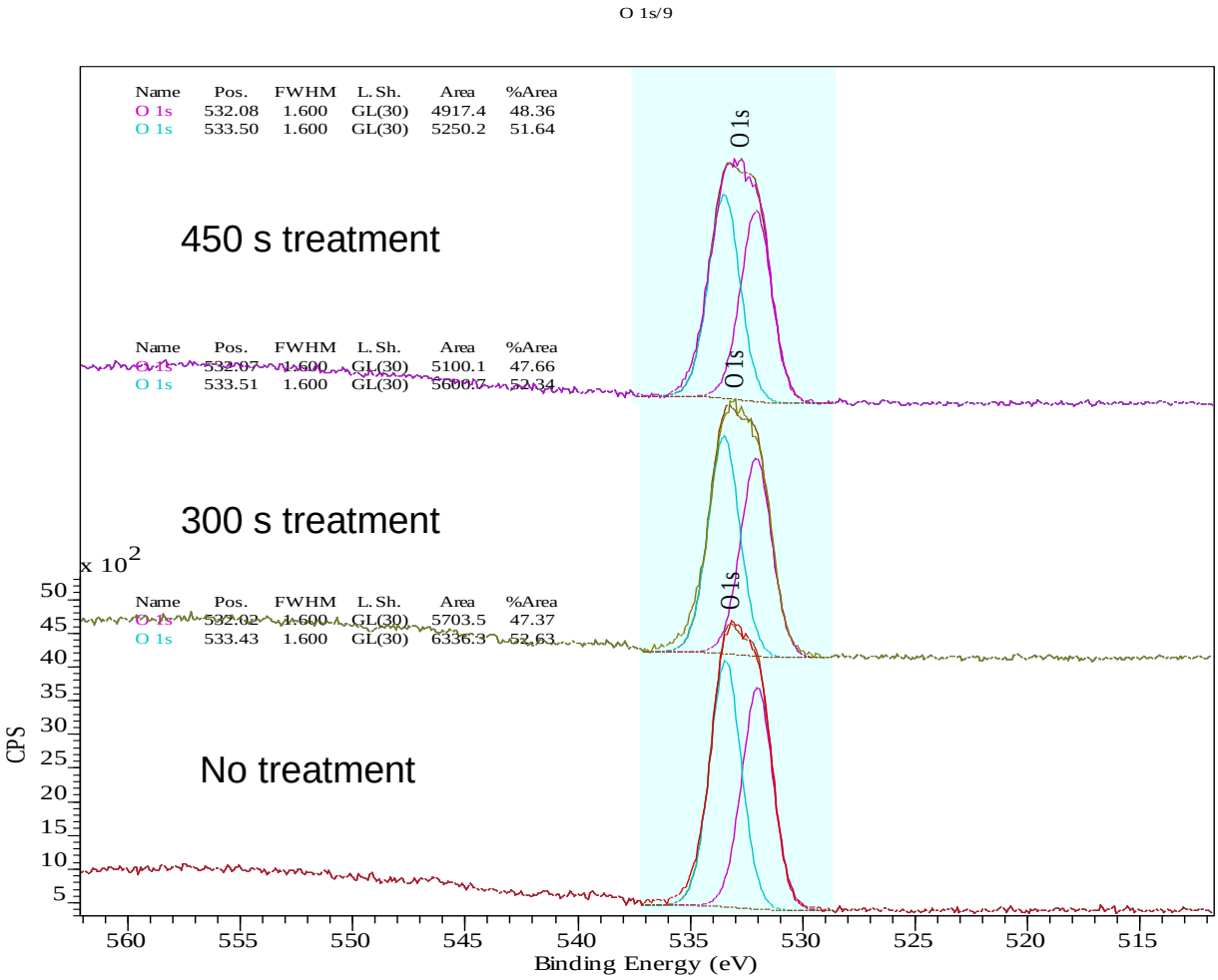
O 1s/9
Name Pos. FWHM L. Sh. Area %Area
O 1s 532.08 1.600 GL(30) 4917.4 48.36
O 1s 533.50 1.600 GL(30) 5250.2 51.64
450 s treatment
O 1s
Name Pos. FWHM L. Sh. Area %Area
O 1s 532.07 1.600 GL(30) 5100.1 47.66
O 1s 533.51 1.600 GL(30) 5600.7 52.34
300 s treatment
O 1s
x 10^2
Name Pos. FWHM L. Sh. Area %Area
O 1s 532.02 1.600 GL(30) 5703.5 47.37
O 1s 533.43 1.600 GL(30) 6336.3 52.63
No treatment
O 1s
CPS
50
45
40
35
30
25
20
15
10
5
560
555
550
545
540
535
530
525
520
515
Binding Energy (eV)

Figure 9

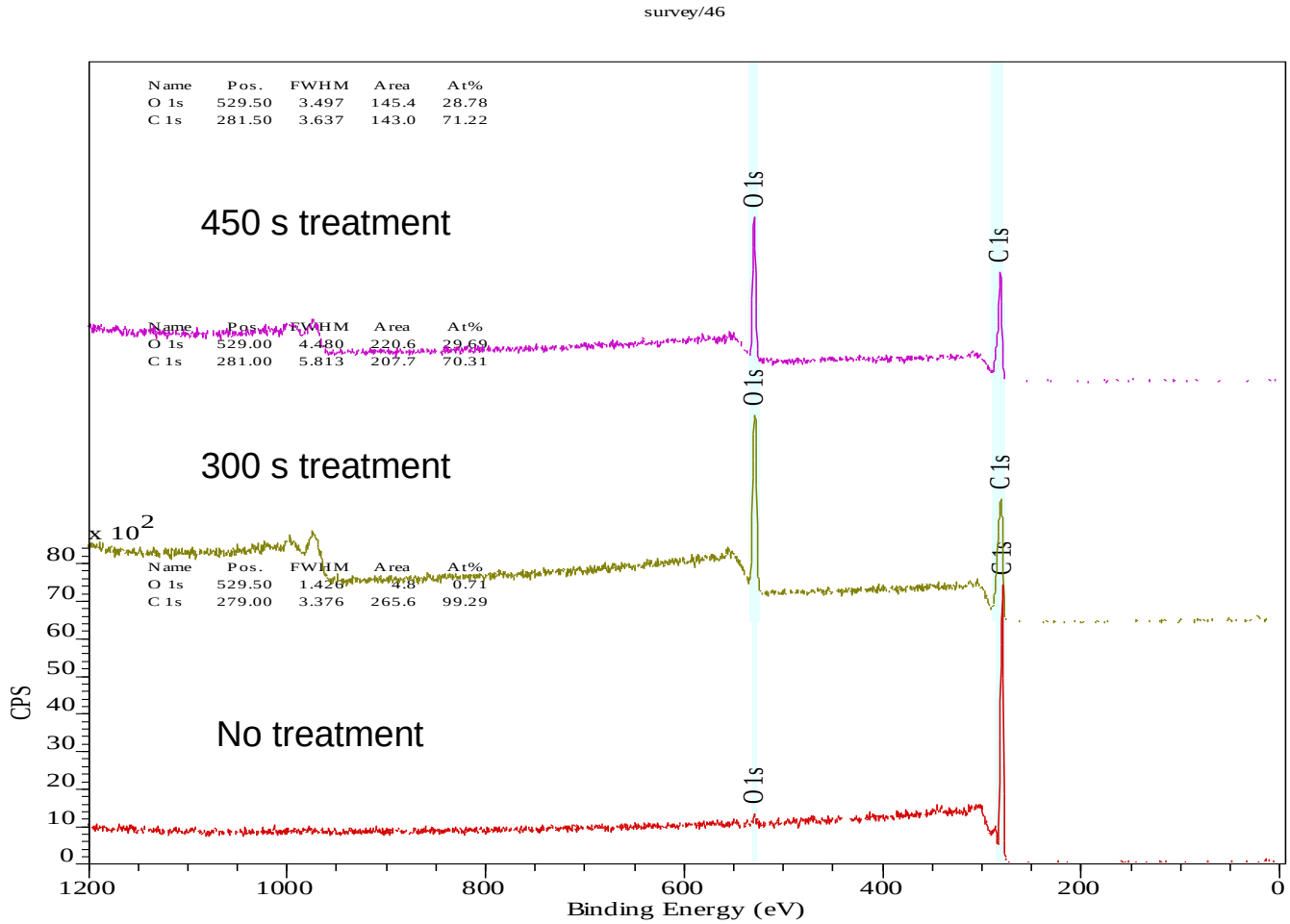
survey/46
Name Pos. FWHM Area At%
O 1s 529.50 3.497 145.4 28.78
C 1s 281.50 3.637 143.0 71.22
450 s treatment
O 1s
C 1s
Name Pos. FWHM Area At%
O 1s 529.00 4.480 220.6 29.69
C 1s 281.00 5.813 207.7 70.31
300 s treatment
O 1s
C 1s
C 1s
x 10^2
Name Pos. FWHM Area At%
O 1s 529.50 1.420 4.8 0.71
C 1s 279.00 3.376 265.6 99.29
No treatment
O 1s
CPS
0
10
20
30
40
50
60
70
80
1200
1000
800
600
400
200
0
Binding Energy (eV)

Figure 10

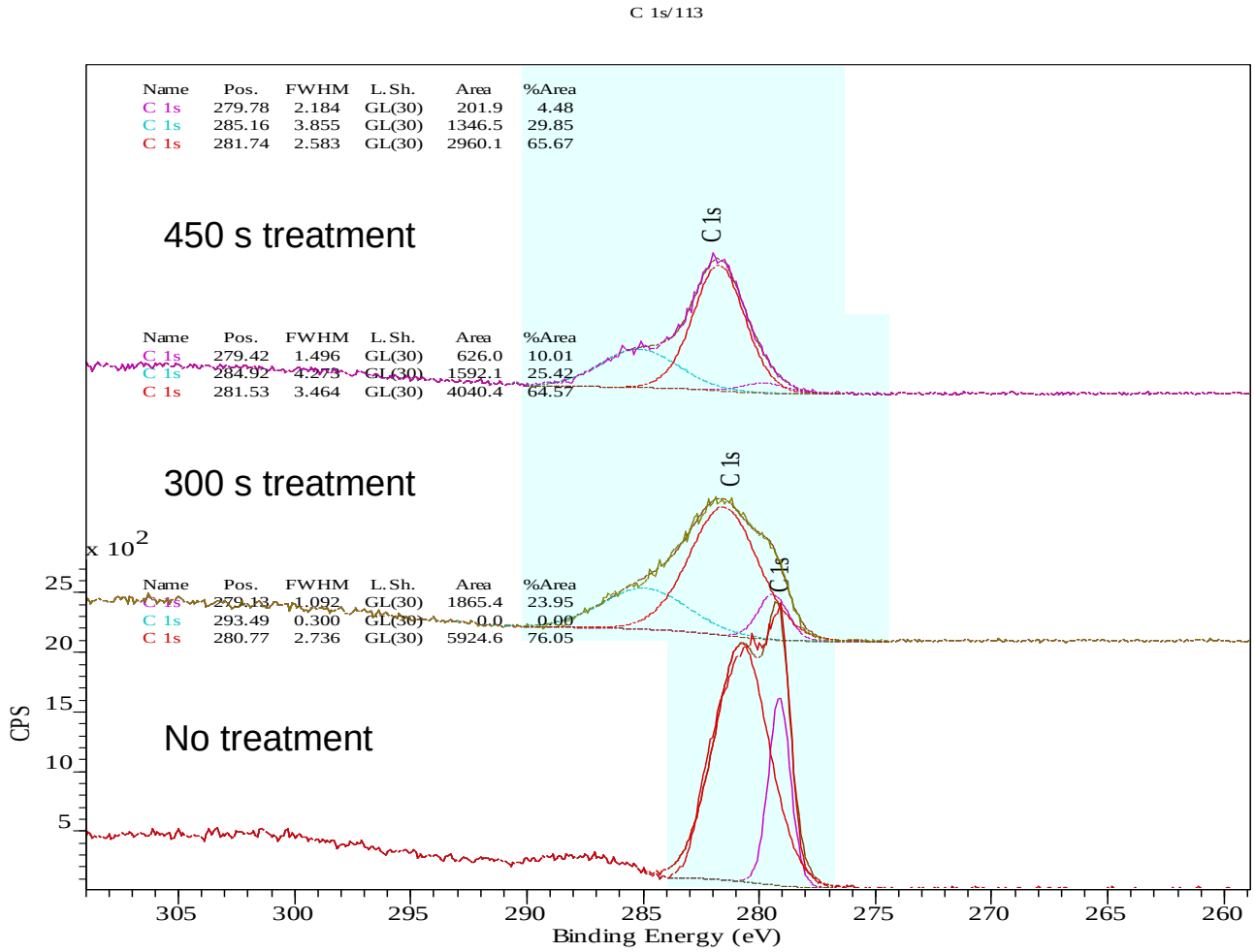
C 1s/113
Name Pos. FWHM L.Sh. Area %Area
C 1s 279.78 2.184 GL(30) 201.9 4.48
C 1s 285.16 3.855 GL(30) 1346.5 29.85
C 1s 281.74 2.583 GL(30) 2960.1 65.67
450 s treatment
C 1s
Name Pos. FWHM L.Sh. Area %Area
C 1s 279.42 1.496 GL(30) 626.0 10.01
C 1s 284.92 4.273 GL(30) 1592.1 25.42
C 1s 281.53 3.464 GL(30) 4040.4 64.57
300 s treatment
C 1s
C 1s
x 10^2
Name Pos. FWHM L.Sh. Area %Area
C 1s 279.13 1.092 GL(30) 1865.4 23.95
C 1s 293.49 0.300 GL(30) 0.0 0.00
C 1s 280.77 2.736 GL(30) 5924.6 76.05
No treatment
CPS
25
20
15
10
5
305
300
295
290
285
280
275
270
265
260
Binding Energy (eV)

Figure 11

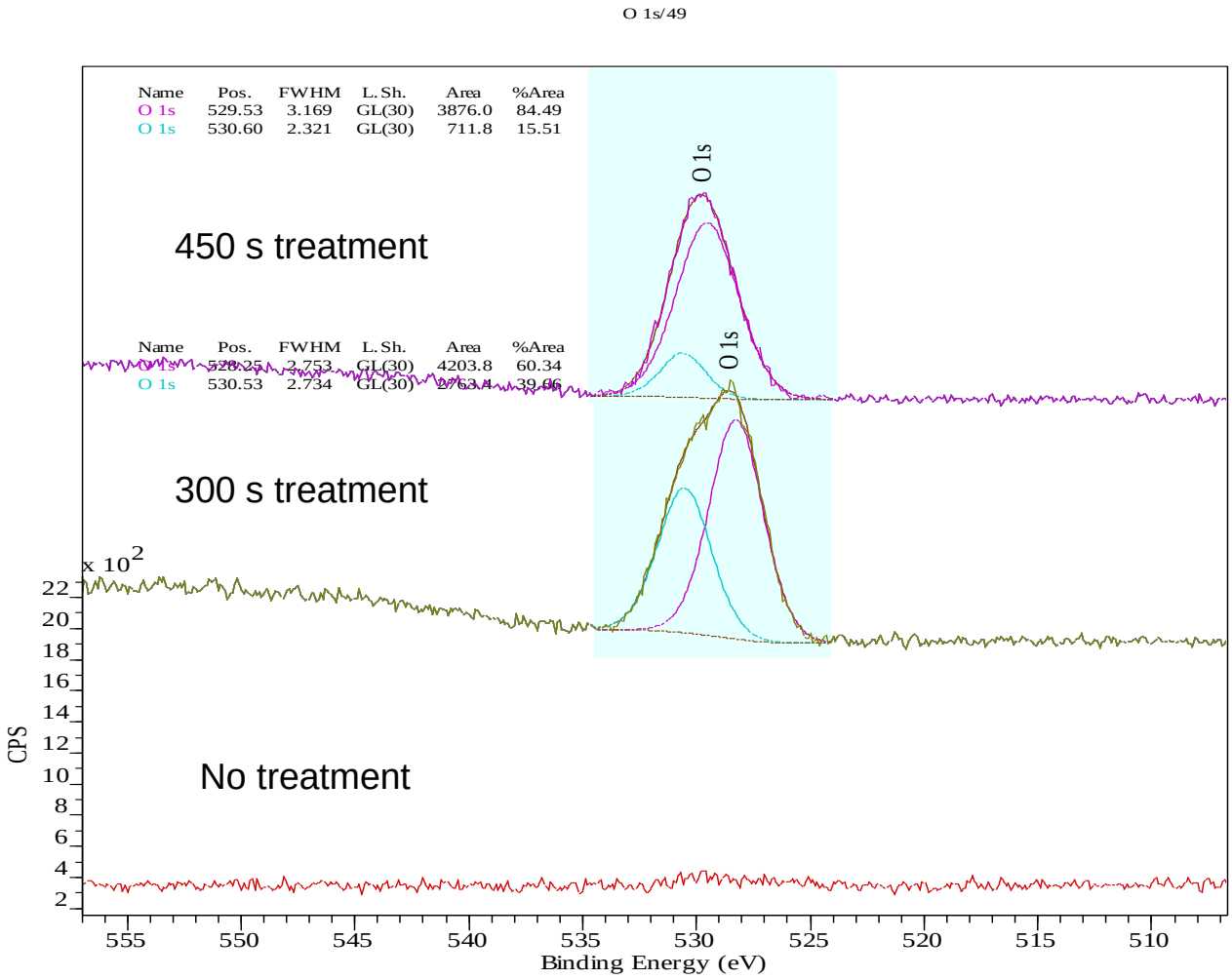
O 1s/49
Name Pos. FWHM L.Sh. Area %Area
O 1s 529.53 3.169 GL(30) 3876.0 84.49
O 1s 530.60 2.321 GL(30) 711.8 15.51
450 s treatment
O 1s
Name Pos. FWHM L.Sh. Area %Area
O 1s 529.25 2.753 GL(30) 4203.8 60.34
O 1s 530.53 2.734 GL(30) 2763.4 39.66
O 1s
300 s treatment
x 10^2
22
20
18
16
14
12
10
8
6
4
2
CPS
No treatment
555 550 545 540 535 530 525 520 515 510
Binding Energy (eV)

Figure 12

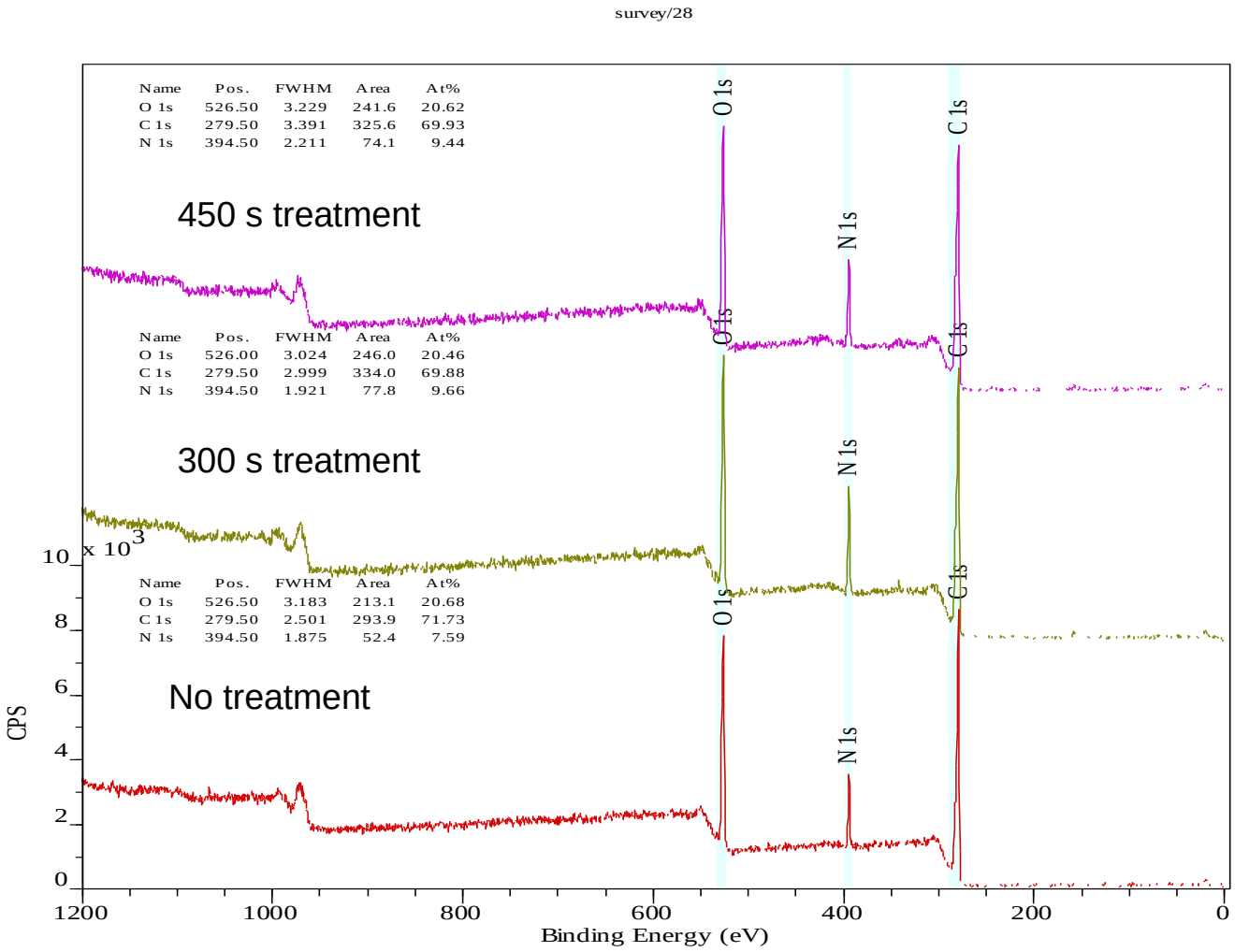
survey/28
Name Pos. FWHM Area At%
O 1s 526.50 3.229 241.6 20.62
C 1s 279.50 3.391 325.6 69.93
N 1s 394.50 2.211 74.1 9.44
450 s treatment
Name Pos. FWHM Area At%
O 1s 526.00 3.024 246.0 20.46
C 1s 279.50 2.999 334.0 69.88
N 1s 394.50 1.921 77.8 9.66
300 s treatment
Name Pos. FWHM Area At%
O 1s 526.50 3.183 213.1 20.68
C 1s 279.50 2.501 293.9 71.73
N 1s 394.50 1.875 52.4 7.59
No treatment
O 1s
N 1s
C 1s
x 10 3
CPS
10
8
6
4
2
0
1200
1000
800
600
400
200
0
Binding Energy (eV)

Figure 13

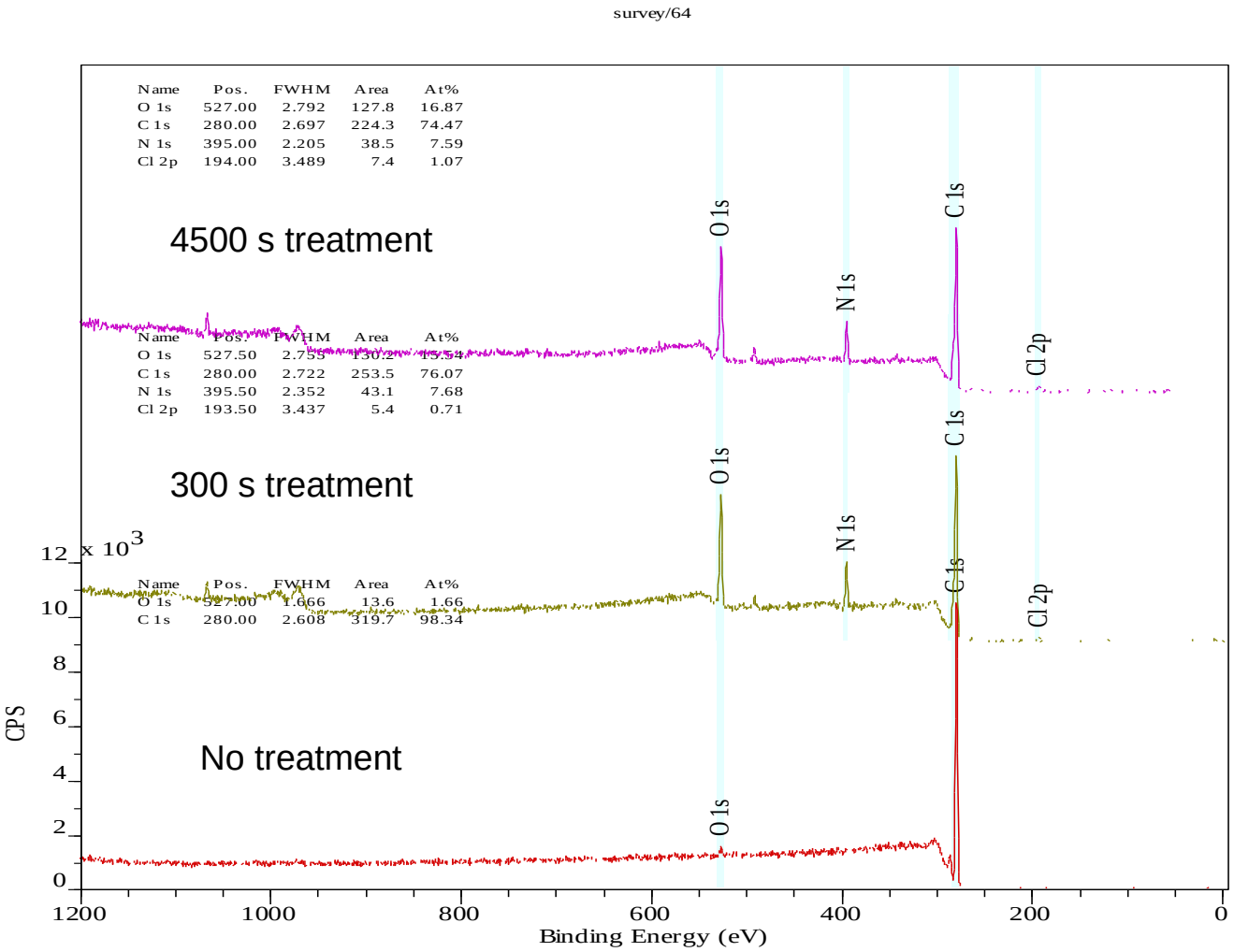
survey/64
Name Pos. FWHM Area At%
O 1s 527.00 2.792 127.8 16.87
C 1s 280.00 2.697 224.3 74.47
N 1s 395.00 2.205 38.5 7.59
Cl 2p 194.00 3.489 7.4 1.07
4500 s treatment
Name Pos. FWHM Area At%
O 1s 527.50 2.755 130.2 15.54
C 1s 280.00 2.722 253.5 76.07
N 1s 395.50 2.352 43.1 7.68
Cl 2p 193.50 3.437 5.4 0.71
300 s treatment
Name Pos. FWHM Area At%
O 1s 527.00 1.666 13.6 1.66
C 1s 280.00 2.608 319.7 98.34
No treatment
O 1s
N 1s
C 1s
Cl 2p
x 10^3
CPS
12
10
8
6
4
2
0
1200
1000
800
600
400
200
0
Binding Energy (eV)

Figure 14

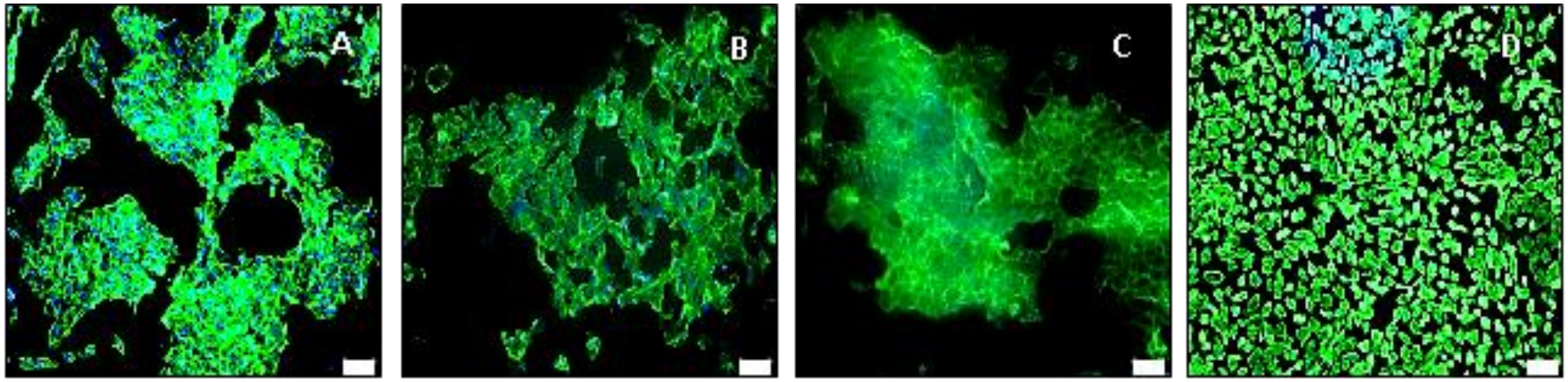

Figure 15

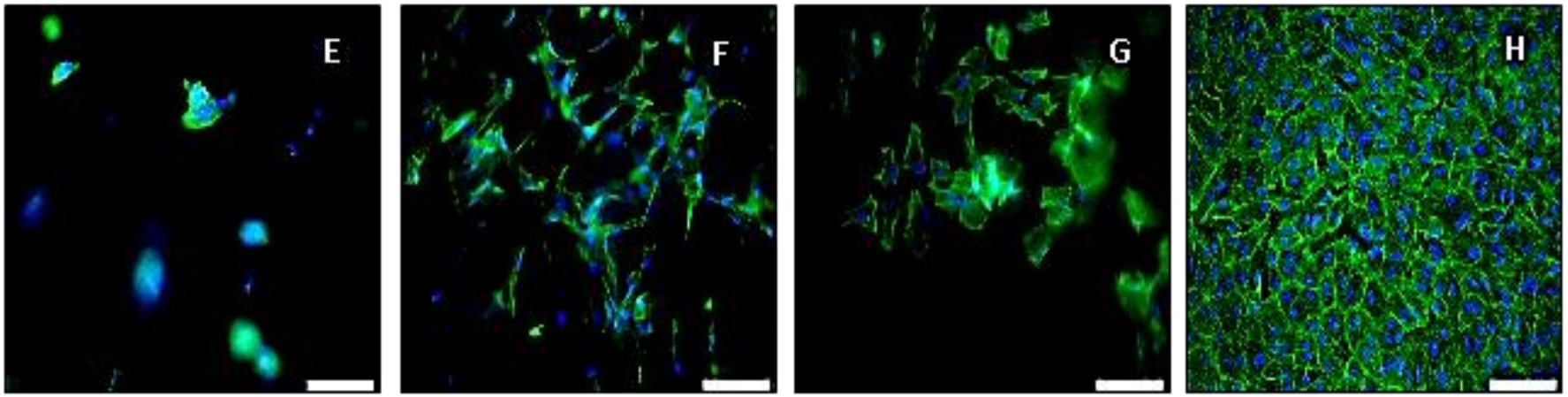

Figure 16

Appendix 2

Here follows the repeatedly measured fibre size frequency distribution graphs for 26.7 % PS in THF/EtOH (A,B,C) and 30 % PET in HFIP (D,E,F). All mean fibre diameters are within 10 % of each other, exhibiting reproducibility within a reasonable range.

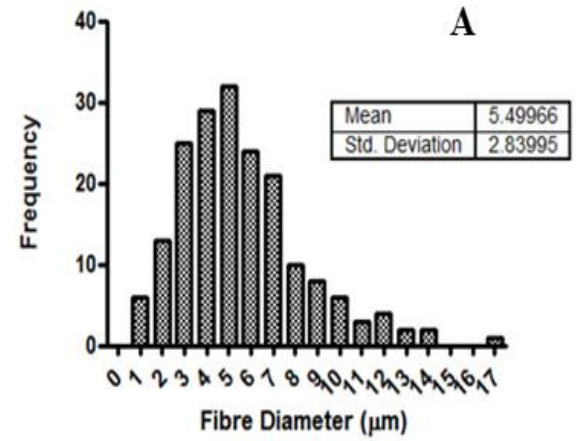

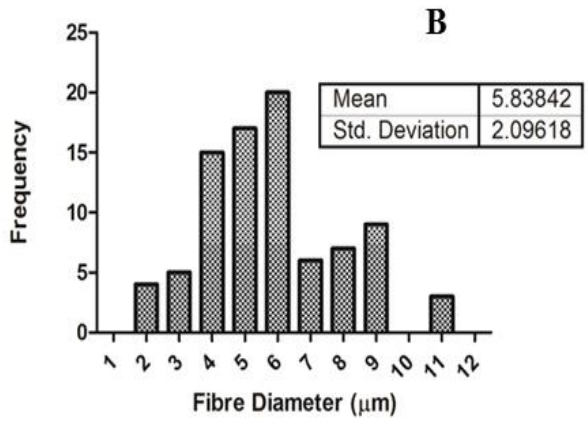

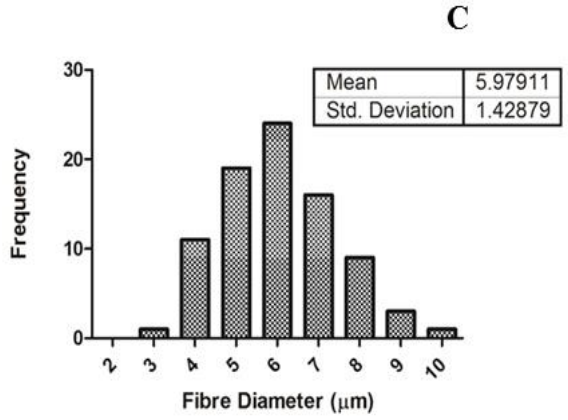

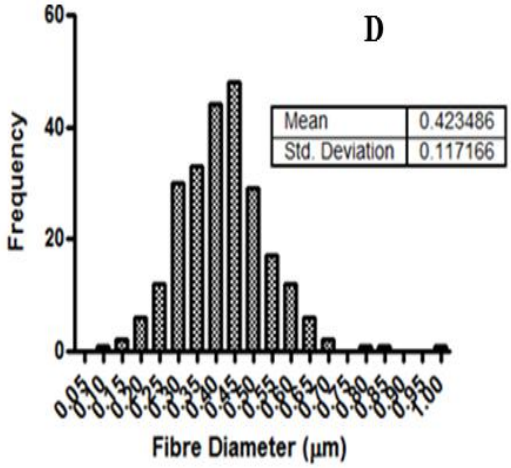
D
Mean 0.423486
Std. Deviation 0.117166
Frequency
Fibre Diameter (μm)

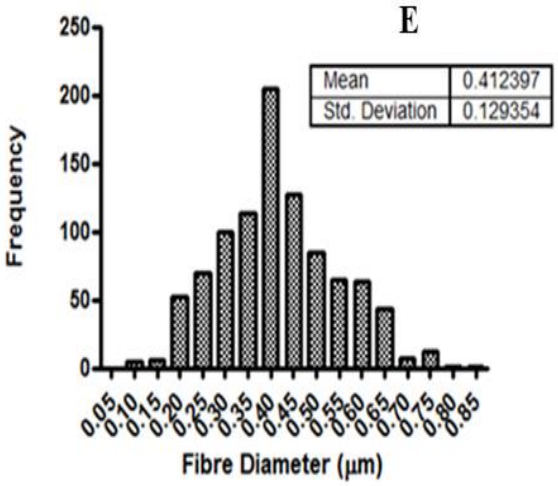
E
Mean 0.412397
Std. Deviation 0.129354
Frequency
Fibre Diameter (μm)

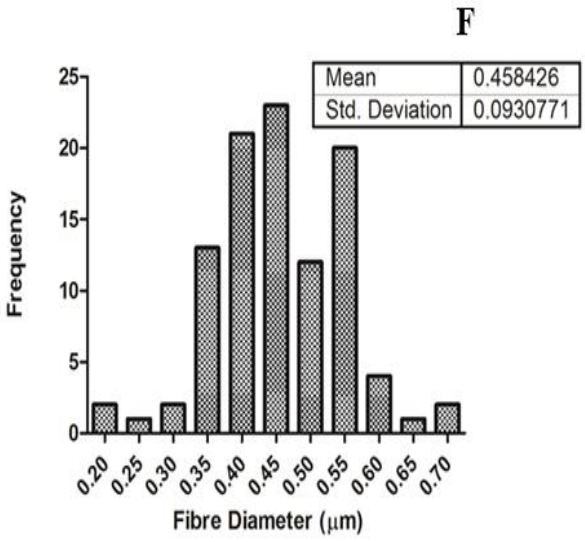
F
Mean 0.458426
Std. Deviation 0.0930771
Frequency
Fibre Diameter (μm)